

**Forschungszentrum Karlsruhe**  
Technik und Umwelt

**Wissenschaftliche Berichte**  
FZKA 5830

**EDITH**  
**Experimental In-Torus**  
**Maintenance System for**  
**Fusion Reactors**  
**Final Report**

**K. Leinemann, B. Dolensky, M. Englert,**  
**B. Haferkamp, R. Krieg, A. Ludwig,**  
**A. Suppan, J. Woll**

**Institut für Angewandte Informatik**  
**Institut für Reaktorsicherheit**  
**Hauptabteilung Ingenieurtechnik**  
**Hauptabteilung Versuchstechnik**

**November 1996**

---



**Forschungszentrum Karlsruhe**

Technik und Umwelt

**Wissenschaftliche Berichte**

FZKA 5830

**EDITH**

Experimental In-Torus Maintenance System for  
Fusion Reactors  
Final Report

K. Leinemann, B. Dolensky, M. Englert\*,  
B. Haferkamp, R. Krieg, A. Ludwig,  
A. Suppan, J. Woll

Institut für Angewandte Informatik  
Institut für Reaktorsicherheit  
Hauptabteilung Ingenieurtechnik  
Hauptabteilung Versuchstechnik

\*Ingenieurbüro für technische Kybernetik

**Forschungszentrum Karlsruhe GmbH, Karlsruhe**  
**1996**

Als Manuskript gedruckt  
Für diesen Bericht behalten wir uns alle Rechte vor

Forschungszentrum Karlsruhe GmbH  
Postfach 3640, 76021 Karlsruhe

ISSN 0947-8620

## **Abstract**

With respect to the special environmental conditions - elevated  $\gamma$ -radiation and temperature - in the plasma chamber of a fusion reactor like NET/ITER, maintenance and replacement tasks can be performed only by means of remote handling systems. EDITH (**Experimental Device for In-Torus Handling**) is the prototype of such a system. It is based on an articulated boom transporter which can be equipped with different end-effectors and tools, respectively, depending on the different tasks to be carried out. EDITH is the central component of a testbed constructed in full scale to investigate experimentally remote handling operations in the simulated section of a plasma chamber. As typical tasks the replacement of protective tiles and divertor plates have been performed. In order to allow the operators a fast and reliable performance of the tasks an advanced guidance and control system has been developed. The guidance system forms a remote handling workstation which, together with the servomanipulator, represents the man/machine interface for the control and surveillance of all devices. The workstation supports the operators at all operations to be manually controlled, at the planning, simulation and programming of automatically performed subtasks. It serves also as a permanently available documentation system and information source. The driving factors for the conceptual design of the control system were the dynamic behaviour, the operational reliability and the cooperation with the guidance system. Qualification tests and first practical experience confirm that this type of remote handling techniques permits to perform in-vessel maintenance tasks safely, reliably and in appropriate time.

### **EDITH**

#### **Experimentelles Handhabungssystem für Wartungsarbeiten im Torus eines Fusionsreaktors**

Wegen der besonderen Umgebungsbedingungen - erhöhte  $\gamma$ -Strahlung und Temperatur - können Reparaturarbeiten in der Plasmakammer eines Fusionsreaktors wie NET/ITER nur mittels eines fernbedienten Handhabungssystems durchgeführt werden. EDITH (**Experimental Device for In-Torus Handling**) ist der Prototyp eines solchen Systems. Es basiert auf einem Vielgelenkarm, der für die jeweiligen Aufgaben mit verschiedenen Endeffektoren bzw. Werkzeugen ausgerüstet ist. EDITH ist die zentrale Komponente eines Teststandes, mit dem in Originalgröße in einem nachgebildeten Ausschnitt einer Plasmakammer Fernhandlungsvorgänge experimentell untersucht werden. Exemplarisch für solche Aufgaben wurde der fernbediente Austausch von Schutzziegeln und Divertorplatten durchgeführt. Um den Operateuren eine schnelle und zuverlässige Durchführung der Arbeiten zu ermöglichen, wurde ein neuartiges Leit- und Steuersystem entwickelt. Das Leitsystem bildet in Form einer Fernhandhabungs-Arbeitsstation zusammen mit den Servomanipulatoren die Mensch-Maschine-Schnittstelle zur Steuerung und Überwachung aller Geräte. Die Arbeitsstation unterstützt die Operateure bei allen manuell zu steuernden Arbeiten, bei der Planung, Simulation und Programmierung automatisch durchzuführender Teilaufgaben und dient mit ihrem multimedialen Dokumentationssystem als ständig verfügbare Informationsquelle. Bei der Konzeption der Steuerung standen das dynamische Verhalten, die Betriebssicherheit und die Kopplung an das Leitsystem im Vordergrund. Qualifikationstests und erste Experimentiererfahrungen bestätigten, daß mit der bei FZK entwickelten Fernhandlungstechnik die gestellten Aufgaben sicher, zuverlässig und in vertretbarer Zeit ausgeführt werden können.

## PREFACE

Work documented in this report was performed within the framework of the Nuclear Fusion Project of the Forschungszentrum Karlsruhe GmbH and supported by the European Fusion Technology Programme.

Contributions are from:

- H. Breitwieser (Institut für Angewandte Informatik)
- G. Dillmann (Hauptabteilung Versuchstechnik)
- B. Dolensky (Institut für Reaktorsicherheit; co-author)
- M. Englert (ITK - Ingenieurbüro für technische Kybernetik, Kuhardt; co-author)
- A. Fiege (Projekt Kernfusion)
- H. Gutzeit (Hauptabteilung für Ingenieurtechnik)
- B. Haferkamp (Hauptabteilung für Ingenieurtechnik; co-author)
- A. Hinz (Hauptabteilung für Ingenieurtechnik)
- H.E. Holler (Institut für Angewandte Informatik)
- F. Katz (Institut für Angewandte Informatik)
- H. Knüppel (Institut für Angewandte Informatik)
- W. Köhler (Hauptabteilung für Ingenieurtechnik)
- R. Krieg (Institut für Reaktorsicherheit; co-author)
- H.G. Krumm (Institut für Angewandte Informatik)
- U. Kühnapfel (Institut für Angewandte Informatik)
- K. Leinemann (Institut für Angewandte Informatik; editor)
- W. Link (Hauptabteilung für Ingenieurtechnik)
- E. Loffl (Hauptabteilung Versuchstechnik)
- A. Ludwig (Institut für Angewandte Informatik; co-author)
- G. Müller (Hauptabteilung für Ingenieurtechnik)
- W. Müller (Hauptabteilung Versuchstechnik)
- W. Olbrich (Institut für Reaktorsicherheit)
- S. Raff (Institut für Reaktorsicherheit)
- J. Reim (Institut für Angewandte Informatik)
- H.A. Rohrbacher (Institut für Angewandte Informatik)
- M. Salaske (Hauptabteilung für Ingenieurtechnik)
- E.G. Schlechtendahl (Institut für Reaktorsicherheit)
- U. Schygulla (Hauptabteilung Versuchstechnik)
- A. Suppan (Hauptabteilung für Ingenieurtechnik; co-author)
- U. Süß (Institut für Angewandte Informatik)
- J. Woll (Institut für Angewandte Informatik; co-author)

# Abbreviations

<b>ABS</b>	Articulated Boom System: complete system consisting of the ABT with working unit
<b>ABT</b>	Articulated Boom Transporter: the transporter itself without the workunit
<b>APC</b>	Axis Positioning Control: In this mode there is performed a path planning for all moved EDITH axes. The axis are synchronised, i.e. the acceleration and deceleration phases as well as the period with constant velocities are equal for all axes within the same path segment.
<b>ASI</b>	Actor/Sensor Bus
<b>AVC</b>	Axis Velocity Control: The axis velocity is given directly using the joystick input. The current nominal position is calculated by integration of the given velocity starting at the current nominal position.
<b>C, C++</b>	C, C++ Programming Language
<b>CAN</b>	Controller Area Network
<b>CDU</b>	Coaxial Drive Unit
<b>DH</b>	Divertor Handling
<b>DHU</b>	Divertor Handling Unit
<b>DM</b>	DOIF Manager
<b>DOIF</b>	Device Operating Interface
<b>EDITH</b>	Experimental Device for In-Torus Handling
<b>EE</b>	End-Effector
<b>EEMU</b>	End Effector Positioning Unit: the EEMU is represented by the three vertical translating axis of the ABT
<b>EMCS</b>	EDITH Motion Control System
<b>EMSM</b>	Electrical Master-Slave Manipulator
<b>ERWS</b>	Edith Remote Workstation
<b>FTP</b>	File Transfer Protocol
<b>FZK</b>	Forschungszentrum Karlsruhe
<b>GWS</b>	Graphical Work Station: The GWS or RHWS provides the user interface for the EMCS.
<b>HB</b>	HandBox: A simple PC based user interface for the EMCS which may be connected serially to the HLCS. This was only used during test phase.
<b>HHL</b>	Handling Heavy Loads
<b>HLCS</b>	High Level Control System: data management system of the EMCS ( parameter handling, sequence files )
<b>HLF</b>	Heavy Load Fork
<b>IO</b>	Input/Output
<b>IRDATA</b>	Industrial Robot Data Transfer Format
<b>iRMX</b>	a real-time operating system provided by Intel, which is running on MB II and PC platforms
<b>ITER</b>	International Tokamak Experimental Reactor
<b>IVHU</b>	In-Vessel Handling Unit
<b>IVT</b>	In-Vessel Transporter
<b>JET</b>	Joint European Torus
<b>KISMET</b>	Kinematics Simulator, Monitor, and Programming Environment for Telemanipulation
<b>LLCS</b>	Low Level Control System: the very control system, containing position controller, path planning and all IO-components needed to control the ABT
<b>MB II</b>	MultiBus II: a special system bus architecture, which is used for LLCS
<b>MHU</b>	Manipulator Handling Unit
<b>MMI</b>	Man-Machine Interface
<b>MPU</b>	Manipulator Positioning Unit
<b>MSM</b>	Master-Slave Manipulator
<b>NRWS</b>	Net Remote Workstation
<b>PEXOS</b>	Procedure Editing, Simulation, Execution, and Monitoring System
<b>POR</b>	Point of Reference

<b>PPC</b>	Point Positioning Control: This mode is used for cartesian positioning of the boom in combination with path planning. The path planning task performs a cartesian path planning and also calls the backward transformation to get belonging axis positions for each path point.
<b>PVC</b>	Point Velocity Control: The cartesian velocity is given directly using the joystick input. The current nominal position is calculated by integration of the given velocity starting at the current nominal cartesian position, which is calculated by forward transformation of the nominal axis positions. Calling the backward transformation gives the new nominal joint positions.
<b>RH</b>	Remote Handling
<b>RHCR</b>	Remote Handling Control Room
<b>RHCS</b>	Remote Handling Control System
<b>RHWS</b>	Remote Handling Workstation
<b>TCP</b>	Tool Centre Point
<b>TCP/IP</b>	Transmission Control Protocol/Internet Protocol (ARPANET Protocol)
<b>TDD</b>	Tile Detachment Device
<b>TFTR</b>	Tokamak Fusion Test Reactor, USA
<b>TH</b>	Tile Handling
<b>TPD</b>	Tile Positioning Device
<b>UDP</b>	User Datagram Protocol
<b>UNIX</b>	Workstation Operating System of AT&T
<b>WU</b>	Work Unit: a device designed to perform special RH tasks, e.g. tile handling or divertor handling. A work unit is mounted to the work unit mounting flange of the EEPU.

# CONTENT

<b>1. Introduction .....</b>	<b>1-1</b>
<b>2. System Overview .....</b>	<b>2-1</b>
<b>3. Mechanics.....</b>	<b>3-1</b>
<b>4. Stress Analysis and Verification .....</b>	<b>4-1</b>
<b>5. Guidance and Control System .....</b>	<b>5-1</b>
<b>6. Motion Control Sytem .....</b>	<b>6-1</b>
<b>7. Qualification .....</b>	<b>7-1</b>
<b>8. Tile Handling .....</b>	<b>8-1</b>
<b>9. Handling Heavy Loads .....</b>	<b>9-1</b>
<b>10. Conclusions .....</b>	<b>10-1</b>
<b>11. Bibliography .....</b>	<b>11-1</b>

# Table of Content

<b>1 INTRODUCTION .....</b>	<b>1-3</b>
<b>1.1 OBJECTIVES OF THIS DOCUMENT .....</b>	<b>1-3</b>
<b>1.2 REQUIREMENTS FOR EDITH .....</b>	<b>1-4</b>
<b>1.3 CONCEPT FOR EDITH AND FULL SCALE MOCK-UP .....</b>	<b>1-6</b>
<b>1.4 RELATED WORK.....</b>	<b>1-6</b>
<b>1.5 REFERENCES .....</b>	<b>1-8</b>

## List of Figures

FIG. 1-1: IN-VESSEL HANDLING.....	1-3
FIG. 1-2: NET CROSS SECTION.....	1-5
FIG. 1-3: NET/TER AND EDITH .....	1-7

## List of Tables

TAB. 1-1 : ENVIRONMENTAL CONDITIONS FOR OPERATIONAL EQUIPMENT AND EDITH .....	1-5
TAB. 1-2: TECHNICAL DATA FOR ABT AND EDITH.....	1-5
TAB. 1-3: MAXIMUM DIMENSIONS AND WEIGHTS OF DIVERTOR MODULES .....	1-5



# 1 INTRODUCTION

In-vessel components of fusion reactors like NET (Next European Torus) or ITER (International Thermonuclear Experimental Reactor) are exposed to high neutron radiation. The high  $\gamma$  dose rate (approximately  $3 \times 10^4$  Gy/h-Si), due to activation already after a short time of operation, prohibits human access for maintenance and repair work. Therefore, maintenance work must be carried out remotely without direct view onto the scene and without the possibility of placing TV-cameras as needed. The unique challenge of this task results from the machine's large size and the complexity of the various maintenance procedures. In addition to the development of task suited devices, the development of software tools for planning, execution, and documentation of maintenance procedures to assist the operators in performing the work as fast as possible to minimise maintenance time.

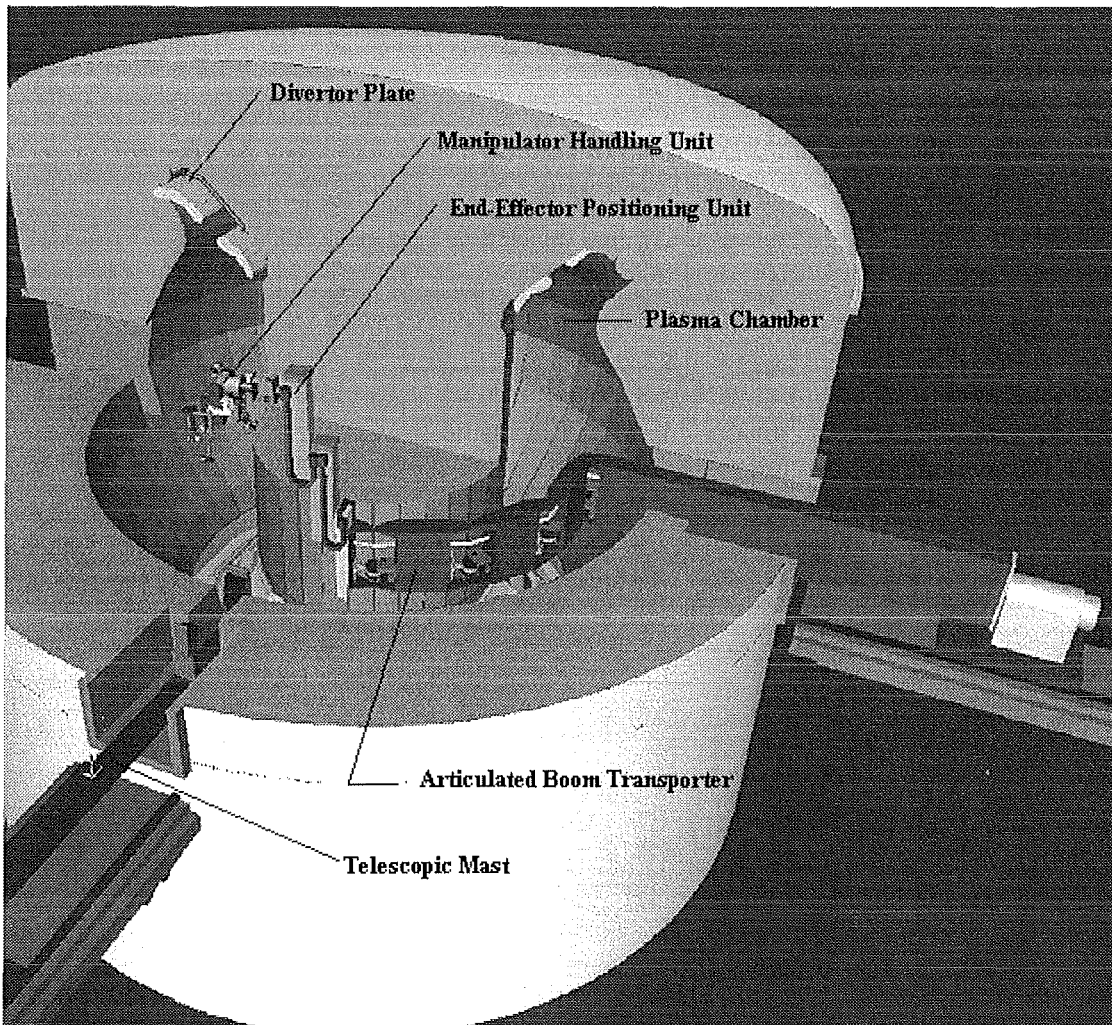


**Fig. 1-1: In-Vessel Handling**

## 1.1 OBJECTIVES OF THIS DOCUMENT

Objectives of this document are

- to give an overview about the testbed EDITH, consisting of the articulated boom transporter (ABT), the full scale mock-up of the upper half of a torus sector, tools for tile exchange and heavy load handling, and the guidance and control system,

- to show the capabilities of the guidance and control system, in particular of the remote handling workstation (RHWS) in a realistic application,
- to summarise the results of the static and dynamic qualification tests at the ABT, and
- to report about tests to demonstrate the handling of heavy loads (e.g. divertor plates) and the performance of delicate tasks like tile handling.

## 1.2 REQUIREMENTS FOR EDITH

EDITH is a prototypic in-vessel transporter (IVT) for the demonstration of maintenance tasks and component replacement inside of the torus of a fusion device like NET/ITER as described in [NET93] and in [HON91]. It is based on the investigations and justification for a full scale prototypic articulated boom as documented in [SH281, SPH988, MAI89, SUP90].

In particular, the objectives of EDITH were:

- Basic investigations of the boom concerning static and dynamic behaviour, manoeuvrability and controllability, positioning and repeatability accuracy.
- Demonstration of the capability to transport and position loads up to 1 ton.
- Demonstration of the suitability to carry out delicate tasks as tile handling.
- Demonstration of reliable remote handling by means of a flexible guidance and control system.

The development of the equipment for demonstration of handling procedures is based on the assumption that no external sensors are available in the in-vessel environment. That means, the development did not include automation of subtasks, in addition to the internal sensors (resolvers) needed for the transport task.

The requirements for EDITH are based on the requirements for the articulated boom transporter which again is part of the basic equipment for in-vessel operations. The requirements differ only by the environmental conditions as shown in Tab. 1-1.

The other requirements for the operational equipment and EDITH are summarised in the Tab. 1-2 and Tab. 1-3. Their basis is the technical specification for NET/ITER in-vessel transporters the document "Divertor Maintenance Using IVHU" and the document "Definition of Requirements for the Design of Prototype Divertor Handling Equipment" as well as the tentative dimensions and arrangement shown in Fig. 1-2.

Since the replacement of divertor modules is the most demanding operation due to the weight of the modules and the required dexterity of the handling operations this task has been the driving factor and the basis for the ABT investigations and thus also for the design of EDITH. For the divertor handling demonstration a radial segmentation of the divertor modules was assumed although the segmentation at NET/ITER is not yet finally decided: The technical data of the divertor modules are listed in Tab. 1-3.

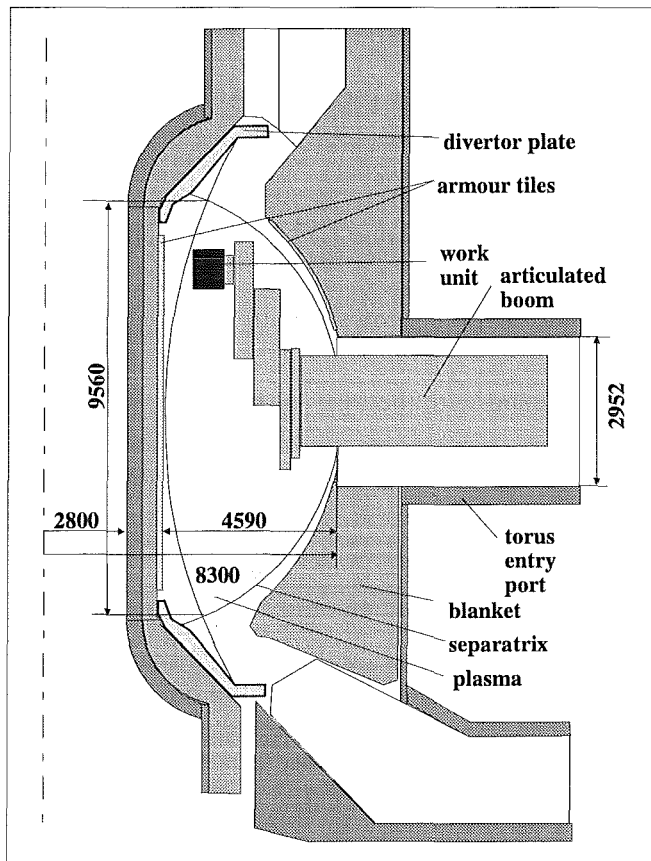


**Fig. 1-2: NET Cross Section**

	<b>Environmental Conditions of Operational Equipment</b>	<b>Environmental Conditions of EDITH</b>
Temperature	+20 to +150°C	0 to +30°C
Atmosphere	He (tbd)	air
Pressure	approx. 1 atmosphere	approx. 1 atmosphere
Radiation	$3 \times 10^4$ Gy/h-Si, negligible $\alpha$ and $\beta$	none
Contaminated dust	tbd	none
Magnetic field	negligible	none

**Tab. 1-1 : Environmental Conditions for Operational Equipment and EDITH**

Number and reach of ABT and EDITH	2 x 90° at full load capacity
Total length of ABT and EDITH	11440 mm
Maximum load capacity of boom at distance of 11800 mm	1200 kg
Number of entry ports for ABT	2
Number of additional ports for components and equipment	2
Height / width of ports	2952 / 1248 mm

**Tab. 1-2: Technical Data for ABT and EDITH**

Number of divertor modules	32 upper / 32 lower ones
Width of one module	745 / 1202 mm
Length of one module	3462 mm
Height of one module	approximately 600 mm
Weight of one module	approximately 1000 kg

**Tab. 1-3: Maximum Dimensions and Weights of Divertor Modules**

### 1.3 CONCEPT FOR EDITH AND FULL SCALE MOCK-UP

Out of several investigated design options for in-vessel handling systems (IVHS) a handling unit based on an articulated boom system (ABS) has been selected. The advantages of this solution are:

- short deployment time because only one port is needed and no support structure has to be installed,
- the available working and manipulation space in the torus is maximal because no space is occupied by rails,
- there is no interaction needed with the torus structure.

EDITH. is the scale 1:1 prototype of such a transporter. Its development and tests were required because of the following reasons:

- JET experience has shown that in-vessel operations that were not rehearsed in a 1:1 test stand turned out to be extremely cumbersome.
- Logical step between existing smaller booms and the final machine: EDITH as a functional prototype in scale 1:1; simple up-scaling not acceptable (non-linearities).
- Demonstration of complete procedures fully remotely executed.

Fig. 1-3 shows the NET torus with the inserted in-vessel handling unit (IVHU) and the EDITH-ABT with the full scale mock-up. As to be seen the mock-up simulates the upper half of a NET torus sector (1/16th of the torus) and includes typical plasma facing components. The EDITH-ABT allows in combination with the mock-up the demonstration of typical maintenance tasks as the replacement of tiles and divertor modules.

### 1.4 RELATED WORK

The EDITH work concentrated on transporter development, workstation development, and the demonstration of selected tasks with standard tools (e.g. tile exchange). To guarantee the performance of the work in a real environment FZK also did research work in the field of radiation resistant motors, lubricants, cables, and resolvers. The result of this task is documented in [SPE95, ENG95, ROH95].

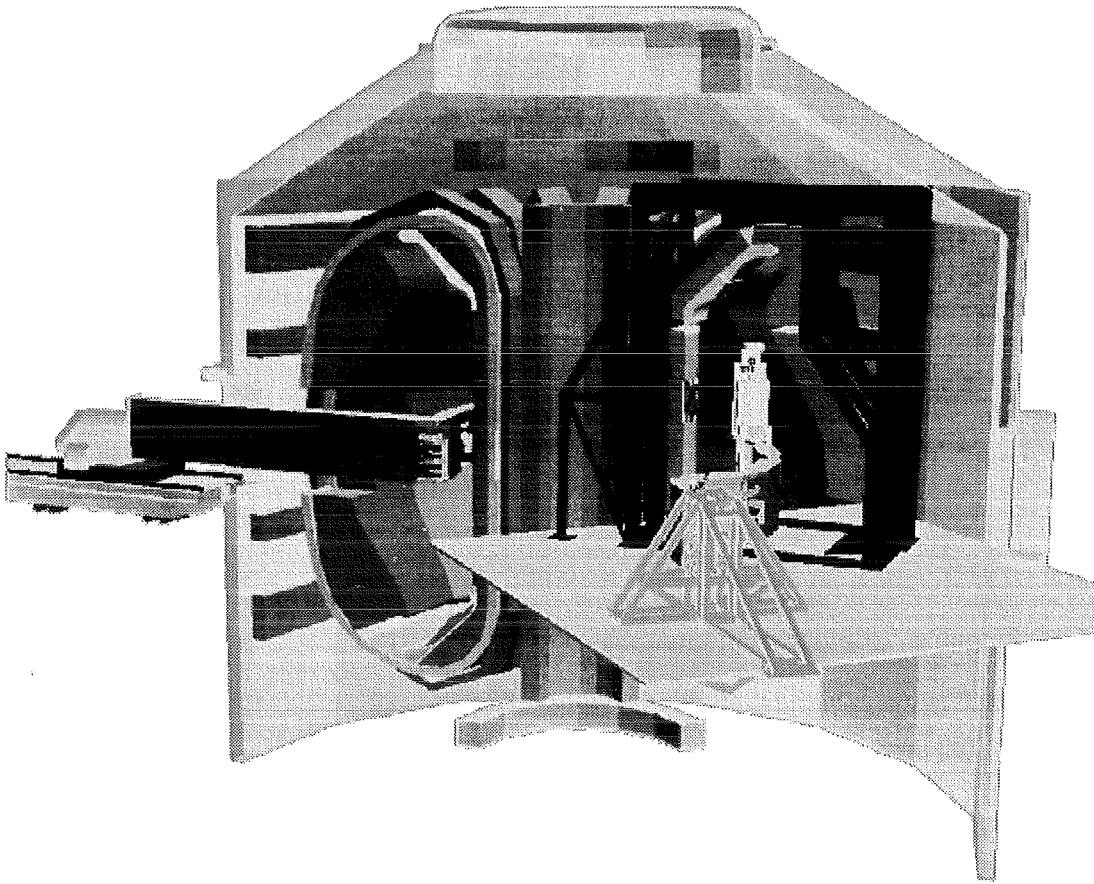


**Fig. 1-3: NET/ITER and EDITH**

At EDITH a support structure substitutes the transporter of the later operational equipment at which the articulated boom will be attached for the transfer into the plasma chamber of the NET/ITER device

## 1.5 REFERENCES

- SH288 Suppan, A., Hübener, J.: Investigations of in-vessel handling concepts for NET. IAEA Technical Committee Meeting on Robotics and Remote Maintenance Concepts for Fusion Machines, Karlsruhe, February 22-24, 1988, Karlsruhe
- SPH988 Suppan, A., Hübener, J.: In-vessel handling unit concept for NET. 15th Symp.on Fusion Technology, Utrecht, NL, September 19-23, 1988 , Utrecht
- MAI89 Maisonnier, D.:unpublished report, 1989
- SUP90 Suppan, A. et al.: The NET Articulated Boom: Preliminary Investigations and Justification for a Full Scale Prototype, KfK 4809, December 1990
- HON91 Honda, T. et al.: ITER Assembly and Maintenance. ITER Documentation Series, No. 34, IAEA, Vienna, 1991
- NET93 The NET Team, NET Predesign Report, Fusion Engineering and Design, Volume 21, Feb. 1993, pp.92-106
- SPE95 Suppan, A., Englert, M.: unpublished report, April 1995
- ENG95 Englert, M.: unpublished report, Feb. 1995
- ROH95 Rohrbacher, H.A.: unpublished report, June 1995

# Table of Content

<b>2 SYSTEM OVERVIEW .....</b>	<b>2-3</b>
<b>2.1 EDITH SYSTEM COMPONENTS .....</b>	<b>2-3</b>
<b>2.2 TECHNICAL DATA OF EDITH .....</b>	<b>2-8</b>
<b>2.3 REFERENCES .....</b>	<b>2-11</b>

## List of Figures

<b>FIG. 2-1: EDITH RELATED TO NET/ITER (SCHEMA) .....</b>	<b>2-4</b>
FIG. 2-2 : EDITH TEST FIELD .....	2-4
FIG. 2-3: EDITH SYSTEM STRUCTURE .....	2-4
FIG. 2-4: EDITH TEST FIELD WITH ABT, MHU, TORUS MOCK-UP .....	2-5
FIG. 2-5 : EDITH TEST FIELD WITH ABT, DIVERTOR, TORUS MOCK-UP, MAGAZINE .....	2-6
FIG. 2-6: EDITH CONTROL ROOM .....	2-7

## List of Tables

TAB. 2-1: ARTICULATED TRANSPORTER SYSTEM DATA.....	2-8
TAB. 2-2: ARTICULATED BOOM DATA.....	2-8
TAB. 2-3: END-EFFECTOR POSITIONING UNIT DATA .....	2-9
TAB. 2-4: MANIPULATOR HANDLING UNIT DATA .....	2-9
TAB. 2-5: MHU VIEWING SYSTEM DATA .....	2-9
TAB. 2-6: CONTROL SYSTEM DATA .....	2-9
TAB. 2-7: REMOTE HANDLING WORKSTATION DATA .....	2-10
TAB. 2-8: MANIPULATING WORKING PLACE DATA .....	2-10



## 2 SYSTEM OVERVIEW

The relation between the EDITH experimental set-up and the NET/ITER reactor is shown in Fig. 1-3 in a 3D-CAD view and schematically in Fig. 2-1. The spatial arrangement of the complete EDITH test site in a FZK building can be seen in Fig. 2-2. In addition to a main hall where the torus mock-up, the articulated boom transporter, and the work units are installed there are two rooms for the guidance and control system. A functional overview over the EDITH system is given in Fig. 2-3 [SUP93, SLW94, FGE94].

### 2.1 EDITH SYSTEM COMPONENTS

An **articulated boom transporter** (ABT) serves for positioning work units (WU) like the manipulator handling unit (MHU), the divertor plate handling unit (DHU), or others in one half of the NET/ITER torus ( $\pm 90^\circ$ ). The ABT is held by a fixed support structure instead of a radially movable carrier system. For the horizontal motion the articulated boom has four links, the vertical positioning is provided by the so-called end-effector (work unit) positioning unit (EPU). The ABT with EPU, MHU and the torus mock-up are shown in Fig. 2-4 and with divertor fork and divertor in Fig. 2-5.

As a basic general purpose work unit a master-slave system is available in form of the **manipulator handling unit** (MHU). This MHU consists of two master-slave systems and a viewing system with four cameras and lights. The master-slave systems can handle 24 kg and 60 kg. The yaw joint of the MHU is only mechanically driven.

For tile exchange the MHU is used together with two special tools: the **tile detachment device** (TDD) and the **tile positioning device** (TPD).

A special simple **load fork** is used for taking over a divertor-mock-up. The planned (and needed) special purpose work unit for divertor plate exchange (DHU) could not be developed.

To use the various devices dedicated **control systems** are available which are accessed via the remote handling workstation (especially its device operating interface subsystem DOIF)

High-level (task level) control, co-ordination, and supervision is done via a general purpose **remote handling workstation** (RHWS) which provides the man-machine interface (together with manipulator masters) and also assists the operator in his work by a group of functions: multimedia multilevel handbook, simulation, co-ordination, documentation.

The NET/ITER reactor is simulated by the upper half of a **torus sector mock-up** (22.5 degree) equipped with two arrays of exchangeable armour tiles and a divertor plate.

Fully remote control of the maintenance procedures is performed from the **control room** (Fig. 2-6) with two working places: one for the co-ordinating/assisting operator and one for the manipulating operator. The control room is equipped with the RHWS, video monitors and the two masters of the MHU.

The control system is located in an adjacent **electronic equipment room**.

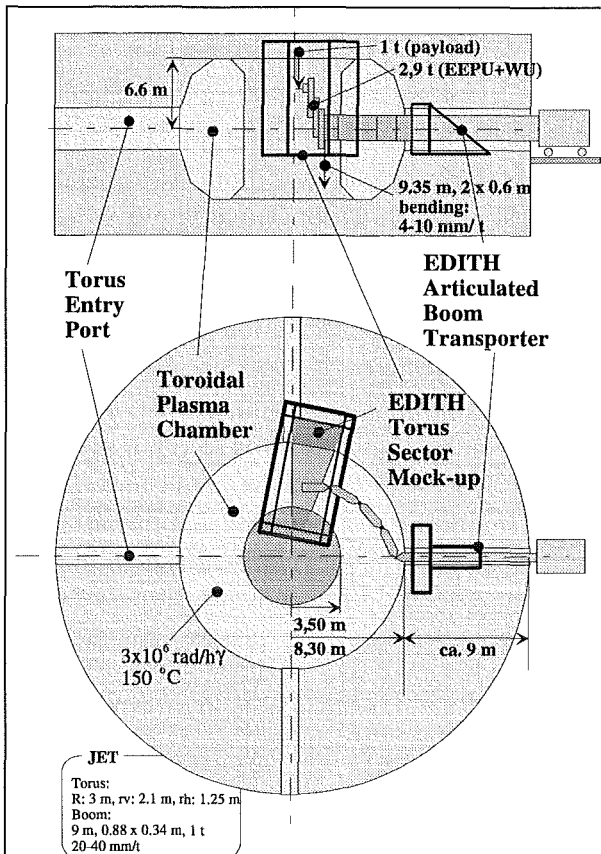


**Fig. 2-1: EDITH related to NET/ITER (Schema)**

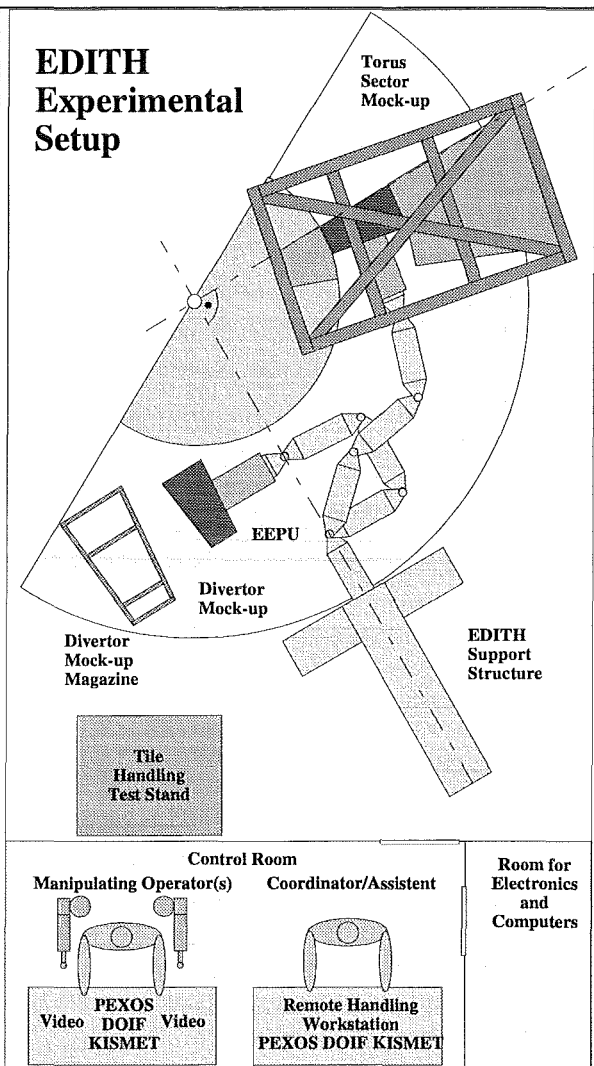


**Fig. 2-2 : EDITH test field**

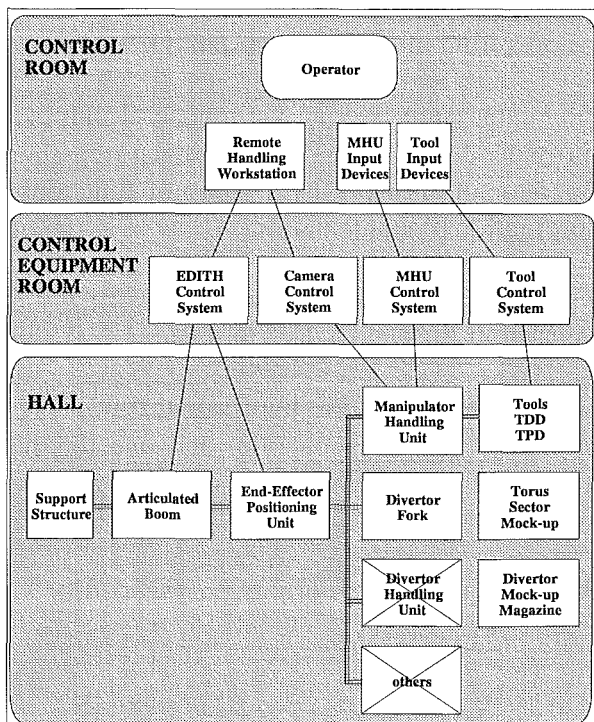


**Fig. 2-3: EDITH System Structure**

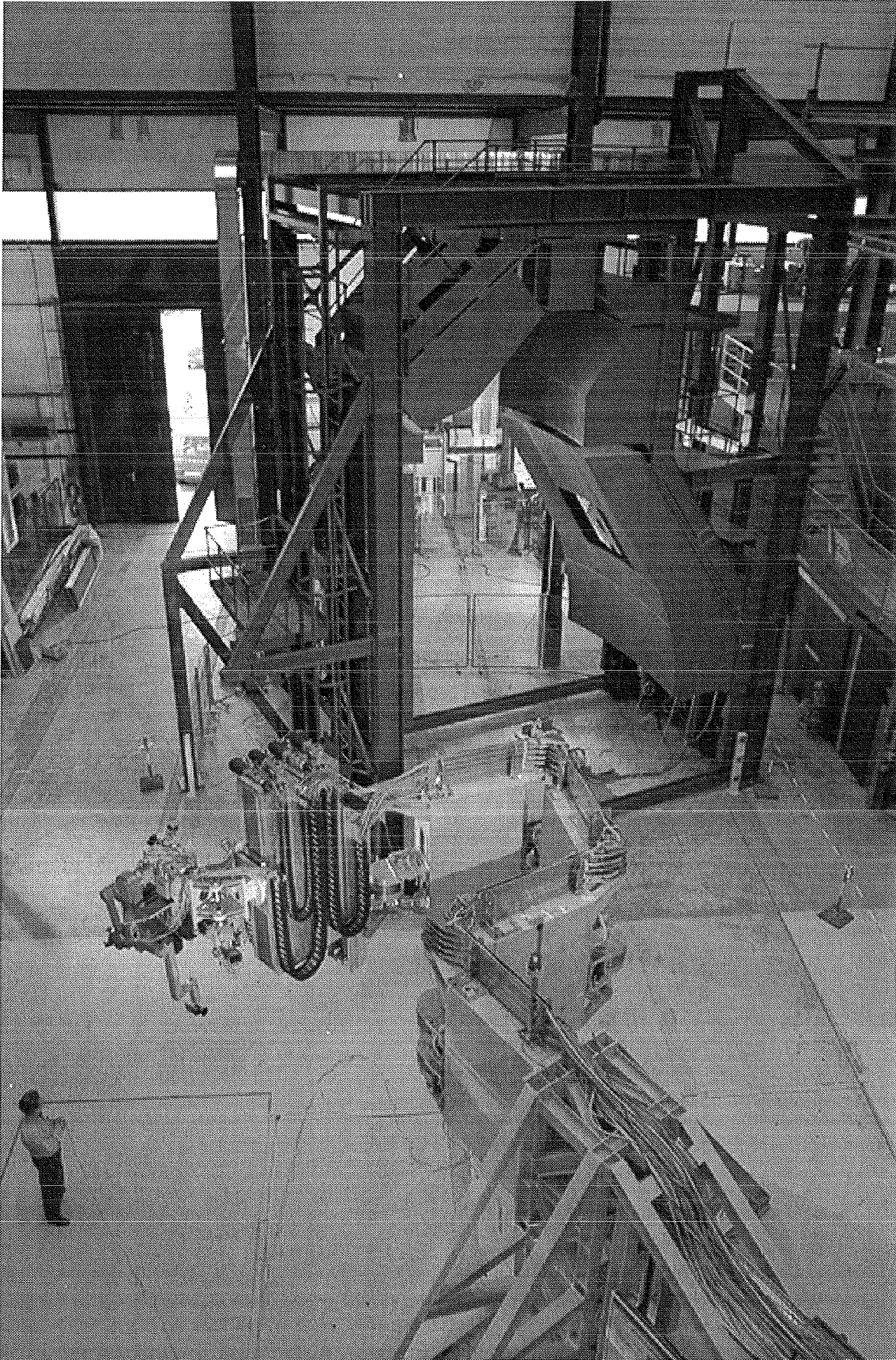


**Fig. 2-4: EDITH test field with ABT, MHU, torus mock-up**

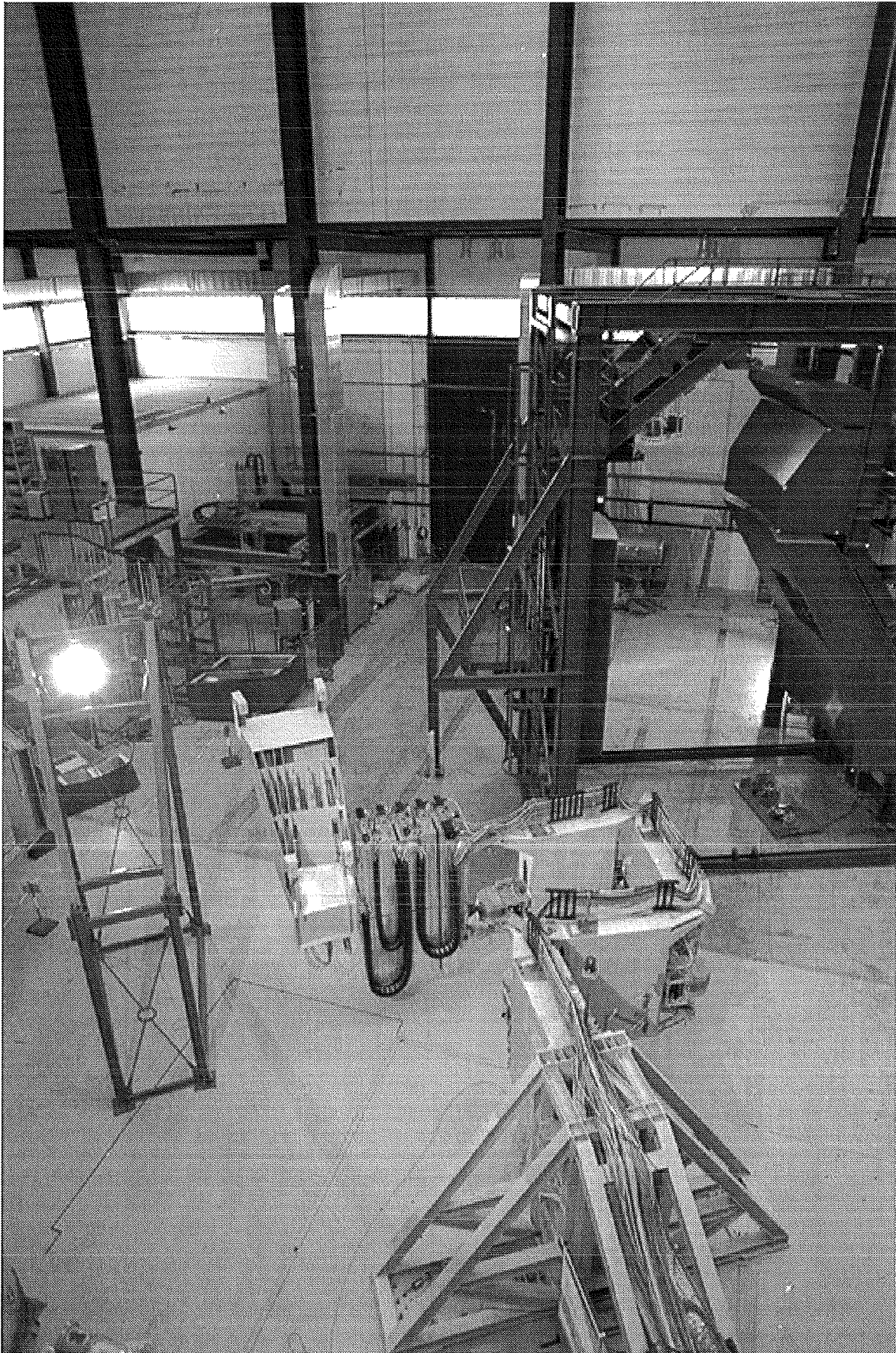


**Fig. 2-5 : EDITH test field with ABT, divertor, torus mock-up, magazine**

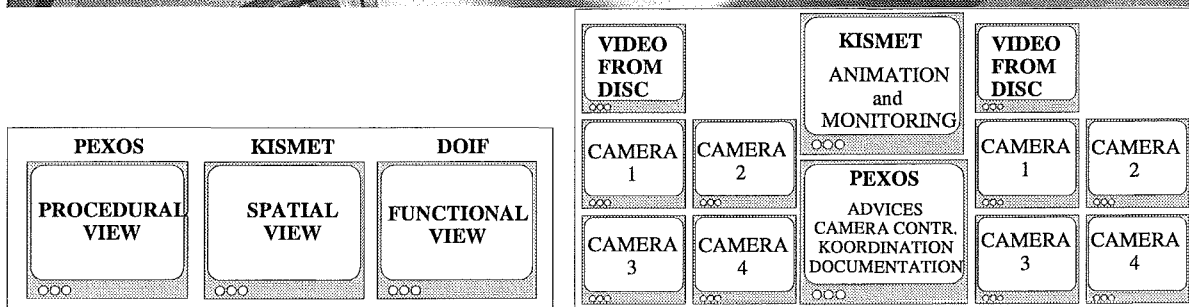
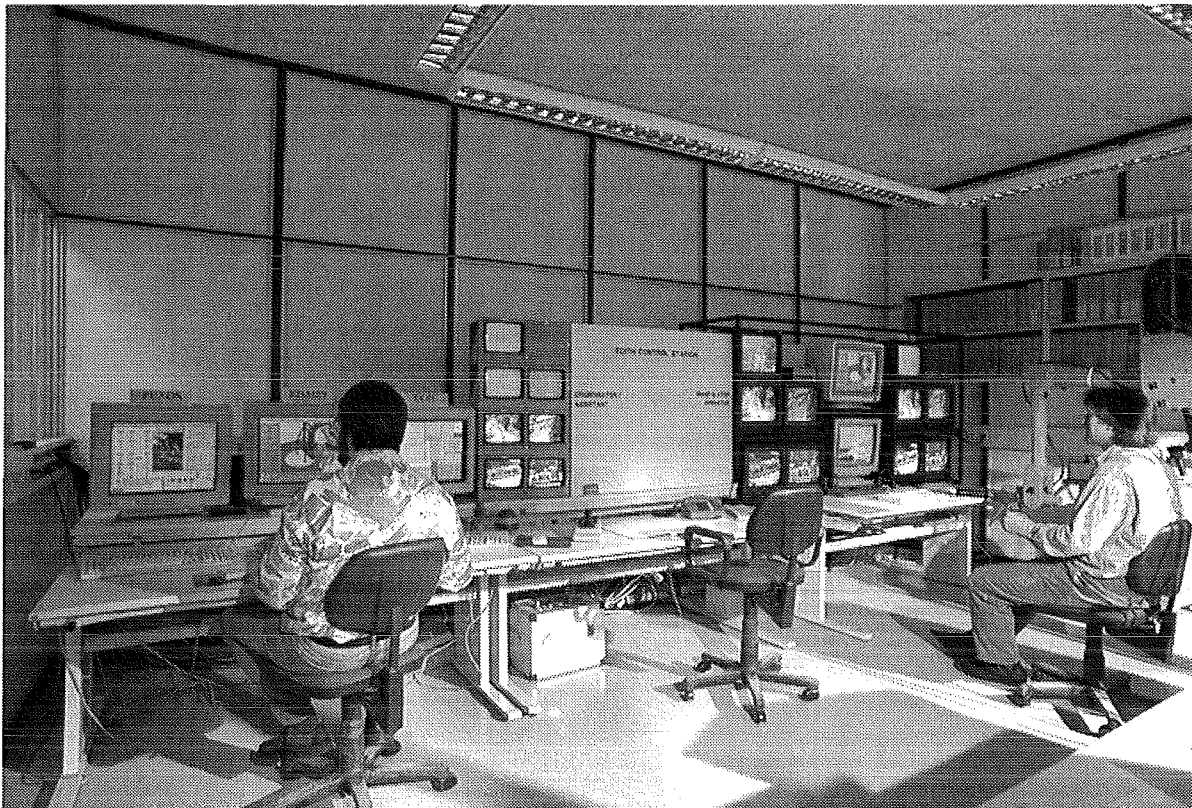


**Fig. 2-6: EDITH control room**

On the left hand side the **co-ordinating operator** with the remote handling workstation and on the right hand side the **manipulating operator** with master arms video monitors of the viewing system and additional computer monitors of the remote handling workstation.

## 2.2 TECHNICAL DATA OF EDITH

The EDITH system will be described in the following chapters in detail. The tables 2-1 to 2-8 will give a rough overview over the technical data of the actual implementation.

Total length excluding support structure	11439 mm
Total weight including end-effector positioning unit	≈ 8.5 tons
Maximum load capacity	1 ton
Weight of the end-effector positioning unit	≈ 2.5 tons
Range of operation related to the torus geometry	±90°
Horizontal positioning accuracy	±50 mm
Horizontal repeatability	±5 mm
Vertical positioning accuracy	±2 mm
Vertical repeatability	±2 mm
POR box during reconfiguration	100*100*100 mm
Vertical deflexion at EEPU/boom flange	10 mm/t

Tab. 2-1: Articulated Transporter System Data

Length	9940 mm
Width / height of links	600 /1825 - 2000 mm
Weight	≈ 6 tons
Number of link joints	4
<b>Link joint parameters</b>	
Range of operation	±115° resp. (±105° at the front link)
Max. angular joint speed	0,15 rad/sec
Max. angular joint acceleration	0.085 rad/sec <sup>2</sup>
Number of coaxial drive units per link joint	2 at the first link, 1 at the front links
<b>Coaxial drive units</b>	
Number of gear trains per unit	2
Nominal motor power	2.2 kW

Tab. 2-2: Articulated Boom Data

Length / width / height	1499 / 974 / 2758 mm
Total stroke	±5075 mm
Total weight	2.5 tons
Vertical positioning accuracy	±2 mm
Vertical repeatability	±2 mm
Max. speed (combined motion of all slides plus trolley)	0.1 m/sec
Max. acceleration	0.1 m/sec <sup>2</sup>
Number of slides	2
Number of trolley with interface for end-effectors	1
<b>Drive parameters</b>	
Number / size of planetary roller spindles - diameter x lead	5 / 39 x 5 mm
Number of motors with fail-safe brakes	6
Nominal motor power	2.2 kW

Tab. 2-3: End-effector Positioning Unit Data

Number / type of electric master/slave manipulators	1 / EMSM2-B & 1 / EMSM3
<b>EMSM2-B</b>	
Number of motions	7
Load capacity of the tong: continuous/ 15 minutes	24 kg/45 kg
Power amplification master/slave	1:2, 1:6, 1:20
<b>EMSM3</b>	
Number of motions	8
Load capacity of the tong: continuous/15 minutes	60 kg/100 kg
Power amplification master/slave	1:2, 1:20, 1:50
<b>Manipulator positioning unit (mech. actuated)</b>	
Number of joints / range of operation	1 yaw joint /±111°

Tab. 2-4: Manipulator Handling Unit Data

<b>Overview cameras</b>	
Number of cameras (colour)	2
Arrangement	pan/tilt heads
<b>Working cameras</b>	
Number of cameras (colour)	2
Arrangement	at camera arms
<b>Camera arms (elt. actuated)</b>	
Number of arms	2
Number of motions per arm	5
Number of drives per arm	4

Tab. 2-5: MHU Viewing System Data

System control	DECstation-3200, VMX
Motion control	Intel-MultibusII iSBC-486/133, iSBC-386/133 360 Digital-I/o, 80 Analog-I/O cycle time: 20 ms controlled axes: 13
Camera arm control	2 PC
Pan/tilt heads control	SBC
Terminal server	1

Tab. 2-6: Control System Data

Subsystem	Hardware	Software
Procedural support PEXOS	SUN SPARCstation2	UNIX, Xview, Lisp, KEE
Spatial support KISMET	Silicon Graphics CRIMSON	UNIX, GL
Functional support DOIF	Silicon Graphics Indigo2, video overlay board	UNIX, Motif
Video disk	SONY LVA-4500P	
Video windowing system	RGB/View 1050	
Video multiplexer	VT, 32 input, 5 output	
Video monitors	6 x 10" bw	

**Tab. 2-7: Remote Handling Workstation Data**

KISMET screen	19", RGB
PEXOS/DOIF-Terminal (X terminal)	Tektronix XP358
Video monitors	2 x 4 x 14" color
Master-slave control	2 master units, separate control panel

**Tab. 2-8: Manipulating Working Place Data**

## 2.3 REFERENCES

- SUP93 Suppan, A., Krieg, R., Krumm, H.G., Kühnapfel, U., Leinemann, K. Reim, J., Woll, J.: Experimental device for in-torus handling - EDITH intermediate report. KfK-5252 (October 93)
- SLW94 Suppan, A. Leinemann, K. Woll, J.: Erste praktische Erfahrungen mit dem EDITH-Teststand für Instandhaltungsarbeiten im Torus eines Fusionsreaktors. KfK-Nachrichten, 26(1994) S.146-55
- FGE94 Fiege, A., Haferkamp, B., Knüppel, H. Leinemann, K., Suppan, A. Woll, J., Maisonnier, D.: Testbed EDITH and first practical experience gained in the operation. Herschbach, K. (Hrsg.) Fusion Technology 1994 : Proc.of the 18th Symp., Karlsruhe, August 22-26, 1994 Vol. 2 S.1379-82 Amsterdam (u.a.) : Elsevier, 1995, Karlsruhe



# Table of Content

<b>3 MECHANICS AND KINEMATICS</b> .....	<b>3-3</b>
<b>3.1 ARTICULATED BOOM</b> .....	<b>3-3</b>
<b>3.2 END-EFFECTOR POSITIONING UNIT</b> .....	<b>3-6</b>
<b>3.3 REFERENCES</b> .....	<b>3-8</b>

## List of Figures

FIG. 3-1: EDITH ARTICULATED BOOM SYSTEM .....	3-5
FIG. 3-2: YAW JOINT Z1 WITH 2 COAXIAL DRIVES AND RESOLVER (TOP) .....	3-5
FIG. 3-3: YAW JOINT Z2 WITH 1 COAXIAL DRIVE AND RESOLVER (TOP) .....	3-5
FIG. 3-4: EEPU SCHEMA .....	3-7
FIG. 3-5: EEPU WITH MHU .....	3-7
FIG. 3-6: EEPU FOLDED .....	3-7
FIG. 3-7: EEPU EXTENDED .....	3-7

## List of Tables

TAB. 3-1: ARTICULATED BOOM TRANSPORTER - LINK DIMENSIONS .....	3-3
TAB. 3-2 : MAIN DATA FOR COAXIAL DRIVE UNITS FOR YAW JOINTS Z1 TO Z4 .....	3-4
TAB. 3-3: TECHNICAL DATA OF THE END-EFFECTOR POSITIONING UNIT .....	3-6

4

### 3 MECHANICS AND KINEMATICS

The EDITH articulated boom system (Fig. 3-1) consist of

- the articulated boom transporter (ABT) with four vertical joints,
- the end-effector positioning unit (EPU),
- the work units (described in detail in chapters 8 and 9),
- the special working tools (described in detail in chapters 8), and
- the working environment mock-ups.

The total length of the ABT, including the cantilever arm which is rigidly connected with the support structure and including also the manipulator positioning unit (MPU) is 12480 mm.

#### 3.1 ARTICULATED BOOM

The support structure replaces a radially to the NET/TER torus movable transport carrier of the later operational articulated boom system (ABS). It consists of a girder construction which is fixed at the floor. The structure and its fixation are calculated for maximum bending moments and maximum torque of 1200 kNm. The structural material is RST.37-2.

The ABT has four links (B1 to B4) plus a cantilever arm (C1) which connects the links with the support structure. Cantilever arm and links have a box cross section. The ABT front link B4 differs from the other ones and consists of the attachment plate with the upper and lower hinges for the link joint Z4. The height of the links is stepwise reduced from the cantilever arm to the link B4. The dimensions of the links are listed in Tab. 3-1. The links are connected by means of yaw joints (Z1 to Z4) which are equipped with spherical roller bearings.

The link boxes contain cable ducts for power supply and signal transmission lines for the yaw joints. The cables for the EPU and the EE's are arranged above the links.

Link Nr.	Link length (mm)	Width (mm) x Height (mm) x Wall thickness (mm)
C1	2000	600 x 2000 x 12
B1	2450	600 x 1930 x 8
B2	2450	600 x 1871 x 6
B3	2450	600 x 1825 x 5
B4	590	600 x 1858 x 15

**Tab. 3-1: Articulated Boom Transporter - Link Dimensions**

The yaw joints are actuated by one coaxial drive unit each (Fig. 3-3). Only the joint Z1 (Fig. 3-2) is driven by two coaxial drive units taking into account the required higher torque.

The link joints Z1 to Z3 have a range of operation of  $\pm 115^\circ$ , link joint Z4 of  $\pm 105^\circ$ .

The motions are controlled by control components which give either position signals of the link joints to the position control system or mechanically of the other systems which have priority fail. The sequence of priority for the control components is the following:

At normal circumstances absolute multi-turn resolvers arranged at the upper joints axles measure the revolutions of the planetary roller spindles and signal the data to the position control system.

Limit switches mounted at the lower link hinges will be actuated by stoppers, arranged at the complementary link hinges, if one of the resolvers fails. They stop the according drive.

The third level are mechanical stops if both resolvers and limit switches fail.

Each coaxial drive unit consists of identical trains of drive, composed of AC-servo motor, spur wheel gear, CYCLO drive and torque arm, acting upon the torque arm constraint. The duplication of the trains of drive results almost in a duplication of the torque and makes optionally possible a mechanical or electrical backlash removal. The main data of the drive units are given in Tab. 3-2.

Parameter	Value
Maximum angular joint speed (rad/sec)	0.15
Maximum acceleration (rad/sec <sup>2</sup> )	0.085
Number of gear trains (motor with fail-safe brake, spur wheel gear, CYCLO drive)	2
Transmission ratio of CYCLO drive	89:1
Transmission ratio of spur wheel gear	5.99:1
Total transmission ratio	532.9:1

**Tab. 3-2 : Main Data for Coaxial Drive Units for Yaw Joints Z1 to Z4**

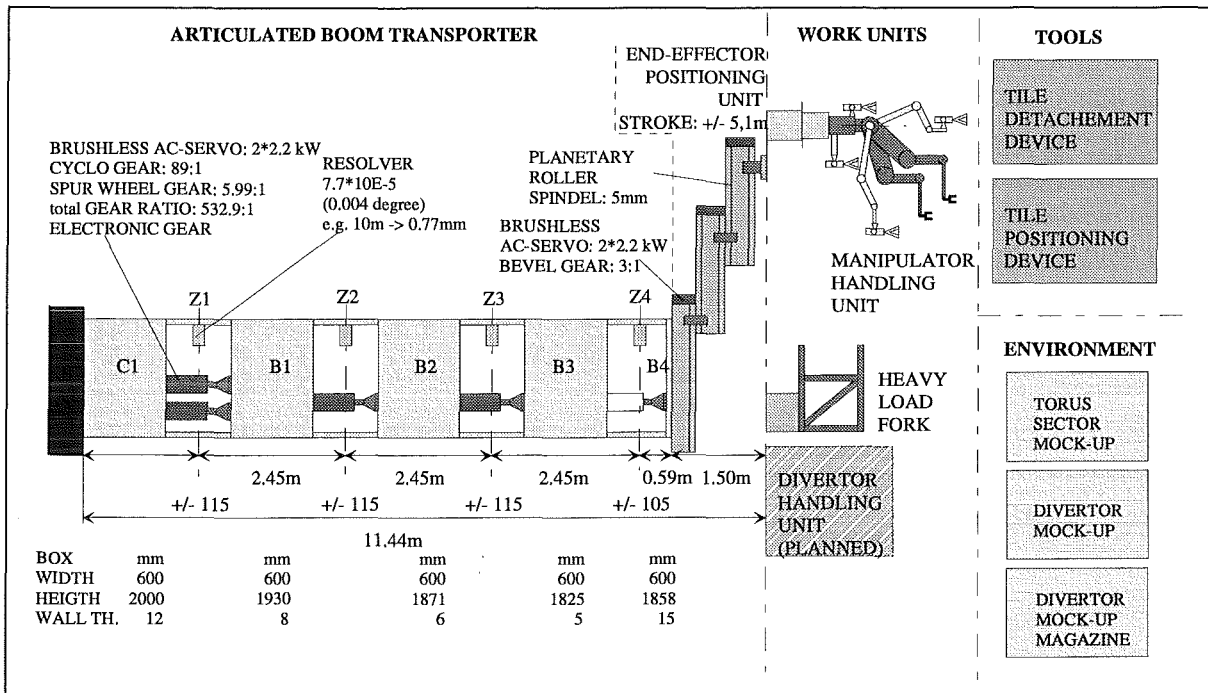


**Fig. 3-1: EDITH Articulated Boom System**

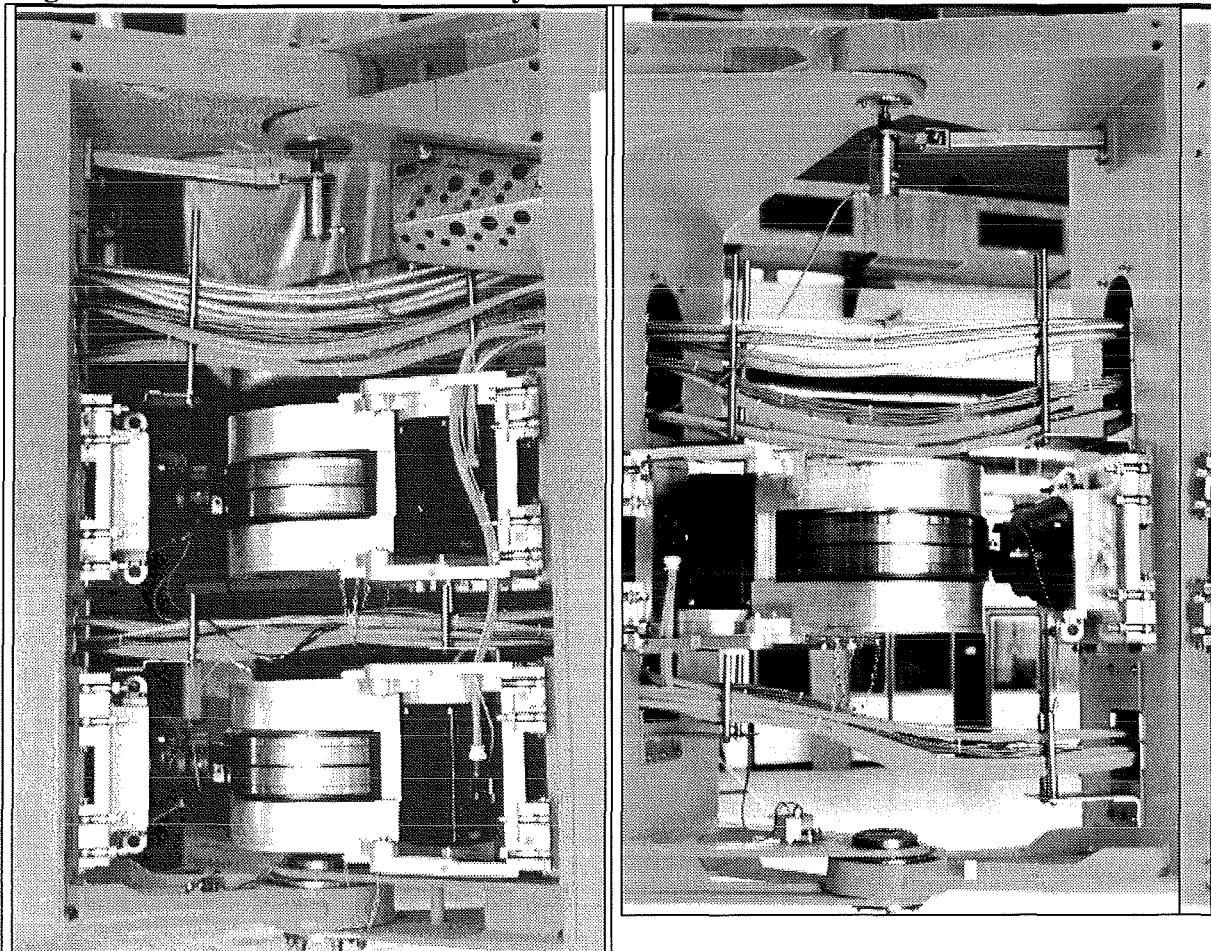


**Fig. 3-2: Yaw joint Z1 with 2 coaxial drives and resolver (top)**

**Fig. 3-3: Yaw joint Z2 with 1 coaxial drive and resolver (top)**

### 3.2 END-EFFECTOR POSITIONING UNIT

The EEPU (Fig. 3-4 - Fig. 3-7) forms the permanently attached connection between the ABT and the different end effectors. It is required to reach the upper and lower torus regions. It is based on a slide and trolley system. To achieve high position accuracy and repetitive accuracy, size and weight of the EEPU were kept as small and low as reasonably possible fabricating the EEPU as compact as possible and using for the large components an Al-alloy (AlZn4,5Mg1(F34)) welded structure. The EEPU was calculated to withstand the maximum peak loads in vertical direction and fully extended. Peak loads may be caused, for instance by bumps during taking over a divertor plate. The main technical data are given in Tab. 3-3.

Parameter	Value
Length x width x height (mm)	1499 x 974x 2758
Total stroke (mm)	±5075
Maximum speed under load - combined motion of all slides plus trolley (m/sec)	0.1
Maximum acceleration under load - combined motion of all slides plus trolley (m/sec <sup>2</sup> )	0.1
Positioning accuracy - not taken into account the deflection of the EEPU (mm)	±2
Number of slides	2
Number of trolleys	1
Number / size of planetary roller spindles - diameter x lead (mm)	5 / 39 x 5
Number / transmission ratio of bevel gears	5 / 3:1
Number of motors with fail-safe brake	6

**Tab. 3-3: Technical Data of the End-Effector Positioning Unit**

The EEPU support frame forms the mechanical connection between the ABT link B4 and the EEPU. The first slide is connected via a carrier with the support frame and simultaneously via a second carrier with the second slide which again is connected with a third carrier, the trolley. The carriers are guided by roller pads. The guiding rails are fixed at the support frame and the slides, respectively. The cables for the EEPU, the end-effectors and the viewing system are distributed into two looms of cables and are then routed in two cable ducts arranged at both sides of the EEPU.

The carriers are actuated by drive units which are composed of AC-servo motors with fail-safe brakes, a bevel gear and a planetary roller spindle. The motors arranged at one slide are coupled to give redundancy for the drives. The drive unit at the support frame is equipped with two motors acting on the bevel gear. For the safety reasons the planetary roller spindles are loaded in tension only.

The positioning control components are similar to those of the ABT and also the hierarchy of safety philosophy is the same.

At the present two types of end-effectors have been manufactured and used to demonstrate typical remote maintenance procedures:

- the manipulator handling unit (MHU) and
- a device (heavy load fork) to grasp loads up to 1 ton.

These devices are described in chapters 8 and 9.

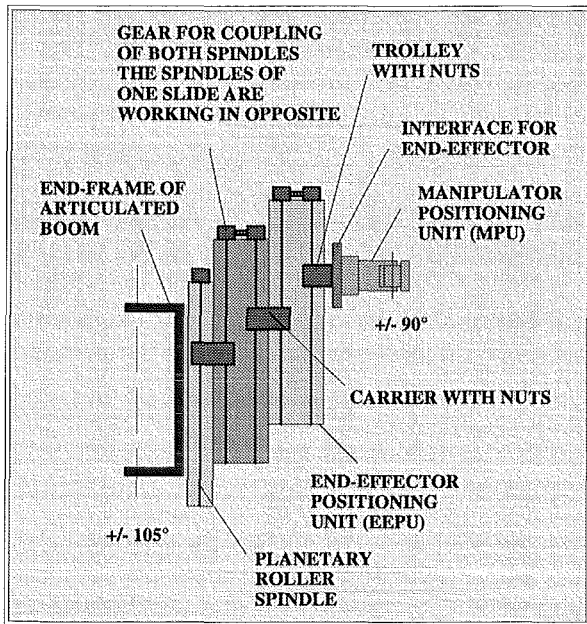


**Fig. 3-4: EEPU schema**

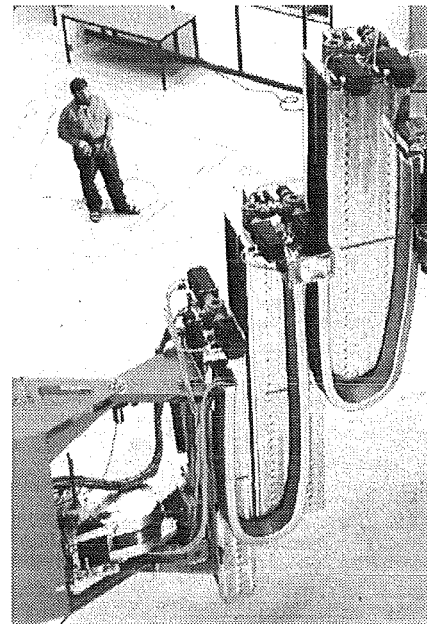


**Fig. 3-5: EEPU with MHU**

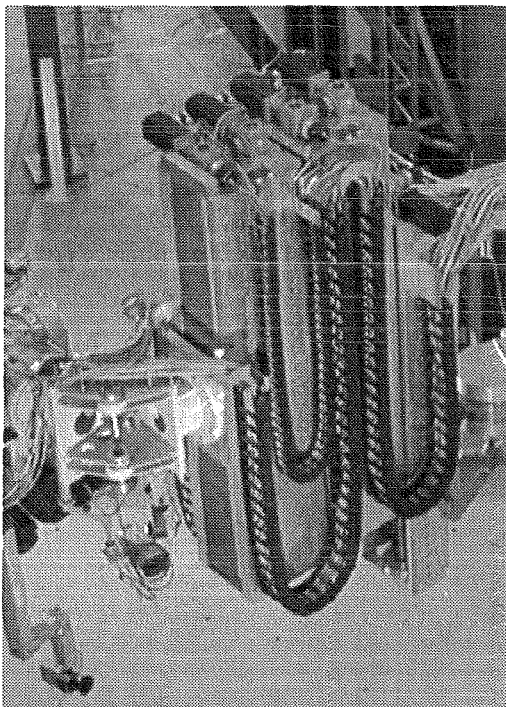


**Fig. 3-6: EEPU folded**

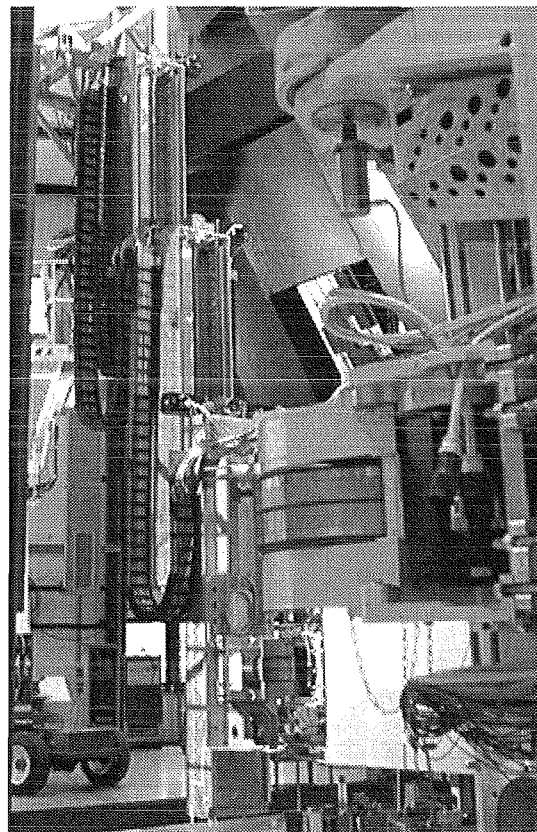


**Fig. 3-7: EEPU extended**

### 3.3 REFERENCES

OGS92 Ognibene, I., Sanguinetti, G.P.: unpublished report, July 1992

RIE93 Rieke, M.: unpublished report, January 1993

# Table of Content

<b>4 STRESS ANALYSIS AND VERIFICATION.....</b>	<b>4-3</b>
<b>4.1 DESCRIBING THE PROBLEMS .....</b>	<b>4-3</b>
<b>4.2 DESIGNING THE CROSS SECTIONS OF THE LINKS .....</b>	<b>4-3</b>
4.2.1 Determination of the Cross Section with Smallest Bending Flexibility under the Condition of a Given Surface.....	4-3
4.2.2 Determination of the Cross Section with Smallest Torsional Flexibility under the Condition of a Given Surface .....	4-5
4.2.3 Determination of the Cross Section Combining Relatively Small Bending and Torsional Flexibility with the Cross-Sectional Area Kept Constant.....	4-7
<b>4.3 MATERIAL SELECTION.....</b>	<b>4-8</b>
<b>4.4 DESIGN OF THE JOINTS AND SPECIFIC PROBLEMS OF LEADING THE JOINT FORCES INTO THE LINKS.....</b>	<b>4-9</b>
4.4.1 Loading of the Front Area of the Links .....	4-10
4.4.2 Loading of the Joint Plates .....	4-12
4.4.3 Connection of the Joint Plates and the Links .....	4-12
<b>4.5 DETAILED COMPUTATIONS USING FINITE ELEMENT CODES AND DETERMINATION OF THE WALL THICKNESS.....</b>	<b>4-13</b>
4.5.1 Building up a Finite Element Model.....	4-13
4.5.2 Calculation of the Tip's Deflection Due to the Payload with Different Configurations of the Links.....	4-15
4.5.3 Computation of the Stresses Caused by Dead Weight and Payload under Unfavourable Configurations of the Links .....	4-16
4.5.4 Buckling Analysis.....	4-16
<b>4.6 COMPARISON OF ACTUALLY OCCURING AND COMPUTED DEFORMATIONS .....</b>	<b>4-17</b>
<b>4.7 CONCLUSIONS OF THE STRESS ANALYSIS .....</b>	<b>4-18</b>
<b>4.8 REFERENCES .....</b>	<b>4-18</b>

## List of Figures

FIG. 4-1: ARBITRARY CROSS SECTION OF A BEAM .....	4-4
FIG. 4-2: LINK CROSS SECTION WITH MINIMUM BENDING FLEXIBILITY .....	4-4
FIG. 4-3: LINK CROSS SECTION WITH LATTICE STRUCTURE, SUITABLE AT BENDING STRESSES	4-5
FIG. 4-4: TORSIONAL FLEXIBILITY OF A HOLLOW STRUCTURE .....	4-6
FIG. 4-5: LINK CROSS SECTION WITH MINIMUM TORSIONAL FLEXIBILITY .....	4-6
FIG. 4-6: DESIGN OF THE LINK JOINTS .....	4-6
FIG. 4-7: TRANSMITTING THE TORSIONAL MOMENT INTO A LINK .....	4-11
FIG. 4-8: FORCES ACTING ON THE LINK HINGES .....	4-12
FIG. 4-9: CONNECTION OF THE JOINT PLATE .....	4-13
FIG. 4-10: FINITE ELEMENT MODEL FOR THE LINKS B1, B2, B3 .....	4-14
FIG. 4-11 : BOOM CONFIGURATION FOR STRESS ANALYSIS .....	4-14
FIG. 4-12: BUCKLING ANALYSIS.....	4-16

## List of Tables

TAB. 4-1: WALL THICKNESS OF LINKS B1, B2, B3 AND THEIR JOINT PLATES 1 TO 6 .....	4-15
TAB. 4-2: COMPUTED DEFORMATION IN DEPENDENCE ON THE WALL THICKNESS .....	4-15
TAB. 4-3: COMPARISON OF THE MEASUREMENT AND CALCULATION.....	4-17

## 4 STRESS ANALYSIS AND VERIFICATION

### 4.1 DESCRIBING THE PROBLEMS

The stress analysis of the ABT [KWHS89] was performed based on the requirement to handle at the boom tip payloads up to 3900 kg without any support inside of the vacuum vessel. In order to allow operating the boom with extremely high accuracy the deformation of the boom caused by its dead weight and the payload should have been kept to a minimum. Therefore, the two requirements mentioned above had the highest priority. Furthermore, considering high speed operation (high acceleration and lag of each link), a small dead weight was desirable. But as will be shown the two requirements, small tip deflection and small dead weight, exclude each other. Based on the port dimensions and the required reach of the boom as listed in Tab. 1-3 and with respect to maintain a particular distance and to avoid horizontal collisions, the number and dimensions of the links were determined as shown in Tab. 3-1. As Fig. 3-1. shows EDITH has one front link B4 and three intermediate swivelling links B1 to B3. On the other hand the fixing link C1 is cantilevered attached to the support structure as it will have been accordingly installed to the transport carrier of the later operational in-vessel handling unit shown in Fig. 1-1.

In former designs smaller ports and a working space including the whole torus were assumed. These assumptions contributed to an unacceptable high boom flexibility.

The necessary considerations and calculations for the new design of EDITH are scheduled in the chapters 4.2 to 4.5. Load experiments are discussed in the chapter 4.6. Especially the actually occurring deformations are compared to those obtained by calculations. This way one can see up to which degree the mechanical behaviour of complicated structures may be predicted by concurrent computational methods.

### 4.2 DESIGNING THE CROSS SECTIONS OF THE LINKS

The cross sections of the links should be determined in a way that the boom's tip deflects as little as possible because of the boom's dead weight. Depending on the configuration of the boom the links are loaded with bending and torsional moments. That's why one is looking for cross sections with lowest possible bending and torsional flexibility. For this selection the interesting cross sections should be comparable in the remaining important qualities. Here the dead weight is an important issue. It is proportional to the cross sectional area (the part of the link's cross section consisting of the walls) and therefore all the cross sections under consideration should have the same cross sectional areas. Furthermore, in the context of stiffness equal distributions of stress (no peaks!) are asked for.

#### 4.2.1 Determination of the Cross Section with Smallest Bending Flexibility under the Condition of a Given Surface

Bending flexibility is proportional to the curvature  $d^2y/dx^2$ . This is approximately derived by the beam bending equation:

$$d^2y/dx^2 = M_b/(E \cdot I_y) \quad (1)$$

Fig. 4-1 shows the bending moment  $M_b$ , Young's modulus  $E$  of the employed material and the moment of inertia  $I_y$ .

$$I_{\eta} = \int \eta^2 dF \quad (2)$$

The determination of the cross section with lowest bending flexibility, e.g. minimum curvature  $d^2y/dx^2$ , under a given cross sectional area of the walls results in the determination of the maximum moment of inertia  $I_{\eta}$ . It can be easily shown that this leads to the cross section depicted in Fig. 4-2. It mainly consists of an upper and a lower chord with a maximum distance, e.g. a maximum height of the cross section. That is why the highest possible value of 2.0 m should be realised. In this case the moment of inertia  $I_{\eta}$  is approximately calculated by

$$I_{\eta} = \frac{1}{2} * a^2 * b * s \quad (3)$$

The width of the cross section is arbitrary because with a constant cross-sectional surface assumed .

$$F = 2 * b * s \quad (4)$$

there is no influence on the moment of inertia. With a pure bending load  $M_b > 0$  in the upper chord there is only equally distributed tensile stress and in the lower chord one only find equally distributed compressive stress. Theoretically the connecting plates between the two chords shown in Fig. 4-2 are not necessary. So their influence is not taken into account. However, if there are also shear forces the connecting plates have to transmit shear stress. Usually this shear stress is so small that there may be break-throughs in these plates. The shear stress acting vertically leads to tensile and compressive stresses in directions inclined at an angle of  $45^\circ$ . So the break-throughs should be arranged in a way that the remaining struts have a sloping position of these  $45^\circ$  (see Fig. 4-3). Thus the shear stress loading leads to cross sections with side walls well known from lattice structures.

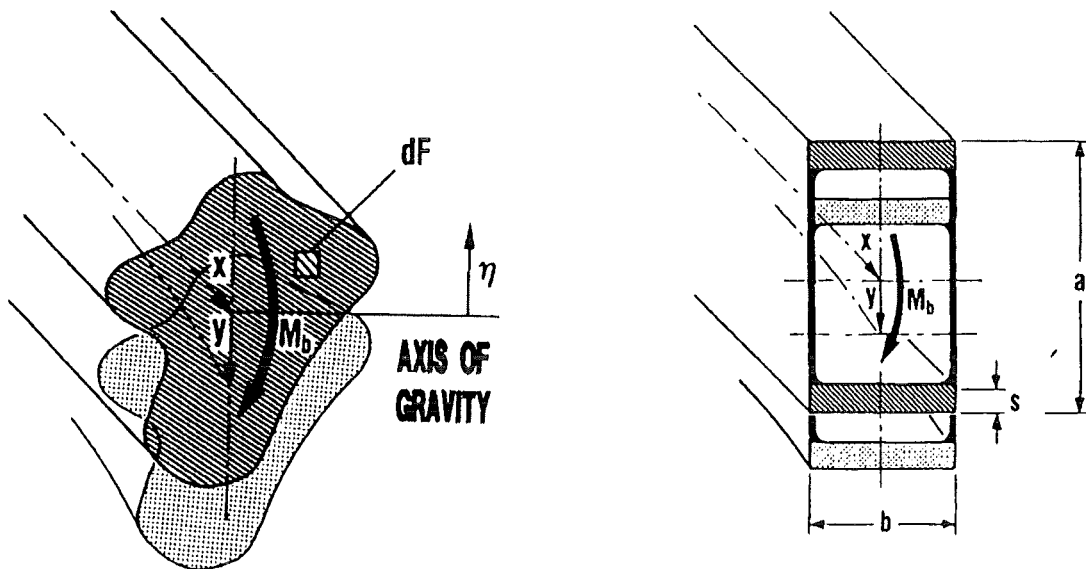


**Fig. 4-1: Arbitrary Cross Section of a Beam**    **Fig. 4-2: Link Cross Section with Minimum Bending Flexibility**

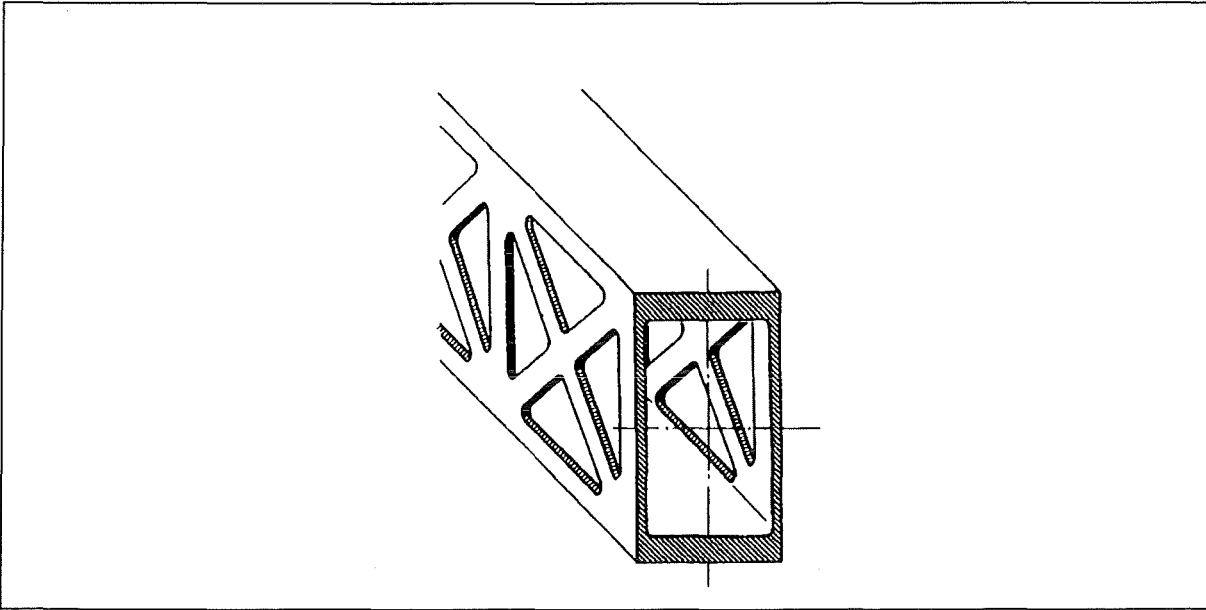


**Fig. 4-3: Link Cross Section with Lattice Structure, Suitable at Bending Stresses**

#### **4.2.2 Determination of the Cross Section with Smallest Torsional Flexibility under the Condition of a Given Surface**

On condition that the cross-sectional area is kept constant hollow sections have relatively small torsional flexibility. This may be illustrated by the torsion of a rolled sheet of paper according to Fig. 4-4. As long as the overlapping parts may slip in axial direction the torsional flexibility is rather high. If the overlapping parts are agglutinated a closed hollow section is generated and the torsional flexibility is reduced distinctively.

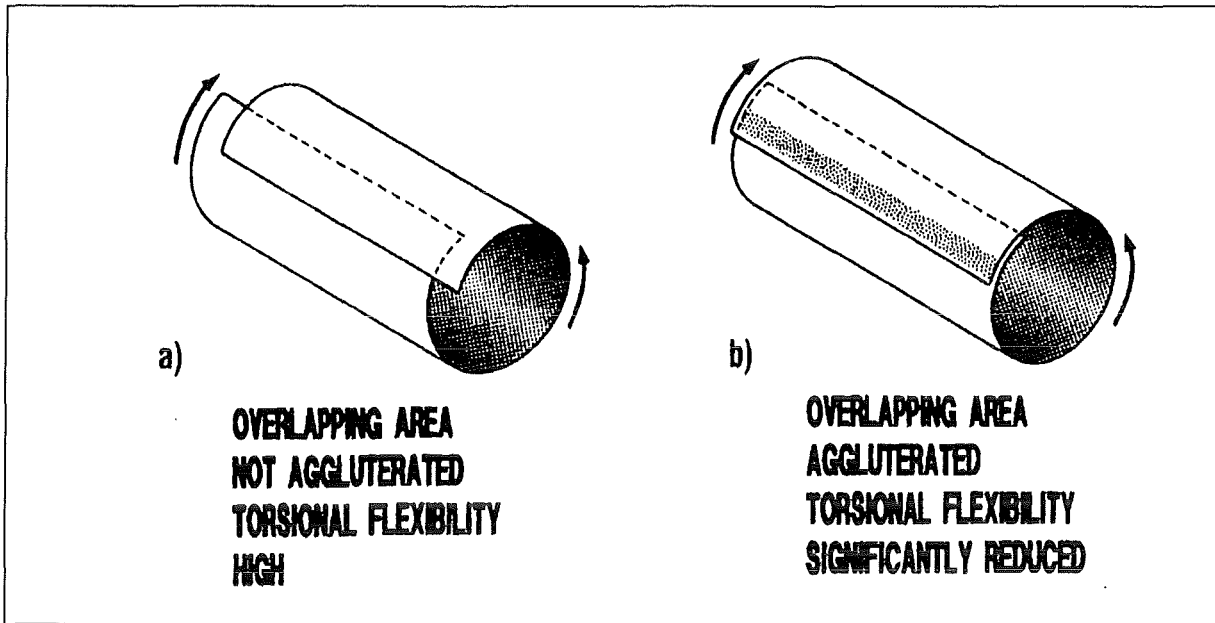


**Fig. 4-4: Torsional Flexibility of a Hollow Structure**

The torsional flexibility of a hollow structure is discussed on hand of rolled sheet of paper: a) If the overlapping area is not agglutinated the torsional flexibility is high. b) At agglutinated overlapping area the torsional flexibility is significantly reduced.

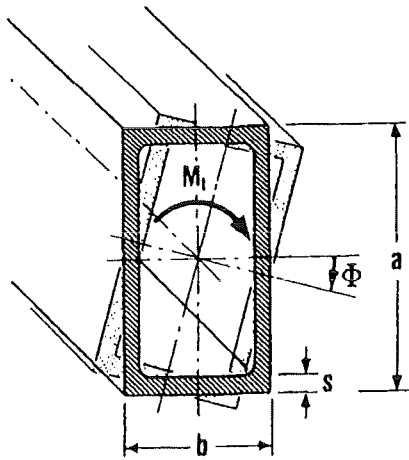


**Fig. 4-5: Link Cross Section with Minimum Torsional Flexibility**

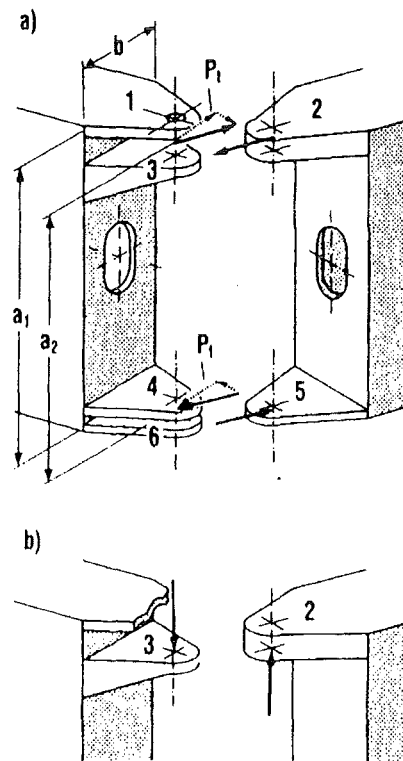


**Fig. 4-6: Design of the Link Joints**

Horizontal forces will be transmitted by all joint hinges, vertical forces only via the joint plates 2 and 3.

Shear stress in thin walls are inversely proportional to the wall's thickness, e.g. the product of shear stress and wall's thickness is constant at every circumferential location. This leads to the cross section depicted in Fig. 4-3.

However, the question remains whether the cross section with a maximum possible height of 2.0 m and width of 0.6 m also leads to a minimum torsional flexibility among all the other cross sections with the same cross-sectional area. According to Bredt's equation [SZAB60] the torsional flexibility (torsion angle per length of the link) is approximated by:

$$\Phi = M_t/G * (a + b) / (2 a^2 b^2 s) \quad (5)$$

where  $M_t$  is the torsional moment and  $G$  the modulus of torsional shear of the applied material. The meaning of the remaining quantities is explained by Fig. 4-3. The cross-sectional area becomes:

$$F = 2(a + b)s \quad (6)$$

With a small increase of the cross-sectional height  $\Delta a$  and a small change in the wall's thickness  $\Delta s$  a small change in torsional flexibility is expected:

$$\Phi + \Delta\Phi = M_t/G * (a + \Delta a + b) / (2(a + \Delta a)^2 b^2 (s + \Delta s)) \quad (7)$$

The cross-sectional area is assumed to be constant:

$$2(a + b) s = 2(a + \Delta a + b)(s + \Delta s) \quad (8)$$

Neglecting the products of small values, equation (8.) gives:

$$\Delta s/s = - \Delta a/(a + b) \quad (9)$$

and inserting this into equation (7):

$$\Delta\Phi/\Phi = - 2 * (b/(a + b)) * \Delta a/a \quad (10)$$

A similar relation may be derived for a change in the width of the cross section  $\Delta b$ .

Equation (10) indicates that keeping the cross-sectional area constant each rise in the cross-sectional height  $\Delta a$  or width  $\Delta b$  reduces the torsional flexibility.

If the height of the cross section is essentially higher than the width a further raise of the height reduces the torsional flexibility only very little. In the case of a quadratic cross section the torsional flexibility increases to the same ratio as the cross-sectional height. Finally assuming a cross section with an essentially smaller height than width a rise in the height results in a double reduction of the torsional flexibility.

#### 4.2.3 Determination of the Cross Section Combining Relatively Small Bending and Torsional Flexibility with the Cross-Sectional Area Kept Constant

The cross sections determined so far optimise only the bending or the torsional flexibility. But in reality cross sections are needed which comply with both requirements. The investigations above suppose that the cross section found last with constant wall's thickness and minimum torsional flexibility, appears to be suitable here. This is supported by the results of subsequently conducted FEM computations which exhibit the crucial influence of the torsional flexibility on the deflections of the boom's tip.

It follows that frame work side walls are not taken into consideration any longer. They would not be suitable to deal with the considerable shear stress caused by torsion. But still great importance is attached to exhausting the full possible cross-sectional height. This is not only meant to minimise the bending flexibility but also to minimise the considerable joint forces.

On the other hand constructive aspects have to be considered, too. That means that the design of the links B3, B2, B1 and C1 is very easy if one increases their heights -in the given order- to the measure of the upper and lower joint hinges. So the heights of the links B3, B2, B1 and C1 have been determined to 1825 mm, 1871 mm, 1930 mm and 2000 mm.

Optimal grading of the wall's thickness starting with rather thin walls for the front link B3 and ending with a rather thick wall for the fixing link C1 is not investigated here. In principal this could be done using the analogy to the preceding procedure. However, some important features cannot be taken into account, as there are manufactural problems of buckling due to thin walls or problems concerning the junction with the joints. Therefore, the grading of the wall's thickness were determined empirically.

On the other hand a determination of an absolute value for a wall's thickness is not possible according to the above considerations. For example increasing the wall's thickness not only reduces the flexibility but also the dead weight. Therefore, at a first approach the deflection of the tip does not change.

### 4.3 MATERIAL SELECTION

Again the decisive criterion is the deflection of the tip caused by the dead weight.

The starting point is again equation (1) describing the bending flexibility. Taking into account that the bending moment  $M_b$  is proportional to the density  $\rho$  and the wall's thickness and, that according to equation (3) the moment of inertia  $I_n$  is proportional only to the wall's thickness, the wall's thickness is cancelled out and it turns out:

$$d^2y/dx^2 \sim \rho/E \quad (11)$$

Another starting point is equation (5) describing the torsional flexibility. Noticing that the torsional moment  $M_t$  is proportional to the density  $\rho$  and the wall's thickness, too, the wall's thickness is cancelled out again and it remains:

$$\Phi \sim \rho/G \quad (12)$$

With basic relations the modulus of shear  $G$  may be expressed by Young's modulus  $E$  and Poison's ratio  $\nu$ ,  $G=E/2(1+\nu)$ . For the materials in discussion  $\nu$  is about 0.3 and so it follows:

$$\Phi \sim \rho/E \quad (13)$$

It does not matter if the deflection under dead weight is due to the bending flexibility (curvature  $d^2y/dx^2$ ) or whether it is due to the torsional flexibility (torsional angle  $\Phi$ ); in both cases the minimisation of the deflection requires the selection of the material with the lowest ratio  $\rho/E$ .

For the most common or available materials this ratio  $\rho/E$  does not differ very much, for instance:

Steel:

$$\rho/E = (7.8 * 10^3 \text{ kg/m}^3)/(2.1 * 10^5 \text{ N/mm}^2) = 3.7 * 10^{-8} \text{ kg/Nm}$$

Aluminium:

$$\rho/E = (2.7 * 10^3 \text{ kg/m}^3)/(0.675 * 10^5 \text{ N/mm}^2) = 4.0 * 10^{-8} \text{ kg/Nm}$$

Titanium:

$$\rho/E = (4.54 * 10^3 \text{ kg/m}^3)/(1.05 * 10^5 \text{ N/mm}^2) = 4.32 * 10^{-8} \text{ kg/Nm}$$

Steels appears to be best qualified. Furthermore among these materials most experience has been gained with steel. But if there were some important reasons to use aluminium or titanium these materials would be acceptable in the context of the tip's deflection under dead weight, too.

Actually a second similar criterion may be derived from minimising the dead weight. If  $\sigma_{zul}$  stands for the maximum acceptable stress this criterion requires that the material with minimum  $\rho/\sigma_{zul}$  is to be selected and that  $\sigma_{zul}$  is exhausted.

Taking into account the following data

Steel:

$$\rho/\sigma_{zul} = (7.8 * 10^3 \text{ kg/m}^3)/(200 \text{ N/mm}^2) = 39 * 10^{-6} \text{ kg/Nm}$$

Aluminium:

$$\rho/\sigma_{zul} = (2.7 * 10^3 \text{ kg/m}^3)/(150 \text{ N/mm}^2) = 18 * 10^{-6} \text{ kg/Nm}$$

Titanium:

$$\rho/\sigma_{zul} = (4.54 * 10^3 \text{ kg/m}^3)/(400 \text{ N/mm}^2) = 11.35 * 10^{-6} \text{ kg/Nm}$$

titanium should be given preference. Now the wall's thicknesses which have not been determined yet may be chosen. But in doing so the tip's deflection under dead weight has to be accepted without any possibility to reduce it. Taking into consideration the requirements presented in chapter 4.1 rather little deflection under dead weight and payload is more important than minimising the dead weight itself. Therefore, it was decided to choose steel as structural material. This way the wall's thickness will be determined later to make sure that the deflection of the tip under payload is sufficiently small. The idea of minimising the tip's deflection is abandoned in order to allow a compromise solution considering the demand for a small dead weight. It shows that for most cases the occurring stresses lie far below acceptable limits. Only a few peak values occurring in complicated structural parts should be paid attention to.

#### **4.4 DESIGN OF THE JOINTS AND SPECIFIC PROBLEMS OF LEADING THE JOINT FORCES INTO THE LINKS**

The design of the joint and the joint plates 1 to 6 is scheduled in Fig. 4-6 (a). The distance from the front surfaces of the links to the joint's axis is determined by the demand for free

space for the driving units. To avoid extreme bending forces the constructively more complicated V-shaped joints have been selected. The joint's forces acting in the horizontal plane and especially the force component  $P_t$  are also shown in Fig. 4-6.

The vertical forces are transmitted only by the plates 2 and 3. That is shown in Fig. 4-6 (b).

#### 4.4.1 Loading of the Front Area of the Links

The joint forces  $P_t$  lead to the torsional moment  $M_t$  into the link:

$$P_t = M_t / a_2 \quad (14)$$

This yields a shear stress  $\tau_1$  in the upper and lower chord of the link (Fig. 4-7 on the left):

$$\tau_1 = P_t / (s * b) * a_2 / a_1 \quad (15)$$

The factor  $a_2/a_1$  accounts for the somewhat different lever arms of  $P_t$  and  $\tau_1$ .

The shear stress  $\tau_2$  loading the torsional moment into the link is not only acting in the upper and lower chord but is distributed equally along the link's circumference (steady shear flux; middle of Fig. 4-7. Additionally the distribution of the shear stress  $\tau_3$  has to be superposed (on the right of Fig. 4-7). Because of its definition no reaction forces may be generated and the horizontal and vertical components of the associated distribution of shear stress have to be equal. From Fig. 4-6 follows:

$$\tau_1 = \tau_2 + \tau_3 \text{ (upper and lower chords)} \quad (16)$$

$$\tau_2 = \tau_3 \text{ (side walls)}$$

This leads to

$$\tau_2 = \tau_3 = \tau_1 / 2 \quad (17)$$

The distribution of shear stress  $\tau_2$  transmitting the torsional moment  $M_t$  in the link may be obtained directly from  $M_t$ . It may be confirmed that this result complies with the results of equations (14) - (17).

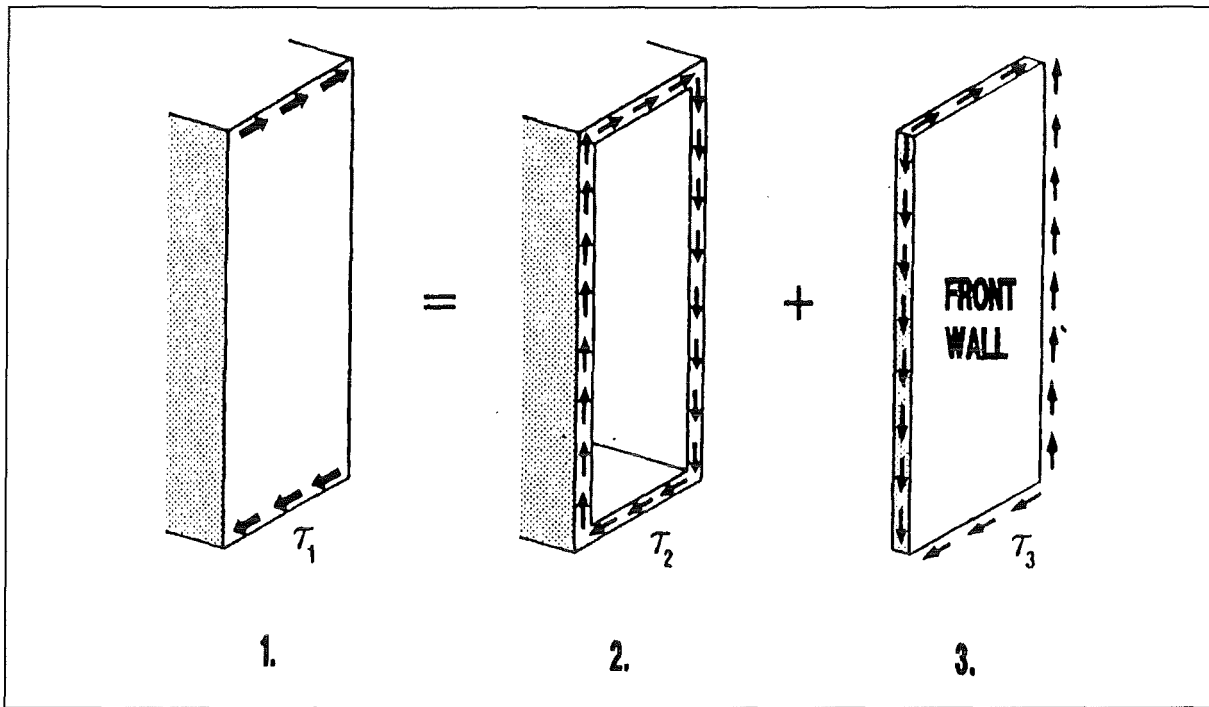


**Fig. 4-7: Transmitting the Torsional Moment into a Link**

The Resulting Shear Stress Requires a Sufficiently Dimensioned Front Wall. Left: Shear stress transmitted from the link hinges. Middle: Shear stress transmitting the torsional moment in the link. Right: Shear stress loading the link cross section by shear.

Practically a thin walled hollow section, built up by the upper and lower chord and the side walls, may not bear the shear stress component  $\tau_3$ . Therefore, the links must have sufficiently dimensioned front walls. The necessity of such walls can also be demonstrated by another consideration. According to Fig. 4-8 the forces acting at the joint plates not only may be interpreted as force couples  $P_1/P_2$  and  $P_3/P_4$ , which distort the link along its longitudinal axis (torsional moment  $M_t$ ) but they may also be understood as force couples  $P_1/P_3$  and  $P_2/P_4$  which distort the link along its vertical axis. A structure which is able to deal with such loadings is in fact a hollow section composed of the two side walls and the front walls. Each of these walls should have similar thicknesses.

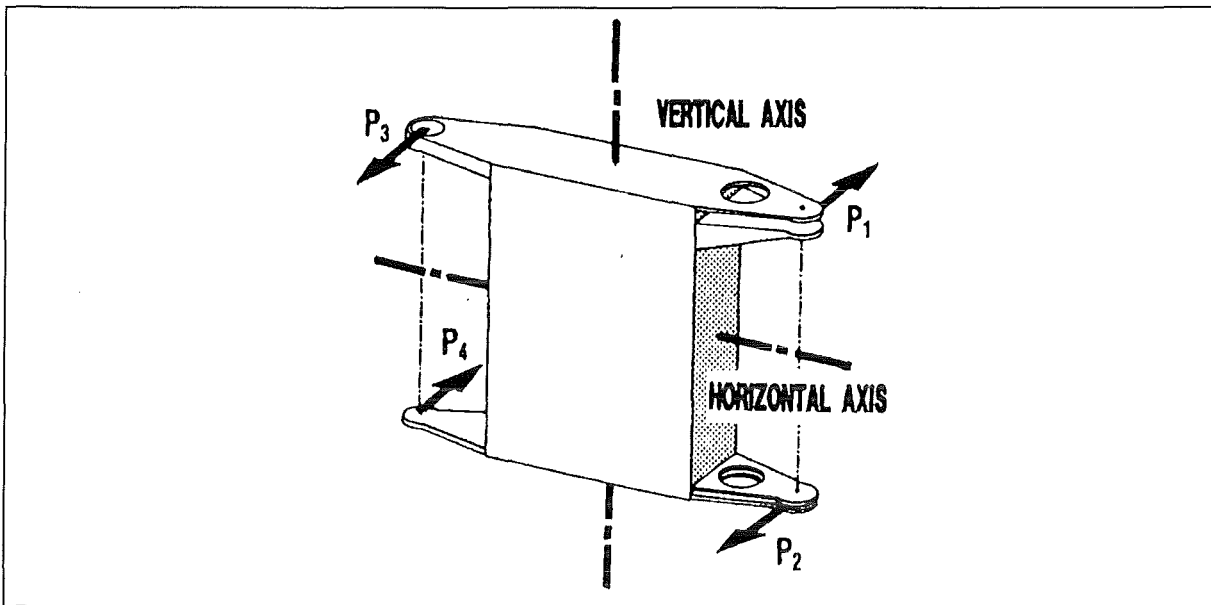


**Fig. 4-8: Forces Acting on the Link Hinges**

Forces Acting on the Link Hinges Distort the Link also along its Vertical Axis. This is the Second Reason for the Necessity of Sufficiently Dimensioned Front Walls.

#### 4.4.2 Loading of the Joint Plates

Particular regard has to be given to the vertical forces acting at the joint plates 2 and 3 (Fig. 4-6 (b)). To bear the resulting bending stresses, respectively to limit the bending deformation to an acceptable degree, thicker joint plates with a sufficient section modulus respectively moment of inertia are necessary. To avoid a strong increase of the dead weight these joint plates are actually designed as box-frame constructions. For the joint plate 2 follows that the upper and lower plate are rather thick. For the joint plate 3 a variable thickness and thus a better adaptation to the demands of mechanical resistance is possible. This leads to slightly thinner walls.

#### 4.4.3 Connection of the Joint Plates and the Links

Some particular constructive measures have to be taken to make this connection bear strong forces. The rather weak front wall of the simple design (Fig. 4-9 (a)) can hardly bear the tensile forces of the joint plates. Only the small surfaces contacting the side walls have to transmit the tensile forces (lumped contact). Therefore, at these spots there is an immense concentration of stress. Even moderate tensile forces (welds) would make the structure collapse.

The improved design (Fig. 4-9 (b)) produces an extended contact area with the force transmitting side walls by prolonging the joint plate into the interior of the link (line shaped contact area). Thus hot spots of stress can almost be avoided. These prolongations of the joint plates are designed for the connection of the joints to the links.

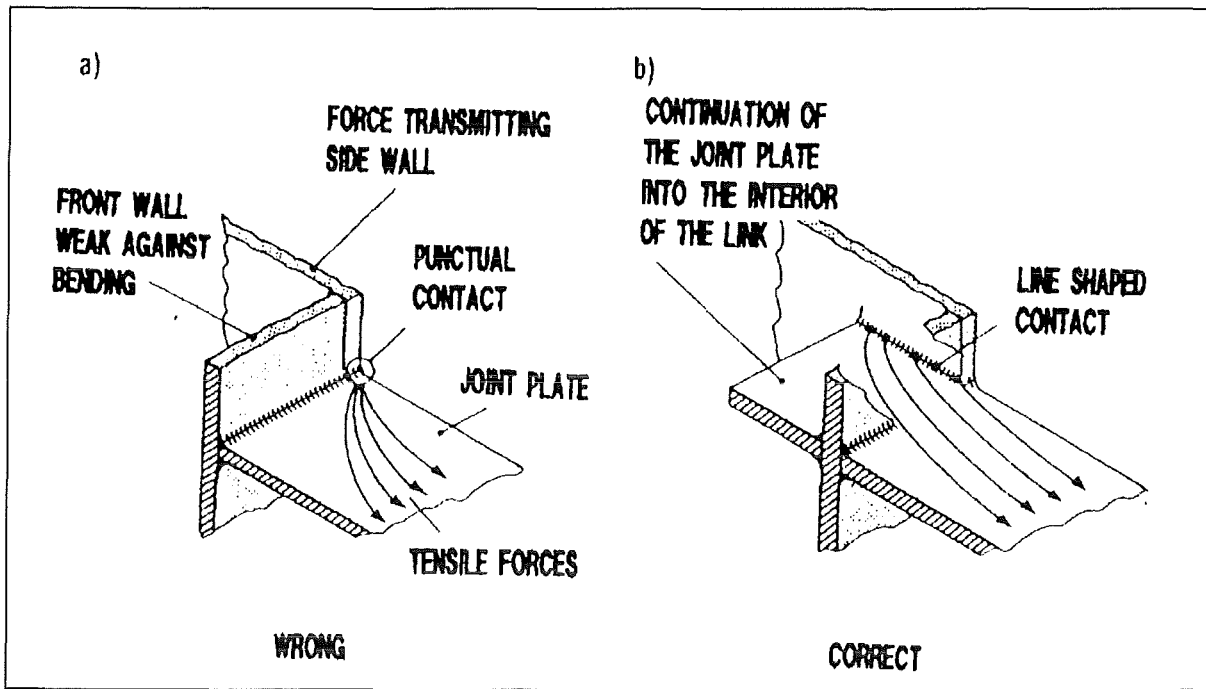


**Fig. 4-9: Connection of the Joint Plate**

Connection of the Joint Plate with the Force Bearing Side Wall of the Link. By Continuing of the Plate into the Interior of the Link the Unfavourable Stress Concentrations are Avoided.

## 4.5 DETAILED COMPUTATIONS USING FINITE ELEMENT CODES AND DETERMINATION OF THE WALL THICKNESS

### 4.5.1 Building up a Finite Element Model

For detailed analyses the finite element model shown in Fig. 4-10. has been applied. It consists of 785 elements (8 node elements). The joint plates 2 and 3 are modelled as hollow boxes. Furthermore it was assumed that the joint plates 1 and 3 as well as 4 and 6 are connected by rigid joint pins.

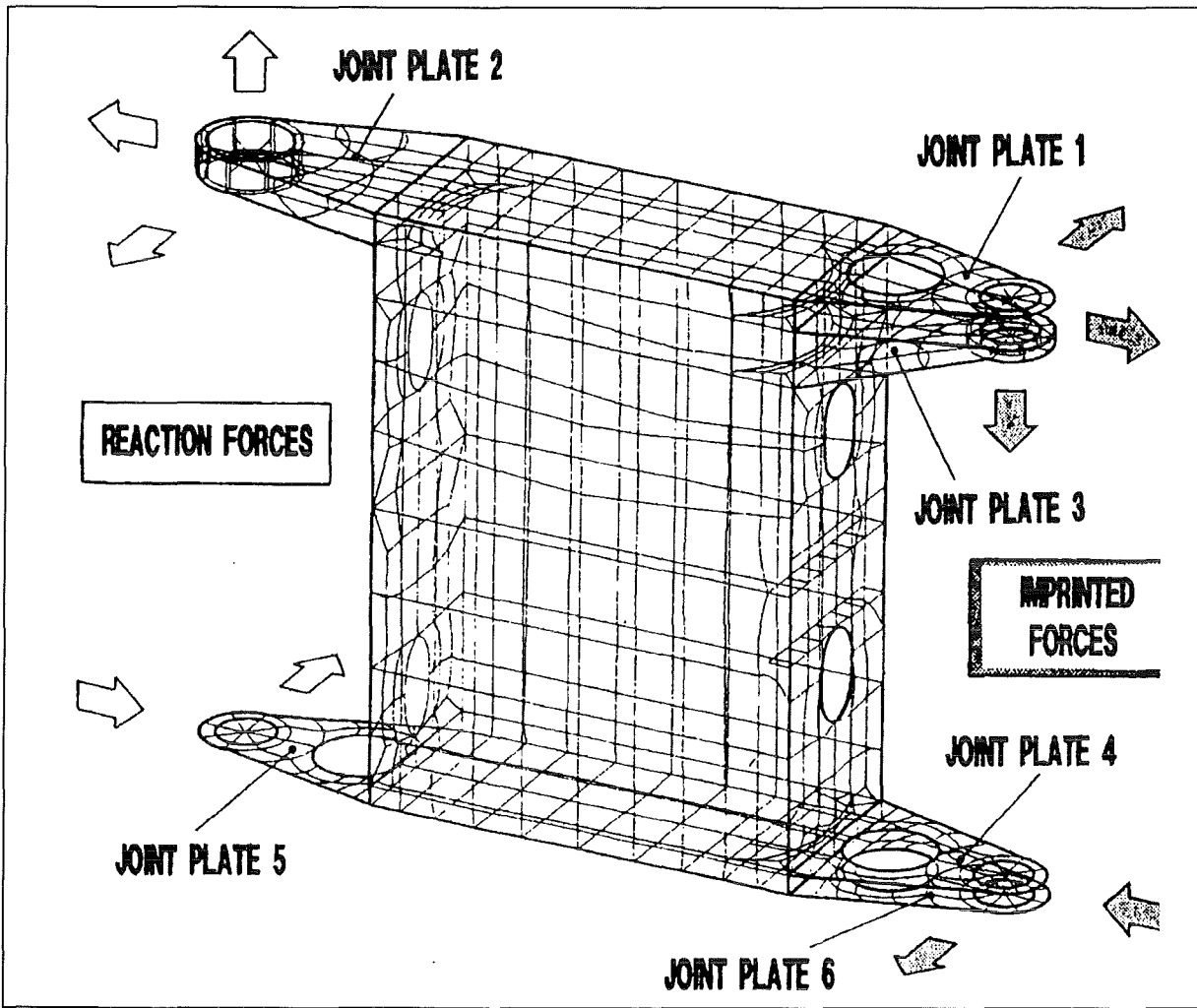


Fig. 4-10: Finite Element Model for the Links B1, B2, B3

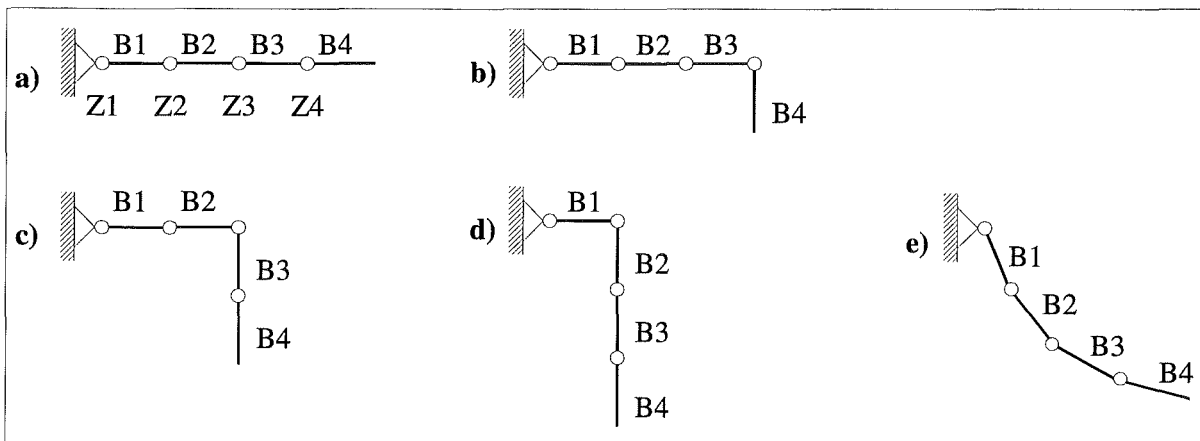


Fig. 4-11 : Boom Configuration for Stress Analysis

The wall's thicknesses for each case are listed in Tab. 4-1. It was assumed that due to constructive reasons the smallest wall's thickness should not be less than 5 mm.

The material behaviour was supposed to be linear elastic with a Young's modulus of  $E=2.1 \cdot 10^5 \text{ N/mm}^2$ . The front link B4 is not designed as a box but in a very simple way. Because of its clearly composed loading no finite element model was employed.

	B1	B2	B3
Links (upper and lower chord, side and front walls)	8 mm	6 mm	5 mm
Joint plate 1	15 mm	10 mm	10 mm
Joint plate 2 - horizontal walls	15 mm	15 mm	10 mm
Joint plate 2 - vertical walls	10 mm	10 mm	10 mm
Joint plate 3 - horizontal walls	8 mm	6 mm	5 mm
Joint plate 3 - vertical walls	8 mm	6 mm	5 mm
Joint plate 4	15 mm	10 mm	10 mm
Joint plate 5	25 mm	20 mm	15 mm
Joint plate 6	15 mm	10 mm	10 mm

**Tab. 4-1: Wall Thickness of Links B1, B2, B3 and their Joint Plates 1 to 6**

#### 4.5.2 Calculation of the Tip's Deflection Due to the Payload with Different Configurations of the Links

To limit the computational effort for each link and each unit force, respectively unit force couple, shown in Fig. 4-10, the corresponding unit deformation was calculated in a finite element analysis. Because the actual forces or force couples are easily determined in a simple calculation. Subsequently a weighted superpositioning of the unit deformations yields the deflection of the tip. Only five interesting configurations are given in Tab. 4-1. (reference configuration). It shows that the deflections of the wedged configurations are higher than the deflection of the straight configuration. In many cases the torsion contributes more to the deflection than the bending. Parallel to this, further analyses have been conducted which vary the wall's thicknesses of the links. The analysis with the smallest increase in the wall's thicknesses from B3 to B1 is of particular interest (variation 1). The resulting deflections are also given in Tab. 4-2. They are up to 17% higher than these of the first analysis. The reduction of the dead weight on the other hand is only about 2%. All in all a certain increase in the wall's thicknesses is useful.

ABT Configuration	Reference case	Variation 1
a)	12.3 mm	13.1 mm
b)	17.9 mm	19.3 mm
c)	32.2 mm	36.7 mm
d)	35.8 mm	42.1 mm
e)	28.2 mm	33.1 mm
	Links B3, B2, B1 have wall thickness of 5, 6, 8 mm	Links B3, B2, B1 have wall thickness of 5, 5, 6 mm

**Tab. 4-2: Computed Deformation in Dependence on the Wall Thickness**

### 4.5.3 Computation of the Stresses Caused by Dead Weight and Payload under Unfavourable Configurations of the Links

The membrane and bending stresses in the wall computed with the help of a finite element analysis (in particular the von-Mises stress and if necessary also the corresponding stress components) have been displayed in many isoline plots. In most cases the numerical values lie far below the allowable stresses. Nearly all over the link B3 only 20% of the material's bearing capacity is used. However, as mentioned above, a reduction of the wall's thickness below 5 mm is not practicable. In the two backward links B2 and B1 the materials's bearing capacity is used to an higher extent but not totally exhausted. Reducing the wall's thicknesses of these links leads to an undesired increase of the tip's deflection. Not acceptable stress peaks may be avoided by, for instance, the constructive measures discussed in chapter 4.4.

### 4.5.4 Buckling Analysis

Such kind of analysis have mainly been conducted for the huge side walls of the links, The critical buckling stress lies partly only 40% above the actual values. But this was accepted, because exceeding the buckling stress in plane shells does not lead to excessive deformations - contrary to cylindrical shells. This has been proved by analyses of not exactly plane side walls. The bulgy deformations are increased by dead weight and payload. For most unfavourable deformations (first eigenmode) according Fig. 4-12. the maximum deflection increases up to 40%. The shear stresses cause a diagonal orientation of the bulge. The negative bending stress in the lower part of the side walls which propagates the buckling moves the maximum of the bulge downward. An important result is that the reinforcing ribs are not necessary for the side walls. For a wall thickness below 5 mm these ribs would be needed.

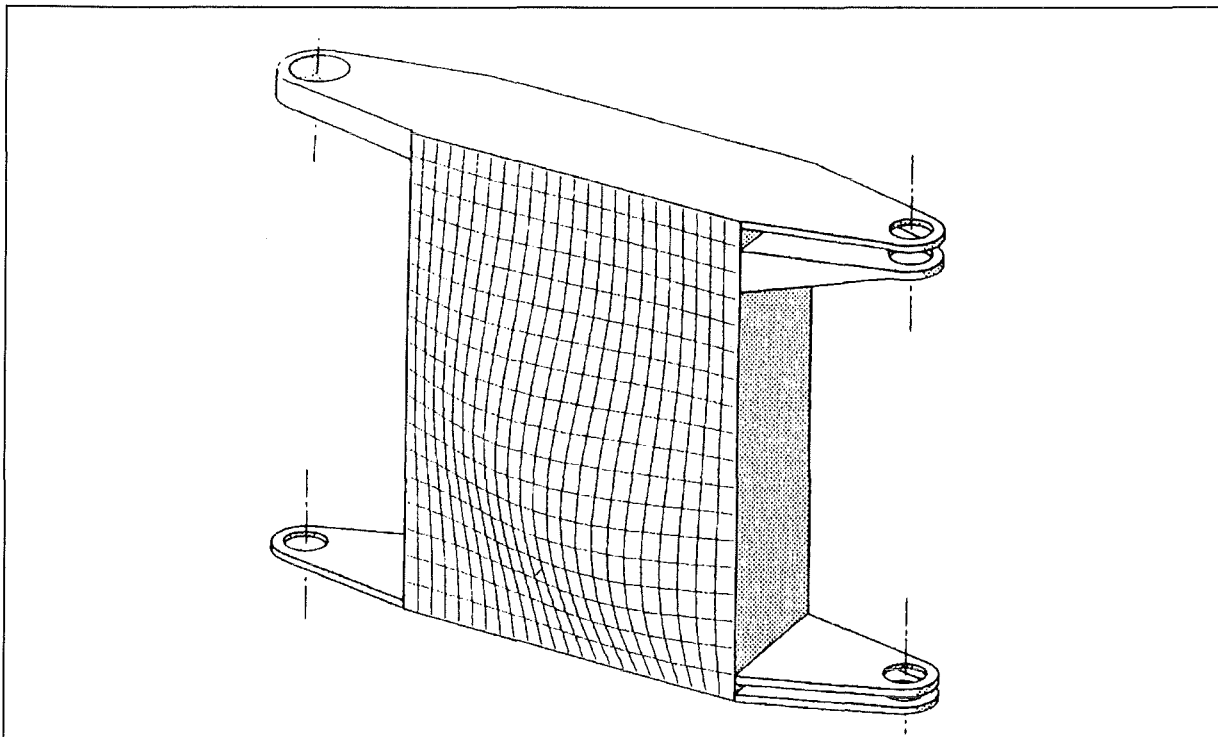


**Fig. 4-12: Buckling Analysis**

Under load the deformation of the side wall increases up to 40%.

#### 4.6 COMPARISON OF ACTUALLY OCCURRING AND COMPUTED DEFORMATIONS

After the assembly the deflections under payload and at the different boom's configurations have been measured at the boom's first joint (Z4 in Fig. 4-11). The results of this measurement are listed in Tab. 4-3, first row. For the last two configurations measurement was only possible up to the deflected link. In these cases the results for the deflection of the first joint could be calculated using the data of the straight configuration, because the wedged part of the boom is loaded like the corresponding part of the straight boom.

ABT-Configuration	Measured deflection at the front link	After subtraction of influences from attachment flexibility	After extrapolation onto the boom tip	Computed deflection of the boom tip
a)	19.1 mm	11.7 mm	15.9 mm	12.3 mm
b)	18.3 mm	13.0 mm	20.3 mm	17.9 mm
c)	26.1 mm	21.3 mm	34.3 mm	32.2 mm
d)	33.5 mm	26.1 mm	38.0 mm	35.8 mm

**Tab. 4-3: Comparison of the Measurement and Calculation**

It should be noticed that the fixing link is also displaced in axial direction and has a sloping position. Both effects have been measured and their influence on the deflection of the first joint has been determined (Tab. 4-3, second row). This influence has to be taken into account if one compares the results of measurement and the results of computation, which postulates an inflexible fixing point. Furthermore, it has to be considered that the results of measurement are related to the first joint. For the comparison with the results of the computations which relate to the boom's tip, the results of the measurement have to be extrapolated to the boom's tip, too (Tab. 4-3, third row). The comparison of these extrapolated data to the calculated deflections shows that the latter are generally smaller. These deviations are known and are probably caused by the following reasons: Finite element computations do not consider details of deformation occurring in domains smaller than a finite element, deformations and free spaces in particular components are neglected totally (hinge pins, roller bearings, etc.), non linear behaviour of the material with reduced Young's modulus under high stresses which may be a result of the superpositioning with high initial stresses. Considering all these effects, the yielded accuracy of the computations is satisfactory.

#### 4.7 CONCLUSIONS OF THE STRESS ANALYSIS

Minimum deflection of the boom's tip under dead weight and under payload has been the essential requirements for the design of EDITH. The dead weight of the boom itself should have been in an acceptable range.

These requirements made necessary a more profound discussion of the basic mechanic effects. Finite element computations have been conducted not before a course design has been chosen and the associated hot spots have been determined.

The result has been a filigree construction. This is directly indicated by the joint plates. But also the walls of the box-shaped links are rather thin. So careful buckling analyses have become necessary.

After assembly the calculated deflections have been compared to those of the corresponding experiments. As it is known the mechanical properties of the articulated boom are satisfactory.

#### 4.8 REFERENCES

- KWHS89 Krieg, R., Wehner, E., Hübener, J., Suppan, A.: Design Optimization of an Articulated Boom for NET In-Vessel Handling Unit. Trans. 10th Int. Conf. on Structural Mechanics in Reactor Technology, Vol. N, Anaheim, Cal. 1989, pp.91-96
- SZAB60 Szabo, I.: Höhere Technische Mechanik, Springer Verlag, Berlin, Göttingen, Heidelberg 1960, pp. 23 and 278

# Table of Content

<b>5 GUIDANCE AND CONTROL SYSTEM.....</b>	<b>5-3</b>
5.1 GUIDANCE AND CONTROL SYSTEM ARCHITECTURE .....	5-6
5.2 CONTROL ROOM.....	5-7
5.3 REMOTE HANDLING WORKSTATION.....	5-9
5.3.1 Synthetic/integrated viewing.....	5-12
5.3.2 Planning and programming.....	5-13
5.3.3 Multimedia handbook and documentation.....	5-13
5.3.4 Co-ordination of RH agents.....	5-14
5.4 PEXOS - WORKING WITH PROCEDURES .....	5-14
5.5 DOIF - WORKING WITH DEVICE FUNCTIONS .....	5-19
5.6 KISMET - MOVING DEVICES IN THEIR ENVIRONMENT .....	5-22
5.7 REFERENCES .....	5-27

## List of Figures

FIG. 5-1: MAN-MACHINE CO-OPERATION .....	5-6
FIG. 5-2: PRINCIPLE RH CONTROL SYSTEM ARCHITECTURE.....	5-7
FIG. 5-3: EDITH CONTROL SYSTEM ARCHITECTURE .....	5-7
FIG. 5-4: REMOTE HANDLING WORKSTATION .....	5-8
FIG. 5-5: SERVO-MANIPULATOR WORKING PLACE.....	5-8
FIG. 5-6: RHWS DATA BASES .....	5-11
<b>FIG. 5-7: SYSTEM ARCHITECTURE .....</b>	<b>5-11</b>
FIG. 5-8: PRINCIPLES OF SYNTHETIC VIEWING .....	5-11
FIG. 5-9: RHWS AS INTERACTIVE MULTIMEDIA HANDBOOK .....	5-11
FIG. 5-11: SIMPLE PEXOS PROCEDURE EXAMPLE.....	5-16
FIG. 5-13: NET WITH INDIVIDUAL TOKENS .....	5-16
<b>FIG. 5-10 : PEXOS MAIN SCREEN .....</b>	<b>5-17</b>
FIG. 5-12: PEXOS SCREEN FOR MANIPULATING OPERATOR (PEXOS-MSM) .....	5-18
FIG. 5-14: DOIF SCREEN .....	5-20
FIG. 5-15: DM MAIN WINDOW .....	5-21
FIG. 5-16 : DM/DOIF MONITOR .....	5-21
FIG. 5-17: KISMET FUNCTIONAL ARCHITECTURE AND RHWS FRONT END .....	5-23
FIG. 5-18: KISMET SCREEN.....	5-24
FIG. 5-19: KISMET DISPLAY WITH CAMERA VIEWING PYRAMID .....	5-25
FIG. 5-20: KISMET WITH VIDEO OVERLAY .....	5-26

## List of Tables

TAB. 5-1: RH GOALS AND RHWS FEATURES.....	5-5
TAB. 5-2: RHWS FUNCTION OVERVIEW .....	5-5



## 5 GUIDANCE AND CONTROL SYSTEM

Maintenance work in fusion plants has to be executed remotely without direct view onto the working site. Because of the high complexity the work has to be performed in a mixed mode of operation: manual work (e.g. with master-slave systems) will be intermixed with automated tasks to be supervised. To make the whole system operable and to give the operators the needed confidence in their judgement of the situation a problem suited control system architecture and a comprehensive operational support for the operators is needed. The architecture of the remote handling control system was developed following structural principles of the general fusion plant control system [BB189, BB289]. Operational support of the operators was investigated with the result of proposing a Remote Handling Workstation as the central high level support system of the operators [LEI84, LVA84, LNO84, LEI90, SUP93].

Remote handling and remote maintenance activities in a fusion plant are divided into areas in which the required equipment is working closely together to perform a special task. One example of an area is the in-vessel handling area. Each device in an area will have a special controller realising together with the mechanical system the required functions (e.g. transport, welding) and providing the function to the operator and/or to a high-level controller co-ordinating the co-operating devices. A very basic task in the EDITH project was to develop a controller for the EDITH articulated boom transporter providing task suited transport functions in the vessel of the NET/ITER machine and between the vessel and the outside. In addition, a controller for the viewing system required for the tile exchange task had to be developed.

Conventionally the device control systems have a hardware or software man-machine interface and no other control connection to the environment. This is sufficient for simple tasks. In a realistic maintenance environment the operator has to put into action a variable group of devices (e.g. Transporters, work units, tools, viewing system). Therefore, a basic requirement is to unify the man-machine interfaces and to **integrate the man-machine interfaces of the devices** for making the system controllable for the operator, to establish a device park control and co-ordination tool.

Maintenance work in fusion reactors must be performed fully remotely without direct view onto the working scene. A basic difficulty results from the spatial restrictions in camera positioning: normally, there are no overviews available what especially is true for in-vessel operations, and in general, it is difficult to locate the camera views. An important requirement therefore is to **enhance spatial viewing**.

But, enhancing the man-machine interface and spatial viewing is not enough in an environment where maintenance procedures (e.g. divertor plate or armour tile exchange) are complex and of long duration and where the procedures are repeated not very often (e.g. once a year). The maintenance procedures, therefore, conventionally, are documented in handbooks, telling the operators how to proceed. To reduce maintenance time a more **advanced operational support tool** is desirable as evaluated in [LEI90] and especially as experiences at JET have shown. To reduce costs, a high-level support, like the operational support, should be designed as a general purpose (generic) software tool applicable to all areas of remote handling. The realisation of such a tool is called **Remote Handling Workstation (RHWS)**. The RHWS has to provide an operational environment to control without direct

view in mixed-mode operation a group of remote handling devices to perform complex maintenance procedures fast, precise, and error free.

Maintenance activities are so complex and partly unplannable that the tasks can not be fully automated: a remote handling system will always be a semi-automated system where manual working sequences will alternate with automated subtasks. This calls for a carefully planned **man-machine co-operation** providing mutual help and mutual supervision.

Summarising, in the context of the over-all control system development for in-vessel handling the following subtasks had to be done:

- Development of a flexible architecture for controlling the devices of a remote handling area and support of the operators
- Development of a device controllers for the EDITH articulated boom transport system for fast, precise, and secure motion and the capabilities to be integrated in a control system architecture.
- Development of a remote handling workstation representing a general purpose (generic) support tool for the operator including working out and defining a modular workstation architecture integrating autonomous subsystems such that it can be configured for different applications.

In Tab. 5-1 the evaluated features of an operating support system are listed in relation to the general remote handling goals.

General Remote Handling Goals	RHWS Features to reach the Goals
minimise time for maintenance	<ul style="list-style-type: none"> <li>• automation of subtasks; problem oriented programming on three levels: procedure, function, motion</li> <li>• computer support for manual operation</li> <li>• facilitate close man-machine co-operation</li> <li>• provide mutual help and mutual supervision</li> </ul>
minimise time losses due to operator errors	<ul style="list-style-type: none"> <li>• enhanced viewing (synthetic viewing)</li> <li>• automation, semi-automation</li> <li>• training for operator</li> <li>• co-ordination of agent and devices</li> <li>• guidance for operator</li> <li>• comprehensive multimedial documentation</li> </ul>
safe operation	<ul style="list-style-type: none"> <li>• motion monitoring</li> <li>• procedure monitoring</li> <li>• function monitoring</li> <li>• simulation in planning and programming</li> </ul>
minimise time for introducing enhancements or special solutions to unexpected situations (extendibility, integration)	<ul style="list-style-type: none"> <li>• modular architecture</li> <li>• software implementation</li> <li>• standard development &amp; maintenance tools</li> <li>• thoroughly defined internal interfaces (hardware &amp; software)</li> </ul>

**Tab. 5-1: RH goals and RHWS features**

WORK PHASES	MODEL TYPES / LEVELS OF ABSTRACTION / VIEWS		
	PROCEDURAL <i>PEXOS</i>	FUNCTIONAL <i>DOIF</i>	SPATIAL <i>KISMET</i>
<b>PLANNING</b>	<ul style="list-style-type: none"> <li>• generation of action/state nets,</li> <li>• procedure simulation</li> </ul>	<ul style="list-style-type: none"> <li>• device function macro programming including graphical interfaces</li> <li>• device function simulation</li> </ul>	support of <ul style="list-style-type: none"> <li>• path generation</li> <li>• motion simulation</li> </ul>
<b>TRAINING</b>	<ul style="list-style-type: none"> <li>• graphical procedure representation</li> <li>• exploration of task structures</li> </ul>	<ul style="list-style-type: none"> <li>• virtual devices</li> <li>• exploration of equipment functions</li> </ul>	<ul style="list-style-type: none"> <li>• virtual working scene</li> <li>• exploration of spatial restrictions</li> </ul>
<b>EXECUTION</b>	<ul style="list-style-type: none"> <li>• state dependent advice &amp; guidance co-ordination</li> <li>• state dependant control support for KISMET and DOIF usage</li> </ul>	<ul style="list-style-type: none"> <li>• graphical device interfaces</li> <li>• device function macro</li> </ul>	<ul style="list-style-type: none"> <li>• integrated (synthetic) viewing</li> <li>• graphical device control (graphical masters)</li> </ul>
<b>MONITORING</b>	<ul style="list-style-type: none"> <li>• task execution</li> </ul>	<ul style="list-style-type: none"> <li>• function parameter</li> </ul>	<ul style="list-style-type: none"> <li>• collision avoidance</li> </ul>
<b>RECOVERY</b>	support of <ul style="list-style-type: none"> <li>• diagnosis</li> <li>• backtracking</li> <li>• alternatives</li> </ul>	support of <ul style="list-style-type: none"> <li>• correction or adaptation of parameter sets</li> </ul>	support of <ul style="list-style-type: none"> <li>• correction or adaptation of paths</li> <li>• backtracking</li> </ul>
<b>DOCUMENTATION</b>	<ul style="list-style-type: none"> <li>• action/state network with multimedia annotations (including DOIF and KISMET usage)</li> </ul>	<ul style="list-style-type: none"> <li>• parameter sets</li> <li>• device (function) macros</li> </ul>	<ul style="list-style-type: none"> <li>• environment and device models</li> <li>• motion paths</li> </ul>

**Tab. 5-2: RHWS function overview**

## 5.1 GUIDANCE AND CONTROL SYSTEM ARCHITECTURE

The guidance and control system architecture is highly modular such that it is easy to exchange modules, to add modules, and especially to use modules in a stand-alone manner. The modules are loosely connected via a simple but sufficient communication. Special attention was paid to an effective man-machine communication and a flexible division of labour between man and machine. A basic result of this was to define a separate module, the remote handling workstation, which represents the operator centred support tools.

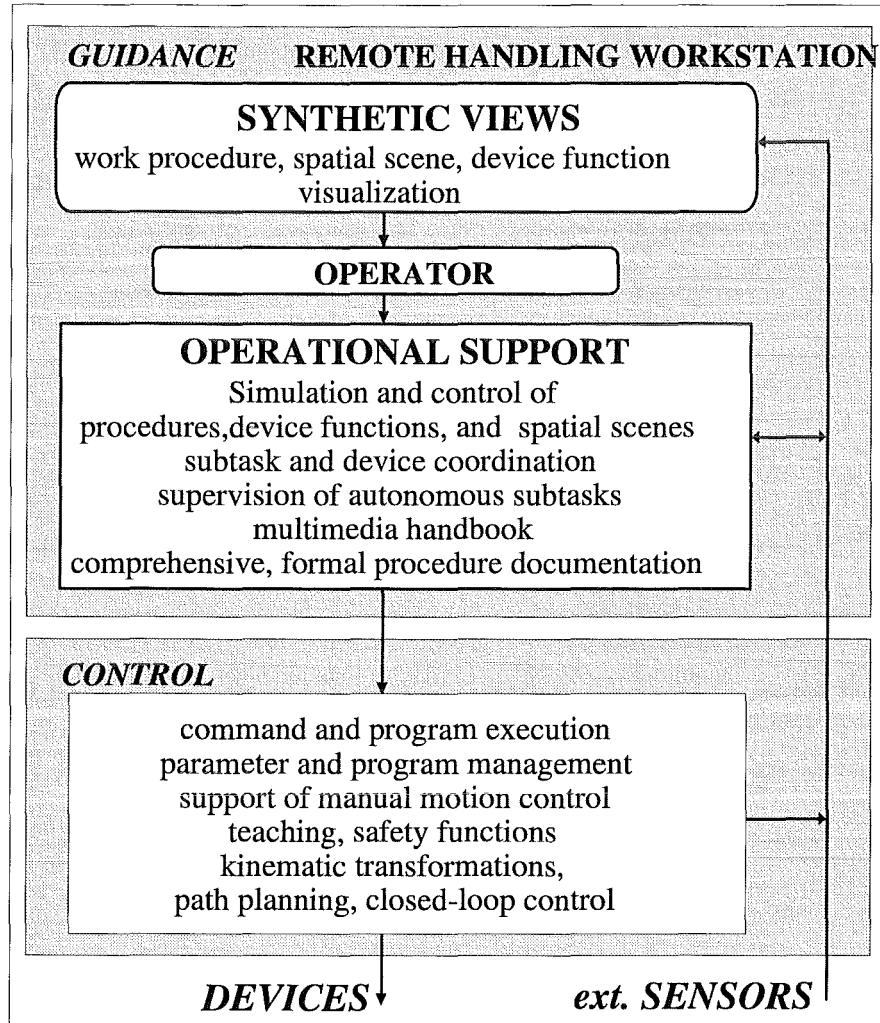


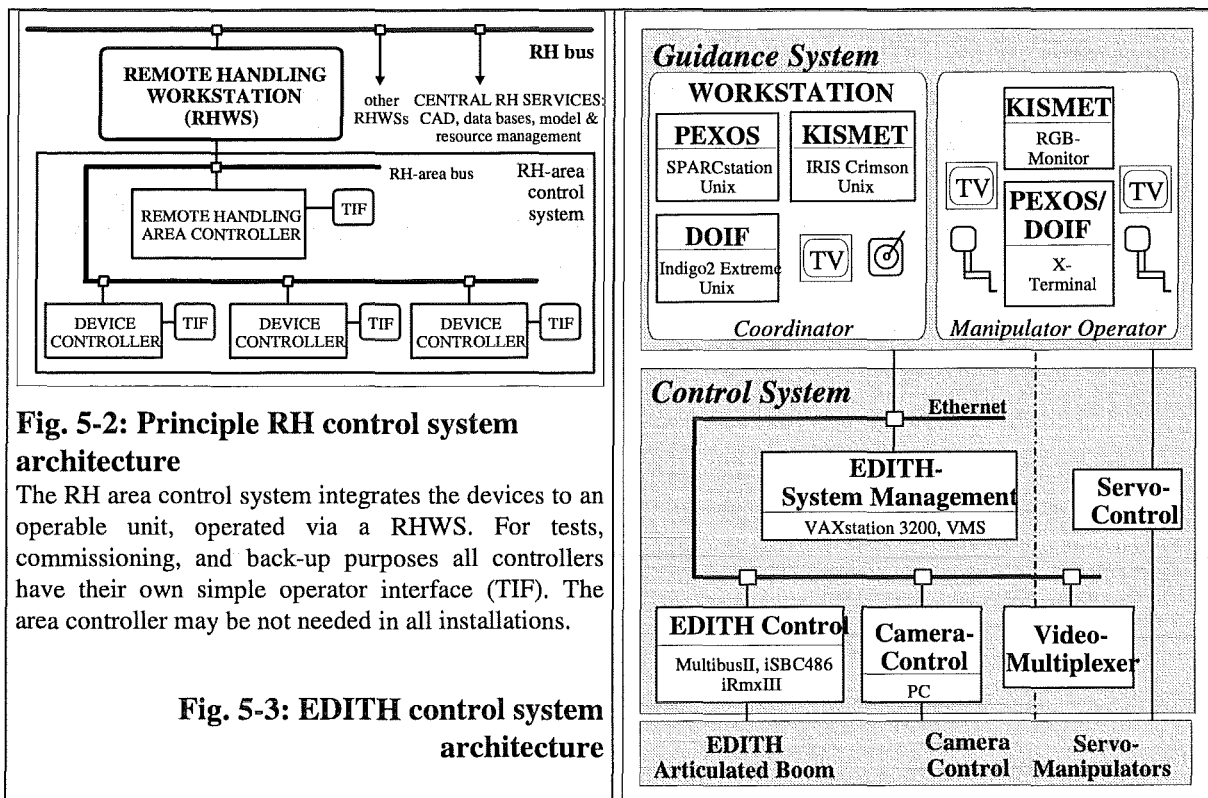
**Fig. 5-1: Man-machine co-operation**

The guidance and control system is organised mainly into two levels (Fig. 5-1):

- the guidance level represented by the RHWS,
- the control level represented by device controllers.

The communication between the units is done via a bus system. In the EDITH installation a Ethernet bus with TCP/IP is used successfully. The device controllers are integrated into this architecture via two interfaces (Fig. 5-2, Fig. 5-3):

- a simple, rudimentary man-machine interface for installation and test purposes and
- a bus interface providing all functions and data of the device controller to the outside. This interface is used for the connection to the RHWS



## 5.2 CONTROL ROOM

The EDITH control room (Fig. 2-7) provides two working places: one for the co-ordinating operator (Fig. 5-4) and the other for the servo-manipulator operator (Fig. 5-5). The place for the manual work provides two master arms, video monitors to look at the working environment, and a graphics screen for additional working scene views. A further computer screen displays the working instructions and enables the operator to call for additional information or to enter or look at notices. If needed the cameras may be controlled via this screen. The second working place serves to co-ordinate the subtasks, to start and supervise the automated subtasks, and to control directly and manually the devices (e.g. EDITH). This working place also serves for preparing the operators for the job or to plan or replan subtask in unforeseen situations. This place is equipped with a remote handling workstation which also provides the operational service for the manipulator operator.

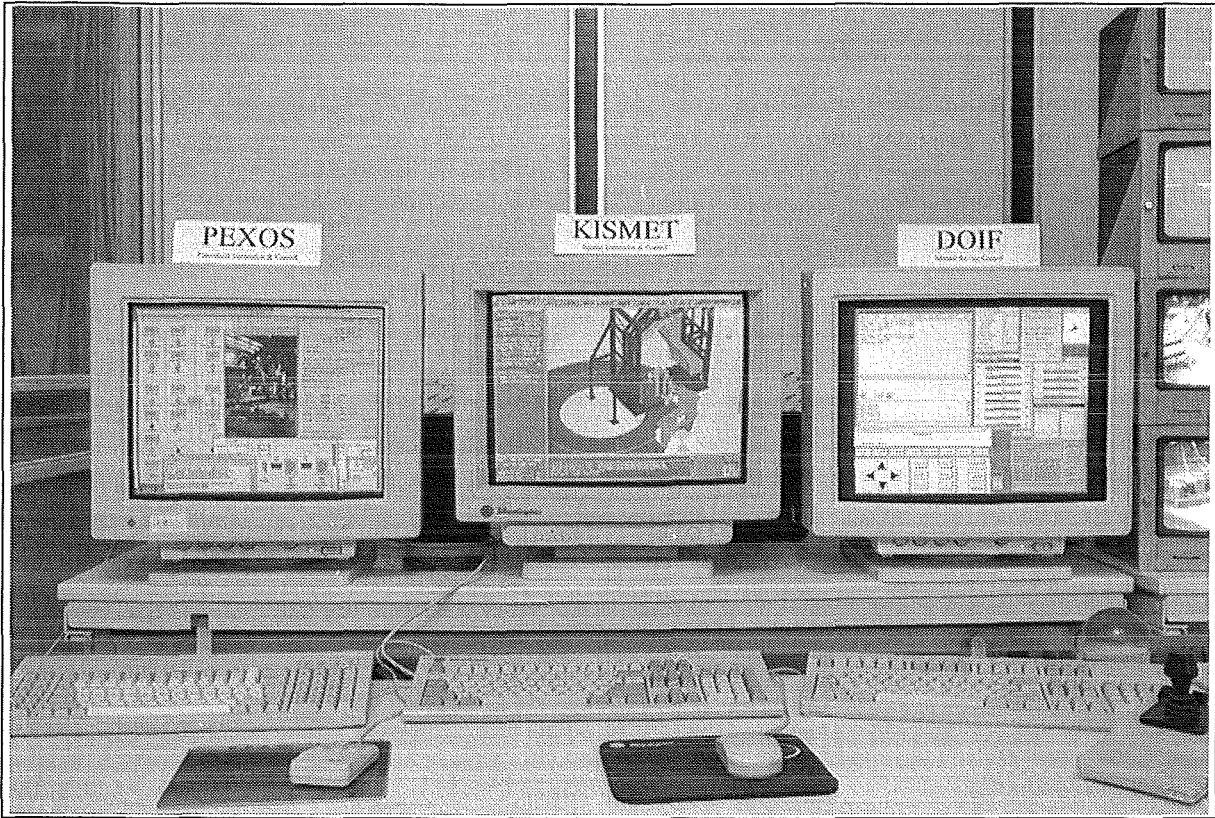


**Fig. 5-4: Remote Handling Workstation**



**Fig. 5-5: Servo-manipulator working place**

### 5.3 REMOTE HANDLING WORKSTATION

One goal of the project was the development of a general purpose Remote Handling Workstation (RHWS) and its application to a simulation of typical remote handling tasks like divertor exchange or armour tile exchange. The remote handling workstation supports the operator during task planning, training, and execution. It is also designed to serve as a procedure documentation tool. The generic and universal RHWS provides ergonomic and transparent remote operation whilst in manual mode and maintains overall supervision control during semi-autonomous operation. The RHWS provides the man-machine interface and operational support tools enabling the operators to perform the work fast, precise, and error free.

The Remote Handling Workstation is a comprehensive general purpose tool supporting the operators in all phases of work, that means during

- planning, including pre-planning and ad-hoc planning,
- training,
- execution, and
- documentation.

Maintenance work is conventionally discussed and described under three aspects or on three levels of abstraction:

- The **spatial aspect** shows where an action of a device takes place and which motion paths have to be used. The spatial domain deals with geometric and kinematics information about the devices and the working environment. This is the representation of the working space *where* the work has to be performed
- The **functional aspect** shows what kind of work a device provides, how a device is controlled and supervised. The functional domain deals with the devices and tools. This is the representation of the functional resources (remote handling devices) *by which* the work has to be performed, *which* are available for performing the work.
- The **procedural aspect** shows how a task is broken down into elementary actions, how the actions are realised by device functions, and where the actions are performed. The procedural domain deals with information on the remote handling procedures to be performed. This is the description and representation of *what* has to be done and *how* the work has to be done (handbook).

These three abstractions are needed and sufficient for a comprehensive support and, therefore, three independent but co-operating support tools were developed: The RHWS therefore consists of three subsystems which are connected but which also may be used stand-alone.

PEXOS (**P**rocedure **E**ditng, **S**imulation, **E**xecution, and **M**onitoring **S**ystem) is a multimedial electronic handbook interacting not only with the operator but also with the other subsystem and the remote handling devices thus co-ordinating the whole work according to the planned procedure. The procedures are graphically visualised by action/state networks and described textually, by drawings, photos, video sequences, and KISMET animations. PEXOS represents the maintenance procedures by a network of actions and states and their causality. It co-ordinates all agents of a maintenance task [LKO95].

KISMET (**K**inematics **S**imulation, **M**onitoring, and **O**ff-Line **P**rogramming **E**nvironment for **T**elerobotics) provides the three-dimensional spatial information for motion planning, device animations, and monitoring. Scripts facilitate the usage of KISMET. KISMET device models can be used as master devices for manual control. KISMET is the spatial support tool providing artificial views onto the working scene. The spatial simulation is based on 3D geometric/kinematics models of the working environment and the devices. The models can be updated by joint sensor signals for device motion monitoring. But the device models also can be animated for spatial procedure visualisation [KLP91, KUE92].

The DOIF subsystem (**D**evice **O**perating **I**nter**F**ace) provides the graphical operating interfaces for manual device control and monitoring and facilitates manual control of a device or a device group by script programming. The DOIF system supports the operator in device function control and monitoring it represents the device park. Each DOIF represents a devices in the RHWS.

Implicitly, there exists a further subsystem the CCSS (**C**onfigurable **C**ommunication **S**ubsystem) integrating the PEXOS, DOIF, and KISMET to the RHWS. The CCSS is not an equivalent independent subsystem but a group of service modules and communication agreements.

The RHWS provides

- the man-machine interface represented by
  - graphical visualisations of the work procedures,
  - the spatial scenes, and
  - the device functions
- operational support represented by
  - simulation of procedures, device functions, and spatial scenes
  - co-ordination of subtasks and devices
  - supervision of autonomous subtasks
  - monitoring of procedure execution, device functions, and spatial motions
  - programming of subtasks in the procedural, functional, and spatial domain
  - comprehensive, formal procedure documentation
  - multimedia handbook

The support of the RHWS is based on models of the reality represented by three data bases (Fig. 5-6). The module and communication architecture of the whole EDITH control system is shown in Fig. 5-7. Tab. 5-2 gives an overview over the RHWS functions related to work phases and support levels.

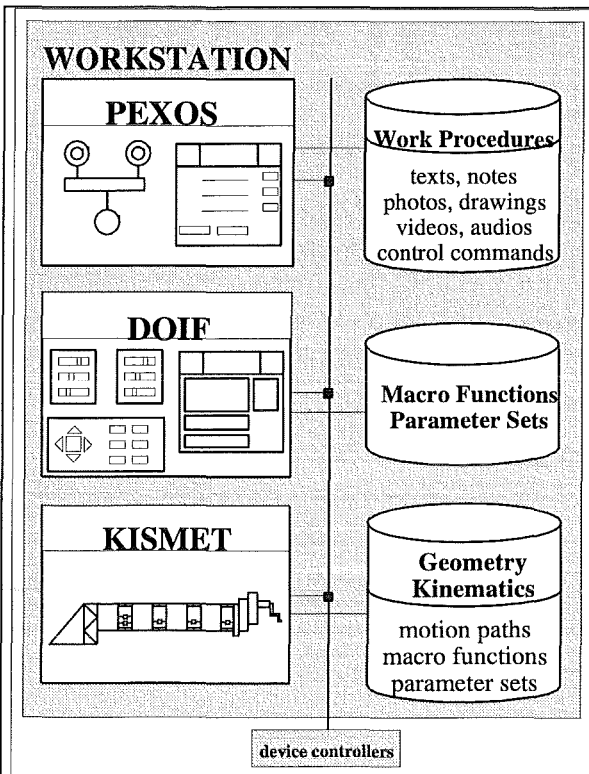


**Fig. 5-6: RHWS data bases**  
The three RHWS subsystems have their own databases.

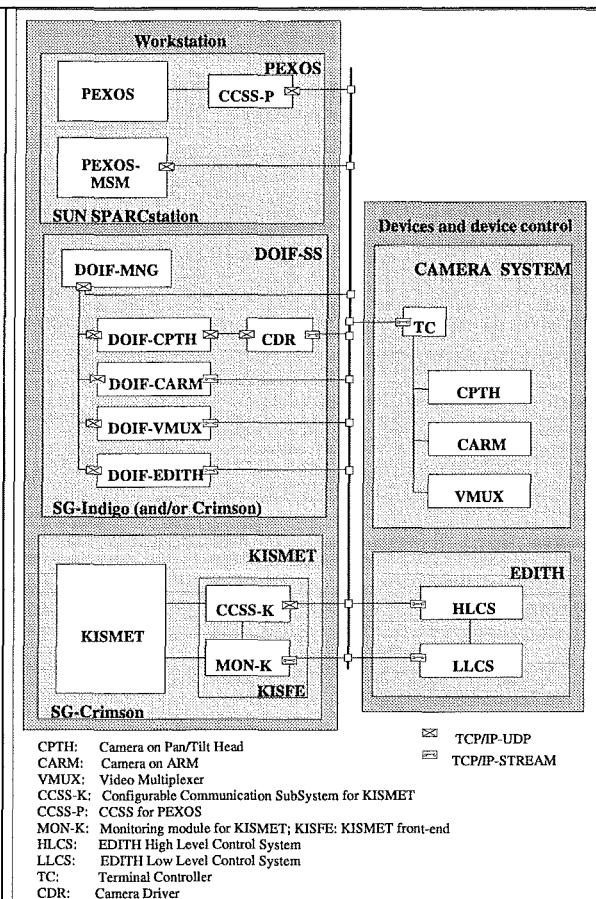


**Fig. 5-7: System architecture**  
The three RHWS subsystems can be used alone or together with others as needed in an application. Due to the communication subsystem the RHWS modules may be allocated on different computers. In the extreme case all systems may be allocated on one workstation

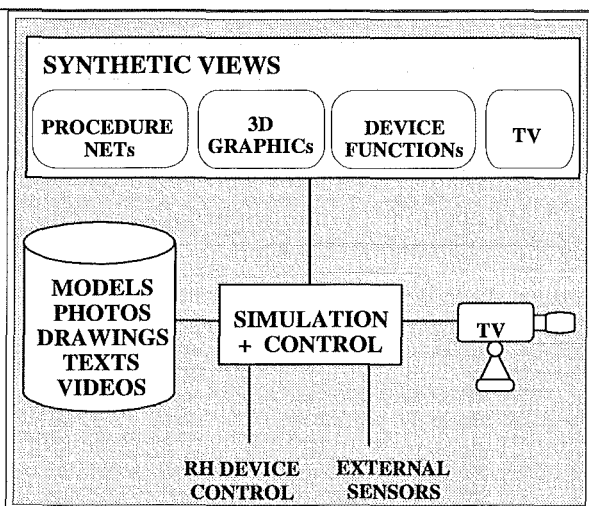


**Fig. 5-8: Principles of synthetic viewing**  
Based on models of the reality and sensor & control system data information views are generated and continuously updated.

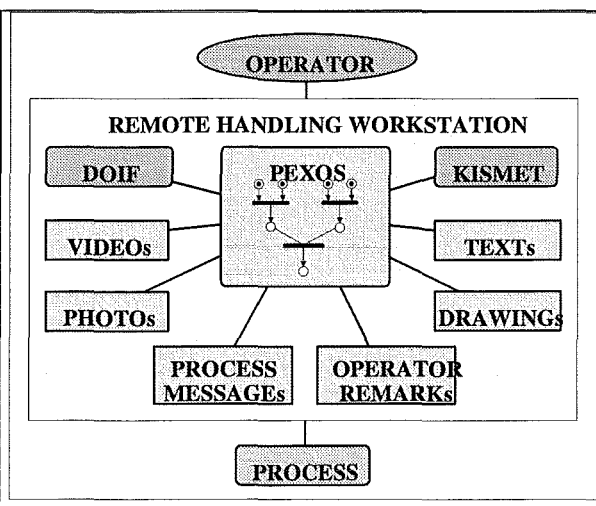


**Fig. 5-9: RHWS as interactive multimedia handbook**  
Via the nodes of the PEXOS ACTION/FACT network various information is accessible

### 5.3.1 Synthetic/integrated viewing

The basic and conventional sources of information about the state of the work are video monitors. In a first development step this viewing channel was enhanced by three-dimensional computer graphics controlled by motion sensors. On the graphics screens the operator can get any needed spatial view especially overviews and views from viewpoints without cameras. In addition, the graphics can be used to control the cameras and to identify the viewing field of a camera. In addition to this basic techniques, an enhanced man-machine interface with programming facilities of the camera control serves to make camera control more easy by pre-programmed camera pre-targeting, storing/recalling camera positions, camera tracking, camera mastering by graphics [LLA95, LHK96].

Practical experience has shown that the concept of viewing needs to be extended to support mainly the work of the co-ordinating/assisting operator. Just seeing were things are is insufficient for the operators to perform their remote handling task properly especially in applications with complex procedures where many device are needed and many interdependent work steps have to be performed. More information is required about the status of all equipment pieces involved and about the status of the entire handling task. Viewing for remote handling applications needs to include the display of such status information in a suitable form. Of special importance in this sense is the representation of the work procedures on the computer display enabling the operator to grasp at a glance the actual state of the work and the details about the subtask which has to be executed next. A similar example is air traffic control where, in addition to radar viewing (spatial viewing), a variety of representations of the traffic situation is available (e.g. sequence graphs and listings).

A task-suited viewing support should open at least three windows onto the work scene for providing three views:

- a spatial view showing the operator the geometry of the scene and the motion of the devices using TV and three-dimensional computer graphics controlled by sensors,
- a functional view visualising the device functions, and
- a procedural view visualising the work procedures by a graph of actions, system states, and their dependencies.

Because the operator thinks about space, device functions, and procedures a complete viewing support has to provide spatial monitoring, device function monitoring, and procedure (action/state) monitoring. The integration of these views is constituting "synthetic viewing", a technique visualising as many information as possible to overcome the problems of having no direct view, to help the operator in making-up and maintaining a mental model of the reality. The principle of synthetic viewing is to visualise by graphical techniques and models of the reality supporting information in addition to TV monitoring (Fig. 5-8). A natural enhancement of synthetic viewing is pre-viewing, looking into the future by simulation because models are needed for both. There is yet another important aspect of viewing for the operator: viewing into documents representing devices, assembly principles, spatial details, and special experiences.

A comprehensive state presentation (synthetic or integrated viewing) is essential for remote work but it can not be separated from its counterpart, controlling. The state visualisation (synthetic viewing) on computer screens should best be combined with the related control functions (graphics-based input devices) and operational support to facilitate the control. The

tool designed for providing the state presentation together with the required control support for the operator is the remote handling workstation.

### **5.3.2 Planning and programming**

To support planning (basic planning and ad-hoc or on-the-fly) planning on all three domains simulation systems and programming aids are available.

- In the spatial domain motion paths can be programmed using the IRDATA language.
- In the functional domain device commands can be bundled to scripts (macros) such that complex functions can be programmed.
- In the procedural domain programming by graphically supported action/state net generation integrates and connects all agents (devices, KISMET, DOIF, and the operators) to a co-operating and co-ordinated system. The operators are integrated via advices which have to be acknowledged.

### **5.3.3 Multimedia handbook and documentation**

Because maintenance procedures are complex, long, and performed infrequently a comprehensive documentation is of great importance. Conventionally this is done by handbooks. Bringing the handbook on the computer provides new possibilities especially the possibility to use various media for describing actions and states and to introduce enhanced information access by using direct links between information elements. The RHWS provides the following techniques for description of procedures (Fig. 5-9):

- graphically represented action/state networks (graphs) showing procedure dynamics by token flow
- texts (hypertexts)
- video sequences
- photos (with pick sensitive areas if needed)
- drawings (with pick sensitive areas if needed)
- audio sequences
- remarks of the operator
- graphical representation of device function and states
- 3D spatial simulations (animations) of devices in their environment

### 5.3.4 Co-ordination of RH agents

To perform a complex procedure enclosing various agents (devices, operators, tools) fast and error free a co-ordinating tool should be available to assist the human co-ordinator. This can be realised partly by the DOIF system on the functional level but is especially provided by PEXOS on the tasking level. PEXOS not only communicates with the operators but also, via the DOIF system, with the devices. According to the planned causality between actions and states the agents are co-ordinated in their work. The co-ordination is visualised by the PEXOS graph.

## 5.4 PEXOS - WORKING WITH PROCEDURES

Procedural support means to assist the operator in performing work procedures like tile or divertor exchange effectively as planned. This kind of support is normally available to the operator by written handbooks. The computerised support is based on procedure models representing procedures by elementary actions and states, their causalities, and temporal relations. The procedure nets are based on the well known Petri net technique and visualised by graphs which are simple enough to be interpreted easily by non-experts. They are natural in some sense to represent the structure and dynamics of a procedure. The actions and states are described in detail by texts (hyper-texts), drawings, photos, video sequences, KISMET images and animations, and DOIF visualisations. This information is accessed through the graphical representation (Fig. 5-10, Fig. 5-11, Fig. 5-12). The system allows to co-ordinate actions and to model typical procedural situations like concurrency, alternatives, and joins. Each action instructs and advises the operators but can also send messages to the DOIF subsystem, to the devices, and to KISMET to unburden the operator. Generating procedure models means programming and co-ordinating the whole system on the tasking level including all devices and the operator. The system allows to directly call for automated sequences and to instruct and advice the manipulating operator. The information for the manipulating operator is displayed on a special screen through which this operator can also call for additional information, can add remarks to an action, and on which he has to tell the system when he starts and finishes a subtask thus enabling PEXOS and the supervisor to co-ordinate work. Each step of the procedure (each action) has to be confirmed by the operator. PEXOS is a mission programming and control system allowing the operator to intervene at each step and also allowing to deviate from a given plan and to re-join and synchronise the pre-planned sequence later on. PEXOS is co-ordinating and controlling all resources in relation to the actual task steps whereas KISMET and DOIF are supporting space and function related. For example, if the task state is reached where the operator has to exchange manually tiles, PEXOS can start the pre-targeting of all cameras and can select the problem suited view for KISMET monitoring.

But PEXOS is also a multimedia handbook and formal documentation tool describing procedures by action/state nets, various kinds of high-level programs (scripts), standard motion programs, and animations always related to action and states such that direct access of the information is easy and problem oriented. Especially the documentation of the dynamics of the procedures including all three levels of abstraction is of great value in preparing a maintenance mission as could be demonstrated in the experimental program.

PEXOS provides means for editing, storing, simulating, and executing procedure nets. During execution of a procedure an ACTION trace is automatically written.

Working with PEXOS the operator is confronted with the following objects represented graphically on the screen (Fig. 5-12, Fig. 5-13):

- NETs, representing the working procedures as a whole. NETs are graphs constructed with ACTIONS, FACTs, and ARCs. An example of a NET describing the tile exchange procedure on the top level is shown in Fig. 5-12. A NET can be simulated off-line thus providing a guided training tour through the work package. In the on-line mode the NET communicates with the operator (advising) and with the devices unburdening the operator from direct manual control tasks. A NET can be seen as a high level program integrating all resources even the operators. The basic model structure of a NET is an ACTION with pre-FACTs (pre-conditions) and post-FACTs (post-conditions). An ACTION is READY for execution when all pre-FACTs are true. The execution of an ACTION transports TOKENs from the pre-FACTs to post-FACTs thus representing the NET dynamics by a flow of TOKENs. To enhance the modelling capabilities special ARCs and TOKENs are available but not described in this context. NETs are described by: texts, drawings, video sequences, 3D KISMET animations, operator remarks, audio sequences, photos.
- ACTIONS, describing the work steps (graphically: rectangles). ACTIONS can be detailed themselves by a NET. ACTIONS are described by: texts, drawings, video sequences, 3D KISMET animations, operator remarks, audio sequences, photos. The basic state of an ACTION is the idle IDLE state. If all pre-conditions of an ACTION are fulfilled the ACTION becomes READY for execution. The pre-conditions are fulfilled if all pre-FACTs are true. A READY ACTION may be started by the operator setting the ACTION in the RUNNING state. Starting an ACTION may send a message to a related device. A RUNNING state denotes that the operator is working manually or that a device is working supervised by the operator. The RUNNING is ended by a DONE message from the related device or , in manual mode, by the operator clicking on the DONE button. ACTIONS may also be switched to the ERROR and HALT states.
- FACTs, describing the status of the work (graphically: circles). A FACT is true, if at least one TOKEN is placed on it. FACTs are described by: texts, drawings, video sequences, 3D KISMET animations, operator remarks, audio sequences, photos. The number of the standard TOKENs on a FACT can be interpreted as a capacity e.g. of available machines. In addition to the standard FACTs there are available so-called predicate FACTs. With predicate FACTs a more flexible kind of state description is used: the predicate for individual TOKENs. Individual TOKENs are predicated according to the predicate FACT they are actually related to. With this construct two FACTs „machine-1 available“ and „machine-2 available“ can be modelled by the predicate FACT „available“ and the two TOKENs „machine-1“ and machine-2“ on it. The predicate FACTs together with the individual TOKENs allow for a more compact description of tasks structures, they prevent for repetition of task structures.
- ARCs, describing the causality between ACTIONS and FACTs (graphically: lines with arrows), they represent the TOKEN paths. In the case of a standard FACT as a starting point of an ARC and in the case of a standard FACT as a target of an ARC the ARC attribute denotes the number of standard TOKENs to be transported. In the case of predicate FACTs the ARC attribute describes for which ACTION type which TOKEN type is needed for execution and, therefore, for transport. The ARC in this case represent filters for TOKEN transport.
- TOKENs, placed on FACTs (graphically: points) marking a FACT as true. TOKENs are used for representing the dynamics of a procedure, they are transported by the ACTIONS

from FACT to FACT. In addition to standard TOKENS individual TOKENs are available for modelling. They represent resources (objects) predicated by the predicate FACTs.

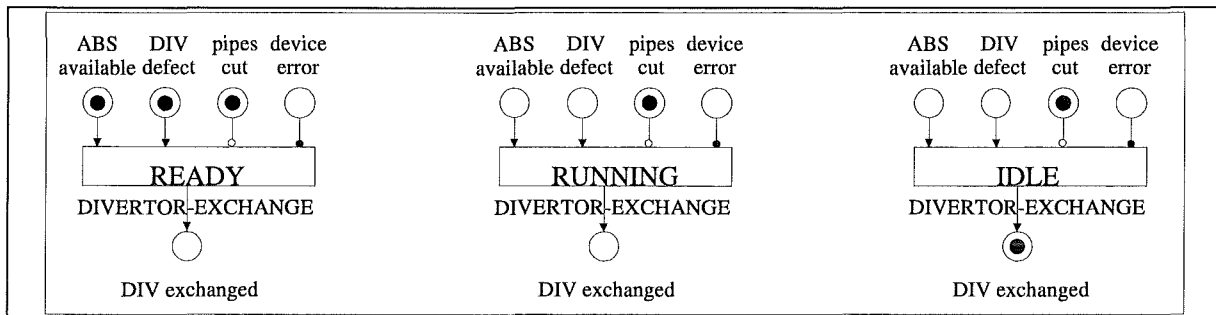


**Fig. 5-10: Simple PEXOS procedure example**

The divertor exchange ACTION is READY because the ABS is available, a divertor (DIV) is defect, the pipes are cut, and no device error occurred. After execution of the ACTION the ABS is not directly available the divertor is not defect, the pipes are still cut and no device error occurred.

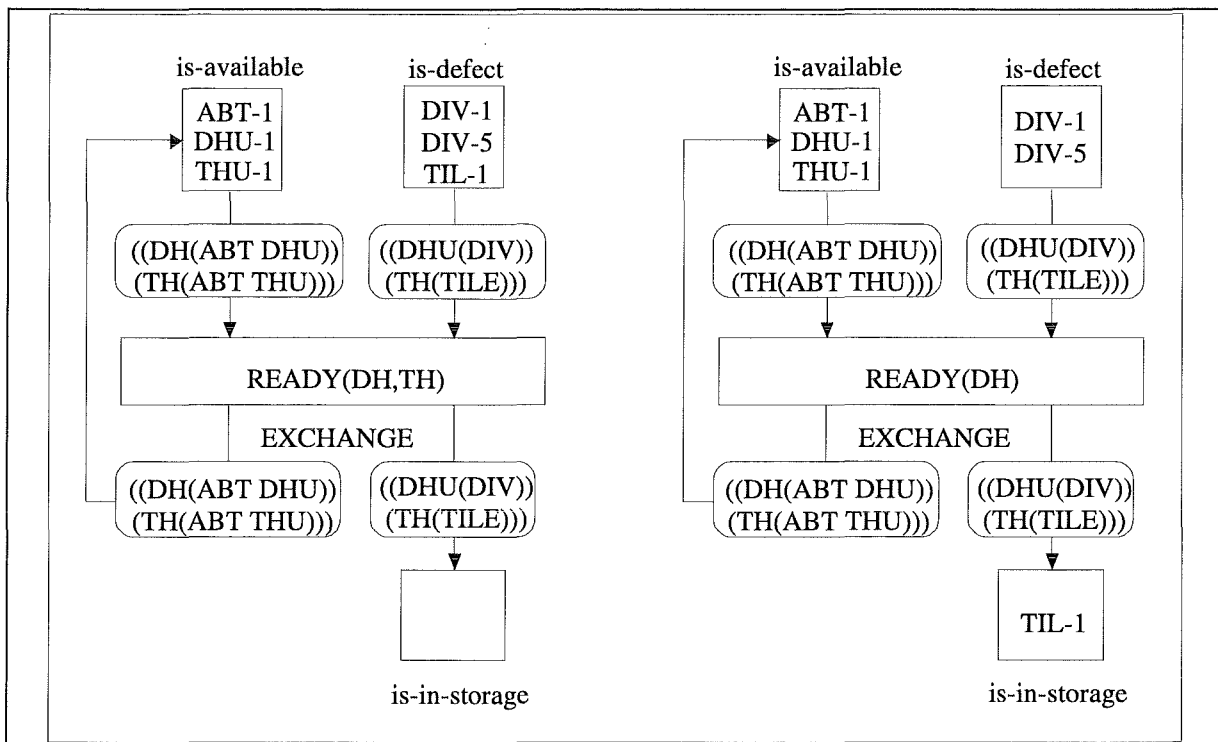


**Fig. 5-11: NET with individual TOKENs**

The articulated transporter 1 (ABT-1), the divertor handling unit 1 (DHU-1), and the tile handling unit 1 (THU-1) are available. Divertor 1 (DIV-1), divertor 5 (DIV-5), and tile 1 (TIL-1) are defect. The system is READY for divertor handling (DH) and tile handling (TH). The exchange task can start e.g. for TH: it needs an ABT, a THU and a TIL for execution. During execution ABT-1, THU-1 and TIL-1 are allocated by the EXCHANGE ACTION. After tile exchange (execution of TH-type EXCHANGE) the exchanged tile is in the storage and the ABT-1 and THU-1 are available but now the ACTION is only READY for DH.

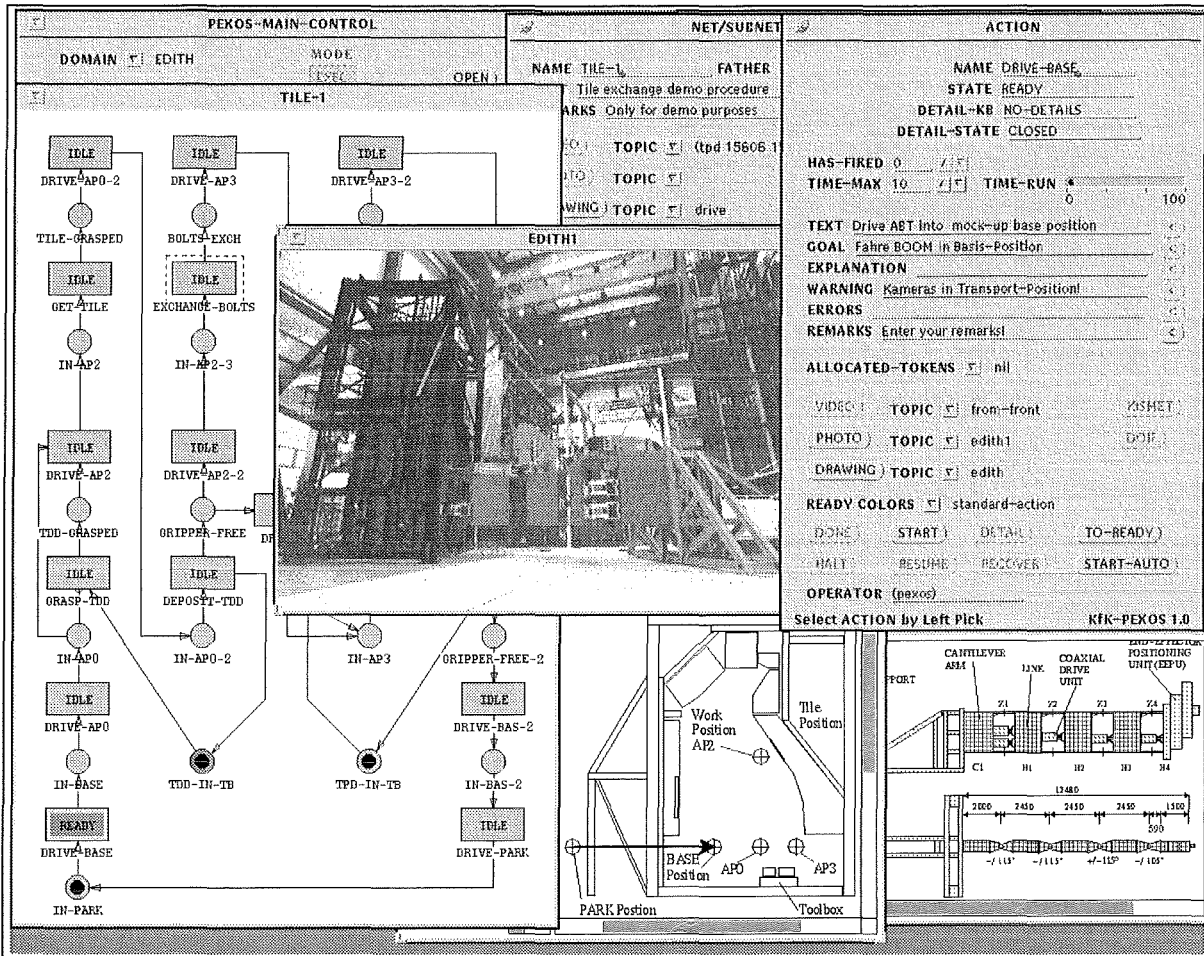


**Fig. 5-12 : PEXOS main screen**

The PEXOS screen shows the work procedure graph consisting of action nodes (rectangles) and fact nodes (circles). Actions and facts can be described by texts, video sequences, KISMET animations, drawings, photos, and operator annotations. The example shows the procedure net for the EDITH tile exchange procedure. The ABT is in the park position (IN-PARK) and the system is ready for driving into the torus (DRIVE-BASE). This action is described by the action panel (upper right side). Using this panel the operator can ask for additional information: photos, video sequences, drawings, KISMET animation. The execution of the automated work sequence can be started directly by a button click (START-AUTO).

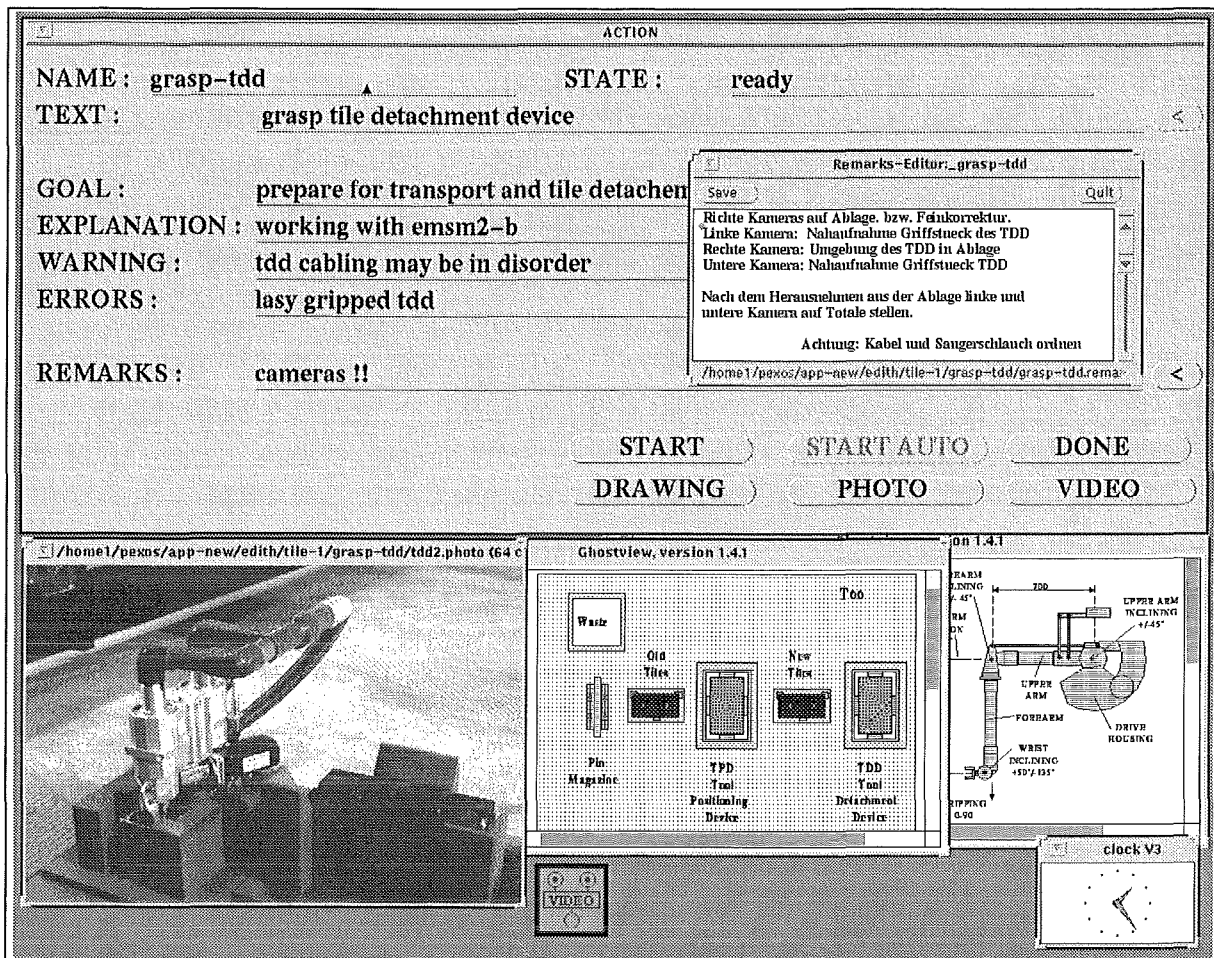


**Fig. 5-13: PEXOS screen for manipulating operator (PEXOS-MSM)**

This PEXOS screen displays advices for the manipulating operator. In addition to the basic textual explanations the operator can get additional information on the subtask in form of video sequences, KISMET animations, drawings, photos, and hypertext pages. The operator has to signal the start of his work (START) and the end of the execution (DONE). For subtask related remarks a notebook function is available.

## 5.5 DOIF - WORKING WITH DEVICE FUNCTIONS

Functional operator support means to facilitate manual control of a devices or a device park. This is provided by the DOIF (Device Operation Interface) subsystem [LKK96]. The devices are represented graphically using the standard window techniques (Fig. 5-14). Each device interface (DOIF) is implemented a separate operating system process allowing its independent use (if for example needed in a test phase or in a small installation). The connection of a DOIF to the DOIF manager (also running as an OS process) is realised by a standardised interface (DMserver) providing the following functions:

- execution of device functions
- manipulation of DOIF windows
  - window /button enabling/disabling,
  - window positioning
  - window object highlighting
  - window object hiding
  - window iconization/de-iconization
  - message displaying
- communication between the DOIF manager and the DOIFs
- DOIF status requests (e.g. ALIVE?)

A special feature of the DOIF system is the DOIF manager (DM) providing the possibility of macro (script) programming (command bundling) of single devices but also writing scripts combining devices. Macros are concurrent processes written in the special DOIF manager language. The macro language provides the following classes of functions:

- macro flow control (e.g. *if...then, while, repeat, ...*)
- start/stop macro
- send/receive message, synchronisation
- variable manipulation including saving/restoring
- string manipulation
- condition handling
- operating system access
- generation of graphical user interfaces (including variable binding for display)

The DM also provides means to support macro programming and management. The management of the DOIFs by the DM is visualised as shown in Fig. 5-15 and Fig. 5-16.

This script programming feature was found to be extremely helpful in **camera control** which is, if manually done, very time consuming. The DOIF systems allows to write scripts bundling cameras and pre-targeting cameras for each working position by this avoiding time-consuming target searching and reducing manual camera control to corrections. In the training or planning phase devices can be simulated together with KISMET. The DOIF system also provides a help

facility and a storage for operator remarks. Command input for devices is accepted in various forms, e.g. EDITH can be moved by textual commands, by a hardware joystick, by a software (graphic) joystick, or by using KISMET as a master.

All the control functions of the DOIF system are available for other RHWS subsystems, especially for PEXOS. This allows for assigning DOIF commands and scripts to PEXOS procedure elements (actions, states) thus enabling problem (task) suited functional support programming.

In the EDITH experiment the DM co-ordinates the following DOIFs which were developed for the devices used in the experiment:

- DOIF-EDITH: Graphical user interface for operating the EDITH motion control system
- DOIF-CPTH: Graphical user interface for operating cameras with pan/tilt heads
- DOIF-CARM: Graphical user interface for operating operating cameras on multi-link arms
- DOIF-VMUX: Graphical user interface for operating a video multiplexer

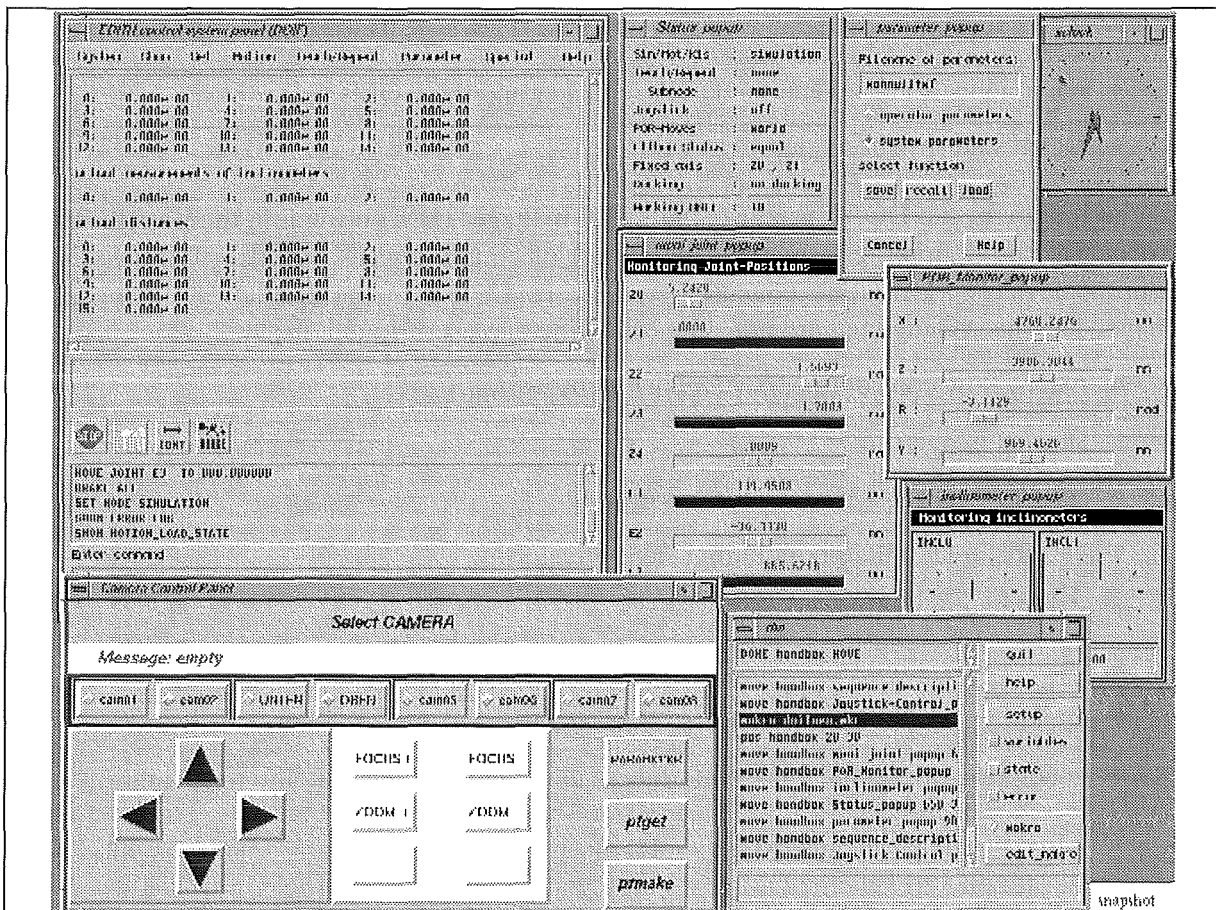


**Fig. 5-14: DOIF screen**

The screen shows the DOIF-EDITH, DOIF-CAM, and the DM window

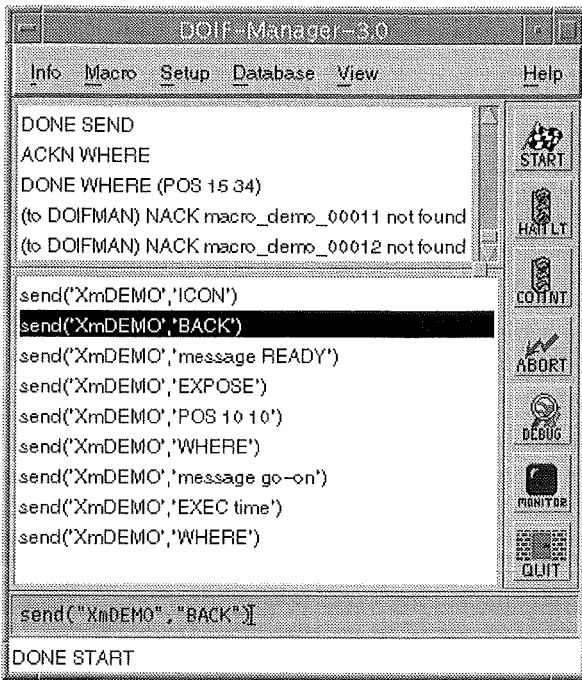


**Fig. 5-15: DM main window**

Main functions: START a macro; HALT a macro; CONTINUE a macro; ABORT a macro; DEBUG a macro; QUIT the DM

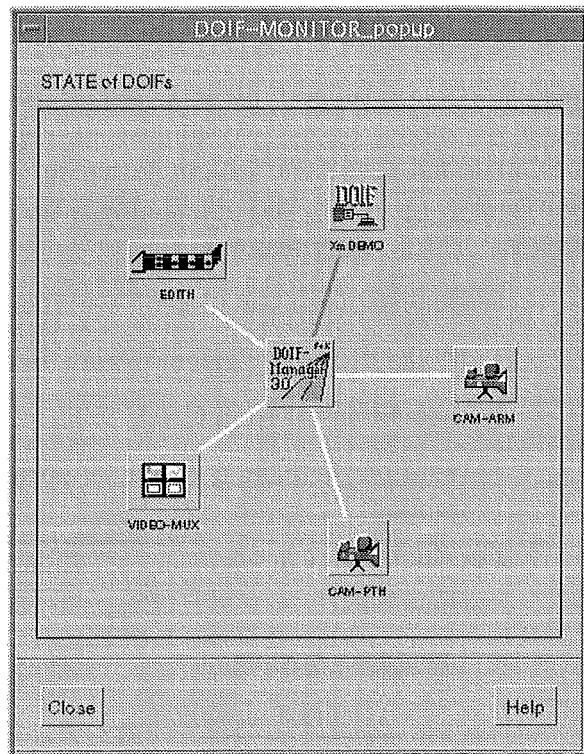


**Fig. 5-16 : DM/DOIF monitor**

The type of line between the DOIF manager in the centre and the DOIFs visualise the state of the connection (CONNECTED, ALLOCATED, BUSY,

## 5.6 KISMET - MOVING DEVICES IN THEIR ENVIRONMENT

Spatial operator support by KISMET [KUE92, KLP91] is based on a three-dimensional geometric model of the working scene (Fig. 5-18, Fig. 5-19). Spatial support is a well developed and successful technique which is now integrated into the RHWS via a special front end (Fig. 5-17) and interacting with the DOIF and PEXOS subsystems. KISMET provides the following features:

- Realistic representation of working scene
- Model control by video overlay (Fig. 5-20),
- model transfer from CAD,
- real-time deflection computation and real-time dynamics simulation for operator training,
- visualisation of geometric auxiliary data like work frames and viewing pyramids (Fig. 5-19)
- Integrated viewing ():
  - Camera viewing
    - + graphical viewing (e.g. overviews)
    - + camera control by graphics (pointing, KISMET as master)
    - + camera tracking
    - + display of camera viewing pyramid (identifications)
- usage of KISMET models as graphical masters transporters,
- collision control,
- motion path tracing,
- off-line programming of devices with IRDATA interface,
- simulation of IRDATA programs,
- motion monitoring of devices,
- animation of subtasks for operator instruction.

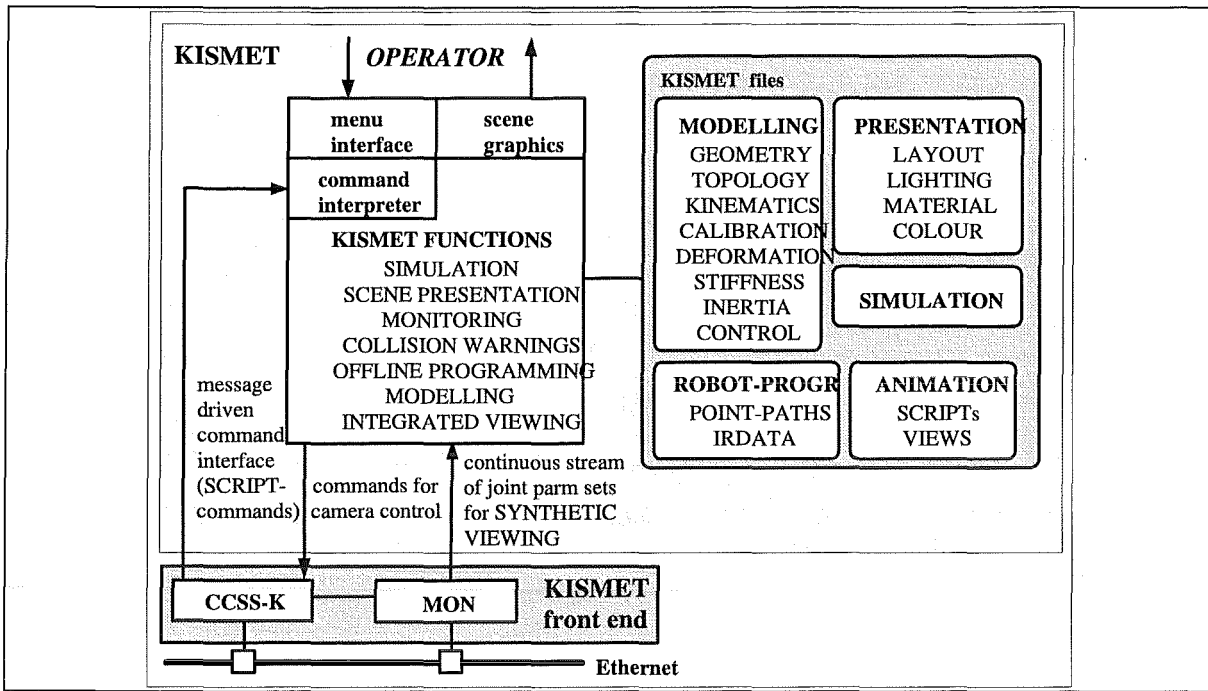


**Fig. 5-17: KISMET functional architecture and RHWS front end**

KISMET is dynamically controlled via the operator interface, the script command interface, and a continuous stream of sensor signals needed for model update (monitoring). The last two interfaces are accessible for external systems through the KISMET front end consisting of two subsystem (CCSS-K: Configurable Communication SubSystem for KISMET, MON: Monitoring interface)

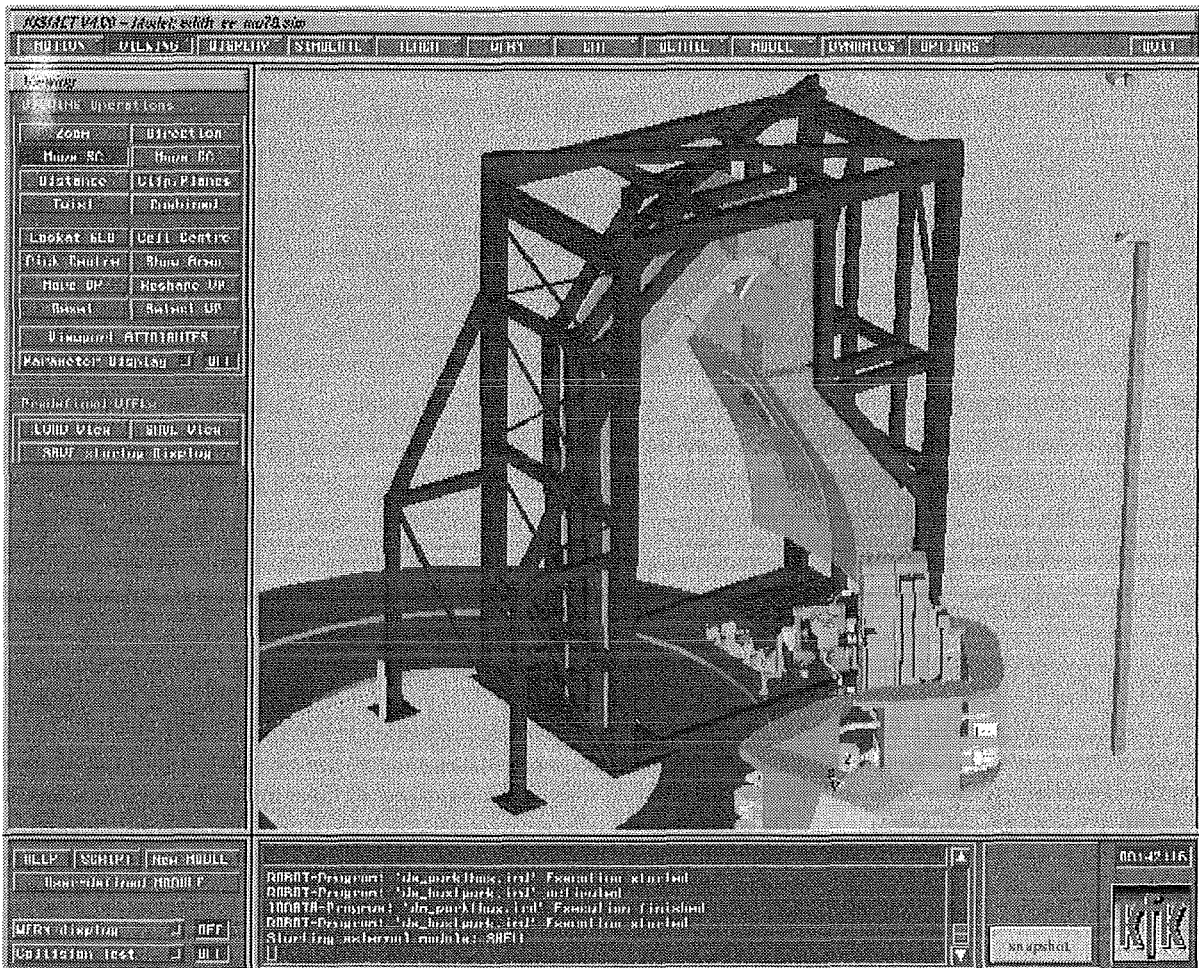


**Fig. 5-18: KISMET screen**

The screen shows EDITH with divertor mock-up, torus mock-up, and magazine. During work monitoring the KISMET system is used for provision of synthetic views not available by cameras. But KISMET is also used in the planning phase and in the execution phase for demonstrating working sequences together with the PEXOS electronic handbook.

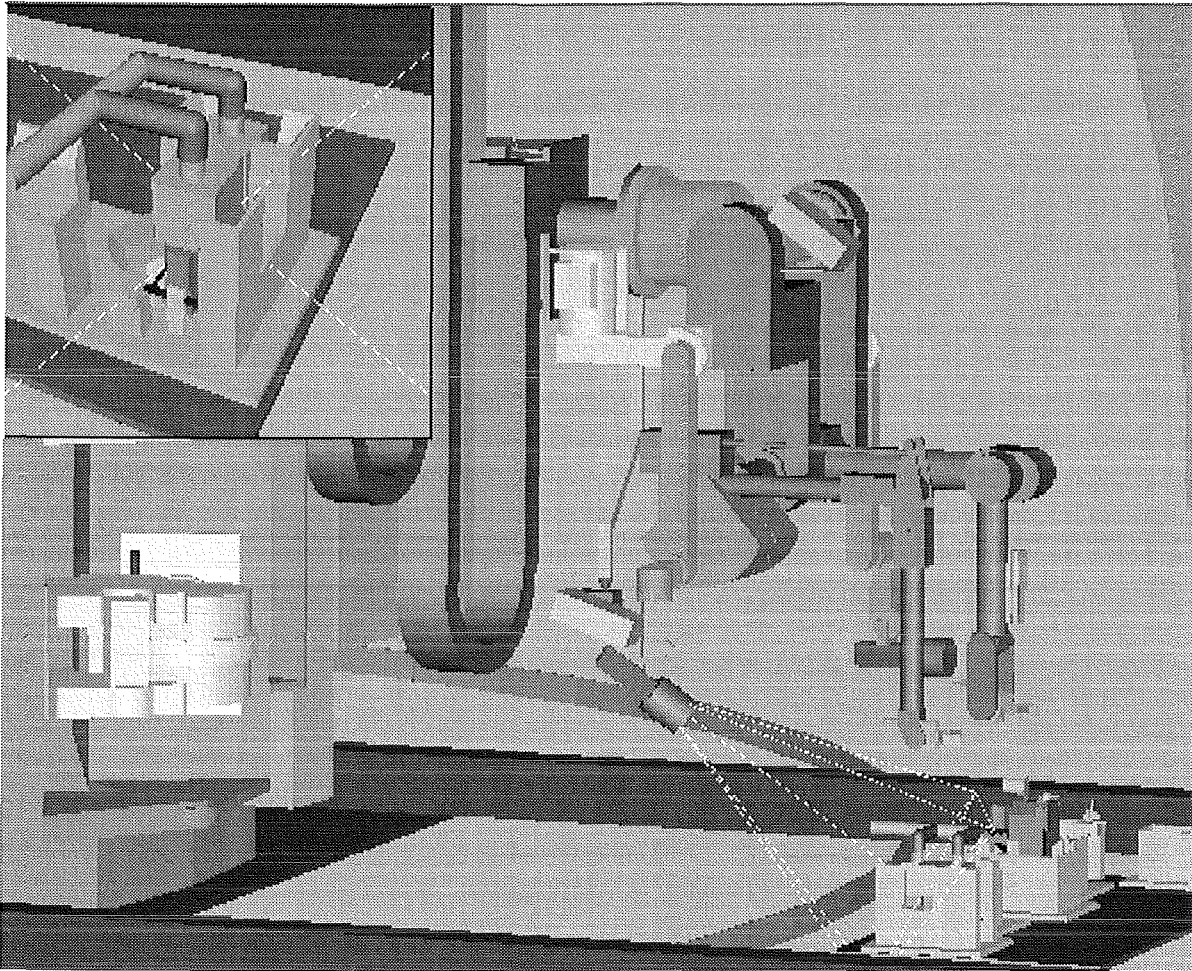


**Fig. 5-19: KISMET display with camera viewing pyramid**

The display of the viewing pyramid of a selected camera supports the operator in identifying screens shown on a video monitor. The graphics camera simulation also is used for camera targeting.



**Fig. 5-20: KISMET with video overlay**

The video overlay feature of the spatial support system assist the operator in verifying the correctness of a spatial model at a glance.

## 5.7 REFERENCES

- LEI84 Leinemann, K.: A Graphics Based Remote Handling Control System. KfK-3788, 1984
- LVA84 Leinemann, K.: Man-machine co-operation in remote handling for fusion plants. Fusion Technology 1984. Proc.of the 13th Symp., Varese, I, September 24-28, 1984. In Two Volumes. Vol. 2 S.1311-16 Oxford (u.a.): Pergamon Pr. 1984 Varese
- LNO84 Leinemann, K., Schlechtendahl, E.G.: Computer graphics support for remote handling simulation and operation. Proc.of the 32nd Conf. on Remote Systems Technology, held in Conjunction with American Nuclear Society Summer Meeting, New Orleans, La., June 3-7, 1984 La Grange Park: American Nuclear Soc. 1985 Vol. I S.10-16 Transactions of the ANS, 46(1984) S.771-72 (Abstract) New Orleans
- BB189 Browne, M.L., Bombi, F.: unpublished report, September 1989
- BB289 Browne, M.L., Bombi, F.: unpublished report, September 1989
- LEI90 Leinemann, K.: NET remote workstation. KfK-4785 (October 90)
- KLP91 Kühnapfel, U., Leinemann, K.: Verfahren zur Manipulation in unzugänglichen Arbeitsräumen. Patentschrift DE-OS 39 25 275 (7.2.1991) DE-PS 39 25 275 (24.1.1991)
- KUE92 Kühnapfel, U.: Graphische Realzeitunterstützung für Fernhandhabungsvorgänge in komplexen Arbeitsumgebungen. KfK 5052, May 1992
- SUP93 Suppan, A., Krieg, R., Krumm, H.G., Kühnapfel, U., Leinemann, K. Reim, J., Woll, J.: Experimental device for in-torus handling - EDITH intermediate report. KfK-5252 (October 93)
- LKO95 Leinemann, K., Katz, F., Olbrich, W.: unpublished report, March 1995.
- LLA95 Leinemann, K., Katz, F., Knüppel, H., Olbrich, W. Maisonnier, D.: Synthetic Viewing: Comprehensive Work Representation, Making Remote Work More Clearer to the Operator. Fusion Engineering and Design 29(1995)317-323
- LHK96 Leinemann, K., Haist, B., Knüppel, H.: unpublished report, January 1996
- LKK96 Leinemann, K., Katz, F., Knüppel, H.: unpublished report, April 1996



# Table of Content

<b>6 MOTION CONTROL SYSTEM .....</b>	<b>6-3</b>
<b>6.1 REQUIREMENTS .....</b>	<b>6-3</b>
6.1.1 Hardware Requirements .....	6-3
6.1.2 Functional Requirements .....	6-3
<b>6.2 STRUCTURE OF MOTION CONTROL SYSTEM .....</b>	<b>6-5</b>
6.2.1 Hardware Architecture.....	6-5
6.2.2 Software Architecture.....	6-8
<b>6.3 FUNCTIONAL IMPLEMENTATION OF MOTION CONTROL SYSTEM .....</b>	<b>6-13</b>
6.3.1 Communication.....	6-13
6.3.2 Function .....	6-14
6.3.3 Parameter Handling .....	6-14
6.3.4 Path Planning.....	6-14
6.3.5 Inverse kinematics Transformations .....	6-16
6.3.6 Teach-Repeat .....	6-17
6.3.7 Position Controller.....	6-21
<b>6.4 COMMAND SET .....</b>	<b>6-26</b>
6.4.1 Legend: .....	6-26
6.4.2 EDITH command set .....	6-26
<b>6.5 EXPERIENCES AND CONCLUSIONS .....</b>	<b>6-29</b>
6.5.1 General Conclusions .....	6-29
6.5.2 Hardware .....	6-29
6.5.3 Software.....	6-30
6.5.4 Handling of the EMCS .....	6-30
<b>6.6 FURTHER DEVELOPEMENTS .....</b>	<b>6-31</b>
<b>6.7 REFERENCES .....</b>	<b>6-32</b>

## List of Figures

FIG. 6-1: OVERVIEW OVER THE EMCS .....	6-6
FIG. 6-2: HARDWARE ARCHITECTURE OF THE HLCS SUBSYSTEM .....	6-6
FIG. 6-3: HARDWARE ARCHITECTURE OF THE EDITH LOW LEVEL CONTROL SYSTEM .....	6-7
FIG. 6-4: COMMUNICATION PATHS WITHIN EMCS .....	6-8
FIG. 6-5: HLCS TASK STRUCTURE .....	6-8
FIG. 6-6: OVERVIEW OVER THE LLCS TASK STRUCTURE .....	6-10
FIG. 6-7: POSITION (Q) AND VELOCITY SHAPE (QP)GENERATED BY APC-PLAN .....	6-15
FIG. 6-8: PRINCIPLE OF CARTESIAN PATH PLANNING AT A VIA POINT .....	6-15
FIG. 6-9: SQUARE SHAPED CARTESIAN PATH AS RESULT OF EDITH'S PPC-PLANNING. ....	6-16
FIG. 6-10: REDUNDANT KINEMATICS OF THE EDITH ABT .....	6-16
FIG. 6-11: FREEZING JOINTS FOR REDUCTION OF REDUNDANCIES .....	6-17
FIG. 6-12: TEACH/EXECUTE/EDIT OF SEQUENCE FILES .....	6-19
FIG. 6-13: ELECTRONIC SYNCHRONOUS GEAR.....	6-22
FIG. 6-14: CONTROL SCHEME OF EB1_CTRL.....	6-22
FIG. 6-15: STRUCTURE OF INVERSE MODEL BASED CONTROLLER WITH REFERENCE BEHAVIOR	6-24
FIG. 6-16: NOMINAL, REFERENCE, MOTOR AND JOINT PATH .....	6-25

## List of Tables

TAB. 6-1 : IO-CHANNELS OF THE EDITH MOTION CONTROL SYSTEM .....	6-4
TAB. 6-2: FUNCTIONAL REQUIREMENTS (OVERVIEW) .....	6-5
TAB. 6-3: DESCRIPTION OF HLCS TASKS .....	6-9
TAB. 6-4: LLCS UTIL TASKS .....	6-11
TAB. 6-5: DESCRIPTION OF LLCS MAIN TASKS .....	6-12
TAB. 6-6: DESCRIPTION OF LLCS SERVICE TASKS.....	6-13
TAB. 6-7: DESCRIPTION OF LLCS IO-TASKS.....	6-13
TAB. 6-8: TELEGRAM STRUCTURE FOR EDITH MOTION CONTROL SYSTEM .....	6-13

## **6 MOTION CONTROL SYSTEM**

### **6.1 REQUIREMENTS**

The requirements for the EDITH Motion Control System (EMCS) are documented in *Spec*. The following paragraphs give a short summarise of those requirements.

In addition to those requirements, the complete system should be designed that way, that it will be easy to adapt and to extend to future requirements.

A basic demand of NET was to adapt the JET TARM control system thus accepting some design decisions not optimal according to FZK opinion.

#### **6.1.1 Hardware Requirements**

The EMCS was required to control a manipulator up to 12 axis with 26 motors. In consequence, the hardware requirements of the control system are specified by the number off IO-channels (Tab. 6-1)

In addition there should be some reserve for later extensions of the system.

#### **6.1.2 Functional Requirements**

Besides hardware requirements there exist also functional requirements, which describe the function of the system. An overview is given in Tab. 6-2.

Channel Type	NR.	Function
analogue out: -10V...0V...10V	26	set point
sum analogue out	26	
analogue in: -10V...0V...10V	24 12 16 3 6 15	velocity of motors velocity of joints distance sensors inclinometers acceleration sensors forces
sum analogue in	76	
digital out	24 24 4 1 1 6 6	activate servo lift brake watchdog reset docking support servo resolver bus joint resolver bus
sum digital out	66	
digital in	24 24 2 2 3 15 24 24 4	servo controller ready servo resolver warning group control supply group power supply emergency off servo resolver bus joint resolver bus range switch WU-encoding, mating OK
sum digital in	122	

**Tab. 6-1** : IO-channels of the EDITH motion control system

<b>Operation Modes</b>	
APC operation mode	operator controlled synchronous axis positioning
PPC operation mode	operator controlled cartesian positioning
AVC operation mode	joystick controlled joint velocity
PVC operation mode	joystick controlled cartesian velocity
PRC operation mode	point reconfiguration - reconfiguration of redundant kinematics of the ABT
<b>Parametrisation</b>	
system parameters	parameters, which may be changed only by the system manager - those parameters are kept constant during a specific task
operator parameters	parameters, which can be modified by the operator due to the appropriate task (reduction of velocities)
<b>Teach in of Motion Sequences</b>	
named points	points must be attached by name
recycling of point databases	usage of a known point database within a new motion sequence
debug mode	it must be possible to execute a sequence step by step
<b>Additional Functions</b>	
trace function	There should be build in a trace function to record data of the position controller(nominal/actual positions, velocities)
simulation mode	There must be given the possibility of testing the whole system with the servo drive units off-line. The behaviour of the system in simulation mode should be the same as is in motion mode. A dynamic simulator must not be build in.
<b>Man Machine Interface</b>	
graphical operator interface	There should be at least one link to the operator workstation.
graphical on-line monitoring	There should be one link to the graphical kinematics simulator KISMET.

**Tab. 6-2: Functional requirements (overview)**

## 6.2 STRUCTURE OF MOTION CONTROL SYSTEM

### 6.2.1 Hardware Architecture

#### 6.2.1.1 Overview

To meet the requirements there was chosen a modular architecture, which allows to distribute functional features among the different subsystems. An overview over the EMCS is given in **Fig. 6-1**.

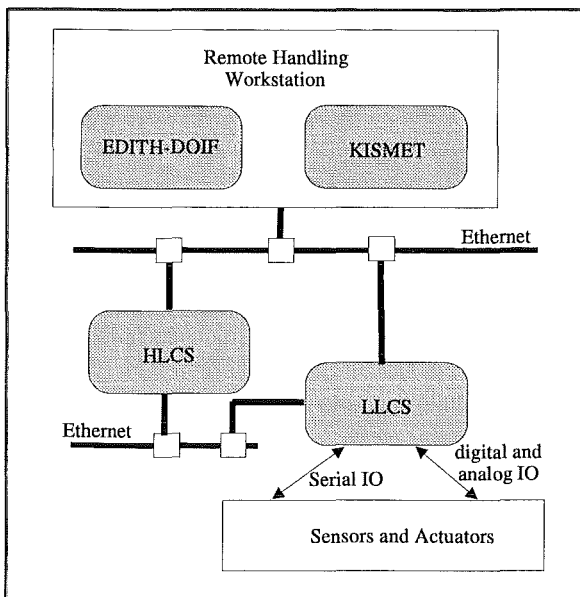


**Fig. 6-1: Overview over the EMCS**

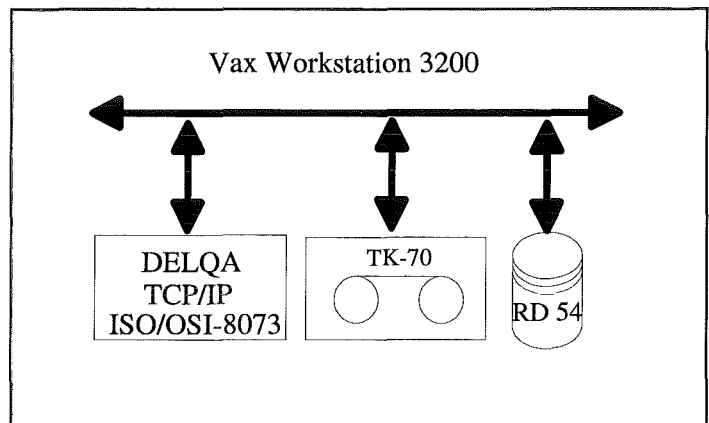


**Fig. 6-2: Hardware architecture of the HLCS subsystem**

The EMCS consists off two components, the high level control system (HLCS) and the low level control system (LLCS). The Remote Handling workstation is not part of the EMCS and is described in an own chapter. Not shown but also available is a serial link to a simple user interface called handbox, which was used for test purposes during development of the EMCS and which is not used any more. Nevertheless it would be possible to control the system from this handbox in axis control mode.

Within the LLCS there is realised the very motion control, i.e. position controller, path planning and the IO subsystem. HLCS however contains higher functions like access control, parameter handling, recording, editing and execution of repeat sequences.

### 6.2.1.2 HLCS

As the EMCS should be a further development off JET's TARM motion control system (requirement of NET) there has been chosen a VAX Workstation 3200 as hardware platform for the HLCS. This offers the possibility off porting and adapting the new control system or parts of it to the JET TARM. The Hardware configuration of the HLCS is shown in Fig. 6-2.

The main tasks are data management (parameter handling, teach in and execution of sequences). In addition to that, it also works as the central communication node. Due to those tasks it consists of mass storage (tape drive and hard disk drive) and communication boards (DELQA).

### 6.2.1.3 LLCS

As platform for the LLCS there has been chosen a Intel Multibus II hardware architecture. Besides a high quality it offers the capability of scaleable system with special features supporting multiprocessing: A special communication processor on MB II CPU-boards, the message passing coprocessor, performs communication with other CPU and relieves the CPU from communication load. It is also possible to address memory global via the MB II as well

as local. This ensures a fast communication with peripheral IO-channels. The LLCS system configuration is shown in Fig. 6-3.

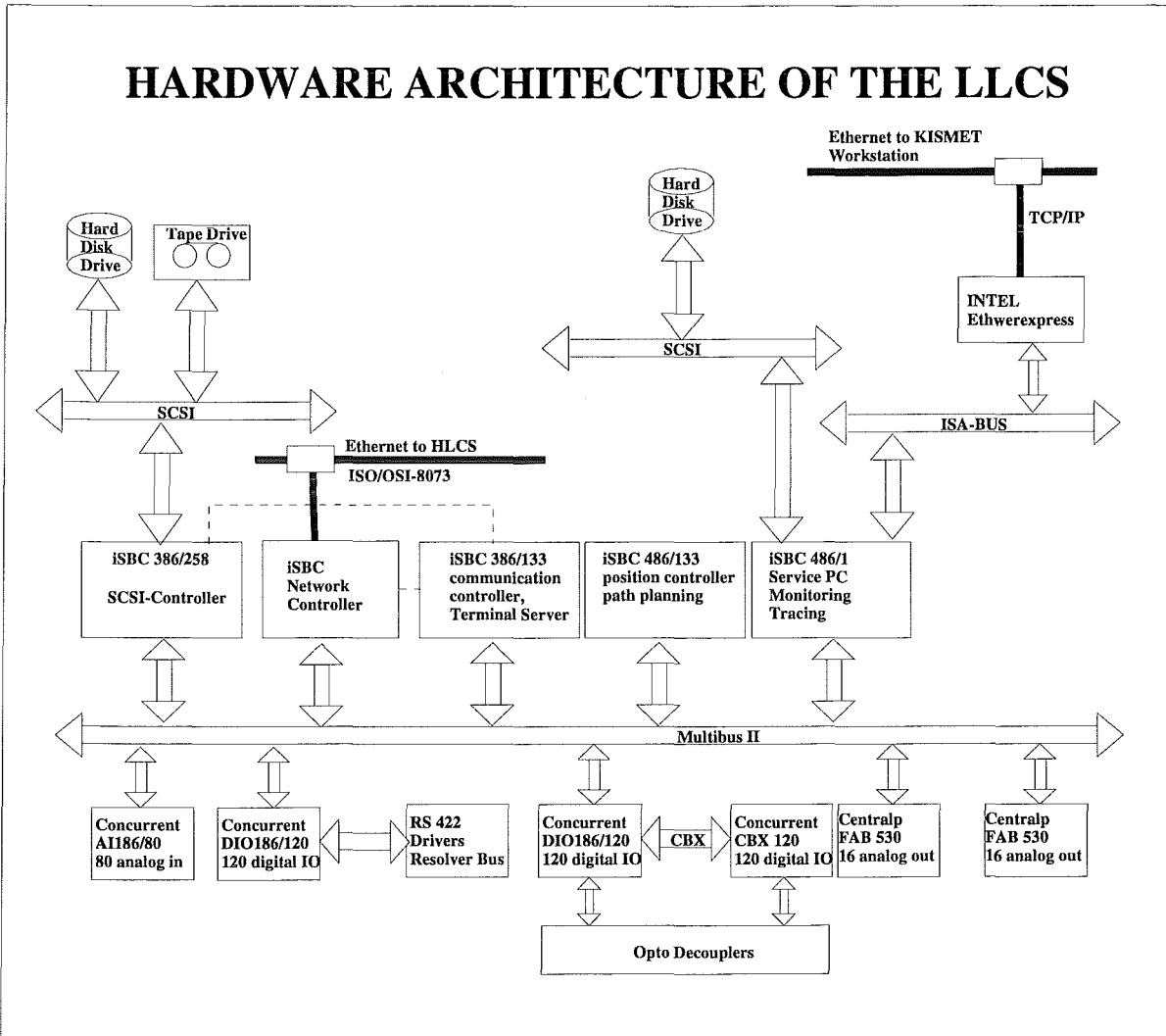


**Fig. 6-3:** Hardware architecture of the EDITH low level control system

There are two MB II CPUs (486/133 and 386/133) built in within LLCS. The first one is computing all critical tasks like path planning, position control, error handling and IO-control. The second is operating as a communication controller, which manages the communication between the HLCS and the LLCS, as well as a service interface, which offers system tracing (recording of LLCS specific messages), and a trace module, which offers on-line tracing. A special architecture is offered by the MB II service PC. It is integrated for recording of traces and also for communication to the kinematics simulator KISMET for on-line monitoring. Traces are recorded in MS-EXCEL 4.0 data file format. This offers the opportunity of manipulating and evaluating data with EXCEL/VISUAL BASIC macro language. As the communication on the resolver bus corresponds to the RS 422 specification, the IO channels of the resolver bus are adapted by a site specific RS422 driver board. All other digital IO-ports are optical decoupled from the peripheral systems.

### 6.2.1.4 Handbox

There had been implemented a simple user interface on a PC with two 3D joysticks connected, which may be either directly connected to the LLCS or to the HLCS. This interface was used for tests during implementation phase and was no longer used, since the EDITH-DOIF was available. In the following it will be mentioned but there won't be described any details.

## 6.2.2 Software Architecture

### 6.2.2.1 Overview

**Fehler! Verweisquelle konnte nicht gefunden werden.** shows the communication between all components of the motion control system. The HLCS is working similar to a gateway between operator station (DOIF) and the LLCS. The MBII service PC is directly connected to the Kismet station via an TCP/IP connection.

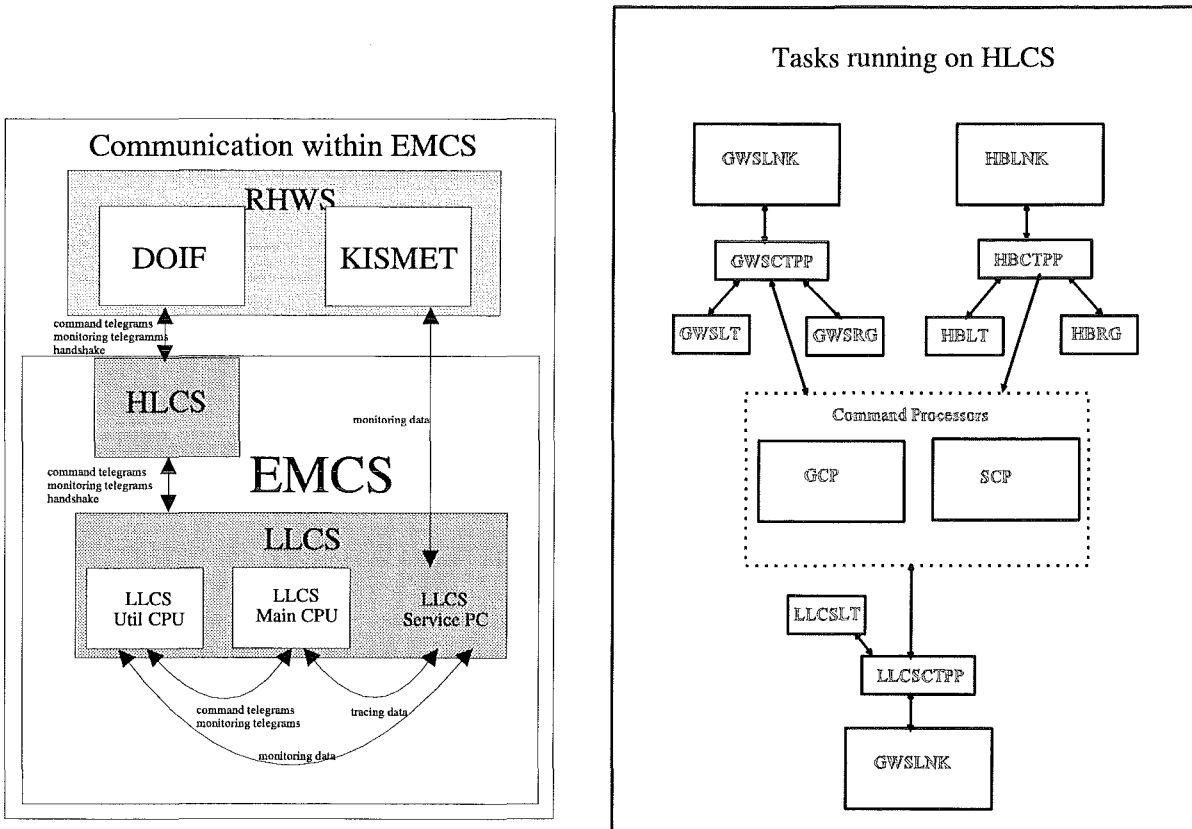


**Fig. 6-4:** Communication paths within EMCS **Fig. 6-5:** HLCS task structure

### 6.2.2.2 HLCS

HLCS operation is joined by several tasks which communicate by a shared memory. The synchronisation between all tasks happens under usage of VMS call „sys\$hiber“ (waiting for incoming messages) and „sys\$wake“ (informing tasks about incoming messages). The „sys\$wake“ call is generated by the telegram pre-processors. The task structure is shown in Fig. 6-5.

Notice, that all arrows in show the functional dataflow. As all tasks communicate using a shared memory, there is no real dataflow. The function of the tasks themselves is explained in following table Tab. 6-3.

LLCSLNK GWSLNK HBLNK	LNK marks the link tasks, which send/receive data to/from the corresponding link partner. There are three links supported: LLCSLNK using ISO/OSI-8073 protocol to the LLCS, GWSLNK using TCP/IP protocol to the graphical workstation and HBLNK using a specific serial protocol to the handbox. Incoming data will just be stored in the shared memory and not be modified by the link task. Outgoing data will be taken out of the shared memory and sent without modification to the desired station.
GWSCTPP HBCTPP	The common telegram pre-processor (CTPP) is running twice for handbox (HBCTPP) and for the graphical workstation (GWSCTPP). The source code is identical as both stations offer the same functionality. The CTPP's process all incoming and outgoing data and correspond to the belonging LNK task. As data are transmitted in the binary number format of the connected stations, the CTPP converts incoming telegrams to VAX number format and distributes them between the other tasks. Outgoing telegrams are converted to the number format of the target system.
LLCSCTPP	The LLCSTPP is the command pre-processor for communication to the LLCS. It operates similar to the GWSCTPP. Data are transmitted in LLCS (Intel) number format.
GWSRG HBRG	Report generators for GWS and HB. They transmit monitoring telegrams, status information and reports (SHOW telegram) to the corresponding operator station.
GWSLT HBLT LLCSLT	Controlled by timers the link testers send test telegrams to all connected stations, which should answer with an acknowledge telegram. If the link to operator station failed, the LLCS operations are stopped.
GCP	The general command processor. There are two command processors, which run exclusively. Excepted in Teach/Execute/Edit mode there is operating the GCP. If there is a Teach/Execute/Modify command, there will switched to the SCP. (special command processor). While all other tasks just convert data the GCP processes data, i.e. it executes the command. That can be setting of parameters, forward a motion command to the LLCS, command execution, changing mode.
SCP	Special command processor: The SCP is operating during Teach/Execute/Edit mode. It handles generation, execution or modification of sequence databases. During point definition submode or manual alignment, the SCP gives control to temporarily back GCP.

**Tab. 6-3:** Description of HLCS tasks

### 6.2.2.3 LLCS

As software platform there has been chosen an iRMX real-time operating system for the LLCS. This offers a high flexibility and offers the possibility porting software between different platforms. As iRMX is a multitasking system, the LLCS function was distributed among different tasks (Fig. 6-6).

The various tasks are shortly described in the following tables:

- Tasks running on util CPU: Tab. 6-4

- Tasks running on main CPU: Tab. 6-5
- Tasks running on service PC: Tab. 6-6
- Tasks running on IO-boards: Tab. 6-7

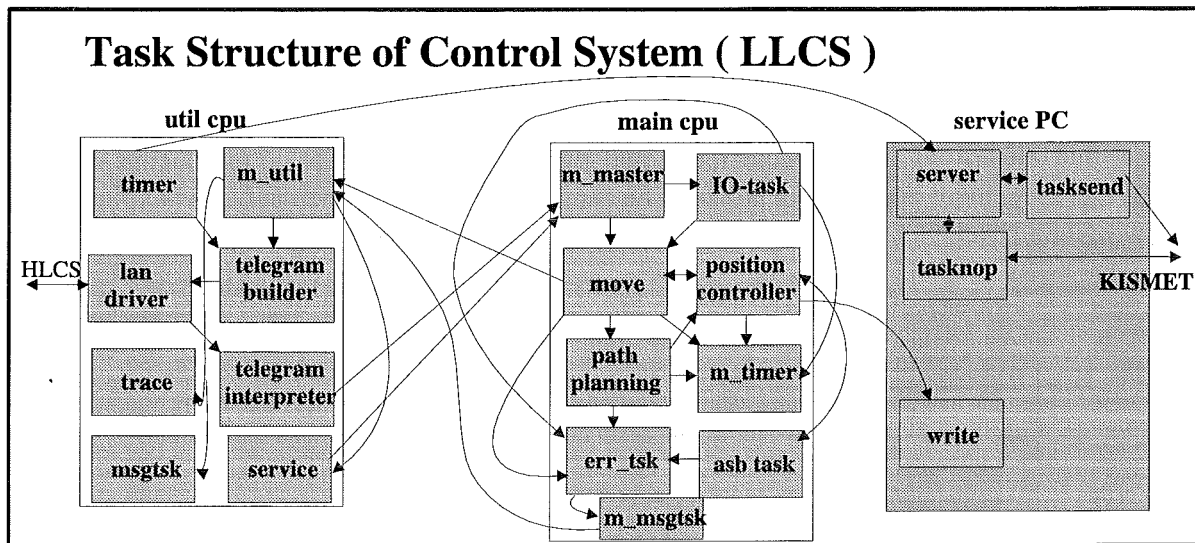


Fig. 6-6: Overview over the LLCS task structure

Task	Description
landrv	The lan driver handles the communication to HLCS using ISO/OSI-8073 protocol. Incoming telegrams are forwarded to the telegram interpreter (telintp), outgoing telegrams are received from the telegram builder (telbld). Lan driver does not modify any telegram data.
telbld	The telegram builder is responsible for any data transmitted to HLCS. It receives data from other tasks, builds the correct telegram structure and sends the complete telegram to landrv, who will transmit data to HLCS.
telintp	The telegram interpreter receives incoming telegrams from the landriver. After interpretation of telegrams the information is distributed to the corresponding tasks.
service	The service task offers the possibility of displaying system parameters and actual measured data. Besides monitoring there exists the possibility of controlling the trace task with its graphical output. It is also possible to control the manipulator by giving in simple APC move commands.
trace	The trace task is controlled by the service task and records position data. It receives the trace data from the u_master task. In combination with the grafik task, it is possible to display recorded data on-line.
grafik	Is also controlled by the service task and offers the possibility of displaying traced data in a diagram.
u_recflg	Reflects the data of the FLAG_DAT data structure, which is located on the main CPU, to the util CPU. It works only in one direction. Flags contained in FLAG_DAT may be modified only on main CPU using special global modules, which cause a message to the u_recflg task. If FLAG_DAT would be modified on util CPU, the data on both CPU would differ.
timer	The timer task is responsible for periodical transmissions to the HLCS or other connected stations. So the timer is responsible for transmission of monitoring data to the user interface or also to the server task (KISMET) on the service PC. It looks up position data in a global segment and causes telbld to transmit data to the corresponding stations.
msg_tsk	This task collects messages, and logs them on harddisk. The global module for sending messages to message task is snd_msg This will check on which CPU it is running and depending on the result select the way for data transmission. Data coming from the main CPU are transmitted via the u_master task.
u_master	u_master collects all data coming from the main CPU and distributes them to the corresponding util tasks. (msg_tsk, telbld, trace)

**Tab. 6-4:** LLCS util tasks

Task	Description
m_master	m_master collects all messages coming from the util CPU and distributes them among the corresponding tasks.
move	move is the central task controlling motions. Any motion (APC, PPC, PVC, AVC) is handled by the move task. If there is an APC, or PPC command, move gives the control to bplarepa (path planning). PVC telegrams cause move to integrate the velocity and calls an inverse kinematics transformation to get the nominal axis values (positions, velocities and accelerations). The communication with the position controller happens under usage of a global segment SOLL_DAT. Move also manages the transmission of position data to util CPU for on-line tracing or monitoring purposes.
bplarepa	bplarepa processes path planning and reparametrisation. In a first step there are processed off-line calculations to get the necessary path parameters. During on-line planning bplarepa calculates path data on demand, i.e. synchronised with the position controller.
posreg	posreg is the position controller. Besides the position control itself posreg manages the synchronisation (timing) of servo drive units including brakes. The cycle time is fixed to 20ms. The synchronisation is managed by a special timer task (m_timer). Cycle time is controlled and monitored managed by the m_timer task.
m_timer	m_timer controls the synchronisation of the central main tasks (move, bplarepa, posreg). At the end of a cycle the tasks suspend themselves. After the desired cycle time is over, the timer task will resume the corresponding tasks. If a task would not have finished its cycle the timer task causes an error. Communication to other tasks happens under usage of a global region.
errtsk	errtsk handles errors, which occurred on any main task. If an error occurs the main task can send an error message to the errtsk. Depending on the settings of the system parameters defining error reaction specifically for each error errtsk reacts with a STOP (immediate stop), HALT (stop with maximal deceleration), INFO (message to msgtsk), SIGNAL (digital output will be set)
iotsk	The iotsk controls the digital IOs as well as the analogue inputs. While there are running project specific tasks on the digital IO boards, the analogue input board is running the table driver. Communication happens via a MB II global data segment. The iotsk is running with 80 ms cycle time.
m_msgtsk	This task was integrated as an extension of the msgtsk. If there occurred too much messages the system collapsed. Now all main tasks entry their message in a global region (module m_sndmsg). The m_msgtsk looks up the data segment and transmits data at a limited rate to the msg_tsk on util CPU. (using snd_msg).
asb_tsk	asb_task realises the communication to the electronic gear (manufacturer ASB) via a serial terminal driver. Starting a motion posreg causes the electronic gear to set the nominal preload angle of the gear for all axis to zero.

**Tab. 6-5:** Description of LLCS main tasks

Task	Description
server	controls the communication to KISMET. The m_timer tasks sends monitoring data to a special MB II port of the service PC. From here server sends data to the KISMET workstation using tasksend.
tasksend	transmits data to the KISMET station.
tasknop	Sends NOP telegrams periodically to the KISMET workstations and waits for response (ACK). If KISMET doesn't respond within a fixed time (time-out) server will be informed and stop data transmission.
write	write receives trace data and stores them in an EXCEL 4.0 data file.

**Tab. 6-6:** Description of LLCS service tasks

Task	Description
ritsk	ritsk reads in axis resolvers and motor resolvers. A shared global MB II memory (RI_DAT) is used for communication with main tasks. ritsk is started and initialized by iotask. During operation it is controlled directly by the position controller.
diotask	diotask, running on the DIO board, reads/writes the digital in/outputs. It is controlled by the iotask using a MB II global shared memory DIO_DAT..
ai table driver	the table driver of the analogue input board is started by the iotask.

**Tab. 6-7:** Description of LLCS IO-tasks

## 6.3 FUNCTIONAL IMPLEMENTATION OF MOTION CONTROL SYSTEM

### 6.3.1 Communication

The communication between different units of the EMCS (HB, HLCS, LLCS, GWS) is done with different telegrams (command telegrams, parameter telegrams, etc.). All telegrams have the same telegram structure, consisting of the telegram head and the telegram contents (Tab. 6-8).

Structure of EMCS Telegrams		
telegram length	2 bytes	telegram head
telegram number	2 bytes	
contents of telegram	between 4 and 1152 bytes	structure different for each telegram

**Tab. 6-8:** Telegram structure for EDITH motion control system

The telegram head contains information about the telegram type (telegram number) and the length of a telegram. As the telegram length is variable there will be just the information transmitted, which is really needed. The telegrams are defined in the EMCS header files tel0.h, tel1.h, tel2.h, tel3.h. As data are transmitted in binary formats data conversion between the different data formats will be necessary. Because the HLCS is the central communication node data conversion is processed on this system. The telegram number format is the number format of the addressed link partner of the HLCS.

## 6.3.2 Function

### 6.3.3 Parameter Handling

There are two types of parameters: System parameters and operator parameters.

System Parameters	kinematics parameters (length of links), limits for velocities, accelerations, deceleration, ranges, parameters defining the error reaction, configuration of IO-logic, tolerance limits for alignment.
Operator parameters	max. velocities, accelerations, deceleration, flypoint tolerance, elbow status

If there exists a corresponding operator parameter for any system parameter, the operator parameter is limited to the value of the system parameter. Parameters can be defined for each work unit separately.

Parameters are stored on HLCS as well as on the LLCS. So the LLCS is able to operate in a stand alone mode and may be controlled by the service task or by the simple handbox connected directly to the LLCS.

### 6.3.4 Path Planning

The EMCS supports an automatic path planning (<bplarepa>). Path planning in case of the EMCS means, that the operator can order a motion by giving in a few path points, which shall be passed. There exist three different modes of path planning: APC, PPC and CHECK planning. While APC commands give the path in form of axis points, PPC commands define the path as cartesian points, with 4 degrees of freedom. The check planning is similar to the APC planning. During check all axis are moved by a certain amount and reverse to the original position.

#### 6.3.4.1 APC Planning

APC planning (<bplarepa/apc\_plan>) processes path planning for axis positioning mode. The input path is given by a telegram containing the number of moved axis, the number of segments, the axis identifiers and the path points. In a first step apc\_plan eliminates useless points, whose distances are smaller than a fixed limit. Afterwards there will be calculated off-line the duration of acceleration, deceleration and constant velocity phases in that way, that all axis will be synchronised, i.e. over all axis the duration for acceleration, constant velocity and deceleration phases will be equal. Based on these parameters and also with respect of the valid system and operator parameters there will be calculated on-line the new nominal data, which are accessed by the position controller <posreg> using a shared memory. On-line in this context means, that new nominal data will be calculated with the same rate as the position controller will consume them. The following picture shows an APC path planning for two axis. An example for APC-planning is shown in Fig. 6-7.

The move command belonging to it has the form

```
MOVE JOINT Z1 Z2 VIA 0.4 0 VIA 0.8 0.4 VIA 0 0
```

### APC-Planning

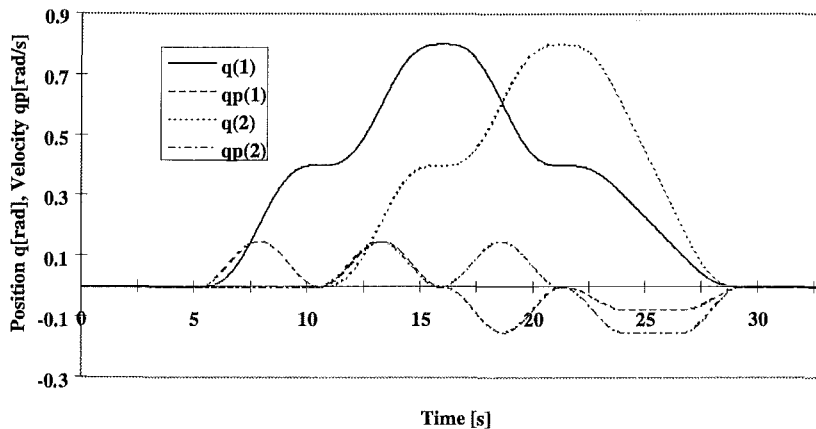


**Fig. 6-7:** Position (q) and velocity shape (qp) generated by APC-Plan

#### 6.3.4.2 PPC Planning

PPC planning (<bplarepa/ppc\_plan>) operates quite similar to the APC planning. There are given several path points each defined by a 4-tupel (x, z, r, y). After elimination of useless points, which is similar to APC planning there will be calculated parameters, which define the latter cartesian path. Besides velocities, acceleration and deceleration for translation and rotation the operator parameter „via radius“ has a great influence. The flypoint is defined as the midpoint of the line segment, which is defined by the points of intersection of two neighbouring linear path segments and a circle with flypoint radius around the via point. The linear segment however will be left at a distance, which amounts two times the flypoint radius, that way, that it will cross the flypoint tangentially (Fig. 6-8)

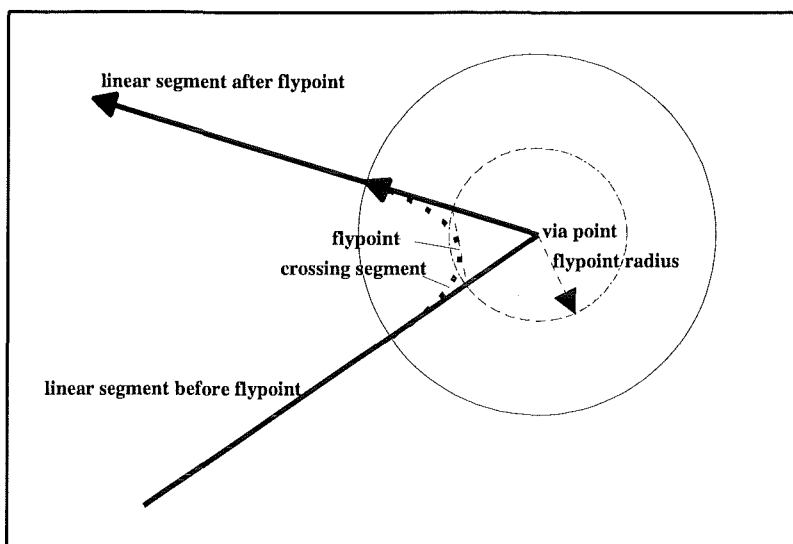


**Fig. 6-8:** Principle of cartesian path planning at a via point

The function of EDITH path planning is illustrated within Fig. 6-9 with rounded corners at the via points. The corresponding move command, when executed in TOOL system, would have the form: MOVE POINT VIA -1000 0 0 0 VIA -1000 1000 0 0 VIA 0 1000 0 0 TO 0 0 0 0.

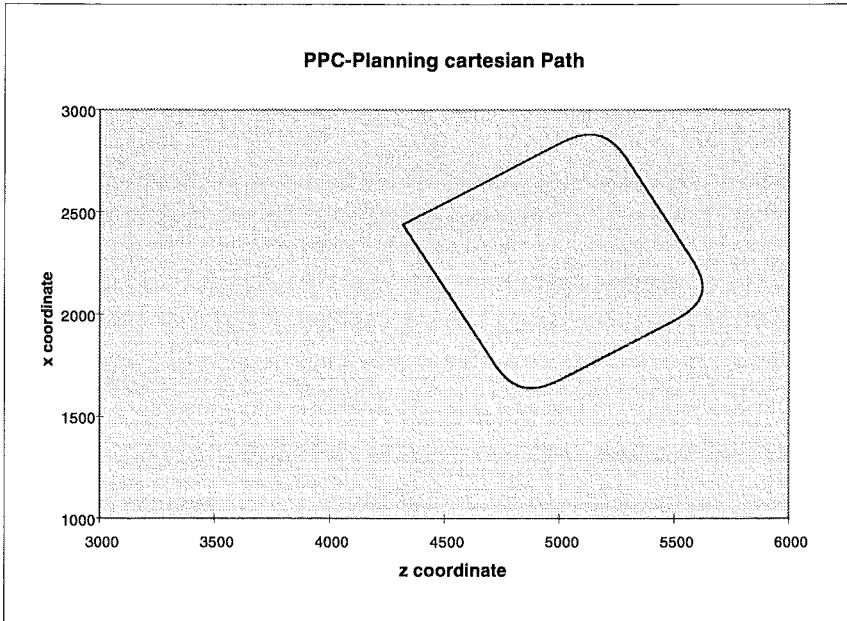


**Fig. 6-9:** Square shaped cartesian path as result of EDITH's PPC-planning.

### 6.3.4.3 Check Planning

Check planning is quite similar to APC control mode. During check planning all axis are moved at a certain amount, which is defined by the system parameter for axis integrity check, and back to the initial position. Check is always performed after execution of a docking operation.

### 6.3.5 Inverse kinematics Transformations

Realising spatial movements with the ABT, there exists the need for implementation of an inverse kinematics transformation. As the ABT has a really complex kinematics, there are kinematics redundancies and in consequence, there exists a infinite number of solutions for a given spatial position.

The problem is illustrated by Fig. 6-10.

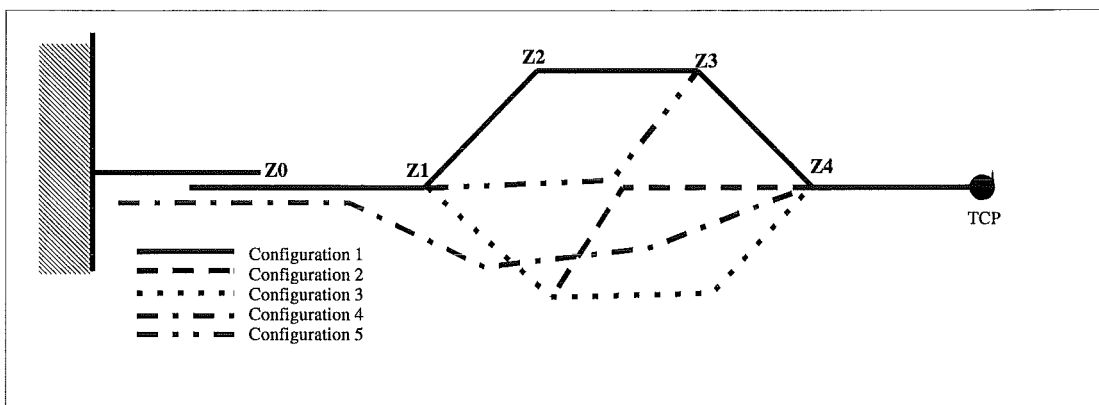


**Fig. 6-10:** Redundant kinematics of the EDITH ABT

As the ABT's TCP has three degrees of freedom (2 position, 1 orientation), the ABT however 5 degrees of freedom, there exists an infinite number of solutions. With exception of the last link, whose spatial position and orientation are defined by the TCP, all other links can take various configurations, to satisfy the given boundaries, i.e. a fixed support structure and the TCP position. To control the inverse kinematics transformation, the degrees of freedom are reduced by fixing 2 of five joints. As axis Z0 (translation) is not realised at the EDITH system this axis is fixed by default. In addition any of the other 4 ABT axis may be fixed.

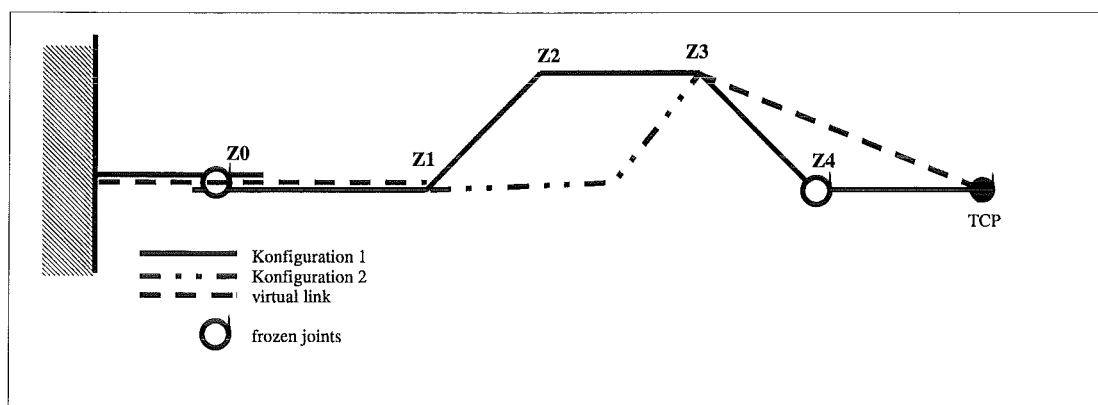


**Fig. 6-11:** Freezing joints for reduction of redundancies

As Z0 and Z4 are fixed, the concerning links can be replaced by virtual links. Now there remain two solutions for the inverse kinematics transformation. (configuration 1 and configuration 2). Further it is possible to choose between the two solutions within a small area around the singularity by choosing the elbow status. Elbow status right would refer to configuration 1 elbow status left to configuration 2. Normally elbow status equal will work sufficiently. When approaching a singularity (when right elbow approaches left elbow) however the selection of a solution must be controlled manually. In this case the joint velocities increase above the given limits and the transformation will abort with an error. When this will happen, there should be performed a reconfiguration. During reconfiguration the axis, which makes problems because of a singularity should be frozen. Assign this axis to the joystick and move it joystick controlled. The position of the TCP will be kept constant, while all other axis positions will be calculated to satisfy this condition

In addition to the boom's kinematics, there also are redundancies in the inverse kinematics transformation for the EEPU. As there are three parallel linear axis, there also exists an infinite number of solutions. The operator is enabled to control this inverse transformation by definition of a ratio, which defines how a given distance will be shared among the three axis of the EEPU.

### 6.3.6 Teach-Repeat

To accelerate the performance of handling tasks and also to avoid human errors, there is implemented a special command processor (<scp>). Using this feature the operator will be enabled to teach motion sequences off-line This also allows the operator to test sequences off-line before executing them on-line, i.e. moving the real machine. The main capabilities are:

- Macrolike sequence

- Parameter integrity
- Symbolic (named) points
- Recycling of point databases
- Execution step by step in forward and backward
- Teaching on-line and off-line
- automatic monitoring during execution (alignment check)

### 6.3.6.1 Macro-like Sequence

The operator can teach in sequences quite similar to macros. The syntax of the commands is the same as used in direct control mode, during execution there will be performed some checks to guarantee the correct function and to avoid operator errors.

In principle there are three possibilities of handling these sequence files:

```
TEACH <filename> [ POINT_DEFINITION <other_filename>]
```

```
EXECUTE <filename >
```

```
MODIFY <filename >
```

While teaching generates a new sequence file with copying the point databases of the other\_file EXECUTE starts execution. MODIFY offers the opportunity of editing the sequence. During editing it is possible to execute sequences step by step, forward as well as reverse with inserting or deleting commands. The connections are shown in Fig. 6-12. The half arrows shall illustrate, that a mode can only be left on the reverse way. The referring command for mode switching is located on the side of the side of the half arrow.

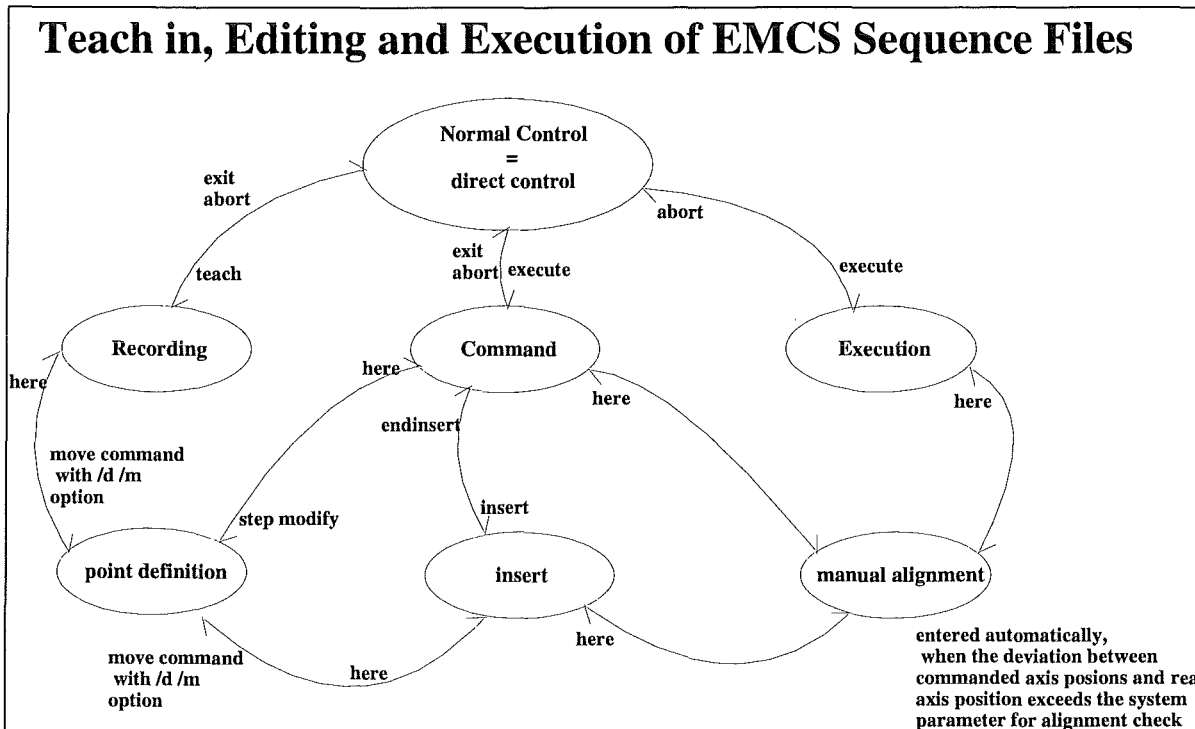


**Fig. 6-12:** Teach/Execute/Edit of sequence files

Notes:

The direct control operation mode is the default operation mode, which will be entered during starting up. Changing between simulation and motion mode is exclusively possible in this operation mode. In direct control operation mode the operator can move the manipulator directly either by APC and PPC commands or in AVC and PVC with joystick control.

The insert submode is similar to the recording submode: While recording inserts new commands at the end of the sequence, the insert command inserts them at the actual position.

The manual alignment mode will be entered automatically in case of the deviation between real position and the commanded position (point database) differs more than the corresponding parameter. During manual alignment the operator has direct control, i.e. moving the machine using move commands or joysticks.

A named point may be marked as to be defined (option /d) or to be modified (option /m). Entering point definition mode gives the operator the opportunity to move the machine in direct control (see above) to the desired position. The actual position is confirmed with HERE.

During step modify there will be executed the next move command, with entering point definition at each named point. (redefinition of all points referenced by that move command)

During command submode there can be entered several commands, which are used as switches between several edit functions:

INSERT	enters insert mode
STEP MODIFY	enters point definition submode
DELETE	deletes the next command
STEP [n]	executes the next n commands (default: n=1), n may also be negative (reverse execution)
SKIP [n]	skip the next n commands (default: n=1 , n > 0)

### 6.3.6.2 Point Databases

Instead of direct positioning of axis or TCP by value, the operator is forced to use named points within teach files. The commands used for those motions are:

*MOVE EDITH via <point1> [via< point2>]\*n TO <endpoint > APC mode*

*MOVE POR via <ppo1> via <ppo2> TO <end\_ppo> PPC mode*

During execution the HLCS generates a move telegram to the LLCS, replacing symbolic names with the position data (joint positions or cartesian position of the POR) from the database.

Each repeat sequence owns two point databases, which are stored in own files. The filename corresponds to the sequence name: sequence\_name.APO and sequence\_name.PPO. While the .APO file contains all axis points including the \$FIRST\_POINT the .PPO file contains the position points, i.e. the cartesian position and in addition the axis positions and configuration of inverse kinematics transformation (elbow, frozen joints).

If a named point shall be defined or modified, the operator marks those points in the move statement with the /d or /m option. The HLCS generates a move command containing all known points, which are located in the path before a point which has to be (re)defined. Then the HLCS switches to direct control mode. In this mode the operator is able to move the ABT directly with APC and PPC motion commands as well as in AVC, PVC using joysticks. During definition of an axis point there are no restrictions. Defining position points there may be used PPC or PVC moves exclusively to ensure the validity of the inverse kinematics transformation. It is also not allowed to change the elbow status or the fixed (freeze) joints during point definition, which would also cause errors, while executing the complete move in execution mode. The point definition mode is left by confirming the actual position as the desired point giving a HERE statement. This procedure will be repeated until the complete move command will be finished. While there are allowed any known points within a APC move, there exist some restrictions teaching PPC moves: Each position point does reference an axis point. There may be combined only position points to a path including the start point, which reference the same axis point and the referenced axis point itself. This enable the operator to teach an existing sequence in reverse direction.

### 6.3.6.3 Parameter handling during execution of sequences

During teach in all system and operator parameters, which were valid, when entering the recording submode, are stored within the sequence head, which is located at the beginning of

each sequence file. While system parameters won't be downloaded during execution or editing, all operator parameters will be compared to those, which were valid during teach in. Parameters, which differ will be downloaded to the LLCs system. This ensures the same operation behaviour (velocities, acceleration etc.) as during teach in phase. Changes of system parameters however will remain. So all adaptations of system parameters will be still available.

#### **6.3.6.4 Alignment Check**

As a feature to check the correct function of the system there has been build in the alignment check function within the HLCS. Alignment check will be performed in edit and execution mode. Before executing a sequence move command (MOVE EDITH or MOVE POR) the current axis configuration will be compared with the axis configuration of the start point (\$FIRST\_POINT in point database). If any joint differs more than the tolerance limit for performing of an automatic alignment, which is a system parameter, the HLCS will switch automatically to manual alignment mode. In this mode the operator can move the manipulator interactively to the desired position. Giving a HERE command, the operator confirms this position as correct and the system will return to the execution mode. If the difference amounts more than a 5th of the tolerance limit for detection of unexpected motion, there will be performed an automatic alignment. During automatic alignment, the HLCS itself generates a motion command, which commands all disaligned axis to the correct position. The complete alignment check procedure will be repeated until all axis are aligned with an accuracy of one 5th of the tolerance limit for detection of an unexpected motion. After leaving alignment mode the move command will be executed.

### **6.3.7 Position Controller**

#### **6.3.7.1 Servo Drive Units**

As the EDITH system was designed under the condition of a favourable relation between payload and its own weight, there have been chosen synchronous AC servo drives to drive the manipulator. This type of drives promised a good relation between power/weight/size and efficiency. To synchronise the two motors of one cyclo drive unit there has been build in an electronic synchronous controller. There have been also performed tests with synchronisation by taking the current monitor of the master servo controller as current set point for the slave controller, what worked not sufficient due to the reluctance torque, which is characteristic for this type of motor.

The present structure of servo drive unit integration into the control system is shown in Fig. 6-13. The motor position of the master servo motor will be measured using the encoder emulation output of the servo controller. The slave motor will be controlled by the electronic gear that way, that the pre-load angle, i.e. the position difference between master and slave motor, will be tuned to the nominal pre-load angle. The electronic gear is connected to the LLCs component of the EMCS via RS232 interface. While starting a motion the electronic gear sets the nominal pre-load to the actual pre-load. With a short delay to the start of motion <posreg> task will force the <asb> task to send a command to the synchronous gear, which sets the nominal pre-load angle to 0. As the encoders works with increments instead of absolute positions, the synchronous gear must be adjusted once to a defined preload state. Therefore the gear preloading will varied interactively, until the current monitor of the servo

drive reaches 10% of the nominal value. In this state the nominal and current preload will be set to zero.

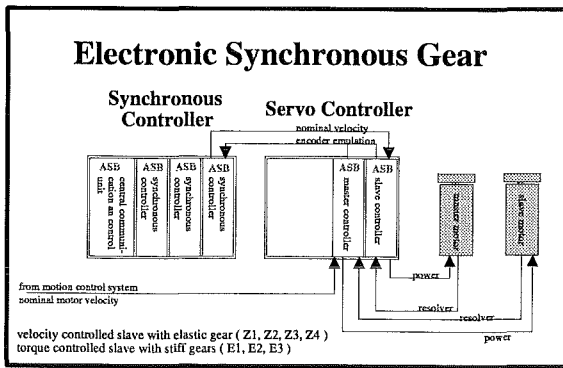


Fig. 6-13: Electronic synchronous gear

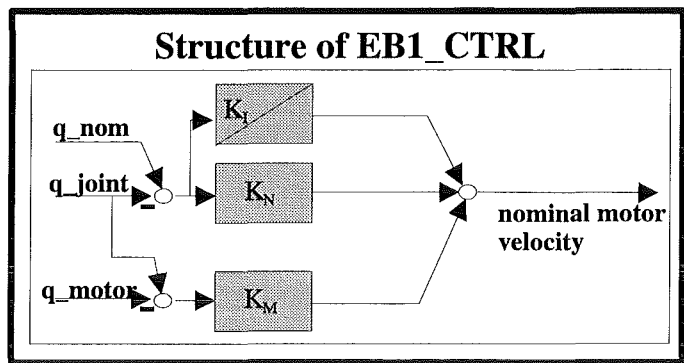


Fig. 6-14: Control scheme of EB1\_CTRL

To support the operator with maintaining the electronic gear, there has been implemented a function, which documents the difference between the position of motor resolvers and the actual value of the encoder counter to a file, which can be evaluated manually by the system manager.

### 6.3.7.2 Position Controller

On LLCS there is implemented a position controller, which supports centralised controllers as well as non central controllers. There have been implemented and tested several control algorithms:

PID_CTRL	a non central PID-controller with a limitation of the integral part
EB1_CTRL	a nom central controller, evaluating the gear preloading
ZR1_CTRL	state space controller
INV_ED	a model based controller, which depends on a inverse dynamic model of the 4 joints

Those control algorithms refer to the 4 main joints Z1 to Z4. All other joints are controlled by the first controller type. The controller type is specified within the system parameter file.

#### PID\_CTRL

The PID\_CTRL controller is some kind of a PID controller. The integral part is limited by a anti windup algorithm, which reduces the integral part that way, that the PID output would not exceed a specified limit. The integral part will be minimally reduced to zero, i.e. limitation will not change its sign. This controller worked not sufficiently. High path precision could be reached with a big proportional part, which however caused increasing oscillations. The compromise with a lower path accuracy and damped oscillation brought no sufficient result. This controller still is used for tuning of the servo controllers analogue inputs with the „monnullfw1“ parameter file as a simple feed forward controller and no feedback term.

#### EB1\_CTRL

This controller is designed to damp oscillations optimally. The algorithm evaluates the difference between motor position and joint position, which is appropriate to the gear preloading. The gain parameters may be calculated from the oscillation frequency of the stretched arm. The structure is shown in Fig. 6-14. The constants  $K_M$  and  $K_N$  are calculated as

$$K_M = \sqrt{3} * \Omega$$

$$K_N = \frac{\Omega}{3 * \sqrt{3}}$$

(corresponds to the first Eigen-frequency of the stretched manipulator. The Eigen-frequency was measured and (calculated to be 5.4rad/s.

ZR1\_CTRL (state space controller)

There has been tested an other non central control structure quite similar to EB1\_CTRL, which was based on a state space control design, with given poles. During design there was supposed only one joint moving all others however were supposed to be stiff. Simulated on a 4 joint model, there could be shown, that the model was no longer stable in all configurations.

INV\_ED (inverse model based controller)

Industrial robots and manipulators, which are controlled with conventional non-central controllers have a very weak coupling between their joints. This can be seen in the matrix of inertia, where the elements beside the main diagonal are much smaller than element, which are located on the diagonal belonging to the same row or column. The EDITH manipulator owns a very complex dynamic structure (4 joints with identical orientation) with a strong dynamic coupling between the for main joints Z1 ... Z4. Evaluating the matrix of inertia for this 4 joint system, there can be seen, that the elements beside the main diagonal have the same dimension as the elements , which are lying on the main diagonal. In some cases they exceed they main elements:

$$M_T = \begin{pmatrix} 324 & 223 & 133 & 56 \\ 223 & 152 & 98 & 42 \\ 133 & 98 & 64 & 28 \\ 56 & 42 & 28 & 16 \end{pmatrix}$$

As the matrix elements vary over a wide range, the matrix cannot be supposed to be constant. As each of its 16 elements consist of highly non-linear terms containing lots of trigonometric functions and vary over a wide range, it obviously costs a high effort to calculate its elements. In this context, *AGRIS Web1* , a modelling system developed by FZK was used to calculate the matrix. Giving in some mechanical parameters (dimensions, inertia, mass, range of position, velocity, acceleration etc.) AGRIS supports symbolic calculation of the inertia matrix. Within given limits for velocity and position those terms, which have a small influence on the dynamic behaviour are removed. AGRIS further optimises the code by extracting and substituting terms. In a final step there is created an autocode. When AGRIS processed the model of EDITH it could be shown, that there was no possibility to ignore terms, what expresses the strong dynamic coupling among the axis. So AGRIS just optimised the algorithm by extraction and substitution of algebraic terms. Simulations showed, that the

system is stable over a wide range of parameters, even if mass and inertia will be doubled or halved.

The structure of this controller type is shown in Fig. 6-15.

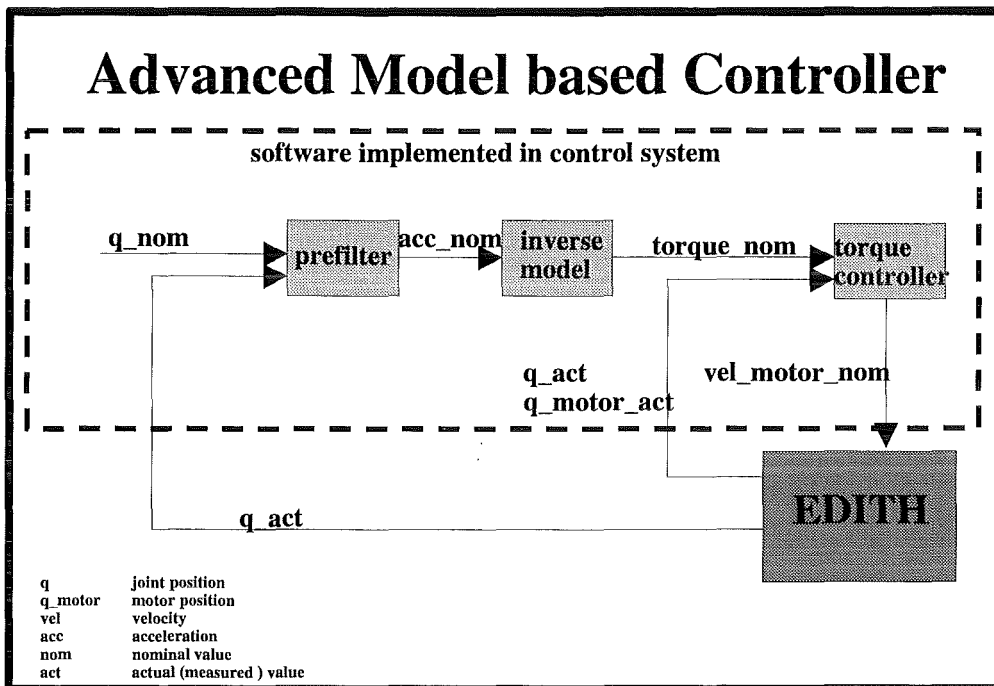


**Fig. 6-15:** Structure of inverse model based controller with reference behaviour

Within this control scheme all signals (arrows) must be taken as a vectors of the dimension 4. The control difference is filtered by a prefilter, which contains the PT2 characteristic, i.e. the output is an acceleration, which would result in a PT2 characteristic when integrated twice. The four signals are not crosscoupled by the pre-filter. The inverse model follows as second step, which contains the reciprocal dynamic behaviour of the EDITH mechanic marked as block EDITH. The inverse model exits nominal torque for each joint, which is controlled by a succeeding torque controller (P-controller with feed forward characteristic). The result is shown in Fig. 6-16.

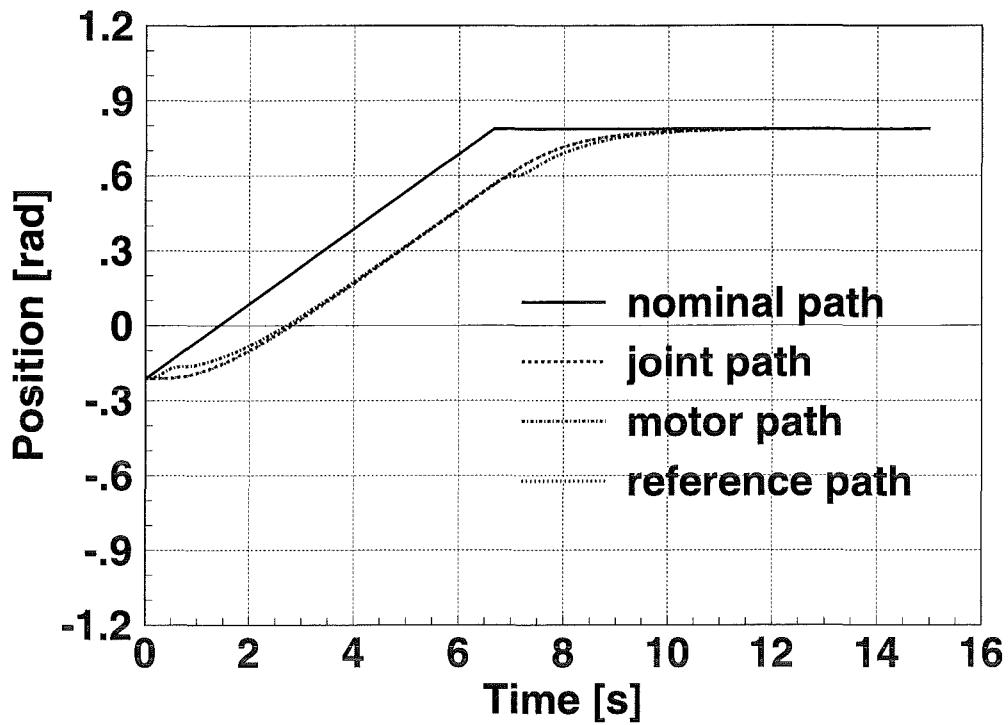


**Fig. 6-16:** Nominal, reference, motor and joint path

As it can be seen in Fig. 6-16 the reference path and the joint path are identical. Gear elasticity results in a difference between joint path and motor path, especially during acceleration and deceleration phases.

## 6.4 COMMAND SET

The following tables give an overview over the EDITH command set.

### 6.4.1 Legend:

priv	is the required user privilege for using this command	- = none required O = operator privilege M = system manager privilege
ctxt	context in which the command can be used	NR = not in conjunction with repeat sequences T = teach mode E = edit mode R = repeat mode
appl	application to control mode	AVC = axis velocity control APC = axis position control PVC = POR velocity control PPC = POR position control
proc	processing system	H = HLCS L = LLCS
POR	Point Of Reference	A point comparable to the TCP in roboter techniques. As the TCP will be reserved for working units, there has been chosen a new name. The POR is related to the work unit mounting flange at the EEPU.

### 6.4.2 EDITH command set

#### 1. Session Control

Command	Qualifier1	Qualifier2	priv	ctxt	appl	proc	Description
login	assistant_operator operator system manager		- O M			H	assistant operator operator system manager
logout						H	terminate session

#### 2. Display Commands producing a single Message Telegram

Command	Qualifier1	Qualifier2	priv	ctxt	appl	proc	Description
show [<wu_grp>]	operator_parameters system_parameters	< group name >	-	all		H	displaying parameter files
show	error_log		-	all		H	display error log file
show	directory		-	all		H	display list of sequence files
show	session		-	all		H	display session information
show	repeat_sequence_description		-	TER		H	display descriptioal text
show	point	< point_name >	-	TER		H	display point data (co-ordinates, references)
show	point	*	-	TER		H	display list of all known points
show	motion_load_state	*	-	all		H	display sensor data
show	switch			all		H	show setting of switches

#### 3. Display Commands producing periodical Message Telegrams

Command	Qualifier1	Qualifier2	priv	ctxt	appl	proc	Description
monitor	positions		-	all	all	H	displaying position data (joints, cartesian, inclinometers)
monitor	joystick_controlled_axis		-	all	all	H	displaying positions of joystick controlled axis
monitor	off		-	all	all	H	switch off monitoring

#### 4. Set System Parameters

Command	Qualifier2	Qualifier2	priv	ctxt	appl	proc	Description
set [< wu_grp>]	system_parameter	<group_name>	M	NR		H,L	setting system parameters
monitor	joystick_controlled_axis		-	all	all	H	displaying positions of joystick controlled axis
monitor	off		-	all	all	H	switch off monitoring

## 5. Set System Parameters

Command	Qualifier1	Qualifier2	priv	ctxt	appl	proc	Description
set [< wu_grp>]	velocity joint i velocity por translation velocity por rotation	to <value>	O	NR,T,E	all	H,L	set velocities for path planning
set [< wu_grp>]	acceleration joint i acceleration por translation acceleration por rotation	to <value>	O	NR,T,E	all	H,L	set acceleration for path planning
set [< wu_grp>]	deceleration joint i deceleration por translation deceleration por rotation	to <value>	O	NR,T,E	all	H,L	set deceleration for path planning
set [< wu_grp>]	left_limit <axis>	to <value>	O	NR,T,E	all	H,L	set left limit of axis range
set [< wu_grp>]	right_limit <axis>	to <value>	O	NR,T,E	all	H,L	set right limit of axis range
set	override transport_unit override working_unit	to <percentage>	O	all	all	H,L	set override factors
set	crp	to <dy,dz,dr,dy>	O	NR,T,E	PVC,PPC	H,L	define CRP position relative to base system
set	por	to <dy,dz,dr,dy>	O	NR,T,E	PVC,PPC	H,L	define POR position relative to working unit mounting flange
set	eepu_ratio to	<e1,e2,e3>	O	NR	PVC,PPC	H,L	Define the ratio for the inverse kinematics transformation of the EEPU axis. They will be standardised to a value of 1 by the HLCS. There may be also negative values allowed.. The vertical component of a cartesian move will be splitted at a ratio of e1:e2:e3 between the axis E1, E2, E3.
set	flypoint_tolerance joint <i>	to <value>	O	NR,T,E	APC	H,L	set tolerance area for axis flypoint
set	flypoint_tolerance por	to <value>	O	NR,T,E	PPC	H,L	set tolerance area for POR flypoint
set	flypoint_tolerance override	to <percentage>	O	NR,T,E	APC,PPC	H,L	set tolerance area for flypoint
set	alignment_check axis <i>	on off	O	T,E	APC,PPC	H	set tolerance area for flypoint
mode	motion simulation		O	NR		H,L	switch between simulation mode
set	configuration to <j>		O	NR		H,L	set actual working unit configuration
set simulation position	joint <i [ j ...]>	to <vali [ valj ...]>	O	NR		H,L	definition of simulated position

## 6. Parameter Disk File Operations

Command	Qualifier1	Qualifier2	priv	ctxt	appl	proc	Description
save	system_parameters	[<filename>]	M	NR		H	save system parameters on file, no filename -> syp\$default
save	operator_parameters	[<filename>]	O	NR		H	save operator parameters on file, no filename -> opp\$default
recall	system_parameters	[<filename>]	M	NR		H	load system parameters file into HLCS memory
recall	operator_parameters	[<filename>]	O	NR		H	load operator parameters file into HLCS memory
load	system_parameters		M	NR		H	transmit system parameters to LLCS file
load	operator_parameters		O	NR		H	transmit operator parameters to LLCS file
copy	system_parameters	to <wu_grp>	M	NR		H	copy system parameters of actual configuration to specified wu_grp parameter set
copy	operator_parameters	to <wu_grp>	O	NR		H	copy operator parameters of actual configuration to specified wu_grp parameter set

## 7. System Integrity Check

Command	Qualifier1	Qualifier2	priv	ctxt	appl	proc	Description
check	all_joints joint <i>		O	NR		H,L	starts an integrity check. This will cause a small motion of the specified axis to ensure the correct working of the system. Check is performed automatically at the end of a docking event.

## 8. Motion Control Mode Changing Commands

Command	Qualifier1	Qualifier2	priv	ctxt	appl	proc	Description
assign	por joint <i,j,k>	to joystick <n>	O	NR,T,E,R	PVC AVC	H,L	Select axis which may be controlled by joystick. Assignment: i (EDITH) -> x (joystick) j (EDITH) -> y (joystick) k (EDITH)-> z (joystick)
joystick_control	axis por reconfiguration off		O	NR,T,E,R	AVC PVC	H,L	Switching on joystick control. This mode is left with qualifier1 = off.
freeze_por_joint	<i,j>		O	NR	PVC, PPC	L	Define, which axis shall be fixed during motion of POR.
por_control	world tool		O	NR,T,E,R	PPC, PVC	H,L	Defines the reference frame for position control. (either CRP or POR)
elbow	left right equal		O	NR,T,E,R	PPC, PVC	H,L	Select the resolution of singularities.
docking	mount dismount		O	NR		H	Enter docking mode for mounting or dismounting working units. In this mode, teach, repeat and edit functions are disabled. This mode is terminated by testing all EDITH joints with CHECK command.

## 9. Motion control Commands

Command	Qualifier1	Qualifier2	priv	ctxt	appl	proc	Description
move joint	<n-tupel> [via <n-tupel>]	to <n-tupel>	O	NR,T ,E,R	APC	H,L	APC command n-tupel is a sequence of n values, which are separated by a comma. The optional via may be repeated.
move edith	[via <p_name> [</d >]] [</m>]]	to <p_name>[</d>] [</m>]	O	T,E	APC	H,L	APC command with named axis points. This command is used while editing or teaching in sequence files. The modifier /d and /m may not occur simultaneously at the same point.
move por	[via <p_name> [</d >]] [</m>]]	to <p_name> [</d>] [</m>]	O	T,E	PPC	H,L	PPC command with named position points. This command is used while editing or teaching in sequence files. The modifier /d and /m may not occur simultaneously at the same point.
move point	<4-tupel> [via <4-tupel>]	to <4-tupel>	O	NR,T ,E,R	APC	H,L	PPC command 4-tupel is a sequence of n values, which are separated by a comma. The optional via may be repeated. Depending on the reference frame (world or tool) the manipulator will move in absolute co-ordinates or incremental, referring the POR.
(joystick telegrams)			O	NR,T ,E,R	AVC, PVC	L	
switch	<i>	on off	O	all		L	switch group i on/off (1 (i 5)
brake	all n_tupel		O	all		L	engage all brakes
stop			O	all	all	L	emergency stop: velocity setpoint = 0 engaging brakes. After short delay (system parameter for switching servos off)servo amplifiers will be switched of too.
halt			O	all	all	L	gentle stop: All moving joints are decelerated at the maximal allowed
continue			O	all	all	L	acknowledge after emergency and gentle stop. After continue, there will be allowed new motion commands.

## 10. Teach and repeat Functions

Command	Qualifier1	Qualifier2	priv	ctxt	appl	proc	Description
teach <seq_file>	[point_definition <old_seq_file>]		O	NR		H	Enter teach mode, start a new repeat sequence file and optionally include point definitions from existing sequence file.
modify	<old_seq_file>		O	NR		H	Enter edit mode.
execute	<old_seq_file>	[skip <n>]	O	NR		H	Execute the specified repeat sequence, optionally skipping the first n commands..
skip	<n>		O	E		H	Skip the next n commands within the edited sequence file. APC command
insert			O	E		H	Enter insert submode within the edited sequence to add new commands at the actual position.
end_insert			O	E		H	terminate insert submode
delete			O	E		H	delete the next command within the edited sequence
step	modify		O	E		H	execute the next command with entering point definition at each referenced point.
step	<n>		O	E		H	execute the next n commands
here			O	T,E		H	return to previous submode (from point definition or manual alignment submode)
undo			O	T		H	return to the state before the recorded command and erase the command from the repeat sequence
pause	[<text_string>]		O	T,E		H	define a rest point and optionally store a line of text for displaying, when the restpoint is encountered during execution of the sequence. This interrupt of sequence execution may be continued by giving a resume command.
resume			O	R		H	resume execution of the repeat sequence at a rest point.
exit			O	T,E		H	exit teach or edit mode, preserving the output file (normal exit)
abort			O	T,E,R		H	In teach and edit mode: terminate the mode and delete the output file. In repeat an simulation mode: terminate the execution immediately.

## 6.5 EXPERIENCES AND CONCLUSIONS

### 6.5.1 General Conclusions

- The EDITH motion control system is able to control the EDITH ABT with a high reliability.
- Even with its nominal payload of about 1 to it is possible to move at a joint velocity of 0.15 rad/s horizontally and a linear velocity of 20 mm/s (E1) or 40 mm/s (E2, E3) vertically.
- At the maximal velocity, the path accuracy amounts 100 mm, with slow motions it has be shown to be 10 mm. The repetition accuracy is defined as a fifth of the system parameter for detection of unexpected motions and can be influenced by adapting this parameter. The position controller itself is able to control the joint position at an amount of 1 resolver digit, which should result in a repetition accuracy of about 2 mm. Due to a backlash in the joint resolvers fixing the measured value amounts nearly 5 mm. The absolute positioning accuracy however has be shown to be 85 mm Woll 1, Woll 2, Div Hand.

### 6.5.2 Hardware

- The HLCS hardware and Software (VAX/VMS) is proved to be very reliable and of a high stability. It is a relict of the required TARM compatibility. As it is a normal universal microcomputer without any special hardware it could be also integrated within the remote handling workstation.
- The MBII hardware was shown to be of a high quality and highly reliable.

- As all signals are collected within the LLCS, the density of cabling is very high and therefore there is a high potential for defects. Especially the cabinet build in 57 pin AMD connectors caused troubles with every modification, because crimped wires slipped out of the pin or also pins slipped out of the casing. This might be not an intrinsic problem of the AMD connector but more a problem of the mechanic, who build up the system but nevertheless it shows, that it is not easy to handle high density connectors. As the connectors are placed just around the build in heat exchanger it was not easy to repair defects. In a future system there should be integrated industrial field bus systems like InterbusS, CAN or ASI, which are meanwhile state of the art. This will reduce the electromechanical complexity, will result in a hierarchical hardware structure and in sequence maintenance will be much easier than today.
- The electronic synchronous gear has been shown to be a good method to synchronise two velocity controlled motors, which are also coupled by a elastic gear. The previously planned torque control *Spec* was not possible, as synchronous AC servo drives own reluctance torques, which amount about 10 percent of the nominal motor torque. It has been shown that a gear preloading of 10 percent of the nominal torque was reasonable which corresponds more than 1 motor turn.

### 6.5.3 Software

- The iRMX operating system has been shown to be a good choice with very short response times far below 1 ms.
- The CPU load amounts up to 20%, even if there will be running the model based controller which costs 0.3 ms.
- Collecting joint positions is the most time costing operation. Future improvements should aim primarily at this operation. High speed peripheral buses like CAN and InterbusS should be taken into account. The software is well structured and it could be shown, that it is possible to get into the software and make changes, which require a good overview over the functional context.

### 6.5.4 Handling of the EMCS

- Since there had been introduced the EDITH DOIF as a user interface, the EMCS may be operated intuitively. Although it takes some experience to handle the system with all of its capabilities.
- As one of the most difficult parts there must be seen the inverse kinematics transformation, which demands the operator to have a good imagination. Therefore further developments should also include a new transformation, which automatically handles the redundancies while moving all axis simultaneously and which also takes account of the geometry of the torus. Otherwise it will not be possible to perform wide range cartesian movements.
- Supporting the operator with parameter databases has been shown to be reasonable. While downloading of system parameters takes a few seconds, downloading of operator parameters takes one and a half minute for each parameter will be set with transferring an own telegram. It should be possible to transmit operator parameters within one or two telegrams to accelerate downloading of operator parameters.

## 6.6 FURTHER DEVELOPMENTS

- When this documentation was in work, Intel, which is the manufacturer of the Multibus II hardware and the iRMX operating system, announced, that it will stop production of Multibus II architecture and iRMX software. They were just looking for an other company, which will continue with MBII/iRMX. As it is not sure, whether this hardware and software platform will be supported by some manufacturer, a succeeding system could migrate to an other platform.
- As the layout of the EDITH motion control system is more than 5 years old, this layout doesn't represent the current state of the art. This mainly concerns the integration of peripheral units like servo controllers, resolvers and force sensors. The application of peripheral buses (CAN, InterbusS, ASI) should be taken into consideration.
- It has been shown, that the repetition accuracy meets the specification. Changes within the construction of the resolver fixing would be done to reduce backlash. This might be done with preloading the resolver by a spring.
- The inverse kinematics transformation should be improved. Automatic handling of redundancies with flexible freezing of joints should be possible. Torus geometry should be supported to enable spatial movement over a wide range.
- As calculation of the dynamic model takes just 0.3 ms there can be integrated a dynamic simulator in simulation mode. This will make the simulation more realistic.

## 6.7 REFERENCES

- Woll 1: J. Woll: unpublished report, June 1994
- Woll 2: J. Woll: unpublished report, July 1995
- Binz R. Binz: unpublished report, March 1995
- Spec : Breitwieser, Frank, Holler, Süß, Leinemann: Specification of EDITH MOTION CONTROL SYSTEM, KfK-4787, September 1990
- Web1 : Weber, W.: AGRIS: unpublished report, June 1990
- EMCS I EDITH Software Documentation of LLCS, unpublished
- EMCS II EDITH Software Documentation of HLCS, unpublished
- EMCS III EDITH User's Manual of the EDITH Motion Control System, unpublished
- EMCS IV EDITH Hardware Documentation of the EDITH Motion Control System, unpublished
- Div Hand Leinemann, K., Woll, J., Haferkamp, B.: unpublished report, January 1996

## Table of Content

<b>7 STATIC AND DYNAMIC QUALIFICATION TESTS.....</b>	<b>7-3</b>
<b>7.1 VALIDATION OF THE STRESS ANALYSIS .....</b>	<b>7-3</b>
<b>7.2 POSITIONING AND REPEATABILITY ACCURACY.....</b>	<b>7-3</b>
<b>7.3 HORIZONTAL STIFFNESS .....</b>	<b>7-5</b>
7.3.1 Description of the performed tests .....	7-5
7.3.2 Total stiffness referring to the boom tip .....	7-5
7.3.3 Deflection of joints due to boom tip deflection .....	7-7
7.3.4 Forces between drive unit (torque arm) and link .....	7-9
7.3.5 Conclusions .....	7-14
<b>7.4 DYNAMIC BEHAVIOUR.....</b>	<b>7-17</b>
7.4.1 Introduction .....	7-17
7.4.2 Test arrangement .....	7-17
7.4.3 Evaluation of test results.....	7-20
7.4.4 Conclusions from the dynamic test results.....	7-36
7.4.5 References .....	7-36

## List of Figures

FIG. 7-1: TEST ARRANGEMENT .....	7-5
FIG. 7-2: STIFFNESS OF THE BOOM WITHOUT PRELOADING .....	7-6
FIG. 7-3: STIFFNESS OF THE BOOM WITH ELECTRICAL PRELOADING .....	7-6
FIG. 7-4: STIFFNESS WITH MECHANICAL COMPENSATION OF BACKLASH AFTER PRELOADING.....	7-7
FIG. 7-5: DEFLECTION OF JOINTS DUE TO BOOM TIP DEFLECTION (WITHOUT PRELOAD) .....	7-8
FIG. 7-6: DEFLECTION OF JOINTS DUE TO BOOM TIP DEFLECTION WITH PRELOAD .....	7-9
FIG. 7-7: FORCE MEASUREMENT BY MEANS OF LOAD CELLS .....	7-9
FIG. 7-8: REACTING FORCES DUE TO THE LOAD FORCE TIP WITHOUT PRELOADING .....	7-10
FIG. 7-9: REACTING FORCES DUE TO THE LOAD FORCE WITH PRELOADING .....	7-11
FIG. 7-10: REACTING FORCES AT JOINT 1 DUE TO THE LOAD FORCE WITHOUT PRELOADING .....	7-11
FIG. 7-11: REACTING FORCES AT JOINT 1 DUE TO THE LOAD FORCE WITH PRELOAD .....	7-12
FIG. 7-12: REACTING FORCES AT JOINT 1 DUE TO LOAD FORCE WITH/WITHOUT PRELOAD ....	7-12
FIG. 7-13: REACTING FORCES AT JOINT 2 DUE TO LOAD FORCE WITH/WITHOUT PRELOAD ....	7-13
FIG. 7-14: REACTING FORCES AT JOINT 3 DUE TO LOAD FORCE WITH/WITHOUT PRELOAD ....	7-13
FIG. 7-15: REACTING FORCES AT JOINT 4 DUE TO LOAD FORCE WITH/WITHOUT PRELOAD ....	7-14
FIG. 7-16: SCHEMATIC SKETCH OF THE EDITH BOOM CONFIGURATIONS IN THE DYNAMIC TESTS .....	7-19
FIG. 7-17: MEASURED DISPLACEMENTS IN TEST V6 (VERTICAL EXCITATION, EXTENDED BOOM, EEPD DOWN) AT SENSOR WA14 (BOOM TIP, VERTICAL DISPLACEMENT COMPONENT) ..	7-20
FIG. 7-18 : VELOCITY SPECTRUM FROM SENSOR VA24 IN TEST V6 .....	7-23
FIG. 7-19 : VELOCITY SPECTRUM FROM SENSOR VA24 IN TEST V8 .....	7-25
FIG. 7-20 : DISPLACEMENT SPECTRUM FROM SENSORS WA13, WA14, AND WA15 IN TEST V33 ..	7-27
FIG. 7-21: VELOCITY SPECTRUM FROM SENSOR VA20 IN TEST V64 .....	7-35

## List of Tables

TAB. 7-1: INFLUENCE BETWEEN BOOM DEFLECTION AND JOINT DEFLECTIONS .....	7-8
TAB. 7-2: ARRANGEMENT OF THE LOAD CELLS .....	7-10
TAB. 7-3: THEORETICAL CALCULATIONS OF BOOM STIFFNESS .....	7-15
TAB. 7-4: ACTUAL MEASUREMENTS OF BOOM STIFFNESS .....	7-15
TAB. 7-5 : LOCATIONS AND MEASURING DIRECTIONS OF DISPLACEMENT AND VELOCITY SENSORS.....	7-21
TAB. 7-6: EVALUATED EIGENFREQUENCIES OF THE EDITH BOOM FROM VERTICAL EXCITATIONS;EXTENDED BOOM, EEPD DOWN (RETRACTED) .....	7-22
TAB. 7-7 : EVALUATED EIGENFREQUENCIES OF THE EDITH BOOM FROM VERTICAL EXCITATIONS; EXTENDED BOOM, EEPD UP (MOVED OUT) .....	7-24
TAB. 7-8 : EVALUATED EIGENFREQUENCIES OF THE EDITH BOOM FROM VERTICAL EXCITATIONS; BOOM FOLDED BY 90° AT JOINT Z2, EEPD DOWN (RETRACTED) .....	7-25
TAB. 7-9: EVALUATED EIGENFREQUENCIES OF THE EDITH BOOM FROM VERTICAL EXCITATIONS; BOOM FOLDED BY 90° AT JOINT Z2, EEPD UP (MOVED OUT) .....	7-26
TAB. 7-10 : EVALUATED EIGENFREQUENCIES OF THE EDITH BOOM FROM VERTICAL EXCITATIONS; BOOM FOLDED BY 90° AT JOINT Z3, EEPD DOWN (RETRACTED) .....	7-28
TAB. 7-11: EVALUATED EIGENFREQUENCIES OF THE EDITH BOOM FROM VERTICAL EXCITATIONS; BOOM FOLDED BY 90° AT JOINT Z3, EEPD UP (MOVED OUT) .....	7-29
TAB. 7-12: EVALUATED EIGENFREQUENCIES OF THE EDITH BOOM FROM VERTICAL EXCITATIONS; BOOM FOLDED BY 90° AT JOINT Z4, EEPD DOWN (RETRACTED) .....	7-29
TAB. 7-13: EVALUATED EIGENFREQUENCIES OF THE EDITH BOOM FROM VERTICAL EXCITATIONS; BOOM FOLDED BY 90° AT JOINT Z4, EEPD UP (MOVED OUT) .....	7-30
TAB. 7-14: EVALUATED EIGENFREQUENCIES OF THE EDITH BOOM FROM HORIZONTAL EXCITATIONS; MASS AT BOOM TIP 200 KG, PRELOAD 1.5 KN, BOOM EXTENDED .....	7-31
TAB. 7-15: EVALUATED EIGENFREQUENCIES OF THE EDITH BOOM FROM HORIZONTAL EXCITATIONS;MASS AT BOOM TIP 200 KG, PRELOAD 1.5 KN, BOOM FOLDED BY 90° AT Z2	7-32
TAB. 7-16: EVALUATED EIGENFREQUENCIES OF THE EDITH BOOM FROM HORIZONTAL EXCITATIONS;MASS AT BOOM TIP 200 KG, PRELOAD 1.5 KN, BOOM FOLDED BY 90° AT Z3	7-33
TAB. 7-17: EVALUATED EIGENFREQUENCIES OF THE EDITH BOOM FROM HORIZONTAL EXCITATIONS;MASS AT BOOM TIP 200 KG, PRELOAD 1.5 KN, BOOM FOLDED BY 90° AT Z4	7-34

## 7 STATIC AND DYNAMIC QUALIFICATION TESTS

Within the frame of the ABT qualification the following tests have been performed:

- Static and dynamic load tests to validate the stress analysis and to determine the deflection under load
- Tests to determine the positioning and repeating accuracy
- Experiments to determine the horizontal stiffness to improve the positioning accuracy and the backlash removal of the drive units
- Dynamic load tests in horizontal and vertical direction to achieve data for the validation of the dynamic simulation

### 7.1 VALIDATION OF THE STRESS ANALYSIS

Stress measurements using strain gauges and strain gauge rosettes, respectively, have been performed at four link positions in order to determine the maximum load conditions. The measurements have been compared with the results of the stress calculations. The investigations included the straight position of the articulated boom and three positions forming angles where always only one link (Z2, Z3, Z4) has been forming a knee of 90°.

First static measurements have been carried out at unloaded conditions followed by measurements with an equivalent load of 2200 kg. The equivalent load has been corresponding to a payload of 1000 kg completed by a factor of two for the dynamic influence and additional 200 kg for missing add-on pieces. The evaluation at the lower pressure hinges showed a satisfying compliance with the calculations. At the side walls of the links B1, B2 and B3 the measured bending stresses were too small whilst the shear stresses were too high compared with the calculation. The smaller bending stresses resulted from the assumption of a linear stress distribution between the upper and the lower link chords. More precise calculations performed meanwhile show a strong increase of the bending stresses at the upper and the lower edges of the side walls.

For this reason a strain gauge rosette has been positioned at the lower edge of the link B2 side wall for dynamic measurements. The unloaded articulated boom has been loaded with an additional weight of 200 kg and has then been loaded by 1000 kg which became abruptly free via an electric lifting magnet. The measured stresses at the pressured hinges were comparable with those of the static tests. As to be expected the pressure stress at the side wall of the link B2 has been higher than those at the static measurements and is comparable with the calculated value. On the other hand the shear stress has been smaller. Thus the assumed factor for taking into account the dynamics is in accordance with the stress amplitude under load.

### 7.2 POSITIONING AND REPEATABILITY ACCURACY

There have been performed tests that evaluated the repetition accuracy of the Articulated Boom System (ABS). Several movements have been executed repeatedly. The end position of each movement has been measured via the joint resolvers, which are integrated in the ABS, and additionally with an external measurement system. The results gained with the external measurement system have met the specification of the ABS, which was specified as 5 mm. The positioning error calculated via forward transformation of the joint resolver values has been much smaller (2 mm). The comparison of both results showed, that the differences have

been bigger than those, which can be explained with the finite resolution of the resolver system. During further experiments the reason of these differences has been detected as a backlash in the resolver system of about  $5 \times 10^{-4}$  rad. In the worst case, i.e. if the ABS is extended and all the measurement errors add themselves to the greatest error, there must be expected a repetition error of about 14 mm, which is mainly (10 mm) caused by backlash.

During all the experiments such a big error never could be measured. So the probability of it seems to be rather small, but theoretical considerations let seem them to be possible. As measure, the reduction of the backlash to a value of 2 resolver digits may be possible by constructional changes. So the error caused by backlash may be reduced to a theoretical value of about 4 mm.

### 7.3 HORIZONTAL STIFFNESS

The horizontal elasticity is caused by

- the drive unit elasticity,
- the drive unit backlash, and
- the joint backlash.

#### 7.3.1 Description of the performed tests

To determine the stiffness the boom was loaded at the boom tip by horizontal forces up to 1 kN in both directions perpendicular to the tip orientation. The load force was increased by steps of 200 N. The applied force was measured by a load cell and the boom deflection by means of a laser pointer and scaled marks on the floor. The tests have been performed at a straight position of the boom. During the test campaign the drive motors haven't been activated and the brakes have been locked. Fig. 7-1 shows the test arrangement.

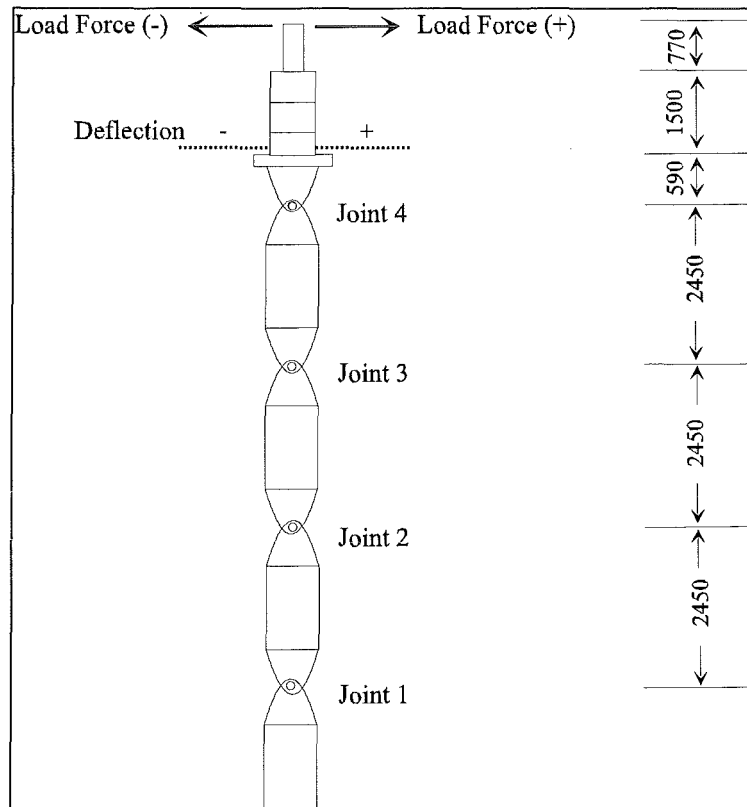
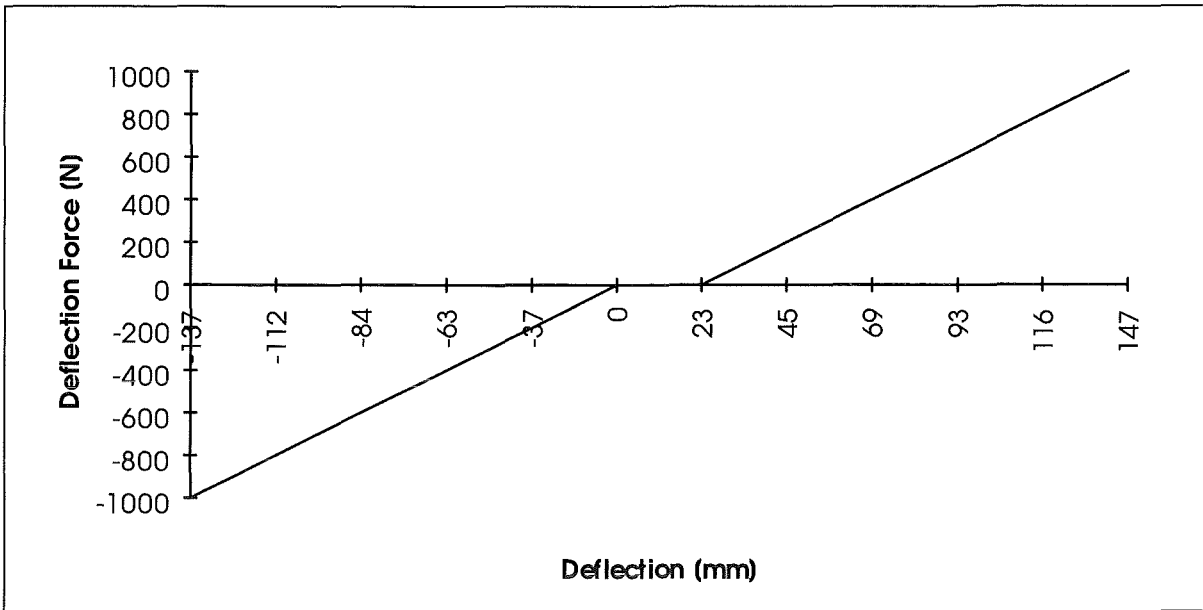


Fig. 7-1: Test arrangement

#### 7.3.2 Total stiffness referring to the boom tip

The stiffness of the boom in horizontal direction without preload was measured to 7042 N/m. The actual backlash at the tip was determined to 23 mm. The measured stiffness curve referring to the tip of the boom is shown in Fig. 7-2.



**Fig. 7-2:** Stiffness of the boom without preloading

The same measurement as described above have been carried out with the first attempt of electrical preloading. The result of this first attempt is given in Fig. 7-3.

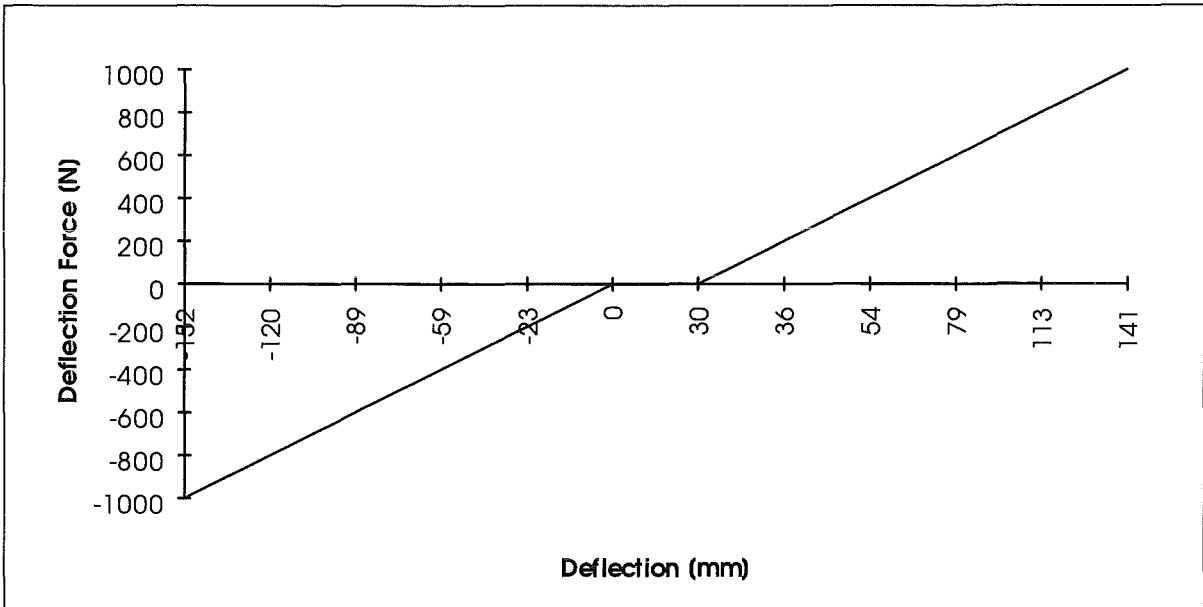


**Fig. 7-3:** Stiffness of the boom with electrical preloading

With electrical preloading in the first step no improvement of the boom stiffness could be realised. The results of the measurements correspond nearly to those without preloading. On the contrary, the total stiffness decreased (6826 N/m) while the backlash increased (30 mm).

To improve the total stiffness of the boom the drive units have been electrically pre-loaded to compensate the backlash of the torque arms. So, the air gap between torque arm and link which results from preloading have been filled up by thin metal sheets. Consequently, the total

stiffness of the boom has been increased and the total backlash has been decreased. In Fig. 7-4 the resulting measurements are shown.

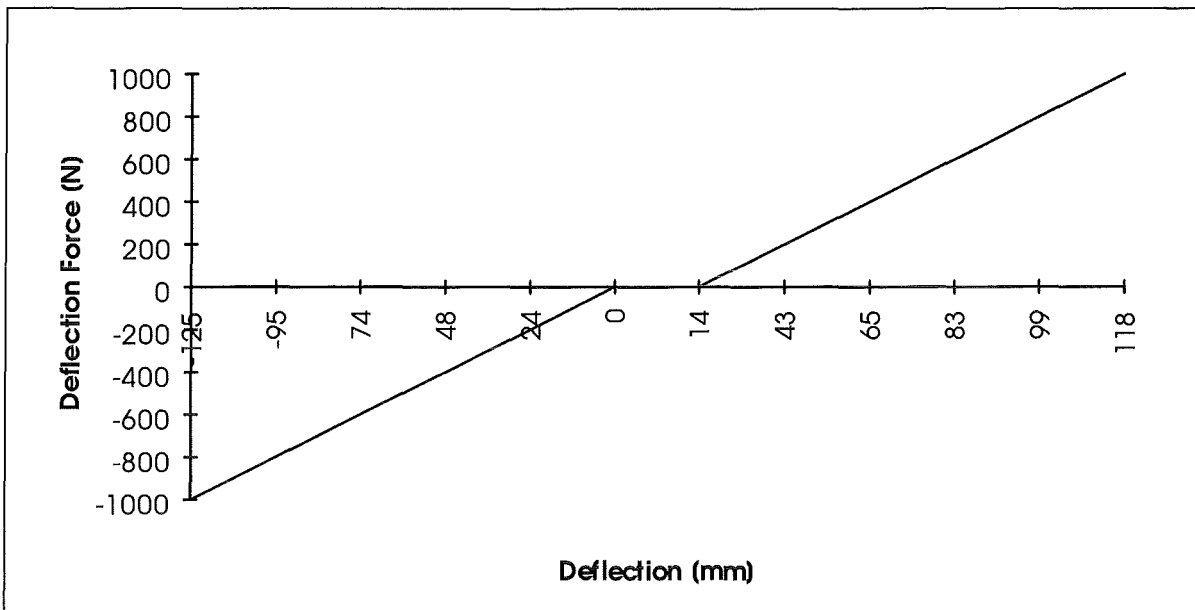


**Fig. 7-4:** Stiffness with mechanical compensation of backlash after preloading

The mechanical backlash compensation and preloading of the torque arms results in an improvement of the boom stiffness up to 8230 N/m and a reduced backlash of 14 mm at the tip.

### 7.3.3 Deflection of joints due to boom tip deflection

The deflection of each joint due to the horizontal load force at the tip of the boom without preloading conditions is shown in Fig. 7-5.

Considering the kinematics structure of the boom the influence of each joint on to the total deflection at the tip was determined.

Due to the dual drive unit in joint 1 the stiffness was increased. Fig. 7-5 shows that in spite of a higher leverage the joint deflection of joint 1 was lower than the deflection of joint 2.

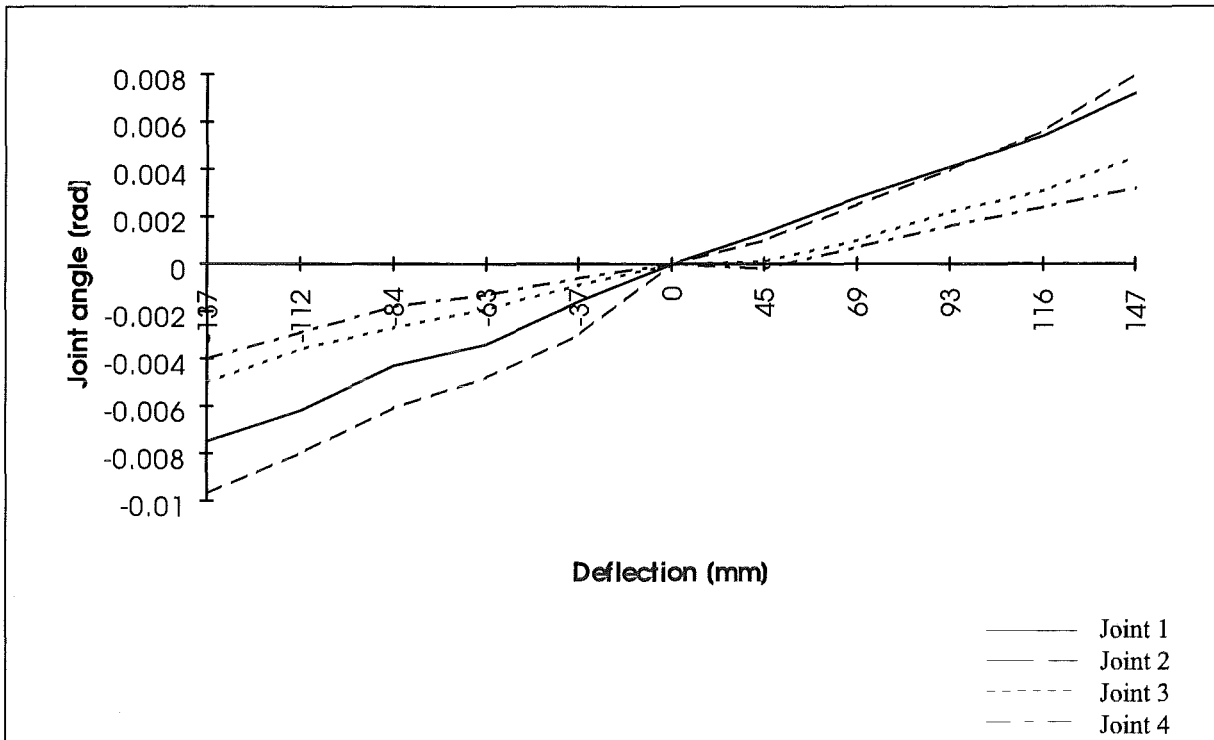


Fig. 7-5: Deflection of joints due to boom tip deflection (without preload)

The corresponding load torques at each joint in dependence on the lever length and the respective joint deflection at the maximum horizontal load are listed in the Tab. 7-1. The resulting joint stiffness has been determined. The influence of each joint deflection on the total tip deflection has been calculated.

	Joint 1	Joint 2	Joint 3	Joint 4
Lever length / load [mm]	10210	7760	5310	2860
Lever length / deflection measurement [mm]	8090	5640	3190	740
Max. load torque [Nm]	10210	7760	5310	2860
Max. joint deflection to the right [rad]	0.008	0.0104	0.0051	0.004
Max. joint deflection to the left [rad]	-0.0075	-0.0097	-0.005	-0.004
Joint backlash [rad]	0.0028	0.0047	0.0017	0.0012
Calculated joint stiffness [kNm/rad]	<b>1608</b>	<b>1008</b>	<b>1264</b>	<b>841</b>
Influence of joint stiffness on tip deflection (right) [mm]	65	59	16	3
Influence of joint stiffness on tip deflection (left) [mm]	61	55	16	3
Influence of joint stiffness on tip deflection (right) [%]	46	41	11	2
Influence of joint stiffness on tip deflection (left) [%]	45	41	12	2
Total influence on tip deflection due to backlash [mm]	23	26	5	1

Tab. 7-1: Influence between boom deflection and joint deflections

The joint stiffness has been calculated by the following relation

$$\text{Joint stiffness} = \frac{2 * \text{Load\_Torque}}{(\text{Joint\_Deflect.}_{\text{right}} + \text{Joint\_Deflect.}_{\text{left}}) - \text{Joint\_Backlash}}$$

Fig. 7-6 shows the joint deflections under electrical preload conditions. No significant changes result from preloading.

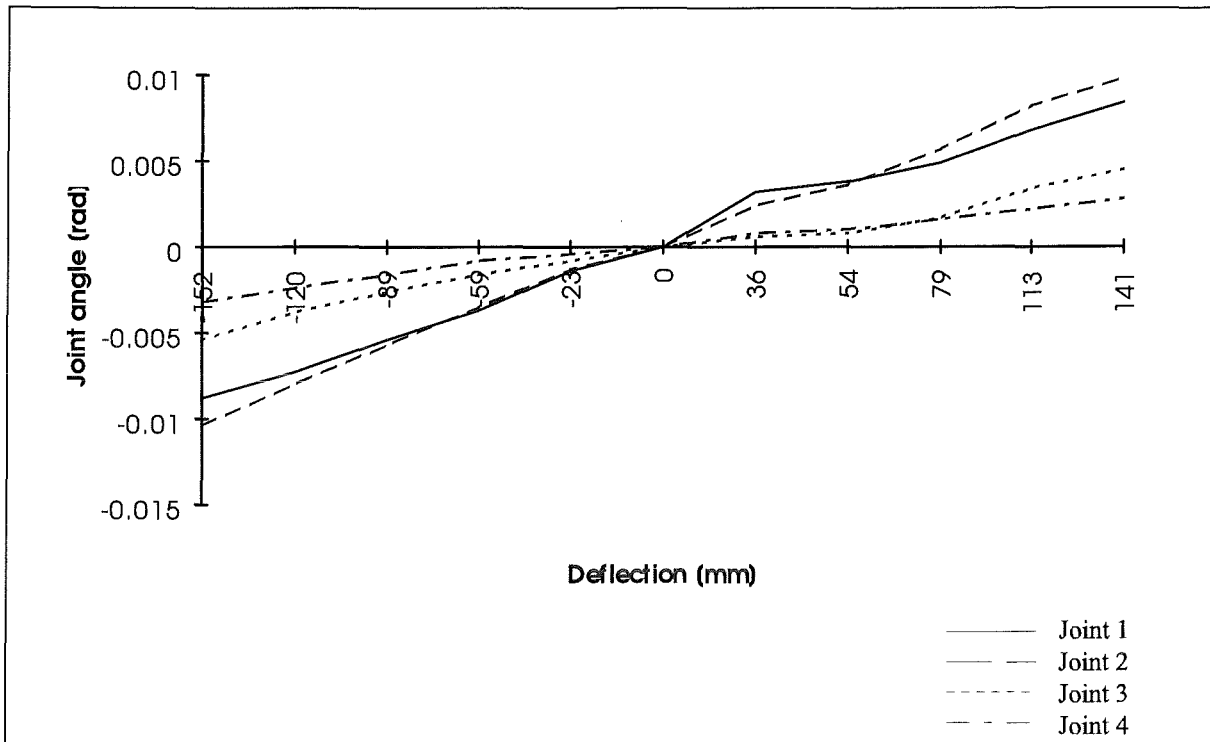


Fig. 7-6: Deflection of joints due to boom tip deflection with preload

### 7.3.4 Forces between drive unit (torque arm) and link

The forces between torque arm and link were measured by means of load cells at both sides of the torque arm. Thus the driving joint torque and the preload force could be measured. Fig. 7-7 shows the several drive components.

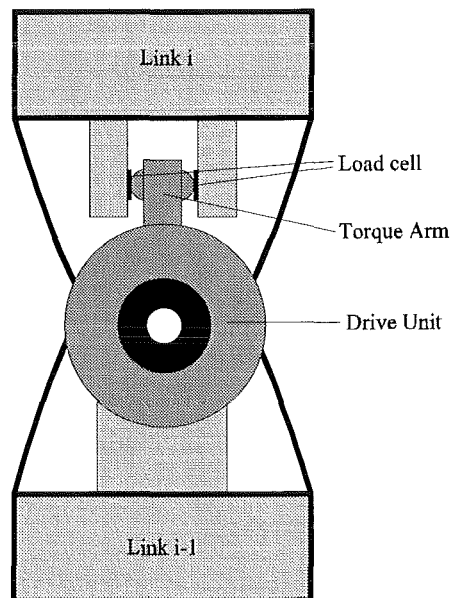


Fig. 7-7: Force measurement by means of load cells

Joint 1 consists of two drive units of the same type. Joint 2...4 consists of one drive unit. The principle of the drive units is shown in Fig. 7-7. The driving torque produced by the two

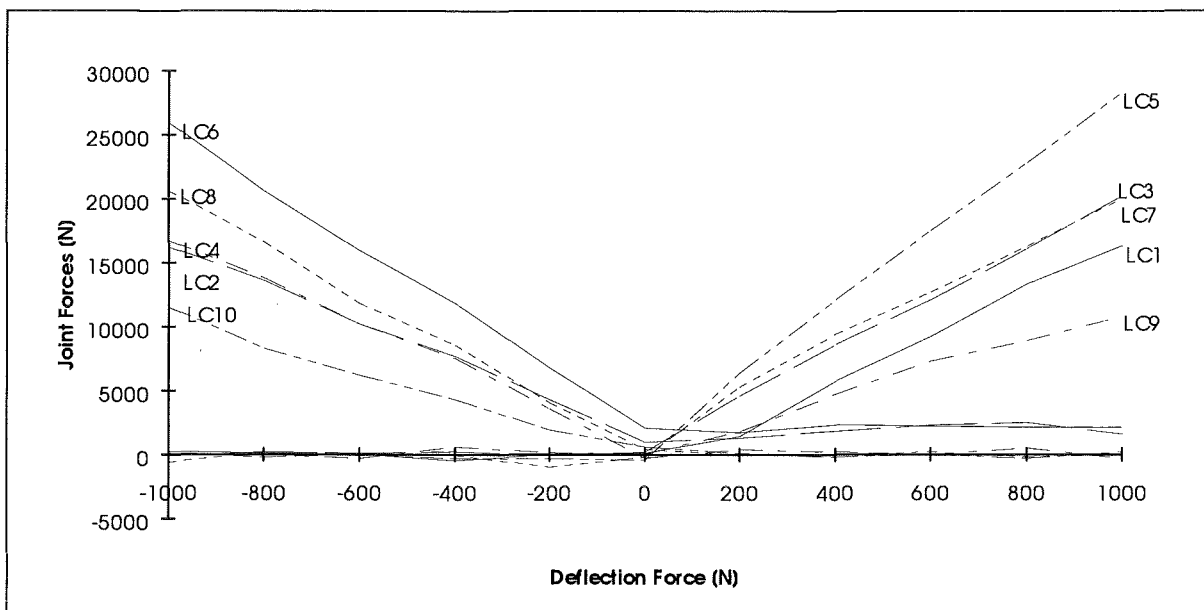
motors of one drive unit will drive the mechanical gears. Both gears will drive the torque arm, which itself drives the link.

Joint 1 contains four load cells (LC1...LC4) and each of the other joints contains two load cells. The arrangement of the load cells referring to the joints is listed in Tab. 7-2.

	Joint 1	Joint 2	Joint 3	Joint 4
Right side	LC1, LC3	LC5	LC7	LC9
Left side	LC2, LC4	LC6	LC8	LC10

**Tab. 7-2:** Arrangement of the load cells

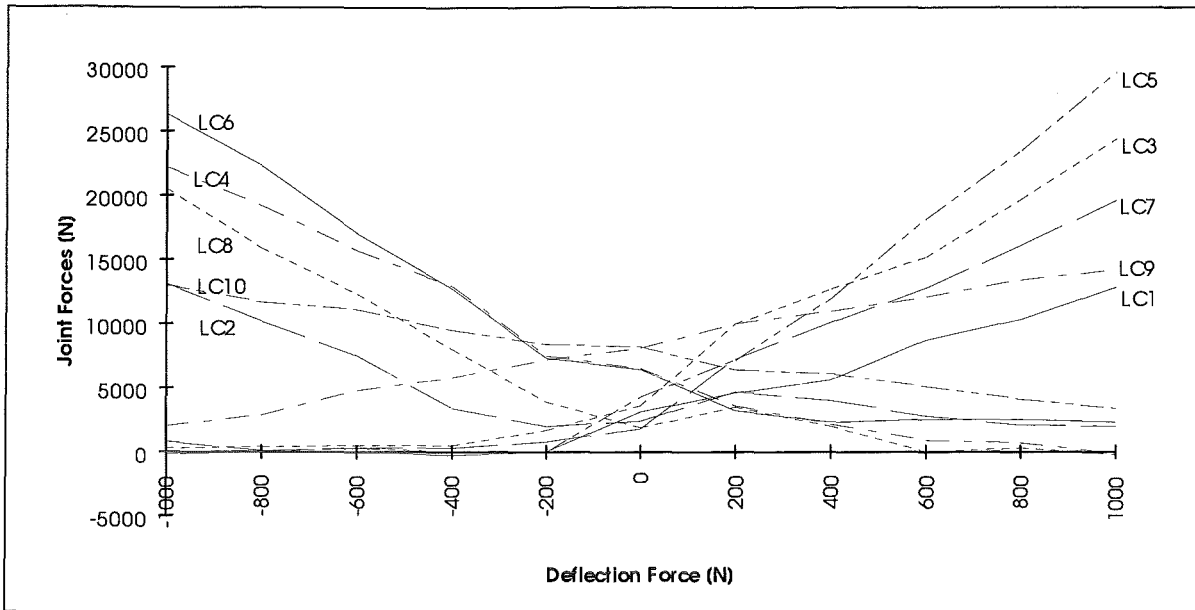
By increasing the deflection force on the right side of the boom, the corresponding load cells will indicate the reacting forces. In the initial (zero) position without deflection the measured forces at the torque arms should be zero (no preload).



**Fig. 7-8:** Reacting forces due to the load force tip without preloading

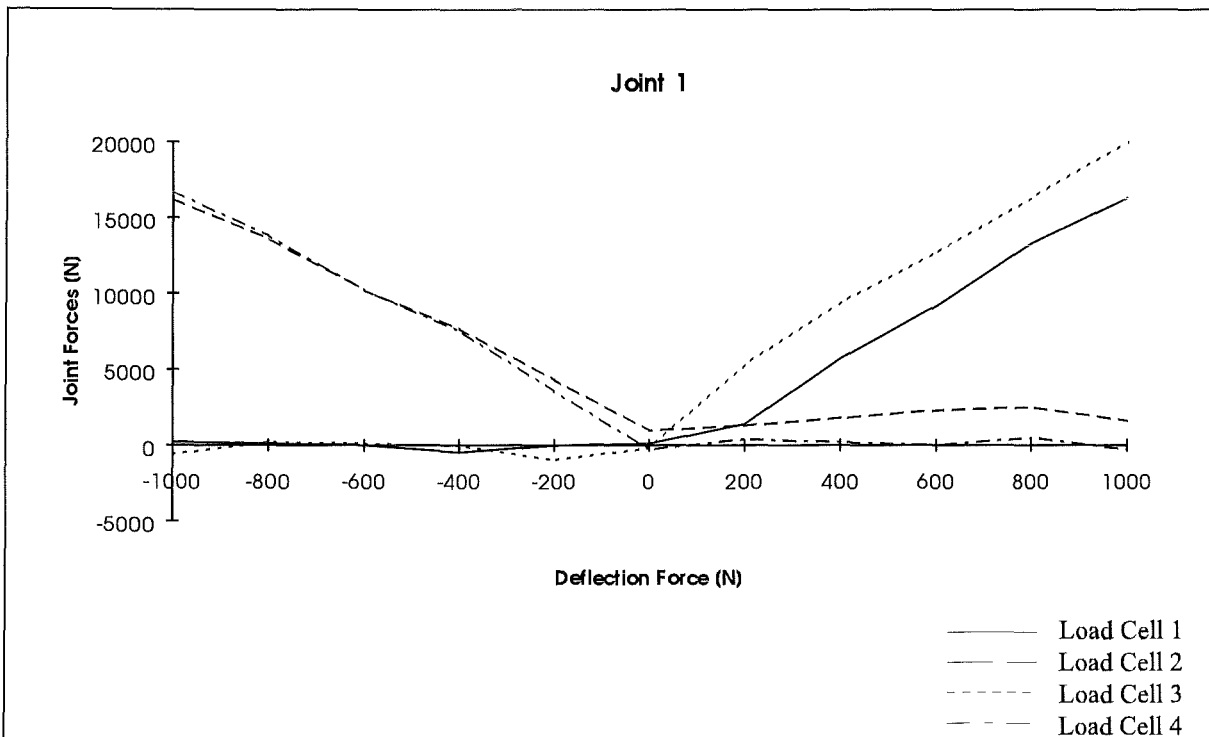
Due to the desired preload force the measured forces at the torque arms will be increased in the zero position (no reacting deflection force at the tip of the boom). The joints which show low zero force have not been pre-loaded enough. By means of the load cells, adjusting a pre-defined preload force should be possible.

Fig. 7-9 shows the forces at the torque arms after preloading the drive units. It shows also the increased zero force compared to Fig. 7-8.



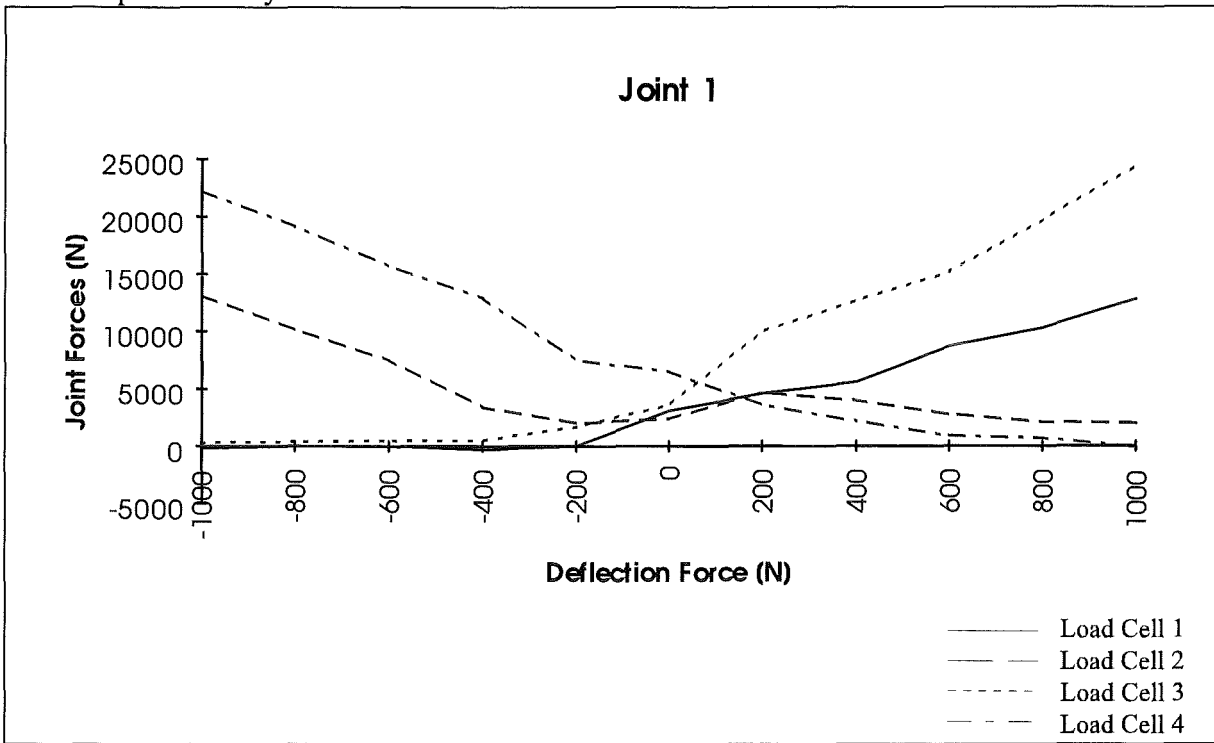
**Fig. 7-9:** Reacting forces due to the load force with preloading

Fig. 7-10 shows the non symmetrical arrangement of the drive units of joint 1. During positive deflection forces to the right side of the boom, LC2 which is on the left side will not become zero. This is the reason why the measured force at LC3 has to be higher as the force at LC1.



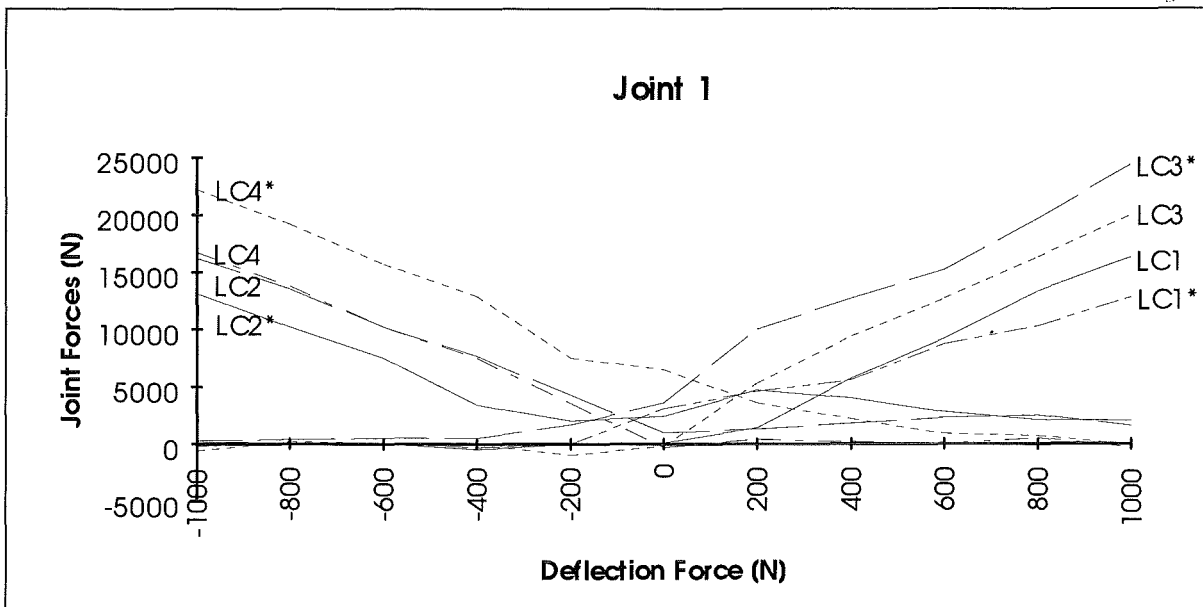
**Fig. 7-10:** Reacting forces at joint 1 due to the load force without preloading

Fig. 7-11 shows the increased forces at the zero position after preloading. It is shown, that the preload of drive unit 1 represented by load cells 1 and 2 will be lower than the one of drive unit 2 represented by LC3 and LC4.



**Fig. 7-11:** Reacting forces at joint 1 due to the load force with preload

Fig. 7-12 shows the measured reacting forces of joint 1 with and without preload.



**Fig. 7-12:** Reacting forces at joint 1 due to load force with/without preload

Fig. 7-13 shows the result of preloading at joint 2. The difference of the curves before and after preloading presents the corresponding preload force. The preload force has been increased by nearly 10 kN.

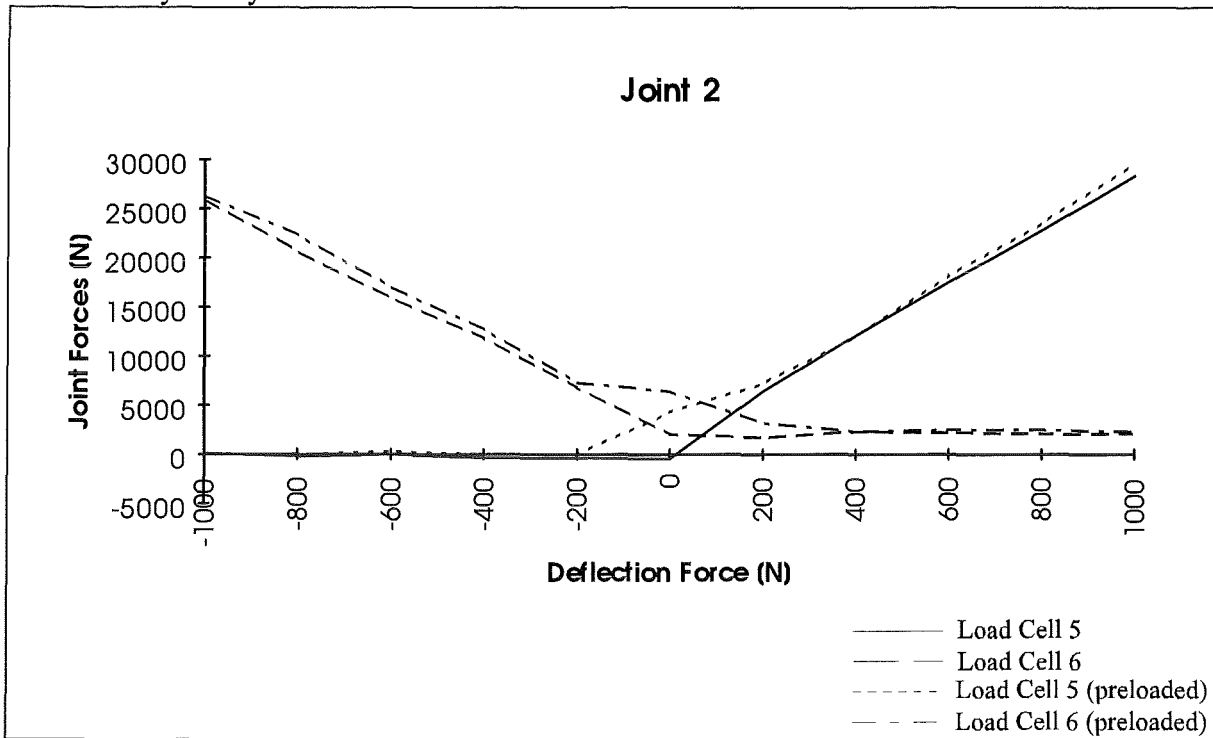


Fig. 7-13: Reacting forces at joint 2 due to load force with/without preload

Fig. 7-14 shows, that the preloading of joint 3 wasn't successful. The forces at the zero position are too low to achieve a sufficient preloading.

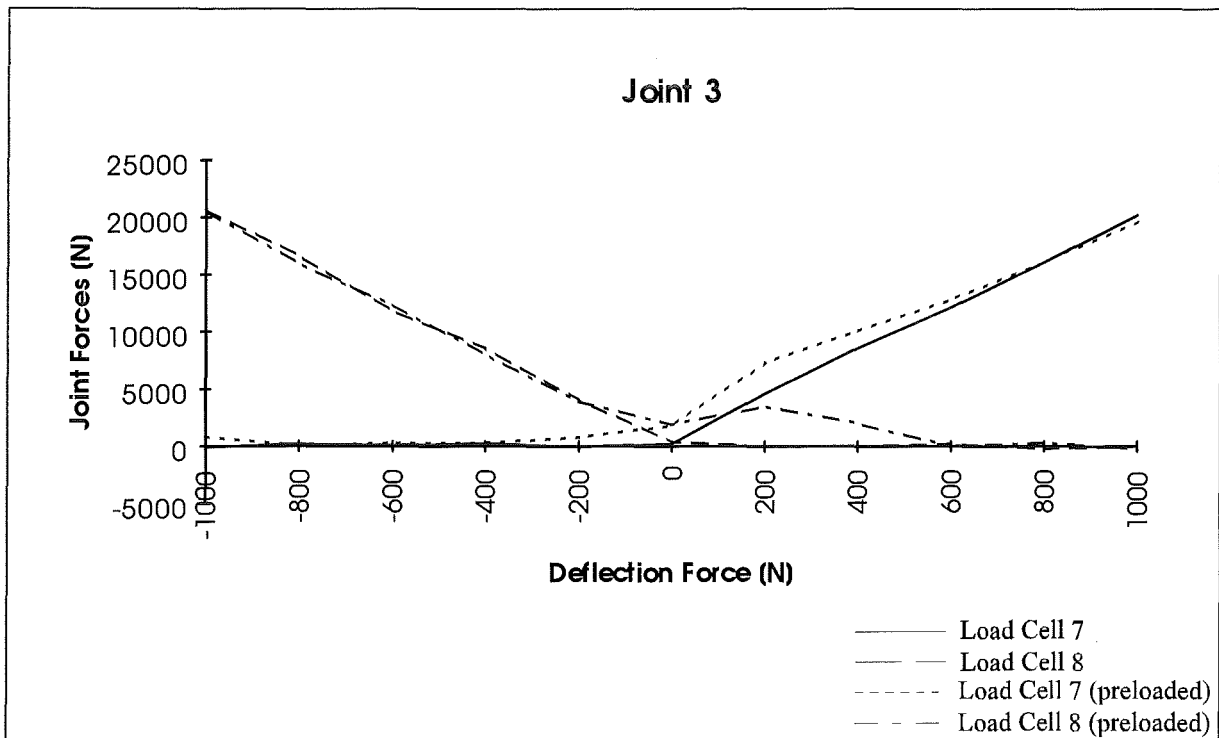


Fig. 7-14: Reacting forces at joint 3 due to load force with/without preload

Fig. 7-15 shows an example for a sufficient preloading. During the whole deflection phase the forces at the torque arm will not reach the zero line. That means, the preloading will be active during the whole load cycle.

At joint 4 a pre-load force of nearly 16 kN has been adjusted by electrical preloading.

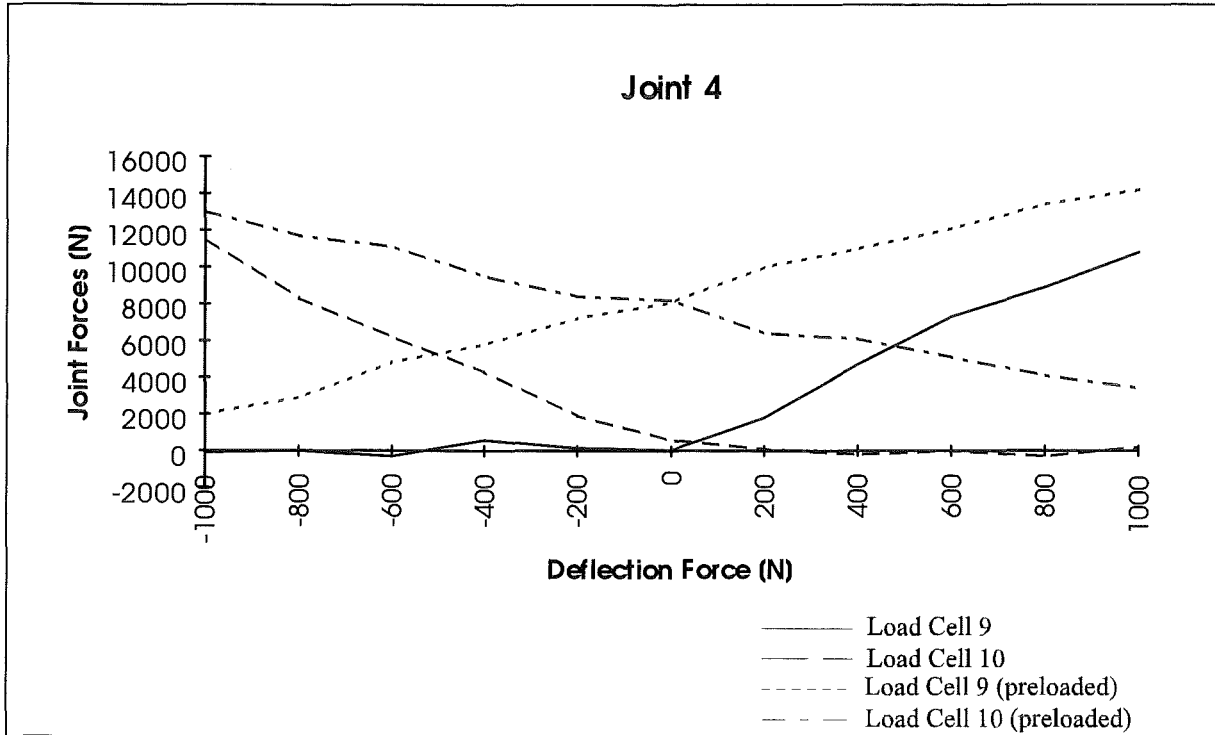


Fig. 7-15: Reacting forces at joint 4 due to load force with/without preload

### 7.3.5 Conclusions

By eliminating the backlash at the torque arms the deflection of the boom tip due to horizontal forces will be reduced by nearly 55 mm referring to the total deflection in both directions. This means about 20% reduction of the total tip deflection.

Fig. 7-4 shows in the first step, that it will be possible to reduce the backlash by preloading the drives and by compensating the resulting air gap between torque arm and the corresponding link. By using this method it should be able to compensate the backlash at the torque arms totally, which will be more considerable than the drive's backlash.

Compared with the measured drive backlash (see Doc-Nr. SGI.RP.421) of about  $3.2E-4$  rad, the joint backlash caused by the torque arm will be dominant. This data have been found out as  $1.2E-3$  to  $4.6E-3$  rad.

By using the measured stiffness and backlash data of the drive units (determined by ANSALDO) a theoretical boom tip deflection of 67.3 mm can be reached, where about 6 mm will be contributed by backlash.

In contrast to this calculations the present tests results in a middle tip deflection of 139 mm. The part, which will be contributed by backlash amount to 55 mm. These data result from calculation of cumulative joint deflections.

In the following tables the results of the theoretical and the actual data are represented.

Theoretical calculations based on drive stiffness measurement by ANSALDO:

Assumptions:      Drive stiffness      1.7E3 kNm/rad  
                          Drive backlash      3.2E-4 rad

	Joint 1	Joint 2	Joint 3	Joint 4	Σ
Prorated contribution to tip de-flection due to stiffness [mm]	24.5	26	10	1.2	61.7
Prorated contribution to tip de-flection due to backlash [mm]	2.6	1.8	1	0.2	5.6
<b>Total [mm]</b>	<b>27.1</b>	<b>27.8</b>	<b>11</b>	<b>1.4</b>	<b>67.3</b>

**Tab. 7-3:** Theoretical calculations of boom stiffness

Actual measurements:

	Joint 1	Joint 2	Joint 3	Joint 4	Σ
Prorated contribution to tip deflection due to stiffness [mm]	40	31	11	2	84
Prorated contribution to tip deflection due to backlash [mm]	23	26	5	1	55
<b>Total [mm]</b>	<b>63</b>	<b>57</b>	<b>16</b>	<b>3</b>	<b>139</b>

**Tab. 7-4:** Actual measurements of boom stiffness

By compensating the backlash to a minimum of 5.6 mm, which corresponds to the data of the drive units, the total tip deflection of the boom could have been decreased down to 89.6 mm instead of 139 mm. This should be able by compensating the backlash at the torque arms.



## 7.4 DYNAMIC BEHAVIOUR

### 7.4.1 Introduction

Dynamic tests aim at the characterisation of the behaviour of a system under conditions when time-dependent forces are applied to the system, either internally by drive units or externally by loads or other external forces, or when the system freely moves due to previously released forces. Among the most significant quantities characterising the dynamic behaviour of a system are the eigenfrequencies, at best together with the corresponding mode shapes of the eigenoscillations.

For a system consisting of multiple parts, however, which form different configurations according to the relative mutual positions of these parts, the eigenoscillations strongly depend on the actual configuration. Hence, dynamic tests must intend to include the influence of the configurations, though, of course, it is impossible to perform tests with all possible configurations.

With EDITH, some series of dynamic tests have been performed. The most significant ones included so called „snap-back“ tests where a vertical or horizontal force, statically applied to the tip of the boom (or, speaking more exactly, to a dummy work unit mounted to the front end of the EEPU) has been suddenly released. During the decay time following this release, a number of relevant response signals have been recorded.

In this type of tests, the joint brakes have been closed, and the dynamic behaviour of the boom is determined completely by its mechanical properties. Controller and motor characteristics do not affect the results. Another test series had been intended to include also these effects; however, an evaluation of such experiments requires comprehensive dynamic models not only of the mechanical system, but also of some electrical, electro-mechanical, and electronic components like controllers and motors. Additionally, detailed mechanical models of all gears would be required. All this turned out to be beyond the capacity of the present EDITH team. Therefore, the following investigation is focused onto the results from the snap-back experiments.

### 7.4.2 Test arrangement

For the dynamic tests, the end effector unit at the front end of the EEPU has been replaced by a dummy box to which an additional mass has been attached. This mass has been varied for the different tests and aimed to substitute the mass of any manipulators as well as that of any payload.

In all tests, a static pulling force has been applied to the dummy end effector box and has been released in order to excite the snap-back oscillations. There have been two principal series with different directions of the excitation. In the first one, the pulling force acted in vertical direction, i.e., parallel to the axes of the ABT joints. In this case, the pulling force has been exerted by the crane the hook of which carried a fish scale (for determining the pulling force) which, in turn, has been connected to the box by an electro-magnetic clutch.

In the second series, a horizontal force has been applied acting perpendicular to the main axis of the front-end link of the ABT, thus inducing also loads on the ABT joints. For this purpose, a fixed weight has been connected to the electro-magnetic clutch by a rope which was guided

by a deflection pulley. This pulley has been located at the same height as the point of attack to the box, but shifted laterally in such a way that the pulling force acted perpendicularly to the main axis of the last link of the ABT (to which the EEPU is mounted), according to the respective boom configuration.

All tests have been performed following the same scheme: First the brakes of all joints have been closed; then the static load has been applied. When the boom had reached a stationary state, the measurements were started and, with a fixed time offset, the electro-magnetic clutch was switched off, thus suddenly releasing the boom. The measured signals have usually been recorded over a period of 30 seconds with a sampling rate of 500 Hz. The recorded period for experiment V68 (see below) covered only about 21 seconds.

The following measuring equipment has been used:

- 12 piezoelectric accelerometers:
  - three at the front side of the dummy box, measuring in three orthogonal directions (vertically and horizontally perpendicular to the main link axis and parallel to the main link axis);
  - three at the bottom side of the EEPU support frame, again measuring in the three orthogonal directions;
  - each two in the mid of the bottom and top walls of the link between joints Z2 and Z3 (see Fig. 7-16), measuring in vertical and horizontal directions perpendicular to the main link axis;
  - each one in the mid of a side wall of the links between joints Z1 and Z2 and between joints Z3 and Z4, measuring in normal direction with respect to the wall to which they were attached;
- 6 displacement gauges:
  - three thread potentiometers, attached to the lower front end of the dummy box and measuring in the three orthogonal directions already specified;
  - two thread potentiometers, attached to the bottom side of the EEPU support frame and measuring in vertical and horizontal directions perpendicular to the main link axis;
  - one probing unit in the mid of a side wall of the link between joints Z1 and Z2, measuring the normal deflections of this side wall;
- 4 velocimeters: Actually, these have been secondary output channels of the thread potentiometers measuring the displacements in directions perpendicular to the main axis of the end link;
- 10 load cells measuring the forces between the torque arms of the drive units and the respective link; see section 7.3.4 above.

Additionally, the number of revolutions and the currents in the motors of all drive units have been recorded; however, for this kind of dynamic tests, these data turned out to be irrelevant.

The vertical displacement measurement at the EEPU support frame failed in the first series of experiments; surprisingly, the same potentiometer gave useful velocity records also in these cases. Thus the redundancy of measuring displacements as well as velocities and accelerations turned out to be helpful.

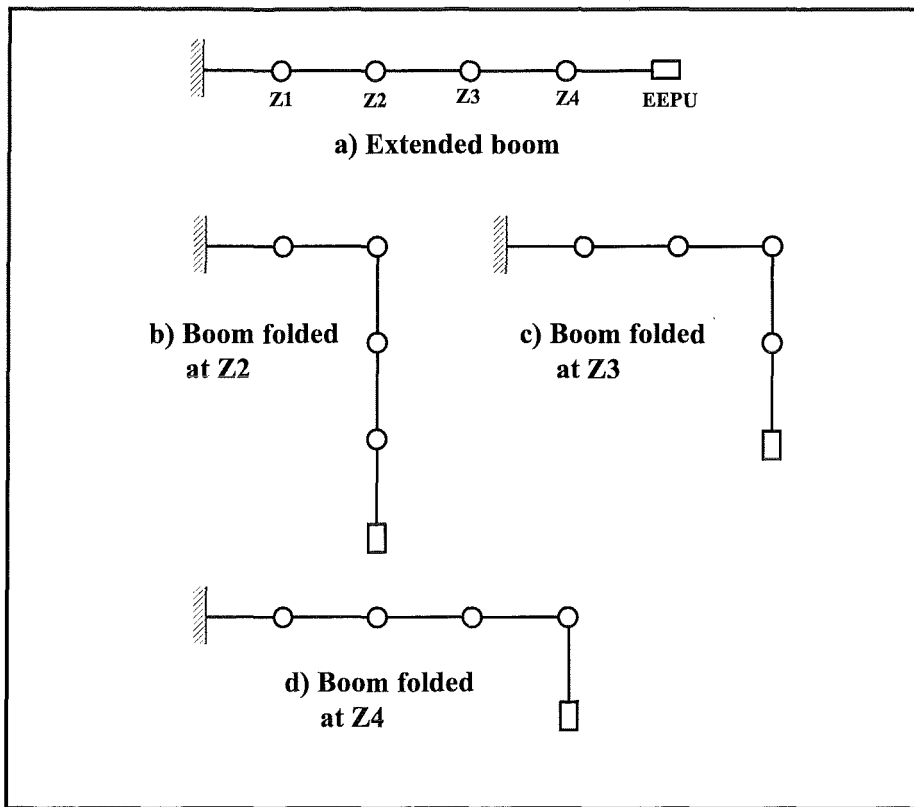


**Fig. 7-16: Schematic sketch of the EDITH boom configurations in the dynamic tests**

The configurations of the EDITH boom in the tests are sketched schematically in Fig. 7-16. For each of these configurations, tests have been performed with both, vertical and horizontal initial loads, as well as with the EEPU being retracted and being moved out (thus elevating the dummy box by about 5 m). In the case of vertical excitation, different tests have been performed with the same configuration and the same EEPU position, but with the additional mass at the boom tip and the preload pulling force being varied. In a linear system, the value of the pulling force does not affect the values of the eigenfrequencies, nor the mode shapes proper; it just influences the amplitude of the oscillations. However, a real system may behave slightly non-linearly; besides this, some weakly excited eigenfrequencies may not be found with low preload values due to the limited resolution of the measuring chains.

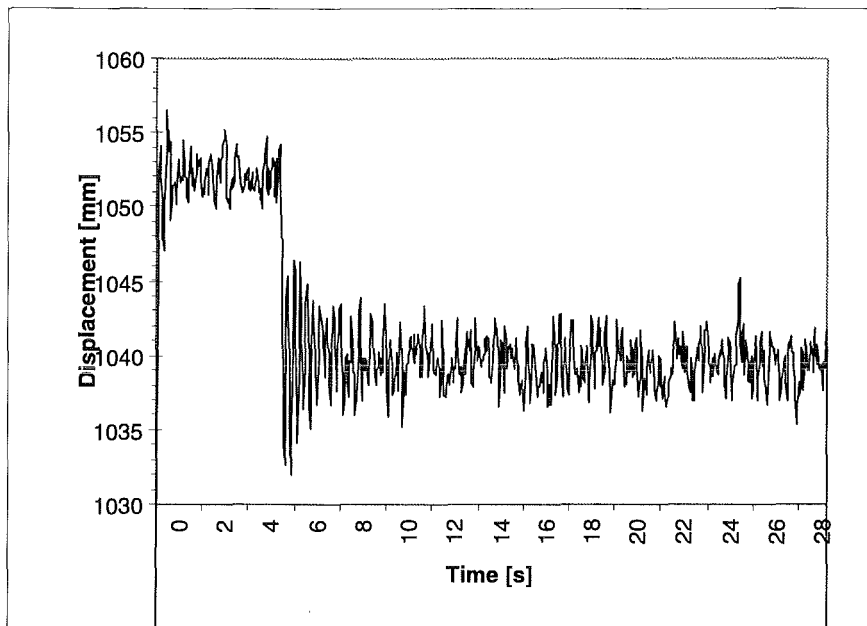


**Fig. 7-17: Measured displacements in test V6 (vertical excitation, extended boom, EEPU down) at sensor WA14 (boom tip, vertical displacement component)**

### 7.4.3 Evaluation of test results

For each single experiment, the measured signals which have been recorded in the time domain were first reduced to a sampling rate of 25 Hz by a suitable filtering technique. The reduced signals were analysed by a modal analysis method. For details of this method see [Eberle1982]. Eigenfrequencies up to 4 Hz have been identified in this way.

Signals from the different measurement groups (i.e., displacements, velocities, accelerations, forces in joints, number of revolutions of the motors, and motor currents) have been analysed separately; in addition, in the case of the displacement and velocity signals also groups of signals from distinct locations or even single signals have been investigated separately. As could be expected from the test arrangement, there have not been any meaningful modal results from the motor revolutions and motor currents, and also the results from the joint forces looked rather accidental, at least for some tests with vertical excitation. With horizontal excitation, the modal force data could be used to support the interpretation of the other data.

Tab. 7-6 through 7-16 list the extracted eigenfrequencies from the displacement, velocity, and acceleration measurements. In the headlines of these tables, the sensors or groups of sensors are noted from the signals of which the data in the corresponding column have been extracted. The locations and measuring directions of the displacement and velocity sensors are compiled in Tab. 7-5.

For each experiment, the frequency data are ordered in the tables line by line in ascending order. Numbers printed in boldface indicate the mode with the highest contribution to the measured signal in that column. Since the modal analysis method employed is strictly valid for linear systems only, the range of the damping ratio is indicated by the style in which the frequency value is printed: Numbers put between parentheses indicate a mode with a damping ratio of 11% or more; numbers printed in italics indicate modes the damping ratio of which is

between 6% and 11%. The frequency numbers of modes with damping ratios less than 6% are not marked specifically.

Sensor name	Signal type	Location	Measuring direction
WA13	Displacement	Dummy box	Horizontal, perpendicular to main axis of last link
WA14	Displacement	Dummy box	Vertical
WA15	Displacement	Dummy box	Horizontal, parallel to main axis of last link
WA16	Displacement	EEPU support frame	Horizontal, perpendicular to main axis of last link
WA17	Displacement	EEPU support frame	Vertical
WA18	Displacement	Sidewall of link between joints Z1 and Z2	Horizontal, normal to the sidewall of the link to which it is attached
VA20	Velocity	Dummy box	Horizontal, perpendicular to main axis of last link
VA21	Velocity	Dummy box	Vertical
VA22	Velocity	EEPU support frame	Horizontal, perpendicular to main axis of last link
VA24	Velocity	EEPU support frame	Vertical

**Tab. 7-5 : Locations and measuring directions of displacement and velocity sensors**

Due to the rather little number of measuring positions, the shape of the modes which correspond to the extracted eigenfrequencies can only be estimated, if at all. Besides this, the accuracy of the calculated eigenfrequencies has been judged from calculations for sensor groups and for sensors within these groups to be about  $\pm 0.1$  Hz. For these reasons, only one frequency is given also in those cases when two almost identical eigenfrequencies have been found.

#### 7.4.3.1 Tests with vertical excitation

Tab. 7-6 lists the eigenfrequencies found in the tests V2, V4, and V6, where the mass on the boom tip (i.e., the additional mass attached to the dummy box) and the preload force have been varied, but the boom has been extended (see configuration a) in Fig. 7-15), and the EEPU has been retracted.

The modes with the lowest frequencies, found from sensors which are sensitive perpendicular to the main excitation direction (WA16, VA20, VA22), probably represent torsional oscillations about the main boom axis which have been excited due to some eccentricity of the initial load. However, the analysis shows that the highest frequencies found from all sensors belong to the most dominant mode; see, e.g., Fig. 7-18. This is the fundamental beam-like mode, where the entire boom behaves like an oscillating cantilever beam. The decreasing values (3.9 Hz in V2, 3.7 Hz in V4, about 3.6 Hz in V6) can easily be explained as consequences of the increasing additional mass at the boom tip (75 kg, 350 kg, and 570 kg, respectively).

All the other modes the eigenfrequencies of which are listed in Tab. 7-6 participate in the movements of the boom only to a minor, almost insignificant extent. They hardly can be

found from a diagram like that given in Fig. 7-17; most of them probably belong to 'local' modes of partial structures of the boom.

Exp. #	Mass at boom tip [kg]	Pre-load [kN]	Frequency [Hz]							Accelerations
			Displacements			Velocities				
			WA13 WA14 WA15	WA16	WA18	VA20	VA21	VA22	VA24	
V2	75	5		<b>(0.25)</b>		<b>(0.3)</b>				
			0.8	0.7	(0.4)					
				1.0	0.8					
				1.4	1.4		(1.2)			1.2
				<b>(1.5)</b>						
			1.9		2.0	1.8	1.8	1.6		1.6
				2.3				2.3		
			2.6			2.5	2.5	2.9		
			3.0		2.9					
						3.5				
			<b>3.9</b>		<b>3.9</b>	3.8	<b>3.9</b>	3.8	<b>3.9</b>	<b>3.9</b>
V4	350	7.5	0.5	(0.5)		<b>(0.6)</b>		(0.5)		
				1.4			(1.1)	1.5		(1.0)
			1.7	<b>(1.6)</b>	(1.8)					
			2.0							
			2.4	2.5				2.6		
				2.8						
				3.2						
			<b>3.7</b>	3.6	<b>3.7</b>	3.7	<b>3.7</b>	<b>3.7</b>	<b>3.7</b>	<b>3.7</b>
V6	570	10	(0.5)	<b>(0.4)</b>		<b>(0.4)</b>		<b>(0.4)</b>		
			1.4			1.2				
			1.8	1.7						
				2.1	2.2					
				2.6		2.7		2.8		
				3.2		3.3				
			<b>3.5</b>	3.7	<b>3.6</b>	3.6	<b>3.5</b>	3.5	<b>3.6</b>	<b>3.6</b>

**Tab. 7-6: Evaluated eigenfrequencies of the EDITH boom from vertical excitations; extended boom, EPU down (retracted)**

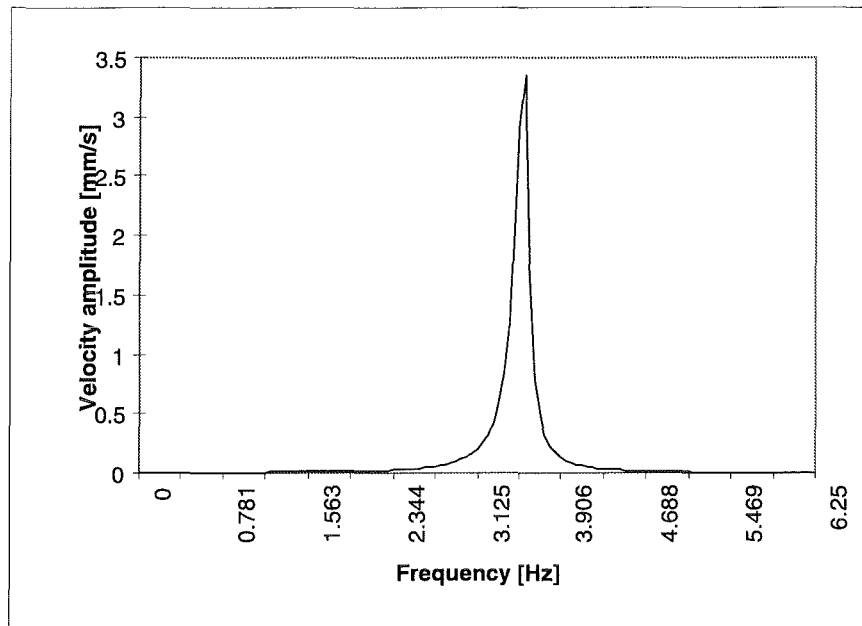


**Fig. 7-18 : Velocity spectrum from sensor VA24 in test V6**

Tab. 7-7 lists the eigenfrequencies evaluated from tests with the same extended ABT configuration like in Tab. 7.6, but with the EEPU (together with the mass on its tip) moved out. The eigenfrequency of the ‘beam mode’ has been diminished significantly for equivalent conditions: 3.2 Hz instead of 3.9 Hz, 2.8 Hz instead of 3.7 Hz, and 2.6 Hz instead of 3.6 Hz. There are at least two effects that induce the eigenfrequencies to decrease. First, the ‘virtual beam length’ of the boom has been increased by moving out the EEPU; second, the extended EEPU is obviously significantly weaker than the ABT, at least with respect to vertical oscillations.

Fig. 7-19 shows the velocity spectrum for test V8 from sensor VA24. It should be compared to Fig. 7-18. Besides the shifting of the main peak from 3.6 Hz to 2.6 Hz, a second peak becomes significant at about 4.6 Hz (not listed in Tab. 7-7 because the evaluation program does not identify eigenfrequencies above 4 Hz). This peak, the height of which is about 20% of that of the main peak, is more or less clearly visible in all displacement, velocity, and acceleration spectra, except those which have been evaluated from sensors that are located at the dummy box on the boom tip. That means, the mutual configuration of the ABT and the extended EEPU is subject to oscillations in this higher frequency mode, whereas the boom tip with its additional mass participates in this oscillation only insignificantly. Thus we have a coupled oscillator, consisting of at least two parts. This interpretation is confirmed by the equivalent spectra from tests V11 and V13, where the additional mass on the boom tip has been smaller: In V11, the second peak shows up at a somewhat higher frequency (about 5.4 Hz) and with a relative height of less than 10%. In test V13 with the small additional mass of 75 kg, this second peak does not show up at all; the mutual oscillation of ABT and EEPU has not been excited.

The other eigenfrequencies listed in Tab. 7-7 are again due to local modes and do not contribute significantly to the overall motion. The little number of relevant sensors inhibits a detailed analysis of these modes.

Exp. #	Mass at boom tip [kg]	Pre-load [kN]	Frequency [Hz]							
			Displacements			Velocities				Accelerations
			WA13 WA14 WA15	WA16	WA18	VA20	VA21	VA22	VA24	
V13	75	5	(0.5) 0.8 1.3 1.6 <b>3.2</b> 3.9		<i>2.1</i> <b>3.2</b>	<b>3.2</b>	<b>3.2</b>		<b>3.2</b>	<b>3.2</b>
V11	350	7.5	(0.4) <i>1.3</i>		<i>1.2</i> <b>1.6</b>	<b>(0.4)</b> 1.2 2.0		<i>1.9</i> 2.4		<b>2.8</b>
			<b>2.8</b> 3.9		2.8	2.8 3.6	<b>2.8</b>	<b>2.8</b> 3.8	<b>2.8</b>	<b>2.8</b>
V8, V9	570	10	0.8	0.6 <i>1.1</i> 1.5	(0.5) 1.1 1.3 1.5	(0.4) (0.9) (1.0) (1.3)				
			<i>1.8</i>	2.3	<b>2.5</b>	<b>2.6</b> 3.3 3.6	<b>2.5</b>	1.9 <b>2.6</b> 3.7	<b>2.6</b>	<b>2.5</b>

**Tab. 7-7 : Evaluated eigenfrequencies of the EDITH boom from vertical excitations; extended boom, EEPU up (moved out)**

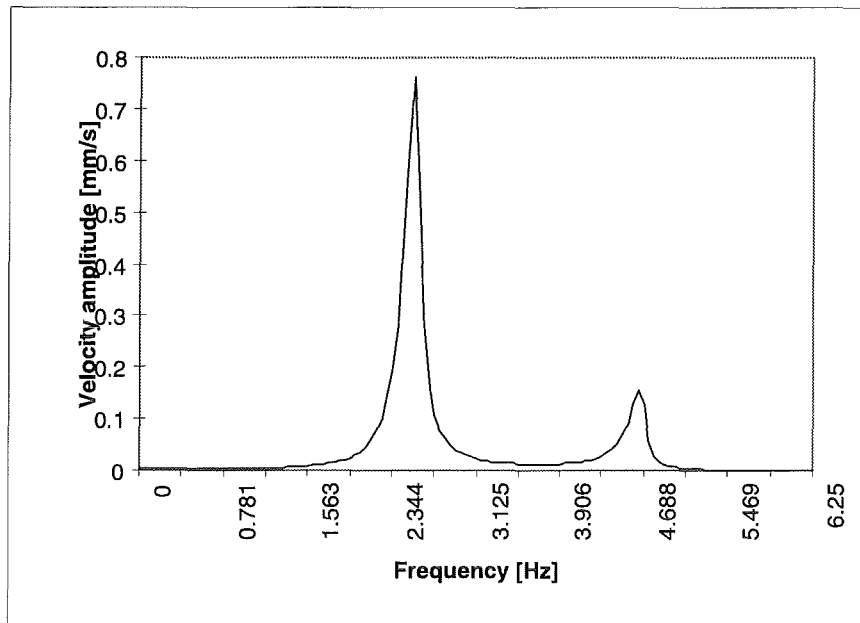


Fig. 7-19 : Velocity spectrum from sensor VA24 in test V8

Exp. #	Mass at boom tip [kg]	Pre-load [kN]	Frequency [Hz]							Accelerations
			Displacements			Velocities				
			WA13 WA14 WA15	WA16 WA17	WA18	VA20	VA21	VA22	VA24	
V27	350	7.5	(0.4)		(0.8)	0.5		(0.5)		
			2.8	2.8	2.8	(2.1) 2.8	2.8	1.2 2.8	2.8	2.8
V29	570	10	(0.6)		(0.9)	0.4	(0.4)	0.4		
			2.7	2.7	2.7 3.6	1.5 2.7 3.5	2.7	2.2 2.7 3.4	2.7	2.7

Tab. 7-8 : Evaluated eigenfrequencies of the EDITH boom from vertical excitations; boom folded by 90° at joint Z2, EEPU down (retracted)

Eigenfrequencies for the ABT configuration b) (Fig. 7-16, joint Z2 rotated by 90°) are reported in Tab. 7-8 and Tab. 7-9. In this configuration, the ABT links up to joint Z2 are subject not only to a bending moment, but also to a twisting moment due to the initial load. Therefore, the lowest frequencies found again probably represent torsional modes. There values are somewhat higher than those for the extended boom. This may be explained by two

effects acting in opposite directions. On the one hand, only the back end of the ABT up to joint Z2 participates in the torsional oscillation; the shorter the ‘torsion spring’, the stiffer it is, and the higher its eigenfrequency. On the other hand, due to the folding of the ABT at Z2, the moment of inertia about the initial ABT axis has been increased significantly. This causes lower eigenfrequencies. Obviously, the first effect slightly exceeds the second one.

The main contributions, however, to the oscillations are also in this configuration due to ‘beam’ modes. Already with the EEPU retracted (V27, V29), we now find a coupled oscillator which consists of the ABT from the base up to joint Z2 on one side and of the remainder of the ABT and the EEPU on the other side. The frequencies of the fundamental beam modes are decreased, as compared to the extended boom; the coupling mode with 3.4 to 3.6 Hz shows up in Tab. 7-8 for test V29.

Exp. #	Mass at boom tip [kg]	Pre-load [kN]	Frequency [Hz]							Accelerations
			Displacements			Velocities				
			WA13 WA14 WA15	WA16 WA17	WA18	VA20	VA21	VA22	VA24	
V33	350	7.5	(0.4) (1.4) (1.5) <b>2.1</b>	(0.4)  <b>(1.5)</b> <b>2.1</b>	  <b>1.5</b> 1.9  <b>2.6</b> <b>2.8</b>	(0.4)  <b>(1.4)</b>  (2.1)  2.7 3.3	  <b>1.4</b> <b>2.1</b>  2.7	(0.4)  (1.5) <b>2.1</b>  2.8	(1.2)   <b>2.0</b>  <b>2.8</b>	  <b>(1.4)</b>  <b>2.0</b>  <b>2.8</b>
V31	570	10	(0.4) (1.3)  <b>1.8</b> <b>2.4</b>	(0.4) (1.3)  <b>(2.0)</b> <b>2.6</b>	<b>1.3</b>  <b>1.8</b> <b>2.6</b> <b>3.1</b>	(0.4) <b>(1.3)</b>  (1.9) 2.5  3.3 3.7	(1.3)  <b>2.0</b> <b>2.6</b>  <b>(3.3)</b>	(0.4) (1.3)  <b>(2.0)</b> <b>2.7</b>	(1.2) (1.6)  <b>2.7</b>	  <b>(2.0)</b> <b>2.6</b>  <b>(3.5)</b>

**Tab. 7-9: Evaluated eigenfrequencies of the EDITH boom from vertical excitations; boom folded by 90° at joint Z2, EEPU up (moved out)**

Moving out the EEPU means to add a third part to the coupled oscillator. As may be found from Tab. 7-9, the frequency of the fundamental beam mode is decreased again, and a lot of internal modes show up in the frequency range up to 4 Hz. To illustrate this, Fig. 7-19 shows the displacement spectrum that has been evaluated from the superimposed signals of WA13, WA14, and WA15 (boom tip) in test V33.

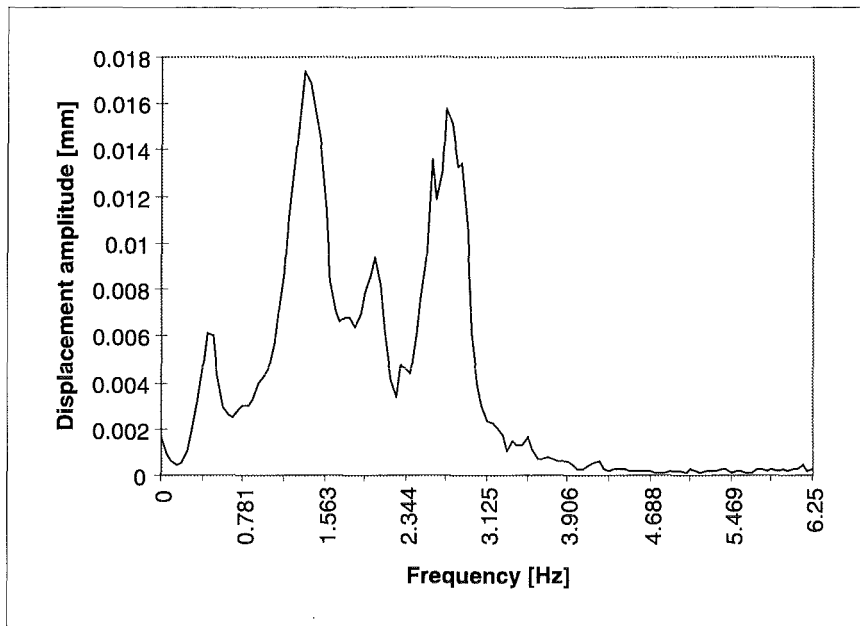


**Fig. 7-20 : Displacement spectrum from sensors WA13, WA14, and WA15 in test V33**

Qualitatively, the same picture is found for the boom configurations with folding the ABT at joint Z3 (Tab. 7-10 and Tab. 7-11). Of course, the length of the ‘torsional spring’ has been increased, and the moment of inertia about the main ABT axis is decreased; furthermore, the link between joints Z2 and Z3 belongs now to the ‘back end’ oscillator. Accordingly, some frequency values have been changed, but all the phenomena of a coupled oscillator show up again.

Unfortunately, the tests with ABT configuration c) from Fig. 7-16 did not include tests with the large additional mass (570 kg) at the boom tip. Thus only the tests with an additional mass of 350 kg can be compared across different configurations: V25/V250 against V27 and V19/V190 against V33. The higher the additional mass at the tip, the more significant become the internal modes of a coupled oscillator.

Exp. #	Mass at boom tip [kg]	Pre-load [kN]	Frequency [Hz]							Accelerations	
			Displacements			Velocities					
			WA13 WA14 WA15	WA16	WA18	VA20	VA21	VA22	VA24		
V23	75	5		(0.5)		(0.5)	(0.5)	(0.5)			
			1.1	1.1	(0.9)	(1.2)					
			1.5			(1.5)	1.5	(1.5)			
			1.6		(1.7)						
			2.0								
			2.3	2.3							
			3.3	2.8 3.1	3.3	3.3	3.3	3.3	3.3	3.3	3.3
			3.5								
V25, V250	350	7.5	(0.5)	0.5	(0.4) 0.8	0.5	(0.5)	0.5			
			1.5	1.6		(1.4)	(1.4)	(1.4)			
			2.1								
			2.3								
			3.1	2.7 3.2 3.6	3.1	3.1	3.1	3.1	3.1	3.1	3.1

Tab. 7-10 : Evaluated eigenfrequencies of the EDITH boom from vertical excitations; boom folded by 90° at joint Z3, EEPU down (retracted)

Exp. #	Mass at boom tip [kg]	Pre-load [kN]	Frequency [Hz]								
			Displacements			Velocities				Accelerations	
			WA13 WA14 WA15	WA16	WA18	VA20	VA21	VA22	VA24		
V21	75	5	(0.5)	0.5	(0.6) (0.8)	0.5	0.5	0.5			
			(1.1)			1.2	1.2			1.2	
			1.9								
			<b>2.8</b>	<b>2.9</b>	<b>2.9</b>	2.9	<b>2.9</b>	<b>2.9</b>	<b>2.9</b>	<b>2.9</b>	<b>2.9</b>
			3.6	3.6							
V19, V190	350	7.5	(0.4)	0.5	0.5	(0.4)	0.4	0.4			
			(1.0)			1.1	1.1	(0.9)		(0.9)	
			<b>2.5</b>	<b>2.6</b>	<b>2.6</b>	2.6	<b>2.6</b>	<b>2.6</b>	<b>2.6</b>	<b>2.6</b>	<b>2.6</b>
									3.3		
			3.5			3.7					

Tab. 7-11: Evaluated eigenfrequencies of the EDITH boom from vertical excitations; boom folded by 90° at joint Z3, EEPU up (moved out)

Exp. #	Mass at boom tip [kg]	Pre-load [kN]	Frequency [Hz]								
			Displacements			Velocities				Accelerations	
			WA13 WA14 WA15	WA16 WA17	WA18	VA20	VA21	VA22	VA24		
V39	350	7.5	(0.4)	(0.3) 1.2		0.4	0.4	0.4			
			1.6								
			1.9		1.8	1.8			(1.9)		
			2.2								
			<b>3.7</b>	<b>3.7</b>	<b>3.7</b>	<b>3.7</b>	<b>3.7</b>	<b>3.7</b>	<b>3.7</b>	<b>3.7</b>	<b>3.7</b>
V37	570	10	0.4	(0.4) (0.5) (1.0)		0.4	0.4	0.4			
			1.2							(1.0)	
				(1.7)		1.7			(1.7)		
			1.9								
			<b>3.5</b>	<b>3.5</b>	<b>3.5</b>	<b>3.5</b>	<b>3.5</b>	<b>3.5</b>	<b>3.5</b>	<b>3.5</b>	<b>3.5</b>

Tab. 7-12: Evaluated eigenfrequencies of the EDITH boom from vertical excitations; boom folded by 90° at joint Z4, EEPU down (retracted)

Exp. #	Mass at boom tip [kg]	Pre-load [kN]	Frequency [Hz]							
			Displacements			Velocities				Accelera-tions
			WA13 WA14 WA15	WA16 WA17	WA18	VA20	VA21	VA22	VA24	
V41	350	7.5	(0.9) 1.2 1.9 2.0 2.3 2.6 3.2 3.5	0.4	(0.3)          (1.7)	0.4          3.9	0.4          2.9	0.4          2.8	(0.4)          2.8	2.9
V43	570	10	0.4  2.6 3.2	0.4  2.6	(0.4)  2.6  3.9	0.4  2.6	0.4  2.6	(0.4)  2.6	(0.4)  2.6	2.6

**Tab. 7-13: Evaluated eigenfrequencies of the EDITH boom from vertical excitations; boom folded by 90° at joint Z4, EEPU up (moved out)**

Tab. 7-12 and Tab 7-13 list the eigenfrequencies which have been found from tests with the ABT configuration d) in Fig. 7-15, i.e., with the ABT folded at joint Z4. In principle, most of the findings from configurations b) and c) apply again; since, however, the front end link in front of joint Z4 forms a rather short and, hence, stiff oscillator, it almost behaves like a rigid lever to the ABT. Thus the main effect of this configuration is that of a considerably eccentric excitation, with bending modes and twisting modes of the ABT (up to joint Z4) being superimposed. Again, moving out the EEPU causes the behaviour of a coupled oscillator to appear.

### 7.4.3.2 Tests with horizontal excitation

In the tests with vertical excitation which have been discussed above, the initial load has essentially caused bending moments in the front end part of the ABT (from any folded joint or from the base to the EEPU support frame) about that principal axis in the boom cross section which is related to the largest areal moment of inertia. Twisting moments were induced only by unintended eccentricities; otherwise they have been restricted to the back end part of the ABT if the ABT has been folded.

The tests with horizontal excitation differ in principle at least in two respects:

- A bending moment is induced in the entire ABT about axes related to the smallest areal moment of inertia in the boom cross sections. Additionally, it causes all joints (i.e., the joint gears) to be loaded.
- At least in the tests with the EEPU moved out, the front end part of the ABT obviously experienced twisting moments. But also with the EEPU retracted, such twisting moments are likely to be induced, since the point of attack and the direction of the preload force can hardly be adjusted precisely to the 'neutral line', which, by the way, has not been known.

For these reasons, the overall picture of the test results changed dramatically. The eigenfrequencies found from these tests are listed in Tab. 7-14 through Tab. 7-17, where each table corresponds to one of the ABT configurations defined in Fig. 7-15.

Exp. #	EEPU position	Frequency [Hz]							
		Displacements			Velocities				Accelerations
		WA13 WA14 WA15	WA16 WA17	WA18	VA20	VA21	VA22	VA24	
V50	down (retracted)	0.3	(0.3)		(0.3)	(0.6)	0.3	0.6	(0.3)
				0.8 (1.3) 1.6 2.4 3.5	2.3		0.9 2.4 2.9 3.2		(1.3) 2.2 3.3

**Tab. 7-14: Evaluated eigenfrequencies of the EDITH boom from horizontal excitations; mass at boom tip 200 kg, preload 1.5 kN, boom extended**

Surprisingly, the lowest frequency found (0.3 Hz to 0.4 Hz) is almost the same in all seven tests, regardless of the boom configuration. It shows up from almost all sensors and turns out to belong to the bending mode or 'beam' mode. The boom behaves in this mode like a straight or curved cantilever beam, and the influence of the 'curvature' is minimal. Of course, the amount of the additional mass would affect the frequency value of this mode, but it has not been varied within this test series.

The signals from the velocity sensors with vertical measuring direction (VA21, VA24) indicate another mode which is to be found in most of the tests, possibly except those with the boom folded at Z4 (Tab. 7-17). Its frequency value varies to some extent from test to test: 0.6 Hz in V50, 0.7 Hz in V67 and V68, and 0.8 Hz to 0.9 Hz in V65. Supposedly, this is a twisting mode of the front end part of the ABT. In V50, where the boom has been extended, the entire ABT forms this front end part; in the other tests, it starts at joint Z2 or Z3, respectively. The decrease of the length of the twisted boom part may have caused the slight increase of the frequency values.

Tab. 7-14 contains the eigenfrequencies which were found with the extended boom configuration. Unfortunately, no test results with the EEPU moved out are available. The higher frequencies listed for V50 probably belong to local modes which cannot be identified in detail, due to limited number of appropriate sensors.

Exp. #	EEPU position	Frequency [Hz]							Accelerations
		Displacements			Velocities				
		WA13 WA14 WA15	WA16 WA17	WA18	VA20	VA21	VA22	VA24	
V67	down (retracted)	0.4	(0.4)		(0.4)	(0.4) (0.7)	0.4 (1.1)	(0.7)	0.4
					(1.8)	1.5 2.3	(1.7) 2.9	2.9	
V68	up (moved out)		(0.4)		(0.4) (0.7)	0.4 1.1 1.7	0.4 1.0 1.9	(0.7) (1.3)	0.4 1.4 1.9
				1.3	(1.3)				
				2.7 3.2 3.7	2.6	3.2		2.2 2.3 2.6	

**Tab. 7-15: Evaluated eigenfrequencies of the EDITH boom from horizontal excitations; mass at boom tip 200 kg, preload 1.5 kN, boom folded by 90° at Z2**

Tab. 7-15 lists the eigenfrequencies for the boom folded at joint Z2. Besides the lowest modes, which have already been discussed, the results from the velocity and acceleration signals in V68 indicate, though rather weakly, some coupled modes involving the boom and the extended EEPU. The frequencies of some local modes decreased in this case, as compared to V67.

Exp. #	EEPU position	Frequency [Hz]							Accelerations
		Displacements			Velocities				
		WA13 WA14 WA15	WA16 WA17	WA18	VA20	VA21	VA22	VA24	
V66	down (retracted)	0.4	0.4	0.8 1.5 2.1 2.4 2.8	0.4 1.2	0.4 (1.2) 1.9 2.8 3.7	0.4 1.2	0.4 3.2 4.0	
V65	up (moved out)	0.4	0.4		0.4 1.0	0.4 (0.9) 1.4 2.5 2.6 3.1 3.6	0.4 2.3 2.7 3.6	0.4 0.8 (1.4) 2.3 2.7 3.7	0.4 1.0 2.3

**Tab. 7-16: Evaluated eigenfrequencies of the EDITH boom from horizontal excitations; mass at boom tip 200 kg, preload 1.5 kN, boom folded by 90° at Z3**

Tab. 7-16 lists the frequency results from the tests with the ABT folded at Z3. Surprisingly, the twisting mode of the ABT front end does not show up in V66 (retracted EEPU); perhaps the line of action of the preload force accidentally hit precisely the neutral line at the boom end. The twisting mode re-appears in V65, where it has been excited in any case, due to the long lever arm formed by the extended EEPU.

The other results indicate a behaviour of the boom that is similar to that with the previous configuration. As the main difference, the frequency values have been increased.

Finally, Tab. 7-17 summarises the results from the tests with the boom folded at Z4. In both tests, V63 and V64, the signals from VA22 and VA24 contain a mode whose frequency is about 0.8 Hz. These velocity sensors are located at the lower end of the EEPU support frame; their measuring direction is parallel to the action line of the preload (VA22) and vertical (VA24), respectively. Possibly also this results indicates a twisting mode, which then would involve only the very short front end link of the ABT, the support frame of the EEPU, and the connecting structure in between. Unfortunately, there is no proof for this conjecture.

Exp. #	EEPU position	Frequency [Hz]							Accelerations
		Displacements			Velocities				
		WA13 WA14 WA15	WA16 WA17	WA18	VA20	VA21	VA22	VA24	
V63	down (retracted)	<b>0.4</b>	<b>0.4</b>		<b>0.4</b>	<b>0.4</b>	<b>(0.4)</b> 0.8	(0.4) <b>0.8</b> 1.8 2.3 2.8 3.8	<b>(0.5)</b>
V64	up (moved out)	<b>(0.3)</b> 0.9	(0.3) <b>(0.9)</b> 1.0 1.4 1.8 2.6	<b>(0.7)</b> <b>1.0</b> 1.4 1.8 <b>(2.7)</b>	(0.4) <b>(1.0)</b>	<b>0.4</b>  1.8  3.3 3.6 4.0	(0.4) <b>(0.7)</b> <b>(1.1)</b>  (2.0) 2.5 2.9 3.4	(0.4) <b>0.8</b>  (1.3) 2.3 2.9 3.4	(0.4) <b>(1.0)</b>    2.9

**Tab. 7-17: Evaluated eigenfrequencies of the EDITH boom from horizontal excitations; mass at boom tip 200 kg, preload 1.5 kN, boom folded by 90° at Z4**

Appart from this, again some coupled oscillations of the various parts of the entire boom become evident, more clearly than in the other tests; even the displacement sensors yield corresponding results. Of course, this effect is stronger in test V64 with the EEPU moved out than in V63. Fig. 7-21 shows the velocity spectrum, evaluated from the signal of VA20 in test V64. The peak of the first coupled mode is almost as high as that from the fundamental bending mode.

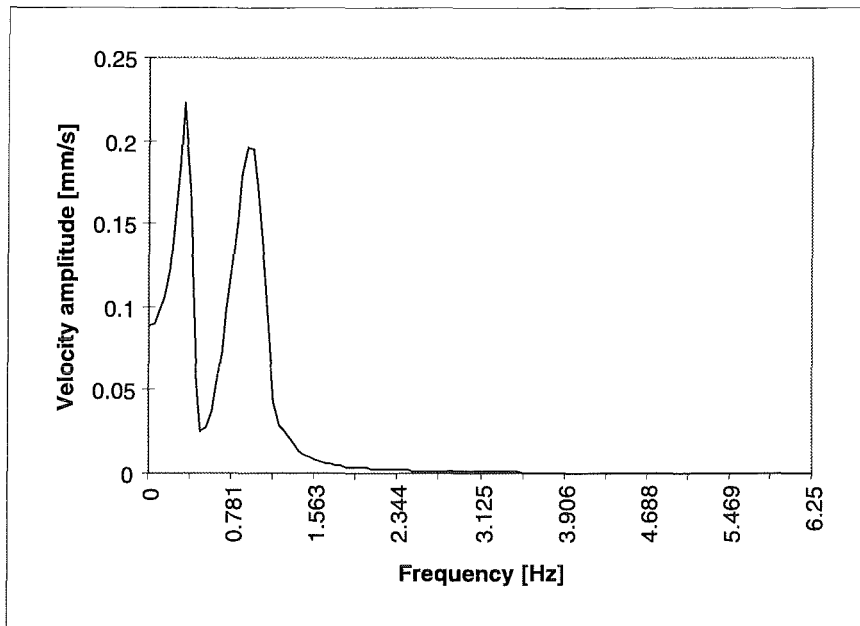


**Fig. 7-21: Velocity spectrum from sensor VA20 in test V64**

#### 7.4.4 Conclusions from the dynamic test results

Although snap-back tests with either purely vertical or purely horizontal excitation provide artificially clean conditions which will rarely be found during normal operation of the transporter, they correspond directly to two important operation modes:

- The tests with vertical excitation are very similar to situations where heavy payloads are transferred either to or from the boom, whereas
- the tests with horizontal excitation are idealised simulations of the transport mode situation.

From the tests with vertical excitation it has been found that the response of the boom in the time domain strongly depends on the actual configuration as well as on the actual payload. However, since the extended boom configuration is extremely unlikely to occur in a normal operation, the twisting modes of the boom will be most dominant in the load transfer situation, with lowest eigenfrequency values in the range between about 0.3 Hz and 0.8 Hz.

The boom response to horizontal excitation is dominated by the fundamental bending mode the eigenfrequency of which certainly depends on the actual payload – this has not been investigated in the present tests – but turned out to be very insensitive to the actual boom configuration. In the tests which have been discussed above, the corresponding frequency value always has been between 0.3 Hz and 0.4 Hz. A former investigation during the design phase of the EDITH boom [Reim1990] had yielded a considerably higher value for this eigenfrequency (0.578 Hz). Since, however, this investigation primarily did not aim on the determination of the actual eigenfrequencies, but on the comparison of different design variants, the difference between this pre-calculated value and the values found in the tests is probably due to an underestimation of the combined masses of the EEPU and of the payload.

As a concise result from both test series, it has to be stated that any controller for the EDITH drives will be faced with lowest values of significant eigenfrequencies of about 0.3 Hz or even less.

#### 7.4.5 References

- [Eberle1982] Eberle, F. and J. Kadlec: Extraction of Eigenfrequencies, Mode Shapes and Critical Damping Ratios of HDR Core Barrel Mockup from Step Relaxation Response Signals Measured in the Snapback Test Series V59, KfK 3408, Kernforschungszentrum Karlsruhe, October 1982.
- [Reim1990] Reim, J.: unpublished report, January 1990.

## Table of Content

<b>8 DEMONSTRATION OF TILE HANDLING.....</b>	<b>8-3</b>
<b>8.1 PROTECTIVE TILE ARRANGEMENT .....</b>	<b>8-3</b>
<b>8.2 REPLACEMENT OF PROTECTIVE TILES.....</b>	<b>8-3</b>
8.2.1 Task Description.....	8-3
8.2.2 Manipulator Handling Unit.....	8-4
8.2.3 Tile Handling Tools.....	8-6
8.2.4 Tile detachment device.....	8-6
8.2.5 Tile positioning device .....	8-7
<b>8.3 PERFORMANCE OF TILE EXCHANGE.....</b>	<b>8-12</b>
<b>8.4 CONCLUSION.....</b>	<b>8-16</b>
<b>8.5 REFERENCES.....</b>	<b>8-18</b>

### Figures

FIG. 8-1: TILE ATTACHMENT AT THE FIRST WALL .....	8-3
FIG. 8-2: MANIPULATOR HANDLING UNIT (MHU) AND TOOLBOX, SIDE VIEW .....	8-4
FIG. 8-3: MANIPULATOR HANDLING UNIT (MHU), TOP VIEW .....	8-4
<b>FIG. 8-4: MHU - COMPONENTS SCHEMA .....</b>	<b>8-5</b>
FIG. 8-5 : KISMET VIEW OF MHU .....	8-5
FIG. 8-6: EMSM-2B MANIPULATOR .....	8-5
FIG. 8-7: EMSM-3 MANIPULATOR .....	8-5
FIG. 8-8: TILE DETACHEMENT DEVICE (DRAWING) .....	8-9
FIG. 8-9: TILE POSITIONING DEVICE (DRAWING).....	8-9
FIG. 8-10: TILE DETACHEMENT DEVICE.....	8-10
FIG. 8-11: TDD WITH GRIPPED TILE .....	8-10
FIG. 8-12: TREPANNING OF TILE.....	8-10
FIG. 8-13: TDD WITH REMOVED TILE .....	8-10
FIG. 8-14: TILE POSITIONING DEVICE .....	8-11
FIG. 8-15: TPD WITH GRIPPED TILE .....	8-11
FIG. 8-16: TPD FIXING SPARE TILE.....	8-11
FIG. 8-17: SPARE TILE FIXED AT WALL .....	8-11
FIG. 8-18 : PEXOS ACTION/STATE NETWORK FOR TILE HANDLING.....	8-13
FIG. 8-19: PEXOS ACTION/STATE NETWORK FOR BOLTS EXCHANGE .....	8-14
FIG. 8-20: TRANSPORT POSITIONS AND TRANSITIONS .....	8-15

### Tables

TAB. 8-1: OPERATION STEPS AND REQUIRED EQUIPMENT FOR TILE REPLACEMENT .....	8-4
<b>TAB. 8-2: TECHNICAL DATA OF THE TILE DETACHMENT DEVICE .....</b>	<b>8-8</b>
TAB. 8-3: TECHNICAL DATA OF TILE POSITIONING DEVICE .....	8-8
TAB. 8-4: TRANSPORT SUBTASKS OF TH .....	8-15
TAB. 8-5: TOOL HANDLING SUBTASKS FOR TH .....	8-15
TAB. 8-6: STATES OF TH .....	8-15



## 8 DEMONSTRATION OF TILE HANDLING

### 8.1 PROTECTIVE TILE ARRANGEMENT

Armour tiles manufactured from Carbon fibres reinforced graphite will protect the plasma facing surfaces of the first wall from sputtering and wear and will prolong thus the life of the exposed components. Depending on the area where the tiles are mounted their size and weight can differ. A typical size for tiles arranged in the equatorial plane is 300 mm high, 160 mm width and 20 mm thick, a typical weight is approximately 2 kg [KS88, RSS91, SUP92, SUP94].

Fig. 8-1 shows the attachment scheme of radiative cooled tiles using two studs in low-conductivity Carbon Fibre Composite fitted in the first wall slots. Each stud carries a coarse M12 thread. A removable pin at the stud ensures alignment and correct thread engagement. Two conical holes in the tiles mate with conical nuts. Graphite circlips permit rotation of the nuts in the holes but hold them captive during handling. Grooves at the small sides of the tiles permit handling by means of grippers as part of the handling devices.

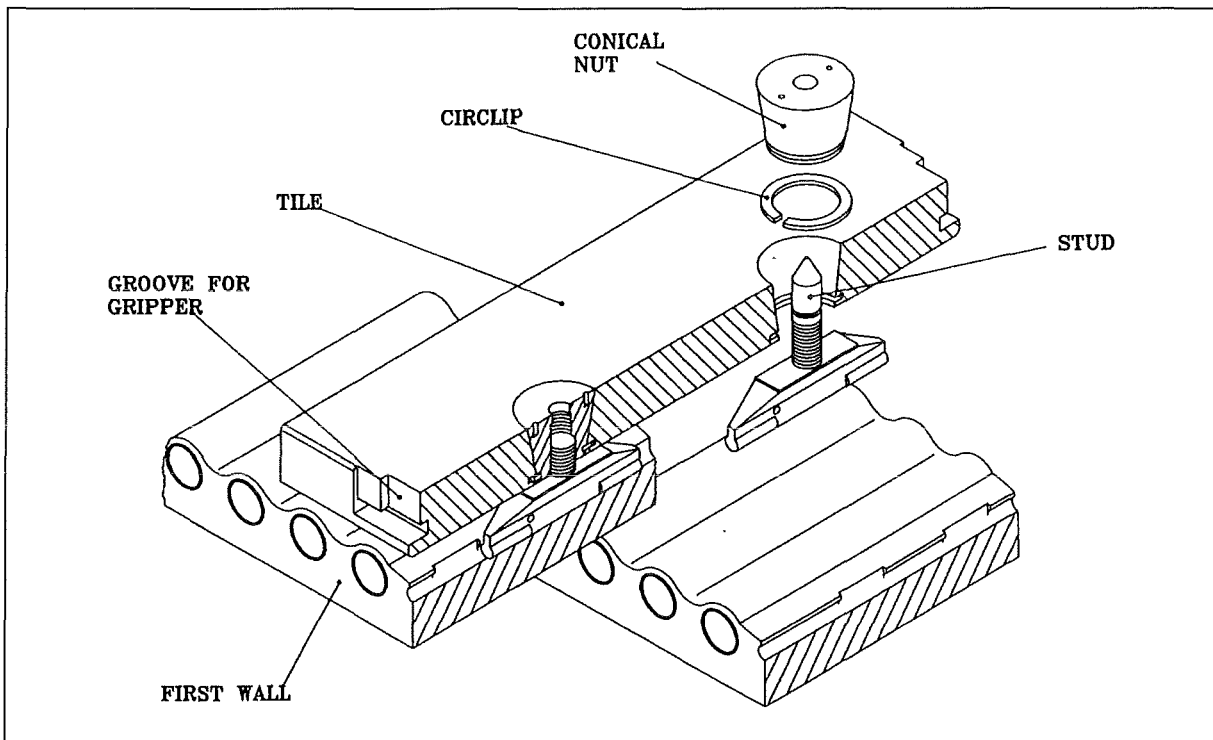


**Fig. 8-1: Tile Attachment at the First Wall**

### 8.2 REPLACEMENT OF PROTECTIVE TILES

#### 8.2.1 Task Description

Tiles are fastened at the first wall by studs and conical nuts. The nuts can be screwed using the slots at the upper surface for engaging the screw driver. According to the possible wear of the tiles and the conical nuts in a fusion reactor it must be assumed that unscrewing will not be possible after some time of operation. Therefore, other solutions than unscrewing the nuts had to be found. The chosen solution was the trepanning of the nuts. This means that removed

tiles, studs and nuts have to be replaced by new ones. For replacing tiles the main operation steps and the required equipment are listed in Tab. 8-1.

Operation steps	Required equipment
Grasping the tile to be replaced and trepanning the nuts	Manipulator handling the tile detachment device
Transfer of the removed tile to a waste magazine for tiles	Manipulator handling the tile detachment device
Removal of the studs and transfer of the removed studs to a waste magazine for studs	Manipulator, no special tools
Picking up of spare studs and positioning of them in slots of the first wall	Manipulator, no special tools
Grasping a spare tile from a magazine and its positioning	Manipulator handling the tile positioning device
Fastening the spare tile	Manipulator handling the tile positioning device

**Tab. 8-1: Operation Steps and Required Equipment for Tile Replacement**

### 8.2.2 Manipulator Handling Unit

The MHU represents a multi-purpose work unit and is mainly used to handle different tools, e.g. to replace armour tiles. It is constructed as an interim solution for the demonstration of maintenance tasks and is composed of one electric master-slave manipulator of FZK-type EMSM3, one electric master-slave manipulator of FZK-type EMSM2-B, and one adaptation unit for connecting the slave arms of both manipulators and for the attachment to the manipulator positioning unit. The technical data of the manipulators are listed in Tab. 2-4. It is the purpose of the adaptation unit to connect both slave arms with the MPU. On the other hand, the adaptation unit has to compensate the geometrical differences of both slave arms. Thus it is possible to operate with both arms almost within the same reach of envelope. The MHU is shown in Fig. 8-2 to Fig. 8-7. The MHU includes a viewing system consisting of two working cameras mounted on special arms and two overview cameras on pan/tilt heads [KS93].

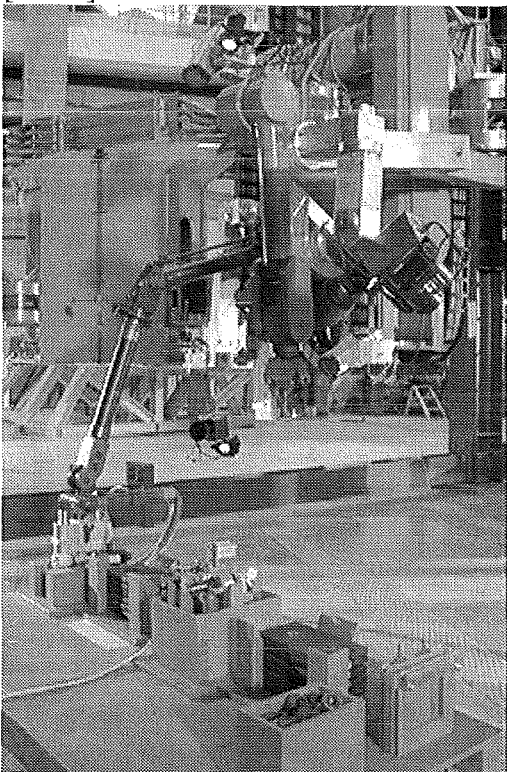


**Fig. 8-2: Manipulator handling unit (MHU) and toolbox, side view**

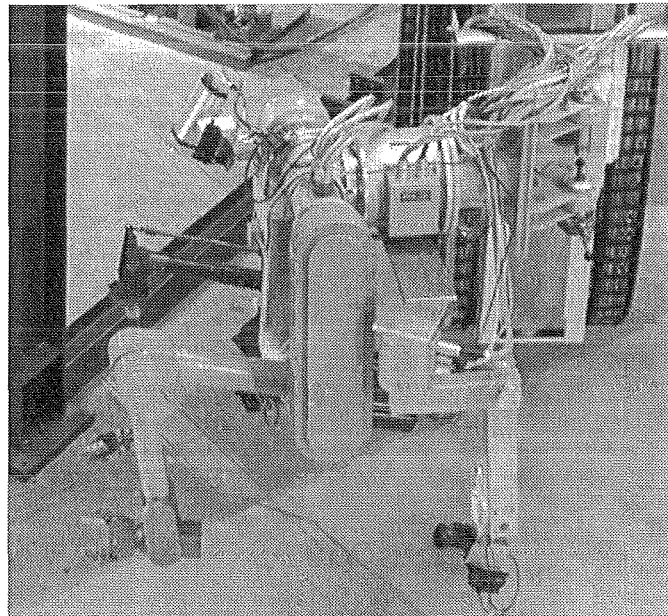


**Fig. 8-3: Manipulator handling unit (MHU), top view**

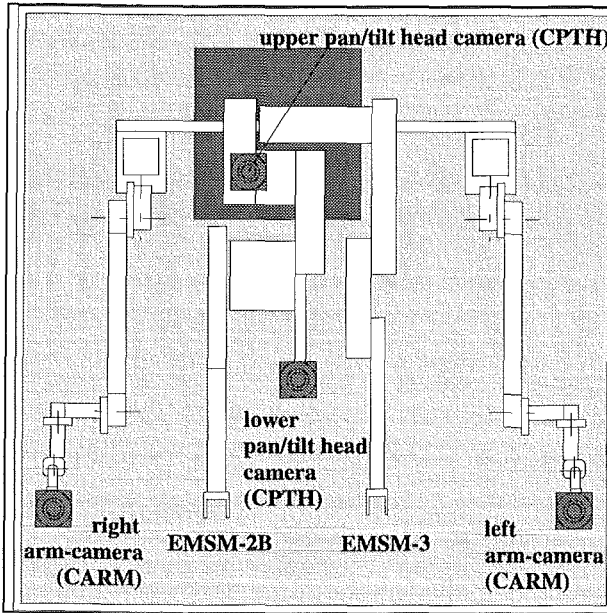


Fig. 8-4: MHU - components schema

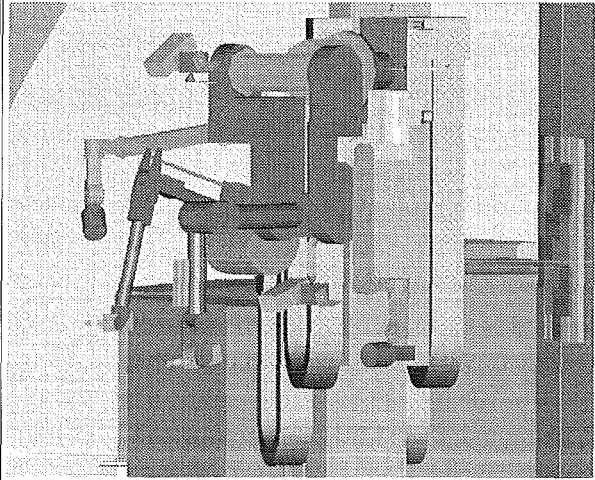


Fig. 8-5 : KISMET view of MHU

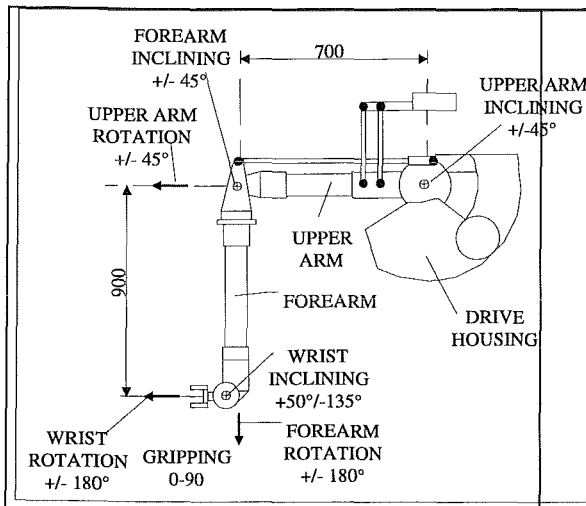


Fig. 8-6: EMSM-2B Manipulator

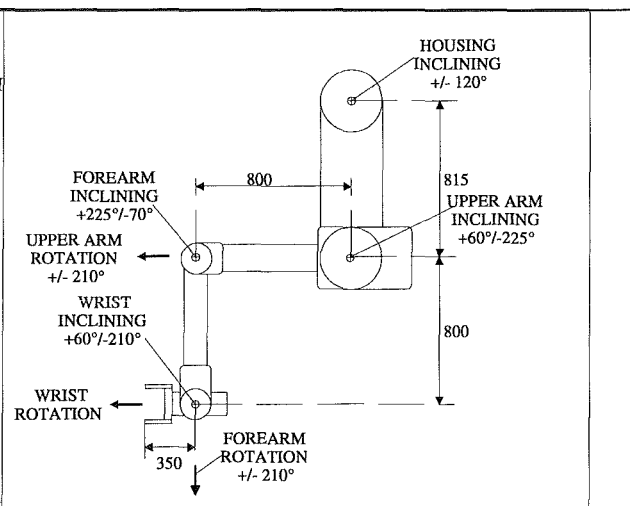


Fig. 8-7: EMSM-3 Manipulator

### 8.2.3 Tile Handling Tools

For the tile handling experiment two special tools were developed which have to be grasped and positioned by a master-slave manipulator:

- the tile detachment device (TDD) for unmounting a defect tile and
- the tile positioning device (TPD) for mounting a new tile.

### 8.2.4 Tile detachment device

The TDD (Fig. 8-8 and Fig. 8-10 to Fig. 8-13) serves to detach and transport the tiles. It includes two parallel arranged trepanning drills which are actuated by one motor via a common drive unit and a fixed forward feed. The device has a mechanism to grasp and hold the tile for transport which mates with the grooves of the tile and positions the drills at once. Limit stops at the drills prevent from possible contact with the first wall behind the tile and its damage. The final positions of the drills are controlled by limit switches. All bearings are double tightened and lubricated by MoS<sub>2</sub>. In order to keep the weight of the device as small as possible mechanically small loaded components are fabricated from AlMgSi1. Other components are manufactured in austenitic steel 1.4541. The weight of the TDD is approximately 12 kg.

The main components of the TDD are

- the drive,
- the trepanning drills, and
- the gripper for the tiles.

The drive consists of the brushless AC servo-motor, the spur wheel gear for drilling and the forward feed. The motor is installed in such a way that it can be replaced remotely.

The motor actuates via a worm gear and additional spur wheel gear simultaneously both drills. The trepanning drills and the spur wheels are connected by means of spline toothings. Via the worm gear and a further spur wheel gear the spindle nuts are actuated. The spindles themselves are part of the drills and have fine pitch threads. The pitch of the thread in connection with the gear ratio determine the forward feed. Thus drilling revolutions and forward feed have a pre-determined ratio. At the final positions the drills are stopped via limit switches and can only be taken into operation with an opposite sense of rotation. The stops of the limit switches can be fixed depending on the tile thickness. The drills stop at least 3 mm in front of the first wall.

The trepanning drills have diamond cutting points. Slots in the drills and hollow axles allow in combination with an externally arranged vacuum cleaner the removal of dust.

The gripper is based on a lever concept. It is actuated by the drill shaft such that the first few millimetres of the drill forward feed close the gripper before the trepanning drill touches the tile. Vice versa are the last few millimetres in the opposite direction of the drill path used for opening the gripper. This operations are controlled by limit switches. The data of the TDD is found in Tab. 8-2.

### 8.2.5 Tile positioning device

The TPD (Fig. 8-9 and Fig. 8-14 to Fig. 8-17) is used to position and fasten the tiles at the first wall. It includes the mechanism to grasp and hold a tile and a parallel arranged set of two screw-drivers. The latter one is used to fasten the tile by means of conical nuts. The gripper mates with the grooves at the small side of the tile. All bearings are double tightened and lubricated by MoS<sub>2</sub>. In order to keep the weight of the device as small as possible mechanically small loaded components are fabricated from AlMgSi1. Other components are manufactured in austenitic steel 1.4541. The weight of the TDD is approximately 12 kg.

The main components of the TPD are

- the drive,
- the screw drivers, and
- the gripper for the tiles.

The drive consists of the brushless AC servo-motor and the worm gear. The motor is installed in such a way that it can be replaced remotely.

The driving shaft of the worm gear actuates the one screw driver directly and the other one via a spur wheel gear. Dynamometric clutches limit the fastening forces for the tiles. The torques of the clutches are separately adjustable. In order to compensate the forward feed during screwing the head of the screw drivers are spring mounted. Pusher dogs mate with the conical nuts.

The gripper is a toggle lever construction. At power loss the gripper stays closed. Thus the tile can not be lost. The gripper becomes opened by a DC lifting magnet. Beyond the dead centre of the toggle lever a set of disk springs keeps the lever in position even if forces act on the tile which would otherwise open the gripper. The closing movement of the gripper is performed by means of a preloaded spring acting on the lifter rod of the magnet.

A set of four spring loaded pressure pads is foreseen to align the TPD and tile. From the first experiments it has to be seen that the pads are unnecessary and can only be used to give the operator orientation for the handling.

The technical data of the TPD are listed in Tab. 8-3.

Drill diameter	50 mm
Cut point	Industrial diamant
Drill revolutions	100 to 400 min <sup>-1</sup>
Forward feed	approx. 0.1 mm/revolution
Maximum forward feed path	25 mm
Drive unit motor	Brushless AC servo motor, D312-002, MOOG

**Tab. 8-2: Technical Data of the Tile Detachment Device**

Revolutions of the screw driver spindles	100 min <sup>-1</sup>
Force of the drivers	20 N
Torque at the nuts	1.5 Nm
Drive unit motor	Brushless AC servo motor, D312-002, MOOG
Torque of the dynamometric clutch	1 to 5 Nm
Force of the lifting magnet	100 N
Stroke of the lifting magnet	10 mm
Duty cycle	25%
Maximum force of the gripper	60 N

**Tab. 8-3: Technical Data of Tile Positioning Device**

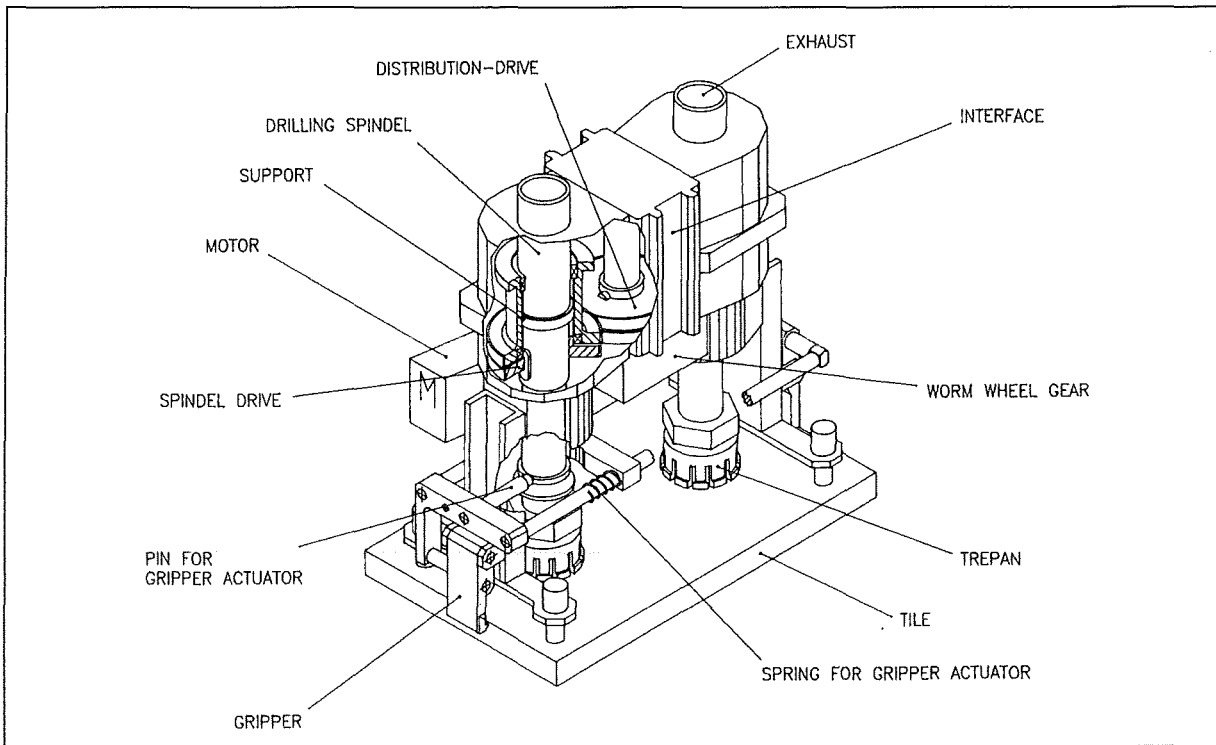


**Fig. 8-8: Tile detachment device (drawing)**

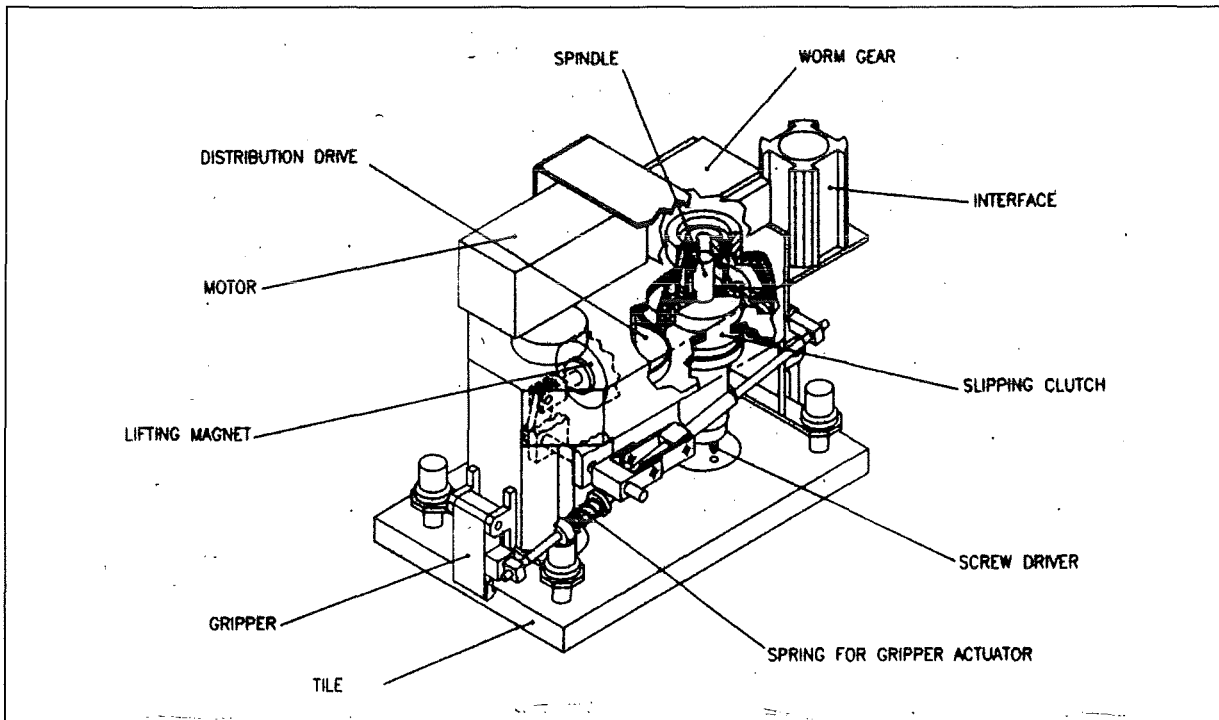


**Fig. 8-9: Tile positioning device (drawing)**

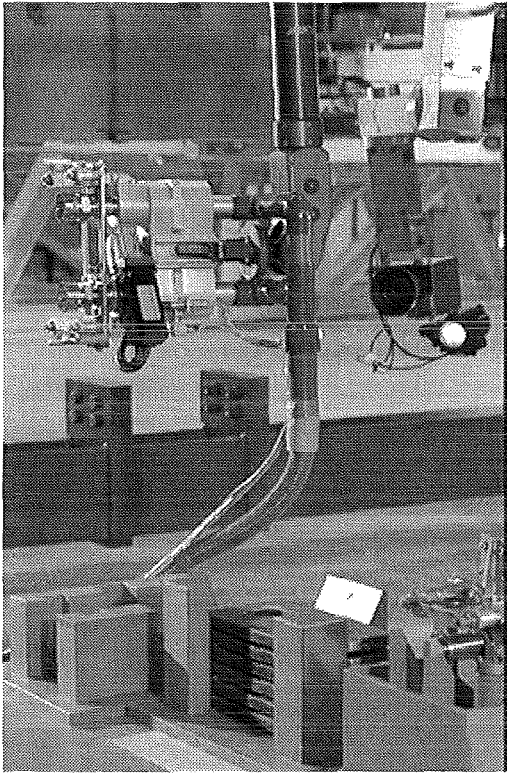


**Fig. 8-10: Tile detachment device**

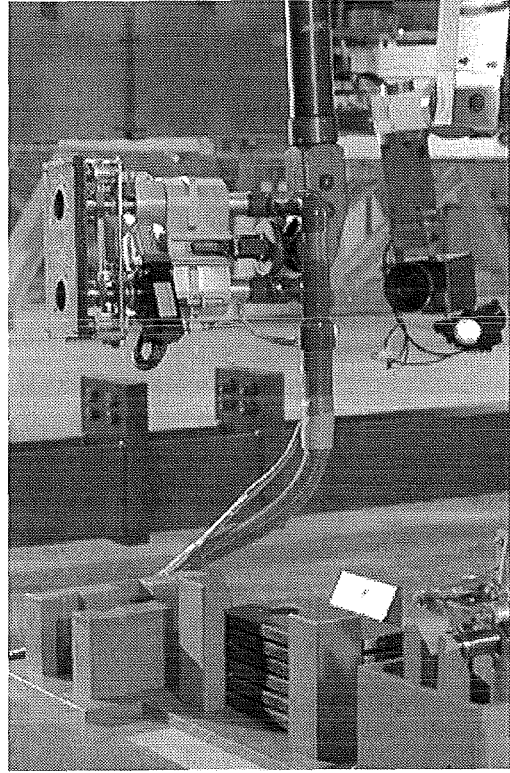


**Fig. 8-11: TDD with gripped tile**

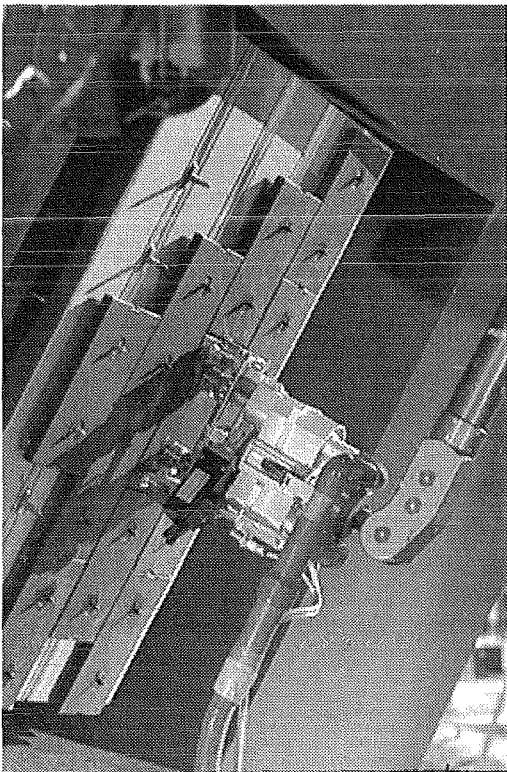


**Fig. 8-12: Trepanning of tile**

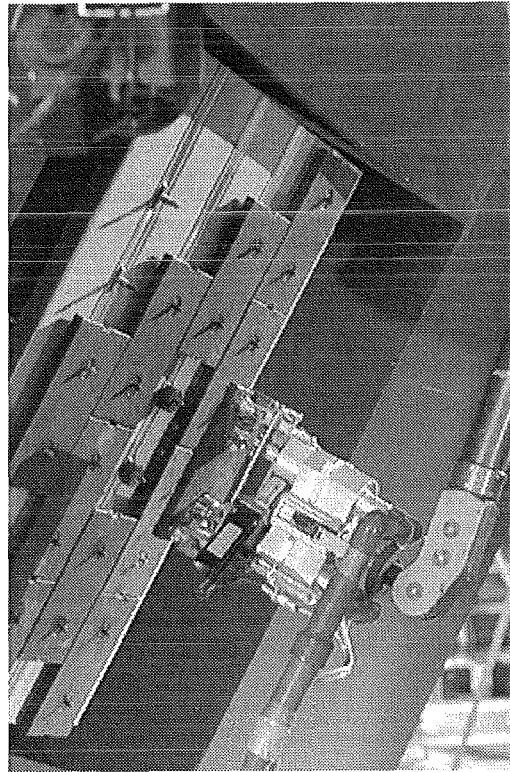


**Fig. 8-13: TDD with removed tile**

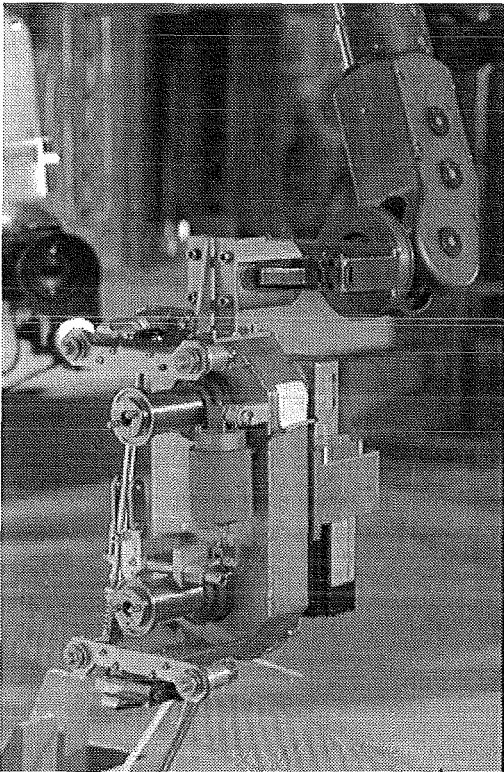


**Fig. 8-14: Tile positioning device**

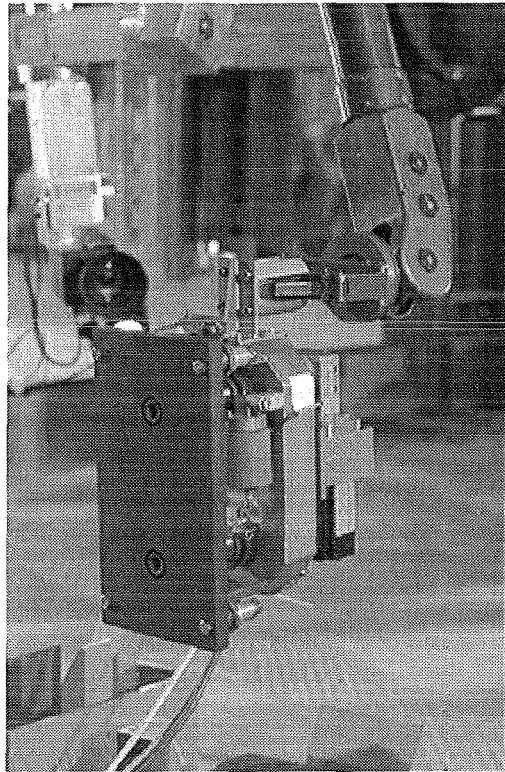


**Fig. 8-15: TPD with gripped tile**

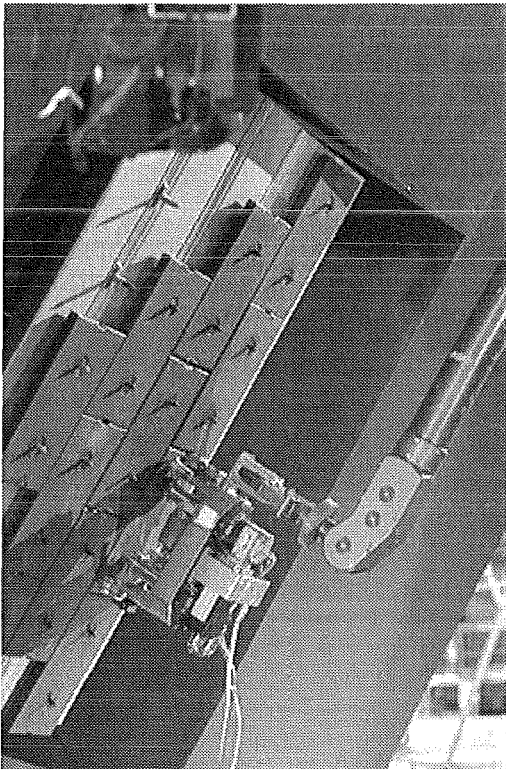


**Fig. 8-16: TPD fixing spare tile**

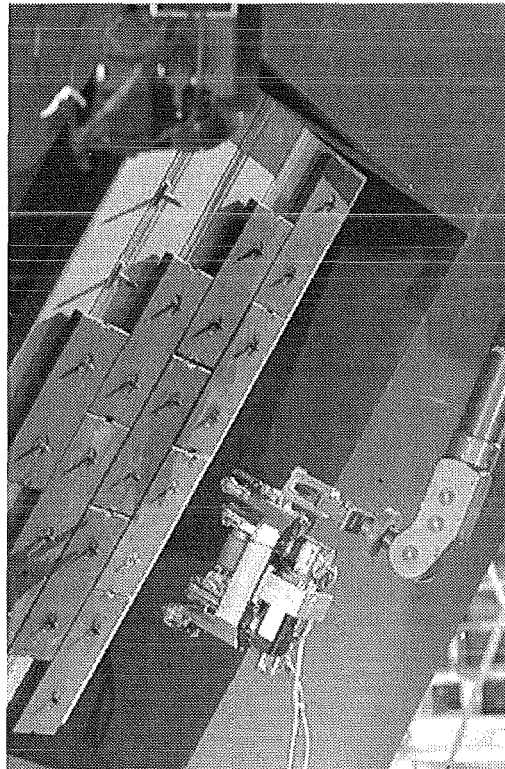


**Fig. 8-17: Spare tile fixed at wall**

### 8.3 PERFORMANCE OF TILE EXCHANGE

For the demonstration of armour tiles work sites in the upper half of the torus mock-up have been arranged. According to the requirements the tiles were fixed by studs and conical nuts. Replacement of the tile was done with the TDD and the TPD both handled with the manipulator handling unit of the ABT. The tools were handled by the EMSM2B and the EMSM3 was used for auxiliary tasks. The magazines for tools and tiles have been arranged at the floor of the mock-up. The supply lines for the tools were not routed at the ABT. In a final version the supply lines will have to be integrated with the consequence that tools and manipulator will have to be remotely connectable in order to allow the tool exchange inside the plasma chamber.

The tests were performed remotely without direct view by two operators from the control room. The ABT and the viewing system has been controlled by the co-ordinating operator, the MHU and the tools by the manipulator operator.

During the planning and preparation phase of the tile exchange task the whole procedure was modelled by PEXOS (Fig. 8-18, Fig. 8-19, Fig. 8-20, Tab. 8-4, Tab. 8-5, Tab. 8-6) and KISMET. Furthermore the EDITH transportation tasks and the camera positions and viewing directions for the different working positions were taught-in and needed device macro functions were developed using the DOIF system to facilitate application dependent controlling. Video sequences, textual descriptions, photos, and drawing of all relevant working steps were produced and integrated. At the end of these preparation not only a complete multimedia documentation was available but also an executable high-level program integrating all agents of the task including the operators. During the task execution PEXOS leads the operators step-by-step through the procedure which is visualized graphically by a network of actions and states (Fig.5-10, Fig. 5-11) . The transportation tasks are directly started via PEXOS by the coordinating operator and they are monitored using the DOIF subsystem (Fig. 5-12, Fig. 5-13) and KISMET (Fig. 5-14). Camera control is reduced to one operator request and probably needed small corrections. The servo-manipulator operator is integrated into the system via a computer screen displaying subtask working instructions and requesting for confirmations of the start and termination of the manual work. Both operator can call for describing information and notices at any time. To cope with unforeseen situations the control system allows to intervene, to left the planned procedure, and to rejoin it afterwards.

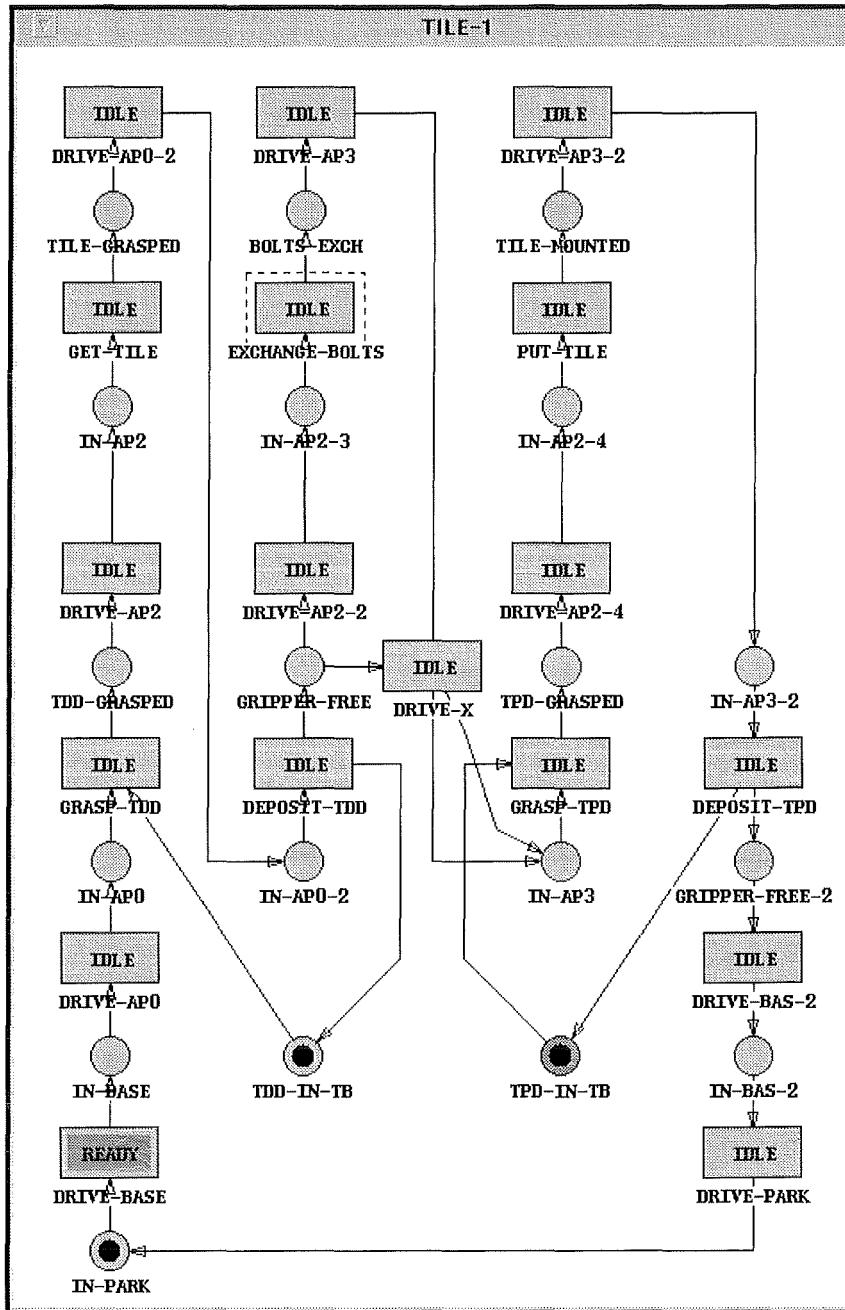


**Fig. 8-18 : PEXOS ACTION/STATE network for tile handling**  
 The subtask EXCHANGE-BOLTS is described in detail by a subnet (Fig. 8-19)

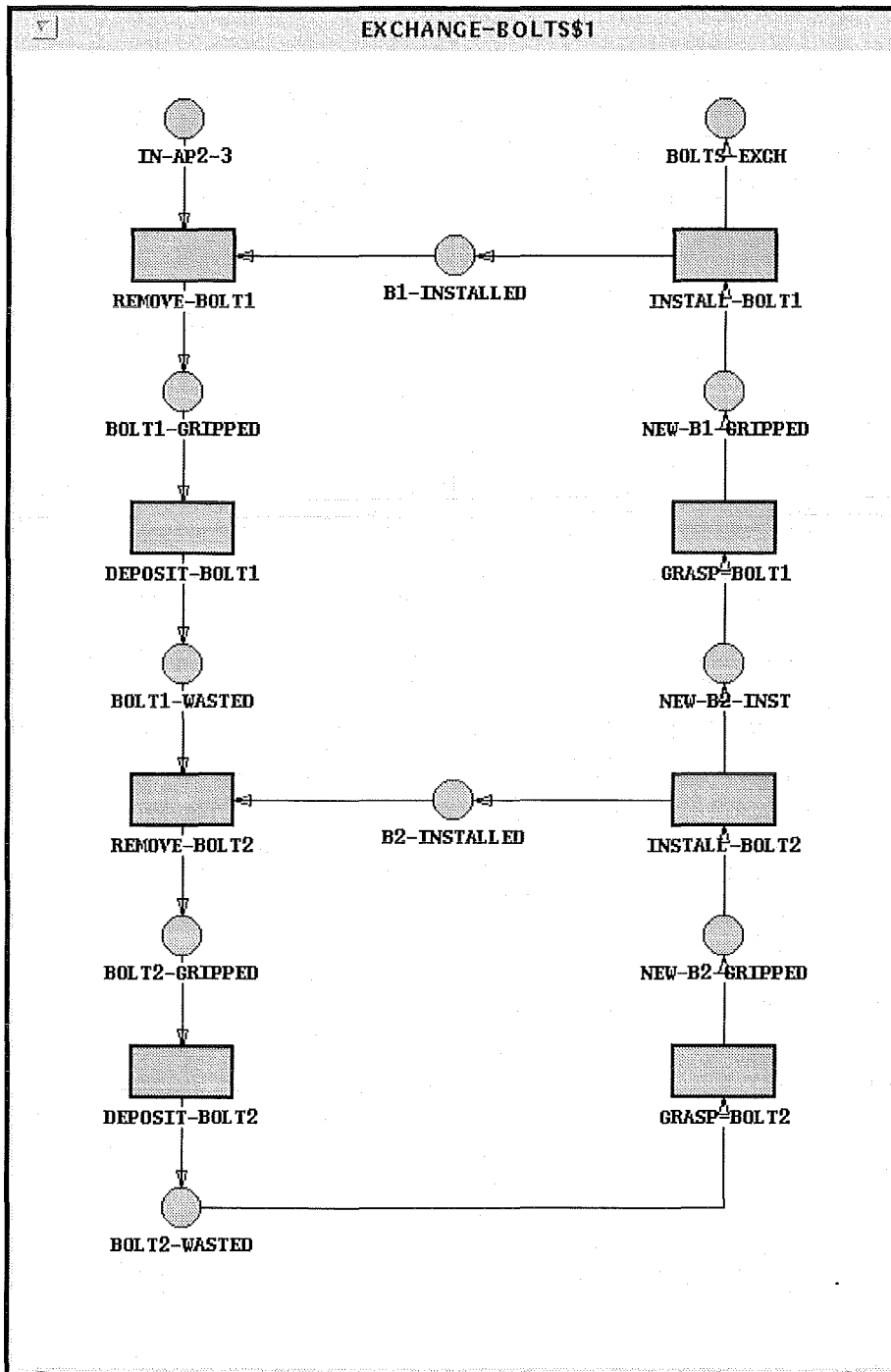
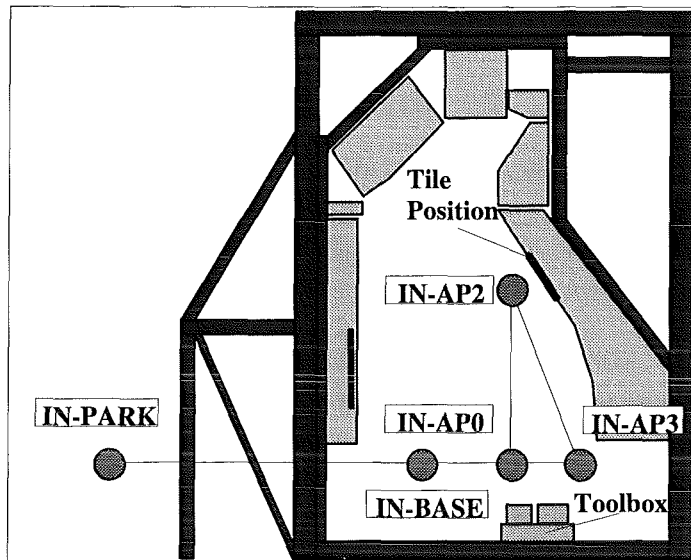


Fig. 8-19: PEXOS ACTION/STATE network for bolts exchange



**Fig. 8-20: Transport positions and transitions**

Subtask Name / ACTION	Description
DRIVE-BASE	Drive EDITH from PARK position into BASE position
DRIVE-AP0	Drive EDITH from BASE position into working position AP0
DRIVE-AP2	Drive EDITH from position AP0 into working position AP2
DRIVE-AP0-2	Drive EDITH from position AP2 into working position AP0
DRIVE-AP2-2	Drive EDITH from position AP0 into working position AP2
DRIVE-AP3	Drive EDITH from position AP2 into working position AP3
DRIVE-AP2-4	Drive EDITH from position AP3 into working position AP2
DRIVE-AP3-2	Drive EDITH from position AP2 into working position AP3
DRIVE-BAS-2	Drive EDITH from position AP3 into working BASE position
DRIVE-PARK	Drive EDITH from BASE position into PARK position
DRIVE-X	Drive EDITH from working position AP0 to working position AP3

**Tab. 8-4: Transport subtasks of TH**

Subtask Name / ACTION	Description
GRASP-TDD	Grasp tool detachment device out of toolbox
DEPOSIT-TDD	Put old tile into waste box, put tool detachment device into toolbox
GRASP-TPD	Grasp tool positioning device out of toolbox, grasp new tile
DEPOSIT-TPD	Put tool positioning device into toolbox

**Tab. 8-5: Tool handling subtasks for TH**

State Name / FACT	Description
IN-PARK	EDITH in park position
IN-BASE	EDITH in base position (in the torus segment)
IN-AP0	EDITH in front of toolbox (near TDD)
IN-AP2	EDITH in working position in front of defect tiles
IN-AP3	EDITH in front of toolbox (near TPD)
TDD-IN-TB	TDD in toolbox
TPD-IN-TB	TPD in toolbox

**Tab. 8-6: States of TH**

## 8.4 CONCLUSION

For the tile replacement the electrical master-slave manipulator EMSM2-B has been used as a multi-purpose handling unit in combination with two special tools, the tile detachment device and the tile positioning device. The second master-slave manipulator EMSM3 supported the EMSM2-B by carrying the waste storage and the magazine for spare studs.

The trajectories of the ABT to the different pre-defined working positions have been pre-programmed and performed in an automatic mode. The articulated boom could be moved with full speed; the positioning accuracy and repeatability were in accordance with the requirements.

The working sequences for the tile replacement have been carried out by the manipulator operator using the master arm and the integrated viewing system. The replacement did not make any difficulties. The special tools worked well.

The tiles were fixed at the wall with a distance of about 5 mm. The trepanning depth resulted from the plate thickness plus 2 mm and was limited by limit switches. The electrical connections have been sensitive for graphite dust and the trepanning part for different inclinations of tile and handling device. An improvement could be possible by using proximity sensors instead of limit switches.

The camera system and lightning was satisfying for working also in the darkness of the mock-up using only the camera lightning. A hand camera was unnecessary.

The required time for the replacement of one tile was approximately 38 minutes included the transport motions needed because of the floor placed tool magazine [SUP94]. The differences of the required time for replacing one tile at daylight and in the darkness of the mock-up was small. The most time consuming operation has been the trepanning. An improvement could be possible by an optimisation of the trepanning gear ratio to increase the speed of the forward feed.

The determined times for the different handling operations can be used for further time estimations, e.g. for the performance of some replacement operations in parallel as moving the EEPU and positioning of the cameras. Time estimations are now also possible for the replacement of more than one tile and changing for this activity the working sequence.

The general functions of the **Remote Handling Workstation** turned out to be sufficient. The realisation of three support tools/domains (procedural, spatial, functional) and a loose coupling between them turned out to be a very flexible architecture. Especially in the pre-tests the possibility of using the RHWS subsystems stand-alone was very helpful because not always the whole RHWS functionality is needed.

The possibilities of switching from planned control to unplanned manual control and back are easy to use. In unplanned situations the operators can interrupt the planned procedure to work manually with the devices via the DOIF and then rejoin the planned procedure as represented by the PEXOS system. The PEXOS coordination techniques (with the possibility to coordinate even parallel action sequences) especially the integration of the manipulating operator is solved satisfactorily by a simple START-DONE message sequence. During the

procedure execution the operators had always a good and sufficient overview over the state of the work and the devices. During the execution no deficiencies in the state presentation became evident.

Very important for the usability of a procedural support tool (PEXOS) is the visual presentation of the task structure, the task state, and the task dynamics because the operator should be able to grasp the work situation at a glance. In all task performances or offline demonstrations we found that the selected graphical representation of the procedure by Petri nets is easily understandable: it seems to be a natural. This type of procedure representation uses only two types of graphical elements and arcs for their logical connections. In addition, those elements are described in more detail by texts and other means. The shown interrelationships are understandable even without an introduction.

In teaching new motion pathes with the EDITH boom the available two modes of simulation had a favourable effect: the motion was first planned (simulated) with KISMET, then simulated in the control systems simulation mode using KISMET as the virtual device (but running the control algorithms without controlling the motors). This enhances the safety and also makes it possible to prepare work without allocating the real device.

The possibility of controlling the DOIF system and KISMET from PEXOS by ACTION/FACT related messages (e.g. opening and positioning of windows, changing views) facilitates the usage of the two subsystems remarkably because this support is problem suited.

The *DOIF manager* was found an important tool for information bundling (compression) to facilitate manual control as well as control from PEXOS. Especially in the preparation phase of the TH procedure when new working subsequences were tried out those could easily put into a DOIF script.

All demonstrations were done with two operators: a manipulating operator and a coordinating/assisting operators but the second operator is only needed if unplanned situations occur. In the normal case all controlling could be done by the manipulating operator because the transport motions and the camera control are reduced to simple button clicks.

Repetitions of the experiment even after longer time were easily performed because the documentation is very comprehensiv such that all questions concerning the performance can be answered. The documentation includes all operational details, even special action related remarks (notices) of the operator.

The interpreted command languages of the RHWS on all three domains and the possibility to refer to programs of another domain was very helpful in the preparation phase as well as in ad-hoc and on-the-fly adaptations during execution.

Model based support systems rely on the accordance of model and reality. Therefore the control systems have to provide state change messages and the capability to respond on state requests to synchronize state representations directly with system states. The capability of PEXOS and KISMET to request for and to evaluate those messages should be enhanced.

## 8.5 REFERENCES

- KS88 Köhler, G.W., Salaske, M.: Elektrischer Master-Slave-Manipulator EMSM2B. Kerntechnik, Carl Hanser, München, 1988
- RSS91 Reeve, T., Shaw, R., Suppan, A., Haferkamp, B.: The remote maintenance of mechanically attached first wall armour tiles in NET. Proc.of the 2nd Internat.Symp.on Fusion Nuclear Technology, Karlsruhe, June 2-7, 1991 Part C Fusion Engineering and Design, 18(1991) S.495-99, Karlsruhe
- SUP92 Suppan A., Hübener, J. Reim, J., Woll, J., Maisonnier, D., Reeve, T.J.: EDITH - A Prototypical Articulated Boom System for NET/ITER, 17th Symposium on Fusion Technology, Roma Sept. 14-18, 1992, Fusion Technology 1992, Vol.2, pp.1599-1603
- KS93 Köhler, G.W., Süßdorf, W.: unpublished report, April 1993
- SUP94 Suppan, A., Gutzeit, H., Haferkamp, B., Knüppel, H., Leinemann, K., Woll, J.: unpublished report, Oct. 1994.

## Table of content

<b>9 HANDLING OF HEAVY LOADS</b> .....	<b>9-3</b>
<b>9.1 OBJECTIVES OF THE EXPERIMENT</b> .....	<b>9-3</b>
<b>9.2 EXPERIMENTAL SET-UP</b> .....	<b>9-3</b>
<b>9.3 WORKSTATION PREPARATION</b> .....	<b>9-7</b>
<b>9.4 CONTROL SYSTEM PREPARATION</b> .....	<b>9-13</b>
9.4.1 Transporting heavy Loads within the Mock-up .....	9-13
9.4.2 Measurements of position accuracy .....	9-15
9.4.3 Reconfiguration .....	9-18
9.4.4 Technical Data .....	9-18
<b>9.5 PERFORMANCE OF THE EXPERIMENT</b> .....	<b>9-19</b>
<b>9.6 CONCLUSION</b> .....	<b>9-19</b>
<b>9.7 REFERENCES</b> .....	<b>9-21</b>

## List of figures

FIG. 9-1: DIVERTOR MOCK-UP AND FORK (DIMENSIONS) .....	9-5
FIG. 9-2: MOTION PATH FOR DIVERTOR EXCHANGE (DETAIL) .....	9-5
FIG. 9-3: DIVERTOR FORK DRAWING .....	9-5
FIG. 9-4: DIVERTOR FORK PHOTO .....	9-5
FIG. 9-5: EDITH WITH DIVERTOR IN TORUS .....	9-6
FIG. 9-6 : PEXOS ACTION/STATE GRAPH FOR DIVERTOR TRANSPORT .....	9-8
FIG. 9-7: SCHEMA OF TRANSPORT PROCEDURE .....	9-9
FIG. 9-8: PEXOS SCREEN FOR DIVERTOR TRANSPORT .....	9-10
FIG. 9-9 : KISMET OVERVIEW OF EDITH SITE .....	9-12
FIG. 9-10: KISMET DIVERTOR NEAR TORUS POSITION .....	9-12

## List of Tables

TAB. 9-1: MAXIMUM DIMENSIONS AND WEIGHTS OF DIVERTOR PLATES .....	9-4
TAB. 9-2: DIVERTOR EXCHANGE PROCEDURE SUBSTATES .....	9-9
TAB. 9-3: DIVERTOR EXCHANGE PROCEDURE SUBTASKS .....	9-9
TAB. 9-5: PARAMETER SETTINGS .....	9-18
TAB. 9-6: EXPERIMENTAL RESULTS .....	9-18



## 9 HANDLING OF HEAVY LOADS

The key experiment with EDITH is the divertor exchange experiment because in this case the maximum load is reached and the most unwieldy load is transported. To handle the divertor in narrow environment during assembly or disassembly a divertor handling unit (DHU) is needed providing a gripper and some special degrees of freedom in addition to the transporter links.

The development and production of the DHU was not possible within the EDITH project though planned in the beginning [DHD90, NET90]: The planned divertor exchange experiment was replaced in agreement with NET by an experiment for **Handling Heavy Loads** (HHL).

In the HHL experiment a divertor plate mock-up is picked-up and placed by the EDITH transporter equipped with a simple load fork. This is done in one torus position and one magazine position. The experiment was controlled from the control room via the Remote Handling Workstation [PKF54].

### 9.1 OBJECTIVES OF THE EXPERIMENT

Because of various reasons the divertor handling unit could not be developed and manufactured as planned. The EDITH experimental program therefore must be reduced to a key problem in divertor exchange: the *transport and transfer of heavy, unwieldy loads* by the EDITH transporter. This experiment is more challenging than using the divertor handling unit because of the missing extra degrees of freedom the transporter has to execute also the required fine motion (positioning). The objectives of the HHL experiment were:

- Demonstration of the mechanical transport capability
- Demonstration of the task suited motion controllability and boom manoeuvrability while carrying heavy, unwieldy loads in narrow environments
- Demonstration of the abilities of the guidance system, to support the operator in all phases of his work in performing lengthy complex tasks without direct view and restricted camera viewing.

### 9.2 EXPERIMENTAL SET-UP

The NET machine was designed with 16 divertors divided toroidally or poloidally into two segments each. The dimensions of the divertors are found in Tab. 9-1. The divertor mock-up simulates the real divertor in its weight and geometric dimensions. It represents a sheet steel box construction with an own weight of 800 kg which is brought to 1 t by tiles of lead. The divertor mock-up has four hooks for attaching it to the console and four holes for inserting the fringes of a fork. The divertor is equipped with a safety-catch working together with its counterparts at the console and the fork.

	<b>Toroidal Segmentation</b>	<b>Poloidal Segmentation</b>
Number	32 (top); 32 bottom	32 (top); 32 bottom
Width (mm)	745/1202	1861/2394
Length (mm)	3462	1657 (3350 inboard)
Height (mm)	ca. 600	ca. 670
Weight (kg)	ca. 1000	ca 1000

**Tab. 9-1: Maximum dimensions and weights of divertor plates**

For the EDITH divertor mock-up a poloidal segmentation was chosen. Fig. 9-1 shows the divertor mock-up in its working position in the torus mock-up, Fig. 9-2 shows the possible narrow motion path for divertor exchange.

To be able to get over the divertor by EDITH a simple fork was installed instead of the planned divertor handling unit. The fork is shown in Fig. 9-3 and Fig. 9-4. The fork is equipped with a simple viewing system consisting of four cameras. The cameras are looking along the four prongs of the fork thus enabling the operator to see the prongs and the related holes in the divertor mock-up during the approach.

The divertor mock-up grasped by the EDITH load fork is shown in Fig. 2-5 and Fig. 9-5.

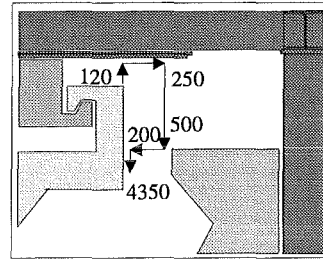
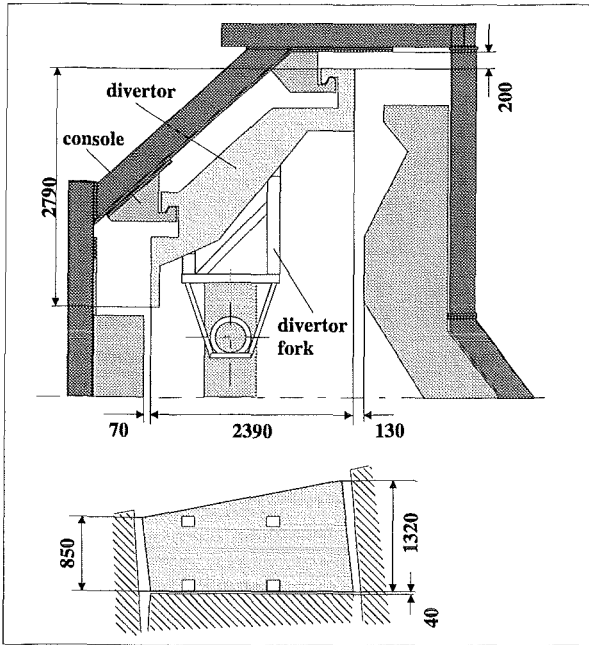


**Fig. 9-1: Divertor mock-up and fork (dimensions)**

**Fig. 9-2: Motion path for divertor exchange (detail)**

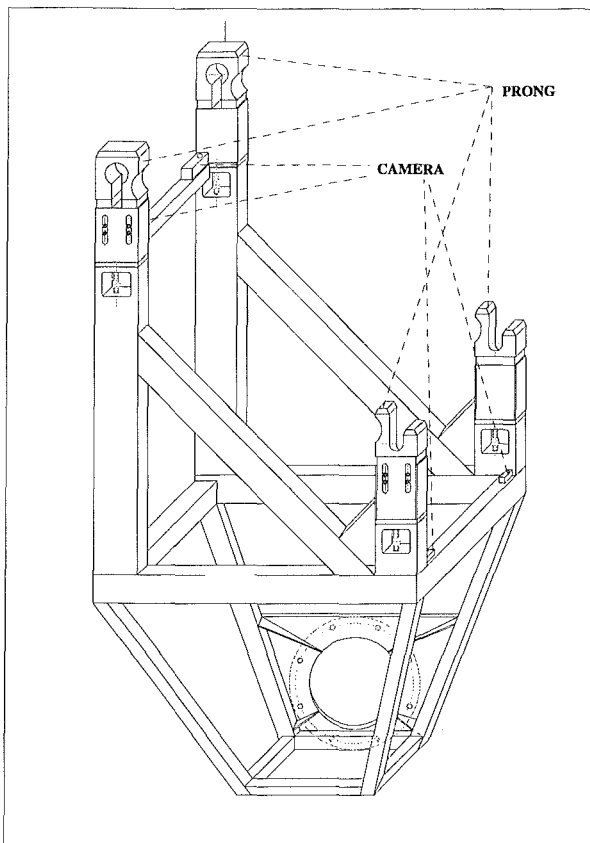


**Fig. 9-3: Divertor fork drawing**

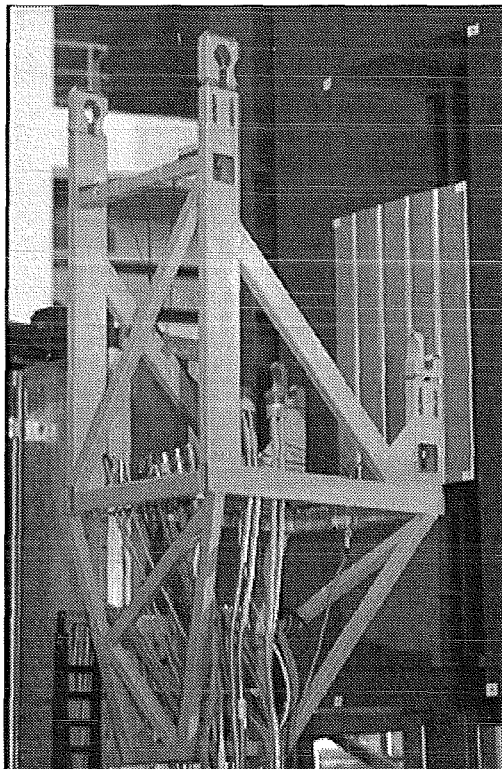


**Fig. 9-4: Divertor fork photo**

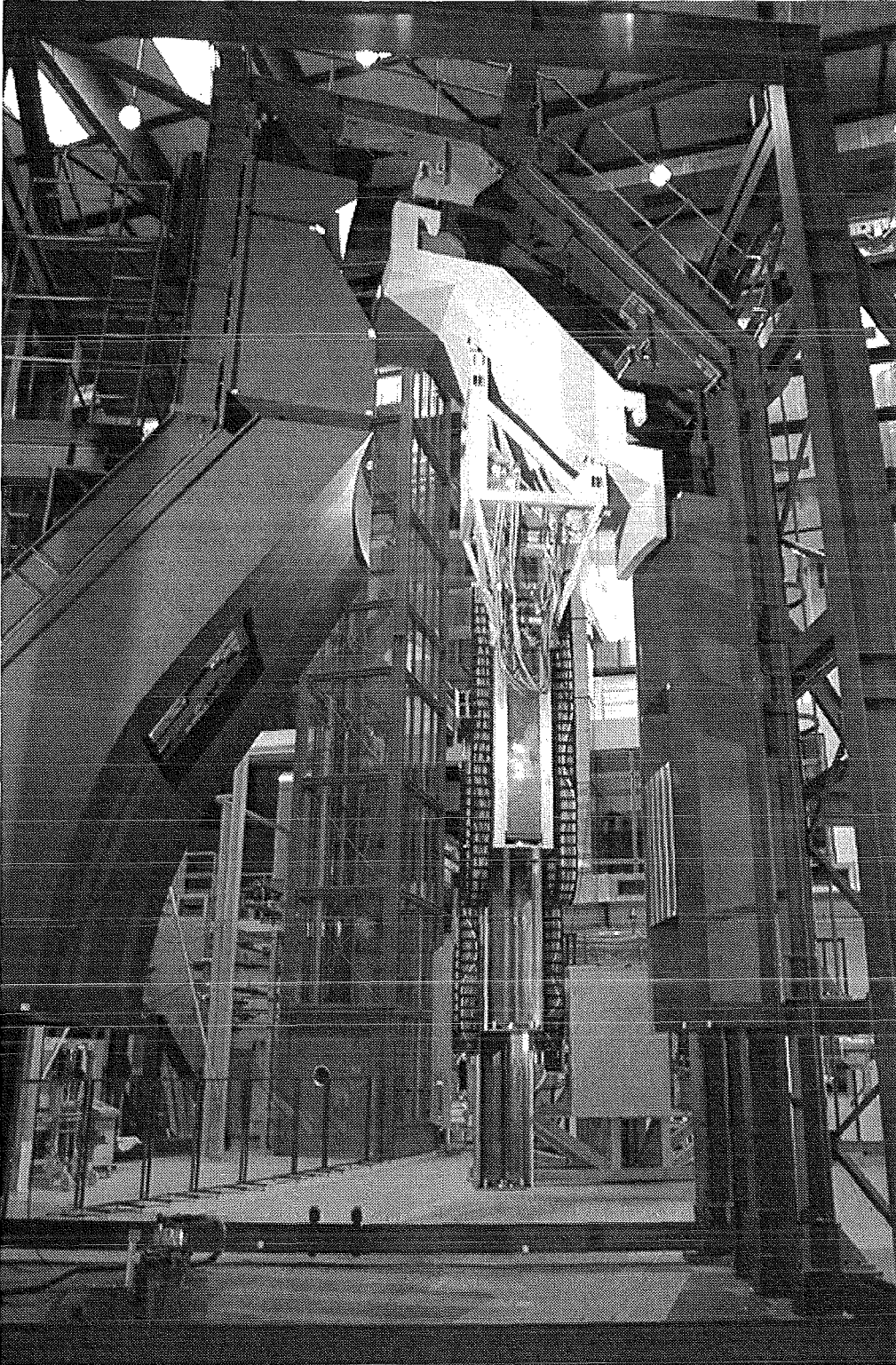


**Fig. 9-5: EDITH with divertor in torus**

### 9.3 WORKSTATION PREPARATION

Preparation of the RHWS for the EDITH divertor exchange procedure is comparable to writing a detailed operator handbook [KFK93].

During the planning and preparation phase of the divertor exchange procedure the work flow was subdivided into simple steps, simple enough to be interpreted by the operator as one instruction or to be executed by the control system automatically. The different types of working steps are:

- Transport with the EDITH boom: in-torus, in-magazine, outside
- Approaching the load transfer position
- Grasping/Depositioning of the divertor

Modelling the EDITH divertor handling procedure with PEXOS starts with the development of a high-level action/state network basically representing the sequence of work steps to be performed. The divertor exchange procedure, as far as the experimental set-up allows to model it, was subdivided into the following steps:

1. Driving the boom fast from the park position (T-PARK) to the divertor magazine base position (M-BASE).
2. Driving the boom in the magazine in a position just below the divertor (M-BELOW). The operator can control the position by the viewing system and by KISMET, which should be in the monitoring mode. Manual corrections are possible if needed.
3. Inserting the prongs of the divertor fork slowly into the divertor mock-up holes. The boom is then attached to the load (M-ATTACHED). The operator can supervise this by looking on the video monitors.
4. Getting over the divertor and lift it a little bit (M-ABOVE). The load should now be free from its attachment.
5. Drive the boom slowly with the divertor around the attachment down to the base position in the magazine (M-BASE). The operator can supervise the motion using KISMET in monitoring mode.
6. Drive the boom with high speed from the magazine base position into the park position.
7. Drive the boom with high speed from the park position into the torus base position (T-BASE).
8. Driving the boom from the torus base position upwards, than slowly around the attachment just above the attachment (T-ABOVE). Supervision is possible using KISMET and, in the experiment, using a camera showing the attachment.
9. Putting the divertor onto the attachment (T-ATTACHED).
10. Getting the prongs of the fork out of the divertor (T-BELOW). This motion can be supervised via the fork cameras.
11. Driving the boom downwards into the torus base position.
12. Driving the boom out of the torus into the park position.

The procedure bringing the divertor from the torus into the magazine is implemented in the same way. The procedures were subdivided into relatively small steps, giving the operator the chance to control a situation thoroughly and then decide for going ahead, to go back, or to deviate from the planned procedure driving the boom manually using the DOIF subsystem for direct EDITH control. Of course, also the execution of repeating sequences can be interrupted by the operator.

The graphical representation of the divertor exchange procedure (as far as implemented in the experiment) is shown in Fig. 9-6 and Fig. 9-7. The meaning of the actions and states/facts is described in Tab. 9-2 and Tab. 9-3.

This action/state network is the basic information describing the sequence of subtasks and states. The bulk of work in modelling with PEXOS is to enter the describing information and to enter the messages PEXOS has to send to the workstation subsystems KISMET, DOIF, and via DOIF to the devices for starting automated subtasks.

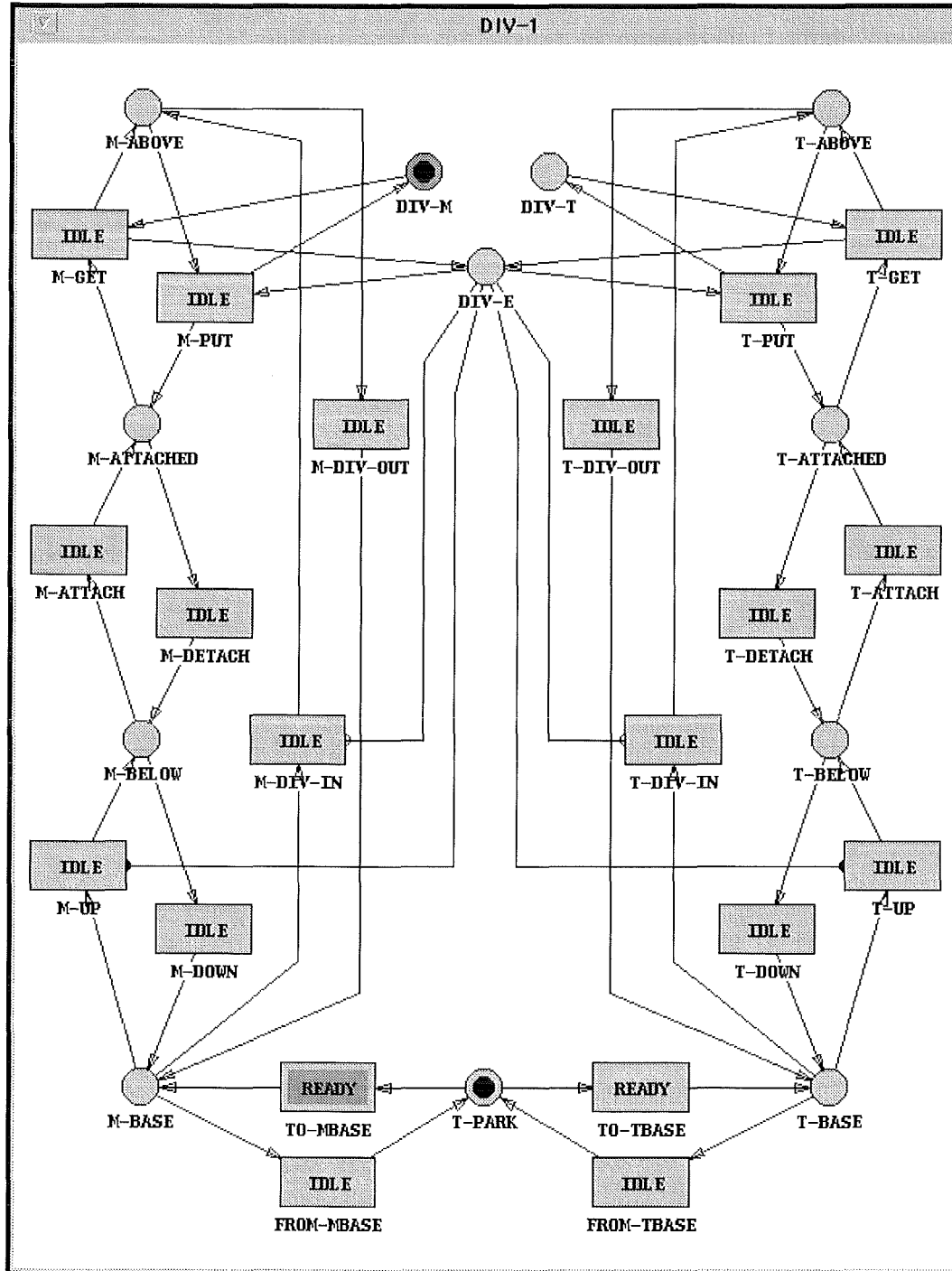
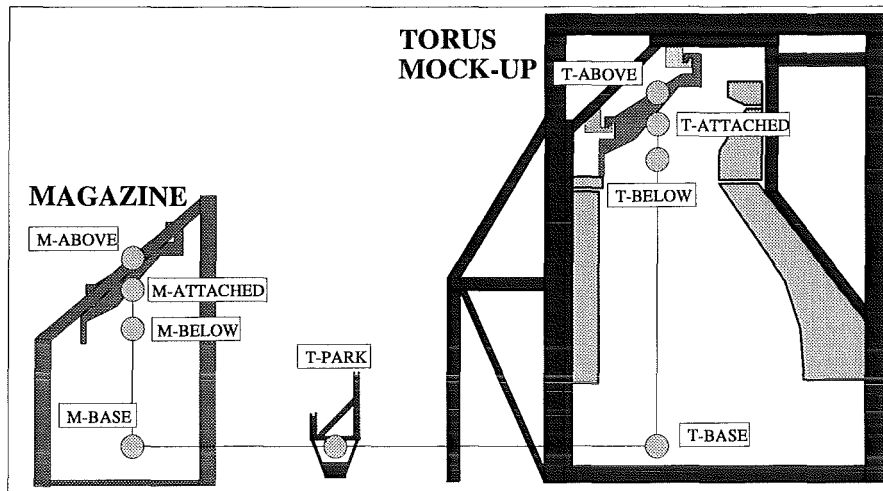


Fig. 9-6 : PEXOS action/state graph for divertor transport



**Fig. 9-7: Schema of Transport Procedure**

State Name	Transport State Description
T-PARK	Transporter in park position
T-BASE	Transporter in torus base position
T-BELOW	Transporter in torus just below divertor position
T-ATTACHED	Prongs of the fork inserted into divertor mock-up holes
T-ABOVE	Transporter with divertor just above divertor working position
M-BASE	Transporter in magazine base position
M-BELOW	Transporter in magazine base position
M-ATTACHED	Prongs of the fork inserted into divertor mock-up holes
M-ABOVE	Transporter with divertor just above divertor magazine position
DIV-E	Divertor mock-up on EDITH fork
DIV-T	Divertor mock-up in torus working position
DIV-M	Divertor mock-up in magazine position

**Tab. 9-2: Divertor exchange procedure substates**

Subtask Name	Subtask (Action) Description
TO-MBASE	Drive EDITH from T-PARK to M-BASE position
FROM-MBASE	Drive EDITH from M-BASE to T-PARK position
M-UP	Drive EDITH in the magazine upwards into M-BELOW position, (only without divertor)
M-DOWN	Drive EDITH in the magazine downwards into M-BASE position, (only without divertor)
M-ATTACH	Insert prongs into divertor holes
M-DETACH	Withdraw prongs out of divertor holes
M-GET	Get over the divertor onto EDITH
M-PUT	Put the divertor onto the magazine attachment
M-IN	Drive EDITH with divertor from M-BASE into M-ABOVE position
M-OUT	Drive EDITH with divertor from M-ABOVE to M-BASE position
TO-TBASE	Drive EDITH from T-PARK into T-BASE position
FROM-TBASE	Drive EDITH from T-BASE into T-PARK position
T-UP	Drive EDITH from T-BASE into T-BELOW position, possible only without divertor
T-DOWN	Drive EDITH from T-BELOW into T-BASE position, possible only without divertor
T-ATTACH	Insert prongs into divertor holes
T-DETACH	Withdraw prongs out of divertor holes
T-GET	Get over the divertor onto EDITH
T-PUT	Put the divertor onto the magazine attachment
T-IN	Drive EDITH with divertor from T-BASE into T-ABOVE position
T-OUT	Drive EDITH with divertor from T-ABOVE to T-BASE position

**Tab. 9-3: Divertor exchange procedure subtasks**



theodolites, and which is convenient for the procedure of result computations. Based on these results the model was corrected.

An important lesson learned during the preparation of this experiment was:

In the phase of model construction the process of model verification should be taken into consideration. This influences already the internal structure of the model with respect to the possibilities of adapting model parts to the measured reality. An environment model derived more or less automatically from standard CAD data is generally not an optimal model for control tasks. This is valid for both aspects: the real-time aspect and the model verification/adaptation aspect.

The first step in the preparation was to teach-in the motion paths of the EDITH boom between positions according to. This was done via the EDITH DOIF together with KISMET in the monitoring mode. The taught-in paths are stored in the EDITH control system. They are called to be executed in various ways:

- directly via the EDITH DOIF
- via a DOIF manager script combining this call together with others to a new operator command facilitating the control task for the operator or the PEXOS programming.

via PEXOS especially by using the START-AUTO command for a READY action.

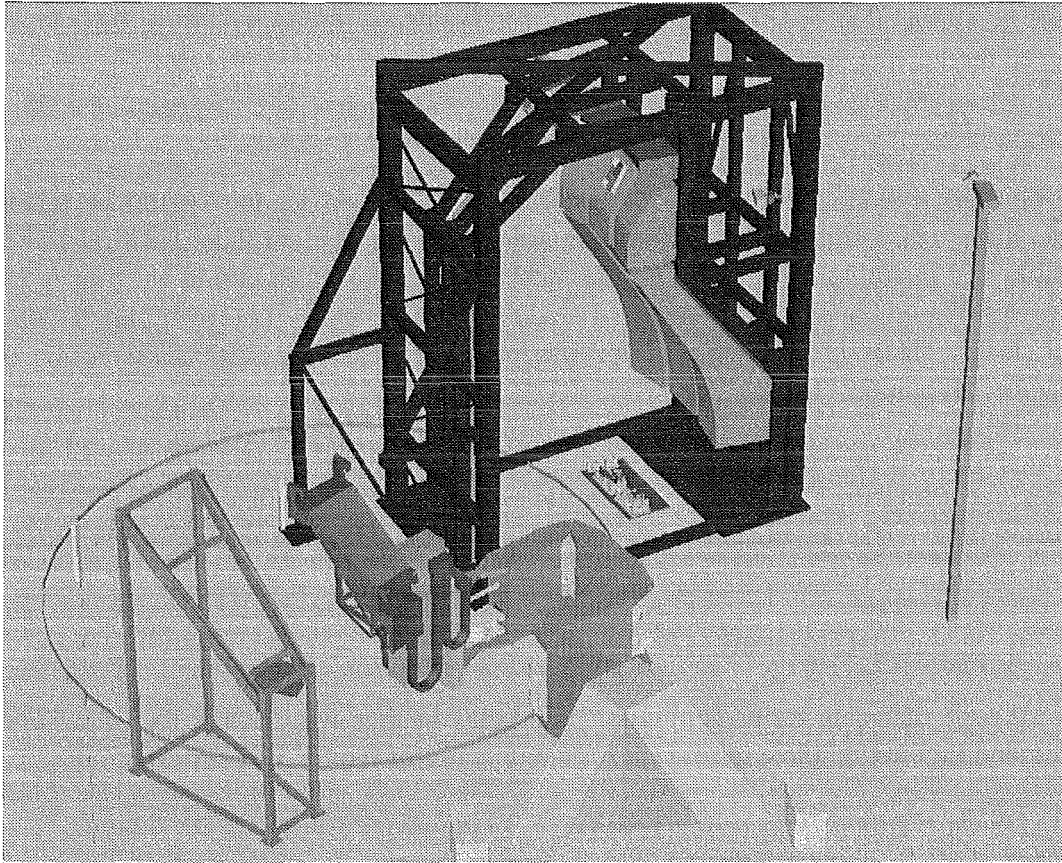


**Fig. 9-9 : KISMET overview of EDITH site**

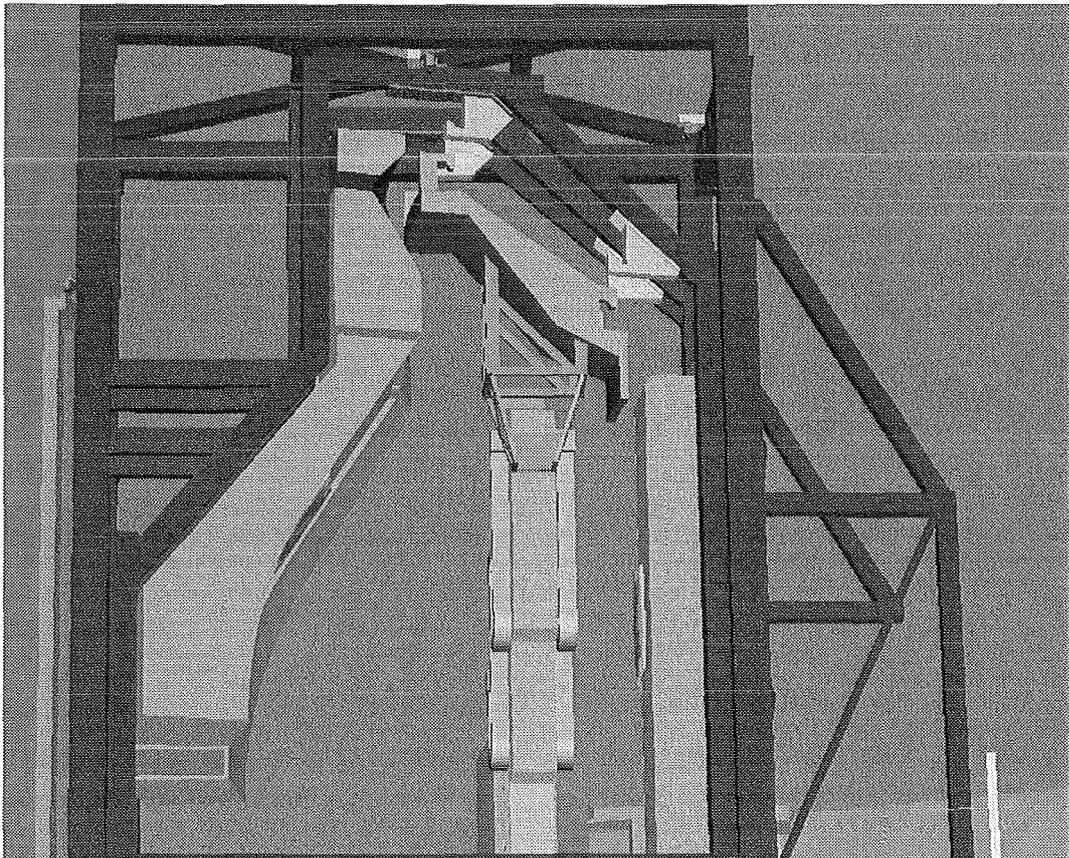


**Fig. 9-10: KISMET divertor near torus position**

## 9.4 CONTROL SYSTEM PREPARATION

The central goal of the HHL experiment was the evaluation of the controllability of the transport motions needed for tasks like divertor exchange. The specification of the EDITH transporter requires an absolute positioning accuracy of 100 mm and a repetition accuracy of 5 mm. These requirements were derived for the transporter taking into account that a work unit (e.g. Divertor Handling Unit) would be used for those tasks. In the actual EDITH test field no work unit was available but with the described fork for divertor „grasping“ and the appropriate console-hook attachment an experiment for divertor mock-up exchange was defined to test the transport dynamics of the boom in a realistic way. The transportation system experiment set-up tolerates arm deflexions of 1 cm. In addition to the transportation of heavy loads under spatial in-torus conditions, a serie of special tests were executed for evaluation of the absolute position accuracy [ECS90].

### 9.4.1 Transporting heavy Loads within the Mock-up

#### Teaching

Rough positioning was done in the well tested and very fast axis positioning mode. Besides the operators had lots of experiences with this motions mode, there are no restrictions in using this positioning mode. Those rough positions were taught in with the kinematics simulation system KISMET, which can operate either as a monitoring system or as a kinematics simulator operating also as master. Exactly the last mentioned operation mode is used with teaching rough positioning: The articulated boom is moved interactively and intuitively in the KISMET simulator. With the KISMET command „move real robot“ a motion telegram is transmitted to the EDITH DOIF. The behaviour of the EDITH system now is like there would have been an operator interaction on the DOIF and the real boom will move. During motion, KISMET may be switched back to monitoring mode and visualise the motion of the real system, using the position data (measured joint positions), which are transmitted from the control system to the KISMET system. As the operators knew KISMET for a long time during rough positioning they prefer the KISMET monitoring to camera viewing due to its better view. Because cameras are fixed and cannot be moved, they are not able to offer useful views in each situation. The operator often is forced to extract the necessary information with a big effort of concentration, comparing and combining the information of different cameras. In opposite to real cameras, KISMET monitoring offers virtual cameras, which may be placed at any position of the test site, even at spots, which are occupied by any subjects. As it is also possible to hide obstacles, there are no restrictions with this synthetic viewing. So the operators can choose a perspective, which offers the desired information without making any compromise. This spares the operator's power and concentration for the task itself. As another feature, KISMET offers off-line teaching of sequences, generating IRDATA file. The IRDATA file can be transmitted to the motion control system using FTP service, where it is converted to EDITH sequence files and executed on the EDITH system. This worked quite well, but it was not used very frequently, because on one hand there are not all features of the motion control system implemented in the KISMET system on the other hand the command interpreter of the KISMET system differed from the command interpreter of EMCS in that way, that complex security functions, which are integrated in the motion control system, stopped sequence execution. This mostly happened during execution of sequences, which contained linear moves mixed with axis moves, because of the referenced axis point check. When using only axis positioning mode, the off-line teaching made no problems. As there were only two operators at the test site and the control system was always available, the

operators preferred the first method, which is also some kind of off-line teaching, when the control system is working in simulation mode.

Because of the divertor's size, the room inside the magazine and inside the torus mock-up is very narrow. With distances below 100 mm to the walls and an absolute positioning accuracy of 100 mm off-line teaching was not reasonable. As the systems kinematics is very complex (4 axis with identical orientation) axis positioning mode was also not possible. This fact forced the operator to use cartesian positioning mode, moving the load on a straight line in areas with small distances to obstacles. Teaching these transport operations forward and backward, while using the same point database, there was the need of extension of the teach and repeat operation mode. Securities, which should ensure the correct working of the kinematics backward transformation in case of combining known points of the point database to new paths, exclusively did allow the execution of cartesian moves, which start at the referenced axis point. The system was extended in that way, that there will be accepted any point in axis positioning mode (cartesian points as well as axis points). During a cartesian move however only position points, which refer the same axis point or the referred axis point itself. This statement is valid for all path points of the movement including its start point. With this extension it is possible to teach sequences backward, using known points, which had been taught in before within other sequences.

As only transport operations can be taught-in off-line, fine positioning was performed relatively in cartesian positioning mode. This relative cartesian positioning mode is a feature, which was implemented for divertor handling. Because of its inertia, the system has a time constant of about 5 seconds. The operator is not able to control the system very precise in joystick mode, which was provided for definition of position points. The extension of the direct ( operator controlled ) relative and absolute point positioning mode enabled the operator to move the machine on a straight line over a certain distance.

During fine positioning, there was the need of using the cameras. Besides the cameras, which were fixed on the fork looking along the prongs for monitoring the attachment and detachment of the divertor, there have been used overview cameras, which were mounted outside the torus in the hall. It was shown, that it is not easy to interpret the video information in the right way and it needs all the knowledge and experience of a well experienced operator. Wrong interpretation of the video often caused the operator to interrupt movements and to check the transporter's position on the spot, although there was no real need. This shows that camera information alone is problematic and often not helpful, because the camera views are very rarely optimally adaptable to a problem. In this context the simulation system KISMET has been shown to be a good tool: While not using KISMET excessively during the beginning of the experiment, because of distrusting the accuracy of the kinematics model, the operators more and more did trust and appreciate this system. KISMET gave the ability of having views even on parts of the system, they never could see with real cameras, although they would be at the spot. The usage of KISMET on-line monitoring culminated in that way, that operators got a little bit schizophrenic: observing the system on the KISMET monitor because of its excellent view, they took fright, when getting aware of it, because there was burned in mind, that the KISMET view is a virtual simulation and that it might not meet reality. As a result there can be fixed, that KISMET monitoring broadens the possibilities of monitoring. Operators must get familiar to KISMET, before they put their trust in it.

## Execution

During execution of taught-in sequences there occurred problems when contacting the hooks. Driven by the integration part of the position controller, the elastic gears wound up, while the boom itself was fixed at the hooks. When losing the contact, the system got an impulse shaped excitation followed by subsiding oscillation. As it made no sense to move in horizontal direction during putting down or picking up the divertor from the hook these phases are taught using vertical movements exclusively. In this context the automatic feature „alignment check“, which was integrated to ensure correct function and to prevent errors, proved to be a hindrance. Before starting a movement, the HLCS compares the desired start position of all axis to the real axis position. If the absolute difference is bigger than the limit for automatic alignment, the HLCS sends an axis motion command containing all positioned axis. As there was requested a very high accuracy for this task, the parameters controlling alignment check were kept very small. So even small changes in joint positions, will request automatic alignment operations. If the transporter moves vertically, the horizontal positions and also the joint positions changes due to the load change, which caused automatic alignment. So windup could also happen, although there was no explicit MOVE command for the horizontal axis. In this situation the operator parameters switching on or off automatic alignment were used the first time. Handled as operator parameters they may be used also within repeat sequences. Using this feature the operator is able to suppress alignment check for any axis during critical movements. After execution of that problematical movement, the alignment check should be switched on again.

Especially in areas, where there is the necessity of a very high precision with a non constant load, it is not possible to use KISMET as the exclusive monitoring system, because deflexions of the system, which are caused by load change, cannot be simulated with the demanded precision.

## Conclusion

- It was shown, that it is possible to transport heavy loads automatically within the repetition accuracy of 5 mm.
- The kinematics simulation system KISMET has been accepted by the operators as a useful tool. As the absolute positioning accuracy amounts 100 mm the simulated position, which is based on the measured axis positions, must be adapted to the reality. As the repetition accuracy was verified to be 5 mm and the deflexion owing to bending amounts to 10 mm ( in vertical ) , it was sufficient to perform this adaptation once. In a later system with various working positions the effort for model adaptation would be too high. For monitoring very narrow sections of the torus, KISMET should be supported by additional (e.g. distance) sensors to correct deviations. KISMET provides real time three-dimensional bending simulation but at the time of the experiment the proper stiffness matrices were not available (man-power problem).
- While contacting the wall, drives belonging to axis, which are fixed by this contact, should be switched in passive state by switching off alignment check or modification of the controller in that way, that the integration will be stopped during the contact. During experiments, the first method was applied.

## 9.4.2 Measurements of position accuracy

To transport material and tools within a narrow fusion torus, the appropriate transport system must have a sufficient positioning behaviour. Besides the dynamic behaviour, which is responsible for path accuracy and settling time, i.e. the time between the planned end of a motion and the real end of the motion, there are some static parameters, which define the accuracy of the end position. These parameters are represented by the absolute and the relative (repetition) accuracy. While the absolute position accuracy defines the position error between the really reached end position and the nominal absolute position, the repetition accuracy is defined as the maximal difference between the position reached at the first trial and all following trials. Further the absolute and the repetition accuracy have different influences on operation:

- A good repetition accuracy enables the system to repeat operations automatically, which have been taught-in once. The specification of the EDITH motion control system specified the repetition accuracy to be less than 5 mm
- A high absolute precision is necessary for off-line teaching. It will be shown, that in case of the EDITH system it is mainly influenced by mechanical parameters, i.e. the stiffness, the manufacturing precision. Based on absolute positioning accuracy you are able to define the minimal approach to the wall or build ins during off-line teaching. The absolute positioning accuracy is specified to be less than 100 mm.

### Repetition Accuracy

The repetition accuracy is defined as the maximal possible deviation of the end positions from the end position, which was reached with a reference move. This definition demands some tests to evaluate the repetition accuracy: The EDITH boom is moved to a specific point repeatedly. When the end position of all axis changes only by 2 or less digits around the desired end position the machine is stopped and the breaks engaged. The end position, which was pointed by a laser on a scale paper is marked. The same procedure was executed 10 times in different positions. The complete description and evaluation of the experiment is documented in [EXP94].

The repetition accuracy has been measured to be less than 5 mm. The external measured repetition accuracy was more than double the size of the internal measured (positions calculated with forward transformation based on the resolver values) repetition accuracy.

To explore the reasons for these differences, there were performed further investigations. Therefore the TCP was moved at a certain amount. Simultaneously there have been measured all axis positions with an external precision measurement system with an accuracy of 1/1000 mm.

The result was surprising: In spite of previous measurements of the resolvers themselves, the resolver system had a backlash up to 0.001 rad. As a single resolver has no backlash, this backlash must come from the way it is mounted. This suspicion was confirmed, but it was not possible to reduce it to zero by slightly modification of the fixing. So without a fundamental reconstruction of the resolver's fixing the backlash was reduced to half the previous value.

### *Conclusion:*

As a final result there can be recapitulated: Measurements showed, that the repetition accuracy amounts up to 5 mm. The positioning accuracy of the position controller itself amounts to 2 resolver digits ( 0.00015 rad ). So the repetition positioning error is mainly caused by a backlash in the fixing of the resolvers and may be reduced with elimination of the backlash to about 3 mm. As backlash normally occurs with load change on the resolvers axis, it may be eliminated by usage of springs, which cause a permanent torque on the resolver axis to avoid backlash.

### **Absolute positioning accuracy**

To define the absolute positioning accuracy there have been done different measurements. As a first step there have been measured the calibration functions of all axis as well as the absolute TCP positions in common with axis positions. There had been fixed spikes centred at the bottom part of each axis. In addition the TCP was marked by a long spike, which was fixed in the centre of the work unit mounting flange of the EEPU. There was measured the cartesian position of all spikes. Taking into account the high effort of these measurements, the fact, that system itself is very complex, and that there was no experience with such measurements at EDITH, there was performed a small campaign to check the usage of these measurements. So in a first step there have been measured 3 different constellations. The complete experiment is documented in [GEO95, EXP95].

### **Axis Resolver Calibration Function**

To define the axis resolver calibration function each axis has been moved over a range of 180 deg. Besides the spatial measurement of axis positions there had been recorded the resolver values.

The axis angle error increases more or less monotonously, starting at negative values ending at positive values. This might be a hint, that these errors mainly are caused by bending, which usually occurs monotonously. The data contained in this diagram have been inserted in forward transformation of the three TCP positions, which are described further on and in addition to those in the forward transformation of the base position within the torus mock-up. Measurements of axis resolver build in calibration function let us expect a horizontal deflexion of 54 mm. This will be checked later in this article against the results of the spatial measurements.

### **Absolute positioning accuracy of TCP**

In a first test sequence, there had been recorded the absolute position of TCP as well as the joint positions in 3 constellations. At the same time there had been recorded the resolver values. Therefore it is possible to compare the results processed by inserting resolver values in forward transformation with those, which were obtained by the measurements with the theodolite system.

In addition to those measurements with the theodolite system, there have been measurements relatively to known points. Those measurements were performed at an accuracy of 5 mm. They are documented in together with the results of measurements with the theodolite system. Those measurements have been executed once for each configuration, as a sufficient

repetition accuracy far below the absolute positioning accuracy had been proved before. As it can be seen the biggest error amounts to 75 mm. This value is congruent to our evaluation of axis calibration, which brought 54 mm horizontal deflexion: Geometric addition of 70 mm ( 60 mm vertical deflexion +10 mm owing to load change when handling heavy loads ) to the horizontal 54 mm gives a total spatial deflexion of 88 mm. This check as well as all experiences made up to now force the conclusion, that the absolute positioning accuracy of the EDITH system amounts to 90 mm.

### 9.4.3 Reconfiguration

Reconfiguration is a special motion control mode providing reconfiguration of the transport arm while the TCP (POR) is spatially fixed. This is important in narrow environments. In this mode one selectable joint is frozen and one is controlled manually. The tests showed that the „fixed“ TCP is moving in a volume of 100 \* 100 \* 100 mm.

### 9.4.4 Technical Data

The basic parameters and results of the experiment with respect to the motion control system are shown in Tab. 9-4 and Tab. 9-5.

axis velocities	Z1...Z4	0.05 rad/sec
	E1	20 mm/sec
	E2,E3	40 mm/sec
axis acceleration/deceleration	Z1...Z4	0.085 rad/sec
	E1	20 mm/ sec <sup>2</sup>
	E2,E3	40 mm/ sec <sup>2</sup>
POR velocity	translation	40 mm/sec
	rotation	0.01 rad/sec
POR acceleration/deceleration		10 mm/sec <sup>2</sup>
		0.005 rad/sec <sup>2</sup>

**Tab. 9-4: Parameter settings**

quality of axis controller	2 digits (0.00015 rad)
absolute axis positioning accuracy	0.008 rad
absolute spatial positioning accuracy	75 mm (measured )
	90 mm (expected maximum)
relative spatial position accuracy = repetition accuracy	5 mm
TCP motion volume during reconfiguration	100 mm box

**Tab. 9-5: Experimental results**

## 9.5 PERFORMANCE OF THE EXPERIMENT

In contrast to the tile handling experiment performed by using a master-slave manipulator for tool positioning the divertor mock-up handling is done exclusively without manual work. All transport, approach, and load transfer operations can be taught-in and repeated in a sufficient precision. But, to get a high flexibility in using taught-in paths and to enforce operator interaction and/or operator acknowledgements the divertor transfer procedure was divided into various steps. For that, a group of intermediate working states were defined together with concatenating transfer actions. The intermediate states were selected to force the operator checking the correctness of the starting point for a new step (e.g. forking the divertor).

The supervision of the automated subtasks were done on three levels:

- Task state supervision using the PEXOS action/state net visualisation showing the dynamics of the state changes
- Position supervision using KISMET and/or the fork cameras
- Device function supervision using the DOIF device parameter presentation.

The experiment was performed several times with larger intervals (demonstrations) without problems. This means that all relevant information for performing a task is easily available such that the operator can act as planned.

The flexibility of the man-machine interaction needed in unplanned situations was proven during the preparation phase in which the divertor exchange procedure was established with manual control.

## 9.6 CONCLUSION

The basic and general result of the experiment is:

- Transport tasks with payloads up to 1 t can be performed with the required precision in realistic narrow environments without problems. The free width in the motion channels for divertor transport was 120 - to 200 mm. For manual control in narrow environments motion steps of down to 5 mm are possible (with load). The absolute positioning accuracy is about 75 mm, the repetition accuracy less than 5 mm. The motion speed used in the experiments
- The Remote Handling Workstation support turned out to be indispensable for those tasks in the preparation and in the execution phase. This is based on a comprehensive multilevel procedure modelling and procedure visualisation.
- Via the Remote Handling Workstation those transport tasks can be controlled and supervised with little operator burden thus avoiding operator errors. In unplanned situations and/or during preparation of tasks the RHWS together with the control system provides high flexibility and good support to solve the tasks effectively.

### Control System:

The EDITH motion control system has been shown to be a good tool controlling an articulated boom transporter. With a positioning accuracy of 2 resolver digits it is able to guarantee a very good repetition accuracy of 3 mm. At the present ABT this was not reachable due to the fact, that there is a backlash at the joint resolvers fixing.

The possibilities of teaching and execution of motion files have been shown to be sufficient. Using all available possibilities the operator has a very comfortable environment. The usage of point databases should be expanded in that way, that databases of several sequences can be combined to a new database. At the present state, the operator selects the point database belonging to one sequence. Security functions as alignment check ensure a high reliability and faultless execution of sequences.

The EMCS has been shown to be flexible in case of necessary extensions. Because of its well structured modularization ( telegrams, tasks, modules ) with well defined interfaces, it is possible to get into the software with an acceptable effort.

Because of the systems time constant, joystick operations are useful for rough positioning of work units at an accuracy of a few cm. There should be used relative move commands if there is demanded a higher accuracy.

The inverse kinematics transformation is working well the way it was planned. Depending on the actual joint configuration it is working within variant areas without any disturbances. Approaching singularities it is a little bit uncomfortable as joint velocities will increase and exceed velocity parameters, what will cause an error and the motion will be aborted. If that happens, the operator must have a good imagination and some experience to manage the situation. In this area there should be investigated some possibilities of automation, which take in account the geometry of a fusion torus and which also avoid the approach of singularities.

Contacting the walls costs some degrees of freedom. As the system is running position controlled this causes problems, as the position is fixed, the controller however tries to correct this fix position. Switching of alignment check has been shown to be a possibility to manage those situations. Further changes can also integrate some switches, controlling the position controller ( i.e. stopping further integration ).

During divertor handling some changes in gear pre-loading had been tested for the first time. The electronic synchronous gear was integrated in the motion control system by an RS232 serial interface. Starting a move at any axis the motion control system causes the synchronous gear to tune the correct preload values. Problems occurred with switching the system on and off. Some increments have been identified, although the system was not moving. In a later system, there should be foreseen the possibility of measuring the absolute position of motors.

## 9.7 REFERENCES

- DHD90 Suppan, A., Hübener, J., Link, W., Ludwig, A.: unpublished report, July 1990
- ECS90 Breitwieser, Frank, Holler, Süß, Leinemann: Specification of EDITH MOTION CONTROL SYSTEM, KfK 4787, September 1990
- NET90 Suppan, A.: The NET Articulated Boom: Preliminary Investigation and Justification for a Full Scale Prototype. KfK-4809, December 1990
- KfK93 Suppan, A., Krieg, R., Krumm, H.G., Kühnapfel, U., Leinemann, K., Reim, J., Woll, J.: Experimental Device for In-Torus Handling - EDITH Intermediate Report -. KfK-5254, October 1993
- EXP94 Woll, J.: unpublished report, June 1994
- EXP95 Woll, J.: unpublished report, July 1995
- GEO95 Binz: unpublished report, March 1995
- PKF54 Leinemann, K., Woll, J., Haferkamp, B.: unpublished report, Jan. 1996



## 10 CONCLUSION

Based on the experience gained during the construction of the ABT, its qualification tests and its operation points of possible improvements and modifications for later operational equipment are summarised in the following.

### 10.1 MECHANICS AND KINEMATICS

#### 10.1.1 Articulated Boom Transporter

At the present ABT the design has been based on the requirement that there should be a direct line from the JET design via the NET/ITER prototype to the operational equipment instead of the design with linear drive units as it was realised for the TFTR manipulator. This means e.g. the application of coaxial drive units for the yaw joints and the arrangement of the cables inside of the link boxes. It should be kept in mind that these requirements have also consequences on the overall design. According to the experience gained, the advantages and disadvantages will be compared in Tab. 10-1.

	Advantages	Disadvantages
Coaxial drive unit	Compact unit. Relatively high stiffness.	Sensitive with respect to deflection of the joint axes due to deflection of the boom. The remote replacement of the CDU is more difficult due to its position between the upper and the lower joint hinges. In case of a CDU failure during operation the movement of the according link joint is difficult since the disengaged CDU forms an obstacle.
Cables inside the link boxes	Cables are protected and can be arranged in the neutral line of the links.	Due to the sensitivity of the cables against radiation they have to be replaced several times during the life of the ABT. Their remote replacement is almost impossible and also the hands-on replacement is difficult.

**Tab. 10-1: Advantages and Disadvantages Coaxial Drive Units and Cable Arrangement**

In our opinion the disadvantages of the CDU and the routing of cables inside the boxes are preponderate the advantages and therefore an improved ABT design could show the following features:

- Each CDU should be substituted by two linear drives acting via levers on the joint axes. Taking into consideration that their drive rods can be linked with the joint axes by spherical bearings deflections of the joints can be compensated. On the other hand, linear drives require a more comprehensive control system to guarantee an uniform motion. But this can be verified by changing the control software relatively easily.
- The best arrangement of CDU's was between the upper and lower hinges of the link joints where also the cables were routed. Linear drives should be located above the link boxes. This arrangement simplifies the replacement of the drives in case of a failure.

- In order to reduce the costs and to reduce also the storage of spare parts only *one* CDU size was applied. The disadvantage of this solution was that on the one hand some of the drives were oversized and that on the other hand at the first link two CDUs had to be used which complicated the electrical backlash removal required to increase the link joint stiffness. Additionally, the weight of the drives and thus also of the boom increased. In the future, the drive units should be adjusted to the required torque taking also into account a possible speed reduction of the joints from the link tip to first link near the support structure and the transporter of the operational ABS, respectively.
- For the arrangement of the cables a suitable solution would be to locate the power and signal transmission lines for the boom above the linear drives and the other cables below the boom. Thus avoiding penetration of the cables at the link boxes and joint hinges. Nevertheless, the cables can be routed in the neutral line of the boom.
- In order to provide enough space for the disengagement and replacement of failed linear drives the cabling above the drives should be easily removable. This requires cable connections at the link joints which are concentrated into one unit designed for a quick disconnection and re-connection, as it has been already developed by the Forschungszentrum Karlsruhe. The disadvantage of deviding the cables into parts equipped with connectors, thus increasing the possibilities of connection faults, seems to be not so severe, since the single connectors used in the connector unit are standard ones which are mechanically and electrically matured and are also highly resistant against radiation.
- The arrangement of the CDUs and the cables above and below the links, respectively allows to re-consider the suitability of the present link and link joint design. Based on the stress analyses and their verification it has been shown that the deflection of the boom is caused to 1/3 by bending moments and to 2/3 by torsion. For torsion the optimum link cross section is circular or tubular. Therefore, it should be taken into account to use for the link boxes tubes and for the joints prismatic parts with square cross sections at the tubes. The joint hinges can become stiffened by connecting the upper and lower hinges rigidly and the joint axes need not to be divided in upper and lower ones but can be formed as one part. Altogether, it seems to be possible to improve the stiffness of the joints where the hinges were the weak points and the stiffness of the link boxes by avoiding the buckling of the box side walls. In addition, increasing the joint stiffness will also increase the accuracy of the position measurement by means of the absolute resolvers mounted at the joints.
- The removal and installation of the cable parts could be facilitated by applying bayonet connections.

## 10.1.2 End-Effector Positioning Unit

The EEPU constructed as a slide and trolley system has the advantage of being useable to reach the upper and the lower torus regions without turning the EEPU as it would be necessary by applying a telescopic mast. Improvements of the present design are mainly possible with respect to the remote and hands-on repair, respectively as well as with respect to the flexibility.

- As to be seen in Fig. 10-1 every two bevel gears are connected by clutches which provide redundancy of the motors and reduce the number of gears. This means that the middle and the front slide as well as the front slide and the trolley will be moved simultaneously. Thus reducing the flexibility of the EEPU during operation in the upper and lower torus regions. By separating the drive units and applying them without clutches but with redundant motors and resolvers above the bevel gears (see Fig. 10-2) the flexibility can be increased but with the disadvantage to increase also the numbers of motors by four and the numbers of resolvers by two. Thus increasing also the required number of cables and signal transmission lines. An advantage of this arrangement is the possibility to replace complete drive units.
- If the present bevel gears would become an additional free shaft the slides and the trolley, respectively could be driven manually and slowly so that by means of spring loaded bolts the movement can be blocked. Thus allowing the removal and re-insertion of drives without supporting the slides or the trolley.
- Taking into account the reduced dead weight of the EEPU from the support frame to the tip the drive units could being adjusted and differ in size. The disadvantage to store more different drives and drive components will be compensated by reducing weight.

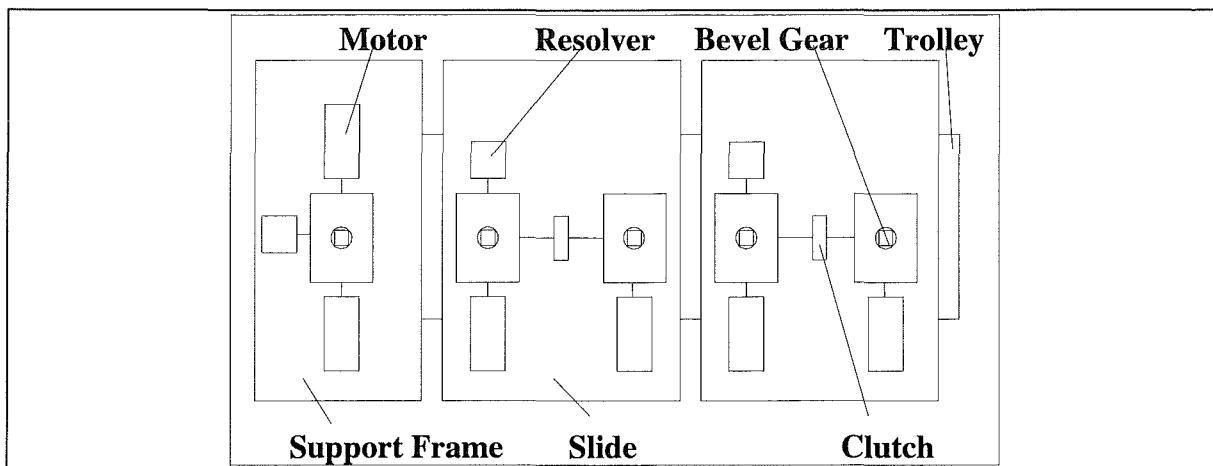
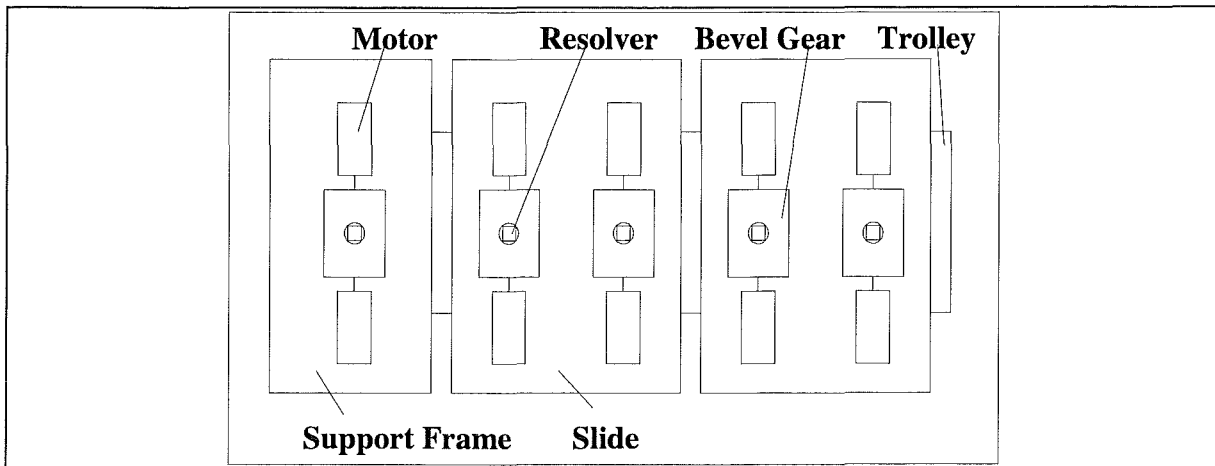


Fig. 10-1: Scheme of the Present Drive Unit Arrangement at the EEPU



**Fig. 10-2: Scheme of a Future Drive Unit Arrangement at the EEPU**

### 10.1.3 Camera System

Work site cameras are mounted onto camera arms and have four driven moments. The motors and gears are located at the links. The power and signal transmission lines are routed inside the camera arms. During the tests some disadvantages became evident and should be considered at a later design of an operational ABT.

- The arrangement of the drives at the link joint makes replacement difficult.
- The space for the routed cables inside the camera arms is rather limited. In connection with the required turn round of the cables at the joints the friction is substantially.
- Both could be improved by arranging all drives near the attachment of the arm and using for the transmission of the torque to the links ropes as it is already standard at manipulators.

## 10.2 PERFORMANCE OF DELICATE TASKS

For the tile replacement the electrical master-slave manipulator EMSM2-B has been used as a multi-purpose handling unit in combination with two special tools, the tile detachment device and the tile positioning device. The second master-slave manipulator EMSM3 supported the EMSM2-B by carrying the waste storage and the magazine for spare studs.

The trajectories of the ABT to the different pre-defined working positions have been pre-programmed and performed in an automatic mode. The articulated boom could be moved with full speed; the positioning accuracy and repeatability were in accordance with the requirements.

The working sequences for the tile replacement have been carried out by the manipulator operator using the master arm and the integrated viewing system. The replacement did not make any difficulties. The special tools worked well.

The tiles were fixed at the wall with a distance of about 5 mm. The trepanning depth resulted from the plate thickness plus 2 mm and was limited by limit switches. The electrical connections have been sensitive for graphite dust and the trepanning part for different

inclinations of tile and handling device. An improvement could be possible by using proximity sensors instead of limit switches.

The camera system and lightning was satisfying for working also in the darkness of the mock-up using only the camera lighting. A hand camera was unnecessary. Nevertheless, some improvements at the camera system are desirable. In particular these are:

- Optimised camera arm lengths to improve the view and to determine the inclination of the wall better which is especially important for fastening the tiles and for the trepanning.
- More powerful motors and changed gear ratios at the camera arms to reduce the time to position the cameras.

The required time for the replacement of one tile was approximately 38 minutes. The differences of the required time for replacing one tile at daylight and in the darkness of the mock-up was small. The most time consuming operation has been the trepanning. An improvement could be possible by an optimisation of the trepanning gear ratio to increase the speed of the forward feed.

The determined times for the different handling operations can be used for further time estimations, e.g. for the performance of some replacement operations in parallel as moving the EEPU and positioning of the cameras. Time estimations are now also possible for the replacement of more than one tile and changing for this activity the working sequence.

It could be demonstrated that the tile exchange is possible with standard general purpose tools (master-slave manipulators), and with the special tools experiences could be gained which are a good basis for an approach with more automation to reduce maintenance time significantly.

### **10.3 HANDLING OF HEAVY UNWIELDY LOADS**

Transport tasks with payloads up to 1 t can be performed with the required precision in realistic narrow environments without problems. The free width in the motion channels for divertor transport was 120 - to 200 mm. For manual control in narrow environments motion steps of down to 5 mm are possible (with load). The absolute positioning accuracy is about 75 mm, the repetition accuracy less than 5 mm. The motion speed used in the experiments

The Remote Handling Workstation support turned out to be indispensable for those tasks in the preparation and in the execution phase. This is based on a comprehensive multilevel procedure modelling and procedure visualisation.

Via the Remote Handling Workstation those transport tasks can be controlled and supervised with little operator burden thus avoiding operator errors. In unplanned situations and/or during preparation of tasks the RHWS together with the control system provides high flexibility and good support to solve the tasks effectively.

## 10.4 GUIDANCE AND CONTROL SYSTEM

The guidance and control system was designed with respect to control systems in comparable areas of control: manufacturing. A manufacturing plant is subdivided into work cells (areas) with device controllers, a cell (area) control, and a super-ordinated guidance system. The most important difference between the applications is the different degree of automation. In fusion plant maintenance the operator stands in the centre and has to be supported. This operational support is concentrated in the guidance system.

### Architecture

The architectural concept of separating high-level generic functions (guidance system) from the device control system and realising them in form of a modular remote handling workstation provides important advantages over the device oriented control system development. Because the RHWS is adaptable to applications, the development costs for a plant with various application areas (remote handling areas) as a fusion plant can be reduced. If work in different areas has not to be executed in parallel, not each RH area has to be equipped with its own RHWS. The separation also makes sense because the hardware requirements (response behaviour, operating system, graphics support) is different from the requirements of the device controllers.

With respect to the maintenance of the whole control system, the device controllers also should be operable by their own equipped with a minimal man-machine interface for tests, installations, and for back-up purposes. Each device controller has to have a standardised interface providing to the RHWS all functions and all state data. Of great importance with respect to the model based support of the RHWS, is the availability of state enquiries and state change messages. For example, the EDITH controller interface does not provide a function requesting for the actual work unit or the actual part gripped, nor does it report a related state change. Because the comprehensive book-keeping of the state of a complex remote device park is extremely important for a future RH control system the implementation of a special system state book-keeping software module should be envisaged in addition to the state request and reporting functions of the devices. A similar book-keeping of the state of the plant is of equal importance and should also be integrated.

### Remote Handling Workstation

#### *General*

The RHWS provides a broad variety of supporting functions and structures for adapting the RHWS to an application ranging from manual work to supervised automated performances. The realisation of three support tools for the three identified domains (procedural, spatial, functional) and a loose coupling between them turned out to be a very flexible architecture. Especially in the pre-tests the possibility of using the RHWS subsystems stand-alone was very helpful because not always the whole RHWS functionality is needed.

In unplanned situations the operators can interrupt the planned procedure to work manually with the devices via the DOIF and then rejoin the planned procedure as represented by the PEXOS system.. During the procedure execution the operators had always a good and sufficient overview over the state of the work and the devices, no deficiencies in the state presentation became evident.

Repetitions of the experiment even after longer time were easily performed because the documentation is very comprehensive such that all questions concerning the performance can be answered. The documentation includes all operational details, even special action related remarks (notices) of the operator.

The possibility to program interactively on all three domains allows for an easily understandable modelling of the procedures which is easily testable and maintainable (due to stepwise information hiding).

The three levels of monitoring are giving the operators sufficient safety in executing complex maintenance procedures of long duration in large intervals without close contact to the equipment and the environment. As the experiences showed it is not sufficient to provide only the device functions in a operator suited manner (graphics device panels): The task suited function bundling, 3D graphics environment representation and the procedural (handbook) support is needed for a real unburdening of the operator.

The possibilities of switching from planned control to unplanned manual control and back are easy to use. In unplanned situations the operators can interrupt the planned procedure to work manually with the devices via the DOIF and then rejoin the planned procedure as represented by the PEXOS system. The PEXOS co-ordination techniques (with the possibility to co-ordinate even parallel action sequences) especially the integration of the manipulating operator is solved satisfactorily by a simple START-DONE message sequence. During the procedure execution the operators had always a good and sufficient overview over the state of the work and the devices. During the execution no deficiencies in the state presentation became evident.

The tile exchange demonstrations were done with two operators: a manipulating operator and a co-ordinating/assisting operators. Controlling could be done by the manipulating operator alone because the transport motions and the camera control are reduced by using the RHWS support functions to simple button clicks.

### *Model based support*

Model based support broadens the support significantly but the drawbacks have also to be taken into account. Model based support systems rely on the accordance of model and reality. Enhanced techniques and procedure to verify the models and to maintain consistency have to be developed to cope with larger more realistic applications. As the experiments have shown two basic areas have to be differentiated: Generation of a problem suited model and continuous update during operation. Therefore the control systems and/or additional external sensor systems have to provide state change messages and the capability to respond on state requests to synchronise state representations on the workstation directly with system states. The capability of PEXOS and KISMET to request for and to evaluate those messages should be enhanced. An example for this feature is the signalling/request of actual divertor attachment: DIVERTOR-ON-EDITH (DIV-E), DIVERTOR-IN-MAGAZINE (DIV-M), DIVERTOR-IN-TORUS (DIV-T). In the actual implementation the operator is only asked to check the situation in the beginning of a procedure. On the most abstract level, the procedural level (PEXOS models) this is relatively easy. But on the spatial level this work should be

more supported. In the environment (devices, reactor) as well as in the model reference (surveying targets, points, lines) should be defined together with identification procedures to guarantee an easy surveying and easy model correction. Therefore it is highly recommended to investigate in standard procedures for spatial model generation, verification, and update.

### *Architecture and implementation base*

Ethernet-UDP-TCP/IP is convenient for communications between RHWS subsystems and between the RHWS and the control systems. The mailbox-like communication used between the RHWS modules is very flexible. The architecture allows the allocation of all subsystems on one computer or distributed. This was especially used in the DOIF system. In the actual implementation two restrictions are valid: PEXOS, until now, requires a SUN because of its implementation basis, KISMET a Silicon Graphics machine for getting the required computational power for real-time simulations.

The multiprocessing features of Unix are widely used, Unix turned out to be a good decision as an implementation basis for the workstation level. The X-based graphical user interface in the Unix environment and the availability of X-terminals makes it easy to configure a problem adapted display configuration including remote access.

PEXOS was implemented using a knowledge engineering programming environment (KEE). In the meantime this implementation basis makes the adaptation of PEXOS to new or other versions of the operating system difficult or impossible. PEXOS should therefore be re-implemented on a new and more flexible basis which also supports the portation to other computers. This would also allow to run PEXOS, DOIF, and KISMET on the same computer equipped with additional X terminals.

An important area of research and development for preparing the RHWS for professional usage should be the long term storage and management of all RHWS relevant information in a database instead of the Unix file system used in the prototype. This is important because this includes the complete documentation. This is not a standard database application because the data is multimedia.

### *PEXOS*

Very important for the usability of a procedural support tool (PEXOS) is the visual presentation of the task structure, the task state, and the task dynamics because the operator should be able to grasp the work situation at a glance. In all task performances or off-line demonstrations we found that the selected graphical representation of the procedure by Petri nets is easily understandable: it seems to be a natural. This type of procedure representation uses only two types of graphical elements and arcs for their logical connections. In addition, those elements are described in more detail by texts and other means. The shown interrelationships are understandable even without an introduction.

The graphical representation of the working procedures by PEXOS should be enhanced by using type specific icons for the ACTIONS and FACTs. Furthermore, in order to enhance the readability of a network of ACTIONS and FACTs as a whole the PEXOS editor should

provide free graphics e.g. to highlight permanently groups of actions by a special backgrounds, surroundings, or annotations.

To make the PEXOS procedure network more compact in special situations (e.g. repetition of work on a group of objects) an extension of the modelling features by individual tokens would be helpful. This feature is implemented only in an experimental version until now.

The possibility of controlling the DOIF system and KISMET from PEXOS by ACTION/FACT related messages (e.g. opening and positioning of windows, changing views) facilitates the usage of the two subsystems remarkably because this support is problem suited.

The PEXOS resource database which is helpful in unforeseen situations in assisting the operator in planning the needed work could be enhanced especially to be able to model the structure of the resources.

### *DOIF*

The DOIF system with the central DOIF manager is the basic tool for integrating a group of devices to an operable system for a special application. And it is the basic link between the controllers and the RHWS: The DOIFs are representing the devices on the RHWS. The device function bundling (script programming and management) and the standard DOIF functions are an important basis for the application oriented high level support by PEXOS. The DOIF manager demands for a textual command (function) interface of the DOIFs and those could best be realised if the control system behind the DOIF also provides its functions via a textual command interface. This is not a must but in the EDITH experiments and other applications of the RHWS we learned that this a very flexible and maintainable basis (at least for an experimental installation).

### *KISMET*

In teaching new motion paths with the EDITH boom the available two modes of simulation had a favourable effect: the motion was first planned (simulated) with KISMET, then simulated in the control systems simulation mode using KISMET as the virtual device (but running the control algorithms without controlling the motors). This enhances the safety and also makes it possible to prepare work without allocating the real device.

Continuous update of models is realised automatically with KISMET models by joint angle sensor signals of the devices. In addition to this internal sensors model updates by external sensor (e.g. distance sensors) should be investigated to broaden the usage spectrum of KISMET. This is important in monitoring near-contact motion. In the context of off-line teaching with KISMET the bending simulation available in KISMET is important. To use this feature for the device to be modelled the stiffness matrices at the joints have to be available in addition to the geometry and kinematics of the device.

## Control System

- The EDITH motion control system is able to control the EDITH ABT with a high reliability.
- Even with its nominal payload of about 1 to it is possible to move at a joint velocity of 0.15 rad/s horizontally and a linear velocity of 20 mm/s (E1) or 40 mm/s (E2, E3) vertically.
- At the maximal velocity, the path accuracy amounts 100 mm, with slow motions it has been shown to be 10 mm. The repetition accuracy is defined as a fifth of the system parameter for detection of unexpected motions and can be influenced by adapting this parameter. The position controller itself is able to control the joint position at an amount of 1 resolver digit, which should result in a repetition accuracy of about 2 mm. Due to a backlash in the joint resolvers fixing the measured value amounts nearly 5 mm. The absolute positioning accuracy however was shown to be 85 mm.

## *Hardware*

- The HLCS hardware and Software (VAX/VMS) is proved to be very reliable and of a high stability. It is a relict of the required TARM compatibility. As it is a normal universal microcomputer without any special hardware it could be also integrated within the remote handling workstation.
- The MBII hardware was shown to be of a high quality and highly reliable.
- As all signals are collected within the LLCS, the density of cabling is very high and therefore there is a high potential for defects. Especially the cabinet build in 57 pin AMD connectors caused troubles with every modification, because crimped wires slipped out of the pin or also pins slipped out of the casing. This might be not an intrinsic problem of the AMD connector but more a problem of the mechanic, who build up the system but nevertheless it shows, that it is not easy to handle high density connectors. As the connectors are placed just around the build in heat exchanger it was not easy to repair defects. In a future system there should be integrated industrial field bus systems like InterbusS, CAN or ASI, which are meanwhile state of the art. This will reduce the electromechanical complexity, will result in a hierarchical hardware structure and in sequence maintenance will be much easier than today.
- The electronic synchronous gear has been shown to be a good method to synchronise two velocity controlled motors, which are also coupled by a elastic gear. The previously planned torque control was not possible, as synchronous AC servo drives own reluctance torques, which amount about 10 percent of the nominal motor torque. It has been shown that a gear preloading of 10 percent of the nominal torque was reasonable which corresponds more than 1 motor turn.

## *Software*

- The iRMX operating system has been shown to be a good choice with very short response times far below 1 ms.
- The CPU load amounts up to 20%, even if there will be running the model based controller which costs 0.3 ms.
- Collecting joint positions is the most time costing operation. Future improvements should aim primarily at this operation. High speed peripheral buses like CAN and InterbusS should be taken into account. The software is well structured and it could be shown, that it is possible to get into the software and make changes, which require a good overview over the functional context.

## *Handling of the EMCS*

- Since there had been introduced the EDITH DOIF as a user interface, the EMCS may be operated intuitively. Although it takes some experience to handle the system with all of its capabilities.
- As one of the most difficult parts there must be seen the inverse kinematics transformation, which demands the operator to have a good imagination. Therefore further developments should also include a new transformation, which automatically handles the redundancies while moving all axis simultaneously and which also takes account of the geometry of the torus. Otherwise it will not be possible to perform wide range cartesian movements.
- Supporting the operator with parameter databases has been shown to be reasonable. While downloading of system parameters takes a few seconds, downloading of operator parameters takes one and a half minute for each parameter will be set with transferring an own telegram. It should be possible to transmit operator parameters within one or two telegrams to accelerate downloading of operator parameters.

## **10.5 SUMMARY AND OUTLOOK**

Inside the vacuum chamber of a fusion device like NET/ITER delicate tasks will have to be performed as well as tasks which require the handling of heavy loads. Tile handling has been only an example for such a delicate task. It has been based on NET requirements and may have been not typical for a possible tile replacement at ITER. Nevertheless, experience gained during these experiments will be useful and applicable also for other similar tasks.

In general it has been shown that delicate tasks can be performed with the available equipment and without direct view. The articulated boom transporter has been the suitable basic equipment for this type of tasks. The universal workstation made possible the reliable and continuous work flow by a combination of manual and automatic operation. The repeatability with the same quality is warranted by the extensive multimedial documentation.

### **Remote Handling Workstation Development**

The Remote Handling Workstation providing the man-machine interface and supporting operational software tools was used successfully in all phases of the experiment. The principles turned out to be adequate, details should be added or changed according to the experiences. The subsystem KISMET is in a product state and available on the market. The subsystems PEXOS and DOIF are in a prototypical state and are being brought to a product state ready for external usage. This means especially for PEXOS to change the implementation basis from Lisp to C++. A further area of research and development should be the long term storage and management of comprehensive procedural information in a database instead of the Unix file system used in the prototype.

## EDITH Goals and Results Tabular Overview

Goal	Problem, Condition	Result, solution
Precise and secure <b>transport and positioning</b> of work units and pay loads (1 t) in the torus; reach: +/- 90 degree	<ul style="list-style-type: none"> <li>• long reach, heavy load</li> <li>• small entry port</li> <li>• no support points in the torus</li> <li>• minimisation of deformation by dead weight and payload</li> <li>• minimisation of dead weight (fast motion)</li> <li>• adoption and enhancement of proven design principles from JET (e.g. coaxial drives)</li> </ul>	<ul style="list-style-type: none"> <li>• deflection (at boom tip) due to 3.9 t payload: 16 - 38 mm depending on configuration</li> <li>• dead weight: 6.2 t (link boxes: 1.5 t; joints: 2.2 t; coaxial drives: 2.2 t; cables: 0.3 t)</li> <li>• prediction of behaviour based on FEM computations is satisfactory</li> </ul>
<b>Optimisation of mechanical structure</b> , evaluation of extend to which standard tools allow to <b>predict behaviour of complicated structures</b>		<ul style="list-style-type: none"> <li>• filigree boom construction: thin joint plates, thin link box walls</li> </ul>
Simulation of <b>boom dynamics</b> to provide tool for further designs or design correction	<ul style="list-style-type: none"> <li>• friction</li> <li>• backlash</li> <li>• non-linearities</li> </ul>	<ul style="list-style-type: none"> <li>• Development of the dynamics simulation system AMBOSS</li> <li>• Computational result: sudden load transfer can be mastered</li> </ul>
<b>Dynamic qualification tests</b>	<ul style="list-style-type: none"> <li>• sudden load release</li> </ul>	<ul style="list-style-type: none"> <li>• significant eigenfrequencies in the range between 0.3 Hz and 3.0 Hz</li> </ul>
Selection of radiation hard <b>motors, cables, and sensors</b>	<ul style="list-style-type: none"> <li>• Temperature: 150 ° C</li> <li>• <math>3 \times 10^6</math> rad/h <math>\gamma</math></li> <li>• Integral dose: 100 MGy</li> </ul>	Motors (100 MGy): <ul style="list-style-type: none"> <li>• <i>Moog</i></li> <li>• <i>Maccon</i></li> </ul> Resolvers (100 MGy): <ul style="list-style-type: none"> <li>• <i>GERWAH</i></li> </ul> Cables: <ul style="list-style-type: none"> <li>• <i>PEEK (10...30 Mgy)</i></li> <li>• <i>KAPTON (100 MGy)</i></li> </ul>

**Tab. 10-2:** EDITH goals and results: Mechanics

Goal	Problem, Condition	Result, solution
<p>Demonstration of complete realistic <b>armour tile exchange</b></p>	<ul style="list-style-type: none"> <li>• usage of general purpose manipulators which are also usable in unplanned and complicated situations</li> </ul>	<ul style="list-style-type: none"> <li>• Development of a tile detachment device</li> <li>• Development of a tile positioning device</li> <li>• Armour tile exchange with general purpose manipulators and special tools at realistic working positions and conditions is possible fully remotely</li> <li>• RHWS turned out to be important in operating support (planning, training, guidance, documentation)</li> </ul>
<p>Demonstration of <b>heavy load transfer and transport</b> (divertor exchange)</p>	<ul style="list-style-type: none"> <li>• no divertor handling unit available: usage of a 0-DOF fork for divertor „grasping“, usage of ABT for fine positioning</li> <li>• handling of heavy load in narrow environment</li> <li>• precise realistic motion at load limit</li> </ul>	<ul style="list-style-type: none"> <li>• Behaviour of the boom system even at pay load limit is excellent such that divertor exchange could be demonstrated without DHU (at one DIV position)</li> </ul>

**Tab. 10-3: EDITH goals and results: Procedure validation**

Goal	Problem, Condition	Result, solution
<p><b>Architecture:</b> Development of a control system architecture applicable also to others than in-vessel remote handling area</p>	<ul style="list-style-type: none"> <li>• man-machine co-operation: human has to be integral part of the control loop</li> <li>• system has to be open to extensions and enhancements</li> <li>• system has to be easily operable and maintainable</li> </ul>	<p>Differentiation between</p> <ul style="list-style-type: none"> <li>• guidance system (represented by a general purpose remote handling workstation),</li> <li>• the area controller, and the various</li> <li>• device controllers</li> </ul>
<p><b>Operator Support:</b></p> <ul style="list-style-type: none"> <li>• Demonstration of fast, secure, reliable execution fully remotely</li> <li>• Improvement of reliability and accuracy of performing maintenance tasks</li> <li>• Support of procedure planning, execution, and repetition management</li> <li>• Comprehensive procedure documentation</li> <li>• Organisation of man-machine-co-operation</li> </ul>	<ul style="list-style-type: none"> <li>• no direct view</li> <li>• restricted camera view</li> <li>• co-ordination of many devices (agents)</li> <li>• little repetition rate</li> <li>• complex procedures with long duration and little repetition rate</li> </ul>	<p>Development of a general purpose RHWS consisting of three co-operating subsystems providing:</p> <ul style="list-style-type: none"> <li>• procedural support (PEXOS)</li> <li>• functional support (DOIF)</li> <li>• spatial support (KISMET)</li> </ul> <p>The RHWS supports comprehensive procedure planning, simulation, management, validation, monitoring, documentation, execution, training, agent co-ordination</p>
<p><b>Motion control:</b> Fast, smooth, secure, precise motion and positioning of the ABT in narrow environment with heavy load</p>	<ul style="list-style-type: none"> <li>• friction, backlash</li> <li>• high radiation, high temp.</li> <li>• narrow environment</li> <li>• high inertias</li> <li>• mixed mode: manual - automatic</li> </ul>	<ul style="list-style-type: none"> <li>• Good positioning accuracy</li> <li>• Good path following precision</li> <li>• Various control modes: <ul style="list-style-type: none"> <li>– manual velocity control (joint, cartesian),</li> <li>– manual position control (absolute, relative),</li> <li>– teach/repeat,</li> <li>– reconfiguration</li> </ul> </li> </ul>

**Tab. 10-4: EDITH goals and results: Guidance & Control System**



## 11 BIBLIOGRAPHY

### 11.1 EDITH BIBLIOGRAPHY

- A84 Leinemann, K.: A Graphics Based Remote Handling Control System. KfK-3788, 1984
- B84 Leinemann, K.: Man-machine cooperation in remote handling for fusion plants. Fusion Technology 1984. Proc.of the 13th Symp., Varese, I, September 24-28, 1984. In Two Volumes. Vol. 2 S.1311-16 Oxford (u.a.): Pergamon Pr. 1984 Varese
- C84 Leinemann, K., Schlechtendahl, E.G.: Computer graphics support for remote handling simulation and operation. Proc.of the 32nd Conf.on Remote Systems Technology, held in Conjunction with American Nuclear Society Summer Meeting, New Orleans, La., June 3-7, 1984 La Grange Park: American Nuclear Soc. 1985 Vol. I S.10-16 Transactions of the ANS, 46(1984) S.771-72 (Abstract) New Orleans
- A87 Kühnapfel, U., Leinemann, K., Schlechtendahl, E.G.: Graphics Support for JET Boom Control. Proc. ANS, Pasco Wa., 1987, S.28-34
- A88 Leinemann, K., Kühnapfel, U., Ludwig, A.: CAD-model based remote handling control system for NET and JET. Van Ingen, A.M. (Hrsg.): Proc.of the 15th Symp.on Fusion Technology, Utrecht, NL, September 19-23, 1988 Amsterdam : North-Holland (u.a.), 1989 Vol. 2 S.1381-85 Utrecht
- B88 Leinemann, K., Kühnapfel, U., Ludwig, A.: Remote handling control with graphical man-machine interface for NET and JET. Robotics and Remote Maintenance Concepts for Fusion Machines : Proc.of a Technical Committee Meeting, Karlsruhe, February 22-24, 1988, IAEA-TECDOC-495(1989) S.249-61
- C88 Benner, J., Fischer, C., Leinemann, K., Stratmanns, E., Till, W.: Towards more automation for remote maintenance. Robotics and Remote Maintenance Concepts for Fusion Machines : Proc.of a Technical Committee Meeting, Karlsruhe, February 22-24, 1988, IAEA-TECDOC-495(1989) S.249-60
- D88 Benner, J., Leinemann, K.: Architecture of a telemanipulation system with combined sensory and operator control. Guttropf, W. (Hrsg.): Advanced Sensor Technology : Proc.of the 7th Internat. Conf.on Robot Vision and Sensory Controls, Zürich, CH, February 2-4, 1988 Berlin (u.a.) : Springer, 1988 S.259-70 (IFS Publications, Bedford, UK), Zürich
- E88 Benner, J., Blume, C., Leinemann, K., Schlechtendahl, E.G., Wadle, M.: Advanced carrier systems and telerobotics. Rembold, U. (Hrsg.) Robot Control 1988 (SYROCO '88) : Preprints of the IFAC-Symp., Karlsruhe, October 5-7, 1988 Düsseldorf: VDI/VDE-Gesellschaft Mess- und Automatisierungstechnik, 1988 S.82.1-82.41, Karlsruhe
- F88 Benner, J., Fischer, C., Leinemann, K., Stratmanns, E., Till, W.: Automation of remote maintenance for fusion machines. 15th Symp.on Fusion Technology, Utrecht, NL, September 19-23, 1988, Utrecht

- G88 Kühnapfel, U., Leinemann, K., Schlechtendahl, E.G.: Graphics support for JET boom control. Proc. of the Internat. Topical Meeting on Remote Systems and Robotics in Hostile Environments, Pasco, Wash., March 29 - April 2, 1987 La Grange Park, Ill. : ANS, 1988 S.28-34
- H88 Suppan, A., Hübener, J.: Investigations of in-vessel handling concepts for NET. IAEA Technical Committee Meeting on Robotics and Remote Maintenance Concepts for Fusion Machines, Karlsruhe, February 22-24, 1988, Karlsruhe
- I88 Suppan, A., Hübener, J.: In-vessel handling unit concept for NET. 15th Symp. on Fusion Technology, Utrecht, NL, September 19-23, 1988
- A89 Maisonnier, D.: unpublished report, 24.10.1989
- B89 Reeve, T.: unpublished report, 11.05.1989 and 1990
- C89 Krieg, R., Wehner, E., Hübener, J., Suppan, A.: Design Optimization of an Articulated Boom for NET In-Vessel Handling Unit. Trans. 10th Int. Conf. on Structural Mechanics in Reactor Technology, Vol. N, Anaheim, Cal. 1989, pp.91-96
- D89 Browne, M.L., Bombi, F.: unpublished report, 26.09.1989
- E89 Browne, M.L., Bombi, F.: unpublished report, 26.09.1989
- F89 Holloway, C., Salpietro, E.: Maintenance Concepts for NET. IAEA-TECDOC-495 (1989) pp.75-87
- G89 Suppan, A., Hübener, J., Holler, H.E., Süß, U., Leinemann, K., Schlechtendahl, E.G.: Fernhandlung in der Plasmakammer einer Fusionsmaschine. KfK-Nachrichten, 21(1989) S.280-86
- H89 Krieg, R., Wehner, E., Hübener, J., Suppan, A.: Design optimization of an articulated boom for the NET in-vessel handling unit. Hadjian, A.H. (Hrsg.): Structural Mechanics in Reactor Technology : Transactions of the 10th Internat. Conf., Anaheim, Calif., August 14-18, 1989 Vol. N, S.91-96 Los Angeles : American Assoc. for Structural Mechanics in Reactor Technology, 1989
- A90 Suppan, A. et al.: The NET Articulated Boom: Preliminary Investigations and Justification for a Full Scale Prototype, KfK 4809, December 1990
- B90 Reeve, T.: unpublished report, Jan. 1990
- C90 Leinemann, K.: NET Remote Workstation. KfK-4785, October 1990
- D90 Kühnapfel, U., Ludwig, A.: Graphics and CAD Support for NET/ITER Boom Control. Proc. 16th SOFT, Sept. 3-7, 1990, London, pp. 1347-1352
- E90 Breitwieser, H.; Frank, A.; Süß, U.; Leinemann, K.: Specification of EDITH Motion Control System, KfK 4787, September 1990
- F90 Suppan, A., Hübener, J., Link, W., Ludwig, A.: unpublished report, July 1990
- H90 Suppan, A.: The NET Articulated Boom: Preliminary Investigation and Justification for a Full Scale Prototype. KfK-4809, December 1990

- I90 Suppan, A., Hübener, J., Süß, U., Leinemann, K., Rohrbacher, H.A., Wehner, E.: Der KfK-Beitrag zur Wartung und Instandhaltung von Fusionsanlagen (NET/ITER). Malcher, L. (Hrsg.) 1. Statusbericht des Arbeitsschwerpunktes Handhabungstechnik (HT) des Kernforschungszentrums Karlsruhe, 14. November 1990 Arbeitsbericht Nr. 10-90 Karlsruhe, KfK 1990 S.71-90
- J90 Leinemann, K.: NET remote workstation. KfK-4785 (Oktober 90)
- A91 Honda, T. et al.: ITER Assembly and Maintenance. ITER Documentation Series, No. 34, IAEA, Vienna, 1991
- B91 Reim, J.: Dynamic Simulation of the NET In-Vessel Handling Unit, Fusion Engineering and Design 18 (1991), pp. 471-476
- C91 Suppan, A.: unpublished report, May 1991
- D91 Leinemann, K.: Tele-operator support for fusion plant maintenance: the EDITH remote workstation. Proc. of the 2nd Internat. Symp. on Fusion Nuclear Technology, Karlsruhe, June 2-7, 1991 Part C Fusion Engineering and Design, 18(1991) S.517-23
- E91 Kühnapfel, U., Leinemann, K.: Verfahren zur Manipulation in unzugänglichen Arbeitsräumen. Patentschrift DE-OS 39 25 275 (7.2.1991) DE-PS 39 25 275 (24.1.1991)
- F91 Leinemann, K.: Advanced tele-operator support for fusion plant maintenance. Proc. of the '91 Internat. Symp. on Advanced Robot Technology ('91 ISART), Tokyo, J, March 5-7, 1991 Tokyo : Japan Industrial Robot Association, 1991 S.465-72
- G91 Reeve, T., Shaw, R., Suppan, A., Haferkamp, B.: The remote maintenance of mechanically attached first wall armour tiles in NET. Proc. of the 2nd Internat. Symp. on Fusion Nuclear Technology, Karlsruhe, June 2-7, 1991 Part C Fusion Engineering and Design, 18(1991) S.495-99
- H91 Boehme, G. Suppan, A.: Fernhandhabungstechnik. Kernfusion - Forschung und Entwicklung Karlsruhe: Kernforschungszentrum Karlsruhe GmbH 1991 S.51-56
- A92 Suppan A., Hübener, J. Reim, J., Woll, J., Maisonnier, D., Reeve, T.J.: EDITH - A Prototypical Articulated Boom System for NET/ITER, 17th Symposium on Fusion Technology, Roma Sept. 14-18, 1992, Fusion Technology 1992, Vol.2, pp.1599-1603
- B92 Ognibene, I., Sanguinetti, G.P.: unpublished report, 08.07.92
- C92 Leinemann, K., Kühnapfel, U., Katz, F., Knüppel, H., Krumm, H.-G., Olbrich, W.: KISMET based multi-media workstation for operational support in fusion plant maintenance. 17th SOFT, Roma, September 14-18, 1992, Fusion Technology 1992, Vol. 2, pp.1579-83
- D92 Benner, J., Leinemann, K.: Supervision and automatic control of robotic systems in nuclear environments. Proc. Third Intern. Conf. on High Level Radioactive Waste Management, Las Vegas, April 12-16, 1992, Vol. 1, pp.966-973
- E92 Kühnapfel, U.: Graphische Realzeitunterstützung für Fernhandhabungsvorgänge in komplexen Arbeitsumgebungen. KfK 5052, May 1992

- A93 The NET Team, NET Predesign Report, Fusion Engineering and Design, Volume 21, Feb. 1993, pp.92-106
- B93 Rieke, M.: unpublished report, 15.01.93
- C93 Suppan, A., Krieg, R., Krumm, H.G., Kühnapfel, U., Leinemann, K. Reim, J., Woll, J.: Experimental device for in-torus handling - EDITH intermediate report. KfK-5252 (Oktober 93)
- D93 Suppan, A. Hübener, J. Reim, J. Woll, J. Maisonnier, D. Reeve, T.: EDITH - a prototypical articulated boom system for NET/ITER. Ferro, C. (Hrsg.) Fusion Technology 1992 : Proc.of the 17th Symp., Roma, I, September 14-18, 1992 Vol. 2 S.1599-1603 Amsterdam (u.a.) : North Holland, 1993
- A94 Suppan, A., Gutzeit, H., Haferkamp, B., Knüppel, H., Leinemann, K., Woll, J.: unpublished report, October 1994
- B94 Woll, J.: unpublished report, June 1994
- C94 Suppan, A., Leinemann, K. Woll, J.: Erste praktische Erfahrungen mit dem EDITH-Teststand für Instandhaltungsarbeiten im Torus eines Fusionsreaktors. KfK-Nachrichten, 26(1994) S.146-55
- D94 Fiege, A., Haferkamp, B., Knüppel, H. Leinemann, K., Suppan, A. Woll, J., Maisonnier, D.: Testbed EDITH and first practical experience gained in the operation. Herschbach, K. (Hrsg.) Fusion Technology 1994 : Proc.of the 18th Symp., Karlsruhe, August 22-26, 1994 Vol. 2 S.1379-82 Amsterdam (u.a.) : Elsevier, 1995
- A95 Leinemann, K., Katz, F., Olbrich, W.: unpublished report, March 1995.
- B95 Woll, J.: unpublished report, July 1995
- C95 Leinemann, K., Katz, F., Knüppel, H., Olbrich, W. Maisonnier, D.: Synthetic Viewing: Comprehensive Work Representation, Making Remote Work More Clearer to the Operator. Fusion Engineering and Design 29(1995)317-323
- D95 Binz: unpublished report, March 1995
- E95 Woll, J.: unpublished report, July 1995
- F95 Binz: unpublished report, March 1995
- G95 Leinemann, K., Katz, F., Knüppel, H., Olbrich, W., Maisonnier, D.: Synthetic viewing: comprehensive work representation making remote work clearer to the operator. Proc.of the 3rd Internat.Symp.on Fusion Nuclear Technology, Los Angeles, Calif., June 27 - July 1, 1994 Part C Fusion Engineering and Design, 29(1995),S.317-23
- H95 Fiege, A., Haferkamp, B., Knüppel, H., Leinemann, K. Suppan, A. Woll, J., Maisonnier, D.: Testbed EDITH and first practical experience gained in the operation. Fusion Technology 1994 : Proc.of the 18th Symp., Karlsruhe, August 22-26, 1994 Vol. 2 S.1379-82 Amsterdam, Elsevier, 1995

- A96 Leinemann, K., Haist, B., Knüppel, H.: unpublished report, January 1996  
B96 Leinemann, K., Katz, F., Knüppel, H.: unpublished report, April 1996  
B96 Leinemann, K., Woll, J., Haferkamp, B.: unpublished report, January 1996

## 11.2 IRRADIATION BIBLIOGRAPHY

- A87 Rohrbacher, H.A.: unpublished report, Nov. 1987  
A88 Suppan, A., Rohrbacher, H.A.: unpublished report, June 1988  
A89 Suppan, A., Rohrbacher, H.A.: unpublished report, Nov. 1989  
A90 Rohrbacher, H.A., Wolf, K.: unpublished report, Sept. 1990  
B90 Rahn, A.: unpublished report, March 1990  
A91 Rohrbacher, H.A., Rahn, A., Suppan, A.: unpublished report July 1991  
A92 Rahn, A.: unpublished report, Jan. 1992  
B92 Rahn, A.: unpublished report, Dec. 1992  
C93 Suppan, A., Rahn, A., Englert, M.: unpublished report, July 1993  
D93 Rahn, A.: unpublished report, Dec. 1993  
E93 Rahn, A.: unpublished report, Oct. 1993  
A95 Suppan, A., Englert, M.: unpublished report April 1995  
B95 Englert, M.: unpublished report, Feb. 1995  
C95 Rohrbacher, H.A.: unpublished report, June 1995